Solving Selected Problems on American Option Pricing with the Method of Lines

A Thesis Submitted for the Degree of

Doctor of Philosophy

by

Blessing Taruvinga

B.Sc.(National University of Science and Technology, Zimbabwe)

M.Sc.(National University of Science and Technology, Zimbabwe)

M.Phil.(University of Cape Town)

Blessing.Taruvinga@student.uts.edu.au

in

Finance Discipline Group

University of Technology Sydney

PO Box 123 Broadway

NSW 2007, Australia

July 16, 2019

Certificate

I certify that the work in this thesis has not previously been submitted for a degree nor has it been submitted as part of requirement for a degree except as fully acknowledged within the text.

I also certify that the thesis has been written by me. Any help that I have received in my research work and the preparation of the thesis itself has been acknowledged. In addition, I certify that all information sources and literature used are indicated in the thesis.

This research was supported by the Australian Government Research Training Program.

Signed Production Note: Signature removed prior to publication.

Date 16 July 2019

Acknowledgements

First, I would like to thank God who has been with me throughout this journey. His faithfulness and continuous presence has been a source of strength for me and I am eternally grateful.

I would like to express my sincere gratitude to my principal supervisor, Dr. Christina Sklibosios Nikitopoulos. On the sad passing of Professor Carl Chiarella, who was my initial supervisor, she took me in as one of her students, and for that I would like to thank her immensely. I am also grateful to her for being a wonderful mentor. Her knowledge and insights, guidance and support, patience, kindness and encouragement while I have been working on this thesis has been invaluable. I would also like to thank Professor Erik Schlögl and Dr Boda Kang for their advice, guidance, and knowledge that they shared with me to make this thesis possible.

My heartfelt gratitude also goes to my fellow colleagues and the staff at the Finance Discipline Group of the UTS Business School. The discussions that we had, the encouraging words to one another, and the support that you gave me was priceless.

This thesis would not have been possible without the financial support received from UTS, through the UTS International Research Scholarship and the UTS Business Doctoral Scholarship received from the UTS Business School. For these scholarships, I am truly grateful.

Last but not least, I would like to thank my family for all the love, support and encouragement which you have given me. To my mother, my mother- and father-in-law, sisters, and brothers, I thank them for their prayers. I am grateful to my two daughters, Tuso and Maita for being there to cheer me up on this journey. My research would not have been possible without the support of my best friend and husband, Jona. Thank you for all the sacrifices that you have made for me. I will be forever grateful.

Contents

Abstract

The American option pricing problem lies on the inability to obtain closed form representation of the early exercise boundary and thus of the American option price. Numerous approaches have been developed to provide approximate solution or numerical schemes that derive American prices at a sufficient level of pricing accuracy and computational effort.

Jump-diffusion models have been used in literature with stochastic volatility models to better explain shorter maturity smiles[1]. They are also able to capture the skewness and kurtosis features of return distributions often observed in a number of assets in the market. By including jumps in volatility to the model dynamics, a rapidly moving but persistent component driving the conditional volatility of returns is incorporated (Eraker, Johannes & Polson (2003)).

This thesis considers the pricing of American options using the Heston (1993) stochastic volatility model with asset and volatility jumps and the Hull & White (1987) short rate model. Since the early exercise boundary depends on the term structure of interest rates, stochastic interest rates are important. The American option prices are numerically evaluated by using the Method of Lines (MoL) (Meyer (2015)). This method is fast and efficient, with the ability to provide the early exercise boundary and the Greeks[2] at the same computational effort as the option price. The main contributions of the thesis are:

- *Pricing American Options with Jumps in Asset and Volatility - Chapter 2 and Chapter 3.* In the first chapter, a MoL algorithm is developed to numerically evaluate American options under the Heston-Hull-White (HHW) model with asset and volatility jumps. A sensitivity analysis is then conducted to gauge the impact of jumps and stochastic interest rates on prices and their free boundaries. The second chapter assesses the importance of asset and volatility jumps in American option pricing models by calibrating the Heston (1993) stochastic volatility model with asset and volatility jumps to S&P 100 American options data. In general,

[1] A volatility smile is a graph of implied volatility as a function of strike for options with the same maturity.
[2] Greeks measure the sensitivity of the option price to changes in parameter values on which the option price depends.

jumps improve the model's ability to fit market data. Further the inclusion of asset jumps increases the free boundary, whilst volatility jumps marginally drops the free boundary, a result that is more pronounced during periods of high volatility.

- *Evaluation of Equity Linked Pension Schemes With Guarantees. - Chapter 4.* In the third chapter American Asian option are priced with application to two types of equity linked pension schemes, namely, the investment guarantee and the contribution guarantee schemes. This extends work by Nielsen, Sandmann & Schlögl (2011), where the American feature is introduced and allows for early termination of the policy. The investment fraction of the investors contributed amount that is required to achieve a certain level of investment return guarantee is analysed. A sensitivity analysis shows that asset volatility and interest rate volatility have a positive impact on the free boundary.

CHAPTER 1

Introduction

1.1. Literature Review and Motivation

American options [1] are important derivative contracts in current financial markets. Trading at extremely large volumes, they are written on many underlying assets such as stocks, indices, foreign exchange rates, and futures. Yet the pricing of American options is not trivial and still remains a topic open to research.

In the 70s Black & Scholes (1973) and Merton (1973) made a major breakthrough in option pricing by proposing an option pricing formula for European options, which became a fundamental tool for derivatives pricing in the financial world. Numerous approaches have been proposed in the literature to relax the Black-Scholes-Merton model assumptions for pricing options to create more realistic models that capture the skewness and leptokurtic features observed in the behaviour of market prices. Typical extensions include the stochastic volatility, the inclusion of jumps (Merton (1976)), and stochastic interest rate models.

Even though in most of these models, tractable solutions can be obtained for European option prices, this is not feasible for American options. The early exercise boundary is one of the inputs in the American option pricing formula. The integral equation that derives the early exercise boundary does not have closed form solutions and the problem converts to an optimal stopping problem. Consequently, an extensive literature has been dedicated on numerically solving the American option pricing problem. Myneni (1992) provides a review of the different methods that have been used in literature to price American options. These can be categorised into five general approaches; the free boundary approach,

[1] An option is a financial instrument which gives the holder the right to buy/sell an underlying asset at a future date for a price agreed for at the initiation of the contract. A call option gives the holder the right to buy the asset, whilst, with a put option, the holder of the option has the right to sell the underlying asset. The holder of the option can buy/sell the asset at a specific maturity date (European option) or can exercise the option at any time on, or before, the maturity date after the inception of the contract (American option).

approximate solutions, the use of compound options, numerical methods and regression-based methods (as well as combinations of those). More recent papers compare the various approaches discussed in literature. Lauko & Sevcovic (2010) considers a comparison of a number of analytical and numerical approximation methods used to compute free boundaries for American options discussed in literature. Minqiang (2010) introduces two analytical approaches which he compares to several approximation methods, the Laplace inversion method and the interpolation method of pricing American options.

1.1.1. American Option pricing problem. As early as the 1960s, before the Black & Scholes (1973) model was developed, American put options under no-arbitrage assumptions were evaluated in the context of an optimal stopping time problem. Some existence results for which the mathematical argument was presented by McKean (1965) and Karatzas (1988) provided a framework under which American options could be priced (see Carr, Jarrow & Myneni (1996)), while Van Moerbeke (1976) discussed the mathematical properties of these problems. Myneni (1992) presented the results by Bensoussan (1984) and Karatzas (1988) for the formulation of the early exercise premium for an optimal stopping problem, in which they suggested using optimality property to obtain an integral equation. However, an explicit solution for this integral equation could not be found and they determined that an optimal stopping problem could be re-modelled into a free boundary problem.[2] Under this new approach, an American option pricing problem can be expressed in terms of its free boundary, and the set of evaluation equations consist of a partial differential equation, together with the Dirichlet and Neumann conditions. An additional condition, known as the 'principle of smooth fit' is also required to determine the value of the free boundary. These sets of equations are known as the Stephan problem (Rubinstein (1971)). Treating the pricing of the American option as a free boundary problem was further advanced by research work such as those by Kim (1990), Carr et al. (1996) and AitSahlia & Lai (1999).

[2]An alternative method discussed by Carr et al. (1996), and studied in detail by Jaillet & D. Lapeyre (1990) is the variational inequality approach, and one of its advantages over the free boundary approach is that it does not require an introduction of the free boundary, a property which becomes beneficial especially when considering models consisting of several assets. Its basis is a discussion on the papers by Bensoussan (1984) and Karatzas (1988), in which they price options using Snell envelopes. Jaillet & D. Lapeyre (1990) make use of these formulas in order to price options using diffusion models, i.e. the Black-Scholes model. Under these conditions, they analyse the properties of option pricing formulas, together with their accuracy. The analysis is made possible by the relationship that exists between optimal stopping and variational inequalities.

Following the introduction of the Black-Scholes-Merton model in 1973, and due to the limited computing power at the time, research was dedicated on finding approximate solutions for the American option case. Initiated by Roll (1977) and extended by Whaley (1981) and Geske (1981), American options can be approximated by a portfolio of European options, a representation that does not lead to a unique solution. There are instances in which an American option is equivalent to a European one, i.e. Margrabe (1978) demonstrated that an American option (call or put) with a strike price that grows exponentially at the instantaneous interest rate would be worth the same as the European option. This led to the use of upper and lower bounds used to approximate the value of an American put option. Among these lines, Johnson (1983) presented an analytical approximation for a non-dividend paying American put option as the lower bound of a European put. MacMillan (1986) and Barone-Adesi & Whaley (1987) derived further approximation with application of commodity and futures options. Even though these methods involve low computational cost, they are not sufficiently accurate.

Geske & Johnson (1984) derived an analytic solution satisfying the partial differential equations and boundary conditions, which included the hedge ratios for asset prices with dividends and asset prices without dividends at discrete dates on which early exercise could occur. The pricing formulae for such American options can also be represented as a compound-option problem. This analytic solution was found to be accurate, in contrast to other approximating solutions, which cannot be made arbitrarily accurate. Due to these appealing properties, several papers adopted the compound-option approach to American option pricing such as Whaley (1986) and Selby & Hodges (1987), who proposed methods to improve the computational time. Further, in work by Schoder (1989), analytical solutions for associated partial differential equations are obtained but the required extrapolation methods made the application to American option pricing less attractive compared to numerical method alternatives.

With the advances in dynamic programming, a substantial amount of literature solves the American option pricing problem with numerical methods such as finite differences and trees. Brennan & Schwartz (1977), developed a numerical solution by discretising the 1-D partial differential equation in time and space, using finite differences to price American

put options. They reduced the problem of valuing an American put option to solving a partial differential equation under a given set of boundary conditions.

The finite difference method can be used to evaluate a variety of American style options (at a certain number of dimensions) thus it has widely been used (see Wu & Kwok (1997), Zhao, Davison & Corless (2007) and Ikonen & Toivanen (2009)). Within the space of finite difference methods, the MoL involves an approximation of one or more partial differential equations using ordinary differential equations in one of the independent variables. Time discretisation is performed and the approximation of the rest of the terms (except the second-order partial differential in the underlying asset) in the partial differential equation using finite differences. The resulting set of two ordinary differential equations is solved more easily than partial differential equations and is solved using Ricatti transformations to obtain option prices together with the Greeks. This method was proposed by Meyer & van der Hoek (1997) in the pricing of options for a diffusion process. Subsequently, Meyer (1998) discussed extensions to jump diffusions, Chiarella, Kang, Meyer & Ziogas (2009) assumed stochastic volatility and considered a Heston model with jumps, Adolfsson, Chiarella, Zioga & Ziveyi (2013) looked at the Heston model, and Chiarella, Nikitopoulos, Schlögl & Yang (2016) applied MoL to regime-switching models. The method has been compared to other similar methods such as the sparse grid method, the Crank-Nicholson method, and the Fourier and Laplace transform methods and demonstrated that it is fast and efficient, with the ability to compute free boundaries and Greeks at the same computational level as the option prices.

Another widely used numerical method to approximate the value of an American option is the binomial tree method, pioneered by Cox, Ross & Rubinstein (1979). They developed a discrete time-and-space option pricing formula and demonstrated that, as the number of time steps increase, the option value obtained using binomial trees converges to the Black-Scholes value. Generalisations of the mesh and tree methods include the multinomial methods of Boyle (1988) and further advances by Broadie & Glasserman (2004) and Tavakkoli & Thomas (2014).

Monte Carlo simulation is another common numerical method that was first proposed by Boyle (1977) for the pricing of European options, and later developed to include American options, see Broadie & Glasserman (1997). Broadie & Glasserman (1997) explained that

Monte Carlo simulations can deal with the high dimensionality of American option pricing, while finite methods become less efficient (in terms of computation effort and accuracy) as the dimensionality of the problem increases.

Alternatively, regression-based methods have also been employed to evaluate American options, see Carriere (1996) and Samimi, Mardani & Sharafpour (2017). Longstaff & Schwartz (2001) presents a least squares Monte Carlo (LSM) approach to price American options, in which the conditional expected payoff from continuation is estimated by using least squares regression. Finally, a combination of these approaches have included works such as (Tsitsiklis & Roy (1999), Fu, Laprise, Madan, Su & Wu (2001), Lindset & Lund (2007) and Agarwal, Junega & Sircar (2016)).

1.1.2. American option pricing models. Since the introduction of the Merton (1973) and Black & Scholes (1973) option pricing model, many extensions have been considered in the literature, including stochastic volatility, jump-diffusions, stochastic interest rates and combinations of those. The classical stochastic volatility models are the Hull & White (1987) and Heston (1993), which can fit better volatility smiles compared to the Merton-Black-Scholes model that assumes constant volatility. These models are widely used option-pricing models and are regularly integrated with other models to contribute in explaining market-observed characteristics in prices and volatility.

Jump-diffusion models have also been used in literature to help explain different behaviours in the market, which cannot be explained by stochastic volatility models (see Merton (1976), Naik & Lee (1990), and Bates (1996) for early references). The inclusion of jumps in asset dynamics helps to better explain shorter maturity smiles. They also have the added benefit of being able to capture the skewness and kurtosis features of return distributions often observed in several assets in the market (Bakshi, Cao & Chen (1997)).

According to Bakshi et al. (1997), Bates (2000), Pan (2002), and Eraker (2004) models with stochastic volatility are not capable of fully capturing the empirical features that are observed in option prices since the conditional volatility of returns increases rapidly, and a model with only asset jumps cannot fully capture this. According to Eraker (2004), jumps in returns explain large movements whilst jumps in volatility provide a persistent rapidly moving component driving the conditional volatility of returns. Further, they provide

evidence that volatility jumps tend to remove the mis-specification found in stochastic volatility models.

Different probability density functions (used to evaluate jump integrals) for jump sizes have been proposed in literature, e.g. Merton (1976) proposed a normally distributed logarithm of jump size, Kou (2002) looked at a jump size with an asymmetric double exponential distribution, Kangro, Parna & Sepp (2003) considered the case of a mixture of independent price jumps defined accordingly, Hanson & Westman (2002) presented a normal model, and Hanson, Westman & Zhu (2004) a uniform model.

Option pricing models with stochastic interest rates were considered as early as the 70s by Merton (1976), and later Amin & Jarrow (1992). Some literature which focuses on pricing models for stock options include Rabinovitch (1989) and Kim & Kunitomo (1999). Stochastic interest rates have been used extensively in the pricing of long-term contracts as they tend to improve the pricing and hedging of these contracts and have been combined with stochastic volatility models to produce well-known hybrid derivatives pricing models, see Amin & Jarrow (1992), Kaushik I. Amin (1993), Bakshi et al. (1997), Scott (1997), and Grzelak, Oosterlee & Weeren (2012). In the pricing of American options, stochastic interest rates play an important role in determining free boundaries, and as Ho, Stapleton & Subrahmanyam (1984) explains:

'*Stochastic interest rates add a potentially important dimension to the valuation of American-style contingent claims. To value such claims, it is necessary to compare the exercised value of the claim with the "live" value (the unexercised value) on each date. Since the term structure of interest rates affects the live value of the claim on each possible exercise date before expiration, the probability of early exercise and hence, the early-exercise premium will, in general, be affected by the volatility of interest rates.*'

American option pricing models with stochastic interest rates have different model formulations and rely on numerical solutions. Chung (1999) uses an analytical method and Kang & Meyer (2014) used the MoL. The classical models for stochastic interest rates include the Hull & White (Hull & White (1990)) which allows for negative interest rates and the CIR (Cox, Ingersoll & Ross (1985)).

Many options traded in the financial markets have early exercise features, hence the pricing of American options is considered. Since the paper by Black (1975), there have been

several extensions in the pricing of American options, similar to European options, i.e. stochastic volatility, stochastic interest rates, and jumps. Papers that focus on stochastic volatility include papers by Clarke & Parrott (1999), Ikonen & Toivanen (2009), Beliaeva & Nawalkha (2010), Haentjens & Hout (2015), and Agarwal et al. (2016). The assumption of stochastic interest rates in the pricing of American options is significant since the early exercise feature depends on the term structure of interest rates and the volatility of interest rates becomes important (see Amin & Bodurtha (1995), Chung (1999), and Detemple & Tian (2002)). Further, combination of stochastic volatility and stochastic interest-rate models have been also studied, for instance, Medvedev & Scaillet (2010), Chiarella & Kang (2011) and Kang & Meyer (2014).

Like European options, efforts have been made to improve the pricing of American options through the inclusion of jumps in the model dynamics, i.e. Bates (1996). Boyarchenko & Levendorski (2007) considered the pricing of American options for a Levy model with CIR-type stochastic interest rates, whilst Lamberton & Mikou (2008) looked at a jump-diffusion model in the pricing of American put options. Recently, there have been models that include both asset and volatility jumps in pricing American options, i.e. Durhama & Park (2013), Salmi, Toivanen & Sydow (2014), and Itkin (2016).

Considering the importance of stochastic interest rates in American option pricing as well as the contribution of (asset and volatility) jumps to derivatives pricing, this thesis aims to combine these two modelling specifications in the American option pricing problem. This combination of models is rarely studied in literature due to the computational complexity involving the numerical solution of a three-dimensional problem. The MoL is well suited to providing sufficient accurate solutions at an acceptable computational cost.

Accordingly, an American call option, for which its model assumes stochastic volatility and stochastic interest rate models with jumps in the asset and volatility dynamics, is considered. The volatility dynamics follows Heston (1993)'s model, whilst the interest rate process follows the model by Hull & White (1990). The asset jump is a compound Poisson process consisting of a random variable and a Poisson process. Its jump size is log-normally distributed (Merton (1976), Kangro et al. (2003), Chiarella et al. (2009)). The volatility jump size is exponentially distributed as this ensures that the variance is always positive (Lutz (2010)).

1.2. Thesis Structure

The aim of this thesis is to numerically evaluate American options when the asset price follows the Heston (1993) stochastic volatility model with asset and volatility jumps, while the short rate follows the Hull & White (1990) model, denoted as Heston-Hull-White (HHW). The MoL is used to obtain American option prices as well as their free boundaries and Greeks under jump-diffusion HHW models. The first part considers the pricing of American options under jump-diffusion HHW models and assesses the impact of jumps on prices and early exercise boundaries. The second part presents the calibration of jump-diffusion HHW models to S&P 100 options. The third part deals with the pricing of Asian-American options with applications to two types of equity linked schemes, namely, the investment guarantee scheme and the contribution guarantee scheme. The last section concludes the thesis.

1.2.1. Pricing American options with jumps in assets and volatility. In the first part, an American call option pricing problem with stochastic volatility and stochastic interest rate dynamics, with asset jumps and volatility jumps is presented. The option prices are obtained using the MoL, thus allowing us to compute free boundaries and Greeks with no extra computational effort. Including asset-volatility jumps impacts the free boundaries significantly, especially far from expiry. Including asset jumps lowers the free boundary when the time to maturity is higher and the holder of the option is more likely to exercise the option, whilst the inclusion of both asset and volatility jumps increases this free boundary and the holder of the option is less likely to exercise the option. Jumps were also found to increase the Delta values and OTM and ATM option values, whilst reducing ITM option values. Interest rates and volatility, together with their volatilities were found to have a positive impact on the free boundaries.

1.2.2. The impact of jumps on American option pricing: The S&P 100 options case. The second part of the thesis discusses a calibration procedure, in which the HHW model with asset and volatility jumps is calibrated to S&P 100 options data. Calibration is done under different market conditions, i.e. high/low volatility and high/low interest rates. To assess the impact of jumps, three models are considered: the HHW model, the HHW model, with asset jumps, and the HHW model with asset and volatility jumps. Asset

jumps play an important role in improving the models' ability to fit market data. Asset and volatility jumps shift up the free boundary, an effect that augments during volatile market conditions, while additional volatility jumps marginally drift down the free boundary.

1.2.3. Evaluation of equity linked pension schemes with guarantees. The third part adapts the American option problem to a problem of valuing equity linked pension schemes with guarantees, thus, to an Asian-American option-pricing problem. This will allow investors to surrender the policy at any time on, or before, contract maturity. Since pension schemes are long-term financial products, a deterministic volatility assumption is made, and the model excludes jumps. Equity linked pension schemes with guarantees, namely the investment guarantee and the contribution guarantee schemes, are considered. Under stochastic asset and stochastic interest rate dynamics, the investment fraction of the investor's contributed amount, required to achieve a certain level of investment return guarantee for both these schemes, is a decreasing function of the guaranteed return and much higher for the investment guarantee scheme.

The impact of interest rates, interest rate volatility, portfolio volatility, and correlation on the free boundary is numerically investigated. The results indicate that the asset volatility and interest rate volatility have a positive impact on free boundary values. When time to maturity increases, interest rates have the greatest impact on free boundary values. These results can provide useful insights on designing these contracts to ensure desirable payoffs for policy holders and investors.

CHAPTER 2

Pricing American Options with Jumps in Asset and Volatility

2.1. Introduction

Numerous approaches have been proposed in the literature to relax the Black & Scholes (1973) model assumptions for pricing European options to create more realistic models, which reflect the behaviour of market prices, for example, by including features such as stochastic volatility, stochastic interest rates, jump diffusion, and combinations thereof. For example, stochastic volatility models capture the empirically observed leptokurtosis in the markets, stochastic interest rates improve pricing and hedging of long-dated contracts, and jump-diffusions tend to explain better shorter maturity smiles.[1]

Another extension of practical importance is the pricing of American options, since many options traded in the market have early exercise features. From the seminal paper by Black (1975), many numerical applications in the literature have been considered to value options featuring early exercise, in addition to stochastic volatility, stochastic interest rates, and jumps. Several papers discuss the assumption of stochastic volatility in pricing American options, including Clarke & Parrott (1999), Ikonen & Toivanen (2009), Beliaeva & Nawalkha (2010), Haentjens & Hout (2015), and Agarwal et al. (2016). The early exercise premium for American options at any time before maturity depends on the term structure of interest rates (i.e. Ho et al. (1984)), thus interest rate volatility cannot be ignored, especially for long-term options. Amin & Bodurtha (1995), Chung (1999), and Detemple & Tian (2002) price American options under the assumption of stochastic interest rates. Some American option-pricing models combine both stochastic volatility

[1]Representative literature on pricing European options with stochastic volatility models include Hull & White (1987), Stein & Stein (1991), Heston (1993) and Schobel & Zhu (1999). Stochastic interest rate models have been developed by Merton (1973), Amin & Jarrow (1992), Rindell (1995), Haowen (2012) and Abudy & Izhakian (2013), and combinations with stochastic volatility include the models by Kaushik I. Amin (1993), Grzelak et al. (2012), Haentjens & Hout (2012) and Guo, Grzelak & Oosterlee (2013). Jump-diffusion models have been considered by Scott (1997), Bakshi et al. (1997), Doffou & Hilliard (2001), Kou (2002), Pan (2002), Kangro et al. (2003), Pinkham & Sattayatham (2011), Makate & Sattayantham (2011), Hua, Shancun & Dianyu (2012), Zhang & Wang (2013), Zhang & Wang (2013).

and stochastic interest rates, i.e. Medvedev & Scaillet (2010), Chiarella & Kang (2011), and Kang & Meyer (2014).

Extensions to accommodate jump diffusions have also been considered in American option-pricing literature. These typically help to explain shorter maturity smiles. Bates (1996) developed a method for pricing American options for stochastic volatility/jump-diffusion processes under systematic jump and volatility risk. According to Bates (1996), Bakshi et al. (1997) and Pan (2002), models with jumps in asset dynamics only are not capable of fully capturing the empirical features of equity index returns or option prices. They propose including jumps in the stochastic volatility and provide empirical evidence that models with only diffusive stochastic volatility and jumps in returns are misspecified, as they do not have a component driving the conditional volatility of returns, which is rapidly moving. Duffie, Pan & Singleton (2000) focused on an affine jump-diffusion model, which allows for correlated jumps in both volatility and price. They found that the level of skewness produced by including negative jumps does not fully reflect market data. According to Duffie et al. (2000) and Pan (2002), jumps in volatility increase the Black-Scholes implied volatility for in-the-money options and they labelled this as the 'hook" or "tipping-at-the-end" effect. A comprehensive description on the impact of jumps in both return and volatility dynamics is given by Eraker et al. (2003). They demonstrate that the inclusion of jumps in returns helps to explain large movements in option prices, whilst the inclusion of jumps in volatility allow it to increase rapidly, as jumps in returns are a rapidly moving, but persistent, factor driving volatility. Further, in comparison to stochastic volatility models, models with jumps in returns steepen the slope of the implied volatility, while adding another jump to volatility further steepens this slope. Boyarchenko & Levendorski (2007) priced American options in Levy models with CIR-type stochastic interest rate using an iteration method based on the Wiener-Hopf factorisation, while Lamberton & Mikou (2008) looked at the behaviour of American put option prices in the presence of asset jumps. More recent developments on models with asset and volatility jumps include Durhama & Park (2013) and Salmi et al. (2014). Itkin (2016) considers the pricing and hedging of exotic options, for which the dynamics include correlated jumps in asset, volatility, and interest rates. The literature on evaluating American option pricing models with jumps in asset and volatility, while assuming stochastic interest rates, is rather limited. The current chapter aims to contribute to this stream of literature.

In the absence of closed-form solutions for options featuring early exercise, a variety of numerical methods have been proposed to price these types of options, such as finite difference methods, splitting methods, multi-grid methods, and numerical approximations. Barone-Adesi & Whaley (1987) used an analytic approximation for pricing exchange traded American options on commodities and the futures contracts. They found their method to be accurate and more computationally efficient in comparison to other methods, i.e. binomial methods and finite difference methods. Broadie & Detemple (1996) propose price approximations with one based on the lower bound and the other based on both the lower and upper bounds. Both these methods were based on the Black-Scholes model. As the Black Scholes model was improved to incorporate stochastic volatility, stochastic interest rates and jumps, other methods such as binomial methods, Monte Carlo methods, and finite difference methods have been used. Broadie & Glasserman (1997) priced American options using a simulation algorithm that has an advantage over lattice and finite difference methods when there are many state variables. Carriere (1996), Tsitsiklis & Roy (1999) and Longstaff & Schwartz (2001) also use simulation-based techniques for this purpose, with the latter paper being most commonly referenced when pricing American options by Monte Carlo. Sullivan (2000) used Gaussian Quadrature together with Chebyshev approximation to price American put options, an alternative method to binomial models. Ikonen & Toivanen (2009) priced American options using five finite difference-based methods, namely, the projected SOR, projected multigrid method, an operator splitting method, a penalty method, and the component-wise splitting method under the Heston model to check the speed and accuracy of these methods. Agarwal et al. (2016) combined finite difference methods and Monte Carlo to price American options with stochastic volatility.

This chapter evaluates American call options with stochastic volatility and stochastic interest rate models that allow for asset and volatility jumps. The proposed model assumes Heston (1993) volatility dynamics and Hull & White (1987) type dynamics for the interest rates. The asset jumps part is a compound Poisson process, which consists of a random variable and a Poisson process, and is independent from the continuous part. The jump sizes are log-normally distributed, see Merton (1976), Kangro et al. (2003), Chiarella et al. (2009). The volatility jump size is exponentially distributed to ensure that the variance

jumps are not negative, as normally observed after large downward jumps occur in asset prices (Lutz (2010)).

For the numerical evaluations of American call options under these model assumptions, the MoL algorithm is employed due to its accuracy and numerical efficiency, see Meyer (1998). The MoL for pricing American options was introduced by Meyer & van der Hoek (1997) with the asset price process following a diffusion process. Extensions to jump diffusion with the MoL were discussed in Meyer (1998). Chiarella et al. (2009) evaluated American options under the assumption that asset price dynamics are driven by the jump-diffusion process proposed by Merton (1976), and the volatility follows the square root process by Heston (1993). They also demonstrated the computational efficiency of the MoL compared to component-wise splitting and Crank-Nicholson methods. The MoL was also used by Chiarella & Ziveyi (2011) to price American options with two stochastic volatility processes, Adolfsson et al. (2013) to price American call option under Heston stochastic volatility dynamics, Kang & Meyer (2014) to price American options whose dynamics include stochastic interest rate of the CIR type and Chiarella et al. (2016) to price American options under regime switching. In this chapter, the MoL is applied to numerically solve the American call option pricing problem under stochastic volatility, stochastic interest rates, and jumps in both asset prices and volatility.

A sensitivity analysis is firstly conducted to gauge the impact of the volatility and the interest rates on the free boundaries. It is found that these have a positive impact on the free boundaries. To assess the impact of jumps on the free boundaries and the option prices, models are compared, the Heston Hull White (HHW), Heston Hull White with asset jumps (HHWJ) and Heston Hull White with asset and volatility jumps (HHWJJ). The analysis reveals that jumps shift the boundaries down far from expiry, a relation that reverses close to maturity. Depending on their moneyness, OTM and ATM options become more valuable as we add jumps.

The remainder of the chapter is structured as follows. Section 2.2 describes the pricing model for American call options, which allows for stochastic volatility, stochastic interest rates, and jumps in both the assets and volatility and derives the corresponding PIDE pricing equation. The implementation details of the MoL algorithm are included in Section 2.3. Section 2.4 confirms the accuracy of the MoL implementation and presents a sensitivity

analysis to gauge the impact of stochastic volatility and stochastic interest rates on the free boundary surfaces. Section 2.5 assess the impact of asset and volatility jumps on American call prices, their free boundaries, and Greeks. Section 2.6 provides a conclusion.

2.2. American Call Option Pricing: The Valuation Model

This section describes the model used to price American call options. In line with the model of Duffie et al. (2000), which includes jumps in both the asset and volatility dynamics, the Heston (1993) stochastic volatility model with asset and volatility jumps is considered. The interest rate process follows the Hull & White (1987) interest rate model.

Under the physical measure $\mathbb{P}$, the dynamics of the underlying price are given by the following equations:

$$\begin{aligned} dS &= (\mu - \lambda_1^* k^*)\, S dt + \sqrt{V} S dZ_1 + (Y-1)\, S dN_1, \\ dV &= \kappa\,(\theta - V)\, dt + \sigma_V \sqrt{V} dZ_2 + y dN_2, \\ dr &= a\,(b\,(t) - r)\, dt + \sigma_r dZ_3, \end{aligned} \tag{2.2.1}$$

where S is the stock price, μ is the instantaneous stock return, V is the variance process, Z_i (for $i = 1,\ 2,\ 3$) is a standard Wiener process under the physical measure $\mathbb{P}$, r is the instantaneous interest rate whose dynamics are given by the Hull & White (1987) model, $Y - 1$ is the random variable percentage change in the asset price if a jump occurs, dN_i is a Poisson increment, which is given by:

$$dN_i = \begin{cases} 1, & \text{with probability} \quad \lambda_i^* dt, \\ 0, & \text{with probability} \quad 1 - \lambda_i^* dt, \qquad \text{for } i = 1, 2 \end{cases}$$

where dN_1 and dN_2 are jump processes with jump intensities λ_1^* and λ_2^* respectively. They are not correlated and are also independent from the continuous part of the process (Lutz (2010)),

$$k^* = E^{\mathbb{P}}(Y-1) = \int_0^\infty (Y-1)\, G^*(Y)\, dY, \tag{2.2.2}$$

where $G^*(Y)$ is the probability distribution of Y under the physical measure $\mathbb{P}$, κ is the rate of mean reversion of V, θ is the long run mean of V, σ_V is the instantaneous volatility of V, y is the absolute jump size of the volatility process, a is the rate of mean reversion of

r, $b(t)$ is the long run mean of r which is given as

$$b(t) = c_1 - c_2 e^{-c_3 t} \tag{2.2.3}$$

where c_1, c_2 and c_3 are positive constants and $c_1 > c_2$, σ_r is the instantaneous volatility of r. In order for the variance process to remain positive, $\kappa, \theta,$ and σ_V will have to be selected such that the following Feller condition (Feller (1951)) is satisfied

$$2\kappa\theta > \sigma_V^2. \tag{2.2.4}$$

In addition to the Feller condition, Cheang, Chiarella & Ziogas (2013) show that an additional condition on the correlation between the Wiener processes need to be satisfied. Under the physical measure $\mathbb{P}$, these conditions ensure that the variance does not explode and that the solution to the asset price process is a martingale. The Wiener processes under the physical measure $\mathbb{P}$ are correlated, and the correlation structure is assumed to be given by

$$E^{\mathbb{P}}(dZ_1 dZ_2) = \rho_{12}dt, E^{\mathbb{P}}(dZ_1 dZ_3) = \rho_{13}dt, E^{\mathbb{P}}(dZ_2 dZ_3) = \rho_{23}dt,$$

where $\rho_{i,j}$ for $i = 1, 2$ and $j = 2, 3$ are constants. The correlation coefficients are such that the correlation matrix is positive definite.

The model described in equation (2.2.1) has three sources of Wiener risk and is inherently incomplete (see Harrison & Pliska (1981)). Additionally, the jump components in the asset and volatility dynamics introduce two more sources of uncertainty. In line with Cheang et al. (2013), we assume that the incompleteness, in terms of evaluating the parameters of the suitable Radon-Nikodym derivative for the transformation of the physical measure $\mathbb{P}$ to an equivalent risk-neutral measure $\mathbb{Q}$, can be handled by a calibration or consideration of a financial scenario (Jeanblanc, Klöppel & Miyahara (2007)). [2] Let q be the continuously compounded dividend rate for the stock. Under the risk-neutral measure, the instantaneous stock return μ is equivalent to $r - q$.

2.2.1. Partial integro-differential equation (PIDE) derivation using the martingale approach. The system of correlated Wiener processes (2.2.1) is transformed to a

[2] Lutz (2010) also discusses the Radon-Nikodym derivative for a similar case of an asset jump only and mentions that his results can be extended to vector processes in which the variance jumps could be included. Itkin (2016) considered a model with correlated jumps in asset, volatility and interest rate dynamics and considers his model only under the risk-neutral measure.

system of uncorrelated Wiener processes using Cholesky decomposition, as it is more convenient to work with a system of independent Wiener processes.[3] The resulting system of independent Wiener processes W_1, W_2, and W_3 is given below as:

$$\begin{aligned}
dS &= \left(r - q - \lambda_1^* k^*\right) S dt + \sqrt{V} S dW_1 + \left(Y - 1\right) S dN_1, \\
dV &= \kappa\left(\theta - V\right) dt + \sigma_V \sqrt{V} \rho_{12} dW_1 + \sigma_V \sqrt{V} \left(1 - \rho_{12}^2\right)^{\frac{1}{2}} dW_2 + y dN_2, \qquad (2.2.5) \\
dr &= a\left(b\left(t\right) - r\right) dt + \sigma_r \rho_{13} dW_1 + \sigma_r \frac{\rho_{32} - \rho_{12}\rho_{13}}{\sqrt{1 - \rho_{12}^2}} dW_2 \\
&\quad + \sigma_r \left(\frac{1 - \rho_{12}^2 - \rho_{13}^2 - \rho_{23}^2 + 2\rho_{12}\rho_{13}\rho_{23}}{1 - \rho_{12}^2}\right)^{\frac{1}{2}} dW_3.
\end{aligned}$$

The Feller condition imposed when the physical measure is under consideration in equation (2.2.4) will not necessarily hold under the risk neutral measure. When the Feller condition is used, the variance process remains strictly positive. When it is relaxed, there is a possibility that the variance could be zero. When the variance is zero, it momentarily stays there since the diffusion part of the first equation in equation (2.6.5) is zero and the drift part which is non-zero draws it to the positive region again (Kokholm & Stisen (2015)). A number of empirical studies show that when the Feller condition is imposed, the model fits the market data poorly, and model performance is improved when this condition is not imposed, as shown by the level of errors (Kokholm & Stisen (2015) and Ribeiro & Poulsen (2013)).

We further assume, the conventional choice of a market price of volatility risk given by, $\lambda_V\left(t, S, V\right) = \lambda_V \sqrt{V}$, with constant λ_V and a constant market price of interest rate risk λ_r (see for instance Chiarella et al. (2009) and Kang & Meyer (2014)). [4] Then the infinitesimal

[3]The computation for transforming the system to a set of independent Wiener processes is given in Appendix 2.1.

[4]Lamoureux & Lastrapes (1993) investigated whether volatility risk does affect the option price. They tested whether the strong assumption of market indifference to volatility risk is consistent with data. They concluded that further attempts to learn from the data should explicitly model a risk premium on the variance process as given in the model by Heston (1993).

generator $\boldsymbol{K}$ for this system of equations is given as:

$$\begin{aligned}\boldsymbol{K} &= \left(r - q - \lambda_1^* \int (1 - \lambda_{SJ}(Y))(Y-1) G^*(Y)\, dY\right) S\frac{\partial}{\partial S} + (\kappa(\theta - V) - \lambda_V V)\frac{\partial}{\partial V} \\ &+ (a(b(t) - r) - \lambda_r)\frac{\partial}{\partial r} + VS^2\frac{1}{2}\frac{\partial^2}{\partial S^2} + \sigma_V^2 V\frac{1}{2}\frac{\partial^2}{\partial V^2} + \sigma_r^2\frac{1}{2}\frac{\partial^2}{\partial r^2} + VS\sigma_V\rho_{12}\frac{\partial^2}{\partial S\partial V} \\ &+ \sqrt{V}S\sigma_r\rho_{13}\frac{\partial^2}{\partial S\partial r} + \sigma_r\sigma_V\sqrt{V}\rho_{23}\frac{\partial^2}{\partial V\partial r} + \lambda_1^*\int (1 - \lambda_{SJ}(Y))(f(YS,t) - f(S,t)) G^*(Y)\, dY \\ &+ \lambda_2^*\int (1 - \lambda_{VJ}(y))(f(V+y,t) - f(V,t)) g^*(y)\, dy, \end{aligned} \tag{2.2.6}$$

where $\lambda_{SJ}(Y)$ is the market price of risk for the asset jump, $\lambda_{VJ}(y)$ is the market price of risk for the volatility jump, $g^*(y)$ is the probability distribution of y. Let $f(t,S,V,r)$ be the price of an option with maturity T at time t. Option pricing can be performed under an equivalent martingale measure which is determined by its numeraire. Under the risk-neutral probability measure $\mathbb{Q}$, the current option value is computed by the expected discounted future payoff of the option, since the option price denominated at the money market account is a martingale under the risk-neutral measure. This approach to option pricing in known as the martingale approach. Mathematically:

$$f(t,S,V,r) = \boldsymbol{E}_t^{\mathbb{Q}}\left[e^{-\int_t^T r(s)ds} f(T,S,V,r)\right]$$

The Feynman-Kac formula states that $f(t,S,V,r)$ satisfies the integro partial differential equation:

$$\frac{\partial f}{\partial t} + \mathbf{K}f - rf = 0,$$

subject to the initial condition

$$\lim_{t\to T} f(t,S,V,r) = f(T,S,V,r).$$

Let time to maturity, τ be defined as $\tau = T - t$. Hence, the PIDE is given as:

$$\left(r - q - \lambda_1^* \int (1 - \lambda_{SJ}(Y))(Y-1) G^*(Y)\, dY\right) S\frac{\partial f}{\partial S} + (\kappa(\theta - V) - \lambda_V V)\frac{\partial f}{\partial V}$$
$$+ ((a(b(\tau) - r)) - \lambda_r)\frac{\partial f}{\partial r} + VS^2\frac{1}{2}\frac{\partial^2 f}{\partial S^2} + \sigma_V^2 V\frac{1}{2}\frac{\partial^2 f}{\partial V^2} + \sigma_r^2\frac{1}{2}\frac{\partial^2 f}{\partial r^2} + VS\sigma_V\rho_{12}\frac{\partial^2 f}{\partial S\partial V}$$
$$+ \sqrt{V}S\sigma_r\rho_{13}\frac{\partial^2 f}{\partial S\partial r} + \sigma_r\sigma_V\sqrt{V}\rho_{23}\frac{\partial^2 f}{\partial V\partial r} + \lambda_1^*\int (1 - \lambda_{SJ}(Y))(f(YS,\tau) - f(S,\tau)) G^*(Y)\, dY$$
$$+ \lambda_2^*\int (1 - \lambda_{VJ}(y))(f(V+y,\tau) - f(V,\tau)) g^*(y)\, dy - rf = \frac{\partial f}{\partial \tau}. \tag{2.2.7}$$

2.2.2. The partial-integro differential equation for a call option and boundary conditions. Let the time to maturity, τ be defined as $\tau = T - t$. Let C, a function of τ, S, V, r be the American call option price given by $C(\tau, S, V, r)$. Then:

$$C(\tau, S, V, r) = \sup_{0 \le \tau^* \le \tau} \mathbf{E}_\tau^{\mathbb{Q}}\left[e^{-\int_0^{\tau^*} r(s)ds} C(\tau^*, S, V, r)\right].$$

where τ^* is the stopping time. Using the Feynman-Kac formula $C(\tau, S, V, r)$ satisfies the integro partial differential equation:

$$\mathbf{K}C - rC = \frac{\partial C}{\partial \tau},$$

in the region

$$0 \le \tau \le T, \;\; 0 < S \le d(\tau, V, r), \;\; 0 < V < \infty, \;\; -\infty < r < \infty,$$

where $d(\tau, V, r)$ is the early exercise boundary, subject to the initial condition

$$\lim_{\tau \to 0} C(\tau, S, V, r) = C(0, S, V, r).$$

The domain for r includes negative interest rates since the Hull-White model allows for negative rates. At the free boundary point, the value matching condition

$$C(\tau, d(\tau, V, r), V, r) = d(\tau, V, r) - K,$$

must be satisfied as it ensures continuity of the option value function at the free boundary. To maximise the value of the American call option and avoid arbitrage in the model , the following smooth pasting conditions need to be included at the free boundary:

$$\lim_{S\to d(\tau,V,r)} \frac{\partial C}{\partial S} = 1, \quad \lim_{S\to d(\tau,V,r)} \frac{\partial C}{\partial V} = 0, \quad \lim_{S\to d(\tau,V,r)} \frac{\partial C}{\partial r} = 0. \tag{2.2.8}$$

This condition implies that the American call option value is maximised by a strategy that makes the value of the option and the delta of the option continuous. The computational domain is

$$0 \leq \tau \leq T, \;\; S_{\min} < S \leq S_{\max}, \;\; V_{\min} < V < V_{\max}, \;\; -r_{\min} < r < r_{\max}. \tag{2.2.9}$$

According to Meyer (2015), in pricing the American call using the MoL under the assumption of the HHW model, he observed the following:

For pricing the European call with $y = 0$ the computational domain $(0, Y) \times (0, V_{\max}) \times (-r_{\max}, r_{\max})$ is chosen in Haentjens & Hout (2012) which takes into account that the Hull-White model formally sustains negative interest rates. On its boundary, conditions are imposed which are suggested by the behaviour of the Black Scholes formula for a call as $r \to \infty$ and $V \to \infty$. They would appear to be inconsistent with the expected behavior of the American call and cannot be used here. Here we shall work with the time independent computational domain:

$$D = \{(y, v, r) : 0 < y < Y, 0 < v < v_{\max}, 0 < r < r_{\max}\}$$

In line with these findings, similar considerations will be made since the same method and similar boundary conditions are being used in pricing the American call option.

The maximum value for r in the r-grid has been selected based on the maximum range of realistic values that can be obtained in the market, and this is similar to the way that $V_{\max}$ is selected. $S_{\max}$ has been selected such that it is at least 3 times the strike price. This is to ensure that the choice of $S_{\max}$ has a negligible impact on the option price at the point where the strike price is equal to the asset price (Meyer (2015)). The minimum value of the S - grid, $S_{\min}$ is zero, since we cannot have negative asset prices. A similar argument holds in the way that $V_{\min}$ is selected,since market volatility can never be less than zero. The associated boundary conditions at these points will be discussed. By selecting these minimum points, the behavior of option prices for small values of S, V and r can be

observed. An analysis of the impact of $V_{\max}$ and $r_{\max}$ on the option prices is discussed in the numerical analysis section of this chapter.

Following the results obtained previously, the PIDE that needs to be solved to obtain the option price is

$$\left(r-q-\lambda_1^*\int\left(1-\lambda_{SJ}\left(Y\right)\right)\left(Y-1\right)G^*\left(Y\right)dY\right)S\frac{\partial C}{\partial S}+\left(\kappa\left(\theta-V\right)-\lambda_V V\right)\frac{\partial C}{\partial V}$$
$$+\left(\left(a\left(b\left(\tau\right)-r\right)\right)-\lambda_r\right)\frac{\partial C}{\partial r}+VS^2\frac{1}{2}\frac{\partial^2 C}{\partial S^2}+\sigma_V^2 V\frac{1}{2}\frac{\partial^2 C}{\partial V^2}+\sigma_r^2\frac{1}{2}\frac{\partial^2 C}{\partial r^2}+VS\sigma_V\rho_{12}\frac{\partial^2 C}{\partial S\partial V}$$
$$+\sqrt{V}S\sigma_r\rho_{13}\frac{\partial^2 C}{\partial S\partial r}+\sigma_r\sigma_V\sqrt{V}\rho_{23}\frac{\partial^2 C}{\partial V\partial r}-rC+\lambda_1^*\int\left(1-\lambda_{SJ}\left(Y\right)\right)\left(C\left(YS,\tau\right)-C\left(S,\tau\right)\right)G^*\left(Y\right)dY$$
$$+\lambda_2^*\int\left(1-\lambda_{VJ}\left(y\right)\right)\left(C\left(V+y,\tau\right)-C\left(V,\tau\right)\right)g^*\left(y\right)dy=\frac{\partial C}{\partial\tau}. \tag{2.2.10}$$

The boundary conditions at the points S_{min}, S_{max}, V_{min}, V_{max}, r_{min} and r_{max} are discussed below. At $S=S_{max}$, the value of the call option is

$$C\left(\tau,S_{max},V,r\right)=S_{max}-K.$$

To determine the type of boundary conditions to be used at $S=S_{min}$, $V=V_{min}$ and $r=r_{min}$, Meyer (2015) and Kang & Meyer (2014) use the algebraic sign of the Fichera function for the PIDE. Applying these results, the option price at $S=S_{min}$ is

$$C\left(\tau,0,V,r\right)=0.$$

At the point $V=V_{min}$, the PIDE becomes

$$\sigma_r^2\frac{1}{2}\frac{\partial^2 C}{\partial r^2}+\left(r-q-\lambda_1^*\int\left(1-\lambda_{SJ}\left(Y\right)\right)\left(Y-1\right)G^*\left(Y\right)dY\right)S\frac{\partial C}{\partial S}+\kappa\theta\frac{\partial C}{\partial V}$$
$$+\left(\left(a\left(b\left(\tau\right)-r\right)\right)-\lambda_r\right)\frac{\partial C}{\partial r}-rC+\lambda_1^*\int\left(1-\lambda_{SJ}\left(Y\right)\right)\left(C\left(YS,\tau\right)-C\left(S,\tau\right)\right)G^*\left(Y\right)dY$$
$$+\lambda_2^*\int\left(1-\lambda_{VJ}\left(y\right)\right)\left(C\left(y,\tau\right)-C\left(0,\tau\right)\right)g^*\left(y\right)dy=\frac{\partial C}{\partial\tau}, \tag{2.2.11}$$

and at $r=r_{min}$ the PIDE reduces to

$$\left(r-q-\lambda_1^*\int\left(1-\lambda_{SJ}\left(Y\right)\right)\left(Y-1\right)G^*\left(Y\right)dY\right)S\frac{\partial C}{\partial S}+\left(\kappa\left(\theta-V\right)-\lambda_V V\right)\frac{\partial C}{\partial V}$$
$$+a\left(b\left(\tau\right)\right)\frac{\partial C}{\partial r}+VS^2\frac{1}{2}\frac{\partial^2 C}{\partial S^2}+VS\sigma_V\rho_{12}\frac{\partial^2 C}{\partial S\partial V}+\sigma_V^2V\frac{1}{2}\frac{\partial^2 C}{\partial V^2}$$
$$+\lambda_1^*\int\left(1-\lambda_{SJ}\left(Y\right)\right)\left(C\left(YS,\tau\right)-C\left(S,\tau\right)\right)G^*\left(Y\right)dY$$
$$+\lambda_2^*\int\left(1-\lambda_{VJ}\left(y\right)\right)\left(C\left(V+y,\tau\right)-C\left(V,\tau\right)\right)g^*\left(y\right)dy=\frac{\partial C}{\partial\tau}. \tag{2.2.12}$$

The call option price is not solved for at the boundary points $V=V_{min}$ and $r=r_{min}$ using (6) and (7). Quadratic extrapolation for obtaining the option values at those points is used. At the point $r=r_{min}$, option values obtained at the points $r=\Delta\ r$, $r=2\Delta\ r$, and $r=3\Delta\ r$ by solving the PIDE using Riccati transformation, are used. At the point $V=V_{min}$ option values obtained at the points $V=\Delta V,\ V=2\Delta V,\ V=3\Delta V$ are used. The general quadratic extrapolation formula is given by:

$$f\left(0\right)=3f\left(\Delta x\right)-3f\left(2\Delta x\right)+f\left(3\Delta x\right).$$

At $V=V_{max}$ the PIDE becomes:

$$\left(r-q-\lambda_1^*\int\left(1-\lambda_{SJ}\left(Y\right)\right)\left(Y-1\right)G^*\left(Y\right)dY\right)S\frac{\partial C}{\partial S}+\left(\kappa\left(\theta-V_{max}\right)-\lambda_V V_{max}\right)\frac{\partial C}{\partial V}$$
$$+\left(\left(a\left(b\left(\tau\right)-r\right)\right)-\lambda_r\right)\frac{\partial C}{\partial r}+V_{max}S^2\frac{1}{2}\frac{\partial^2 C}{\partial S^2}+\sigma_r^2\frac{1}{2}\frac{\partial^2 C}{\partial r^2}+\sqrt{V_{max}}S\sigma_r\rho_{13}\frac{\partial^2 C}{\partial S\partial r}-rC$$
$$+\lambda_1^*\int\left(1-\lambda_{SJ}\left(Y\right)\right)\left(C\left(YS,\tau\right)-C\left(S,\tau\right)\right)G^*\left(Y\right)dY$$
$$+\lambda_2^*\int\left(1-\lambda_{VJ}\left(y\right)\right)\left(C\left(V_{max}+y,\tau\right)-C\left(V_{max},\tau\right)\right)g^*\left(y\right)dy=\frac{\partial C}{\partial\tau}. \tag{2.2.13}$$

At $r=r_{max}$ the PIDE is given as:

$$\left(r_{max}-q-\lambda_1^*\int\left(1-\lambda_{SJ}\left(Y\right)\right)\left(Y-1\right)G^*\left(Y\right)dY\right)S\frac{\partial C}{\partial S}+\left(\kappa\left(\theta-V\right)-\lambda_V V\right)\frac{\partial C}{\partial V}$$
$$+\left(\left(a\left(b\left(\tau\right)-r_{max}\right)\right)-\lambda_r r_{max}\right)\frac{\partial C}{\partial r}+VS^2\frac{1}{2}\frac{\partial^2 C}{\partial S^2}+\sigma_V^2V\frac{1}{2}\frac{\partial^2 C}{\partial V^2}+VS\sigma_V\rho_{12}\frac{\partial^2 C}{\partial S\partial V}-r_{max}C$$
$$+\lambda_1^*\int\left(1-\lambda_{SJ}\left(Y\right)\right)\left(C\left(YS,\tau\right)-C\left(S,\tau\right)\right)G^*\left(Y\right)dY$$
$$+\lambda_2^*\int\left(1-\lambda_{VJ}\left(y\right)\right)\left(C\left(V+y,\tau\right)-C\left(V,\tau\right)\right)g^*\left(y\right)dy=\frac{\partial C}{\partial\tau}, \tag{2.2.14}$$

and for $V=V_{max}$ and $r=r_{max}$ the PIDE is

$$\left(r_{max}-q-\lambda_1^*\int\left(1-\lambda_{SJ}\left(Y\right)\right)\left(Y-1\right)G^*\left(Y\right)dY\right)S\frac{\partial C}{\partial S}+\left(\kappa\left(\theta-V_{max}\right)-\lambda_V V_{max}\right)\frac{\partial C}{\partial V}$$
$$+\left(\left(a\left(b\left(\tau\right)-r_{max}\right)\right)-\lambda_r r_{max}\right)\frac{\partial C}{\partial r}-r_{max}C$$
$$+\lambda_1^*\int\left(1-\lambda_{SJ}\left(Y\right)\right)\left(C\left(YS,\tau\right)-C\left(S,\tau\right)\right)G^*\left(Y\right)dY$$
$$+\lambda_2^*\int\left(1-\lambda_{VJ}\left(y\right)\right)\left(C\left(V+y,\tau\right)-C\left(V,\tau\right)\right)g^*\left(y\right)dy=\frac{\partial C}{\partial\tau}. \tag{2.2.15}$$

Hence at the points $V=V_{max}$ and $r=r_{max}$, the option values are obtained by solving the above equations, whilst at the points $V=V_{min}$ and $r=r_{min}$ the option values are obtained through extrapolation. Using these boundary conditions together with the PIDE at the non-boundary points, the call option price is obtained.

Under the risk neutral measure $\mathbb{Q}$, the probability density functions for the jump components can be redefined, and the IPDE is written as:

$$\left(r-q-\lambda_1 k\right)S\frac{\partial C}{\partial S}+\left(\kappa\left(\theta-V\right)-\lambda_V V\right)\frac{\partial C}{\partial V}$$
$$+\left(\left(a\left(b\left(\tau\right)-r\right)\right)-\lambda_r\right)\frac{\partial C}{\partial r}+VS^2\frac{1}{2}\frac{\partial^2 C}{\partial S^2}+\sigma_V^2 V\frac{1}{2}\frac{\partial^2 C}{\partial V^2}+\sigma_r^2\frac{1}{2}\frac{\partial^2 C}{\partial r^2}+VS\sigma_V\rho_{12}\frac{\partial^2 C}{\partial S\partial V}$$
$$+\sqrt{V}S\sigma_r\rho_{13}\frac{\partial^2 C}{\partial S\partial r}+\sigma_r\sigma_V\sqrt{V}\rho_{23}\frac{\partial^2 C}{\partial V\partial r}-rC+\lambda_1\int\left(C\left(YS,\tau\right)-C\left(S,\tau\right)\right)G\left(Y\right)dY$$
$$+\lambda_2\int\left(C\left(V+y,\tau\right)-C\left(V,\tau\right)\right)g\left(y\right)dy=\frac{\partial C}{\partial\tau}. \tag{2.2.16}$$

where

$$\lambda_1 k=\lambda_1 E^{\mathbb{Q}}\left(Y-1\right)=\lambda_1\int\left(Y-1\right)G\left(Y\right)dY=\lambda_1^*\int\left(1-\lambda_{SJ}\left(Y\right)\right)\left(Y-1\right)G^*\left(Y\right)dY,$$

$G\left(Y\right)$ and $g\left(y\right)$ are the probability density function for the asset and volatility jumps respectively under the risk neutral measure $\mathbb{Q}$.

2.2.3. The partial-integro differential equation for a put option and boundary conditions. Let $P\left(\tau,S,V,r\right)$ be the American put option price. The model specifications for the put option is similar to the above specification, with only a few differences. At all computation stages where the option payoff is required, it is computed as

$$P(\tau, S, V, r) = K - S$$

At the free boundary point, the value matching condition takes the form:

$$P(\tau, d(\tau, V, r), V, r) = K - d(\tau, V, r).$$

The smooth pasting condition is

$$\lim_{S \to d(\tau,V,r)} \frac{\partial C}{\partial S} = -1, \quad \lim_{S \to d(\tau,V,r)} \frac{\partial C}{\partial V} = 0, \quad \lim_{S \to d(\tau,V,r)} \frac{\partial C}{\partial r} = 0. \tag{2.2.17}$$

In the section below, we discuss how the computational method (MoL) is implemented for numerically solving this problem, and also specify the differences in computing the call and put option values using this method.

2.3. Method of Lines (MoL)

MoL is an approximation of one or more partial differential equations with ordinary differential equations in just one of the independent variables, and this approach is discussed in detail by Meyer (2015). The MoL algorithm developed in this chapter is an extension of the algorithm for stochastic volatility and stochastic interest rate model proposed by Kang & Meyer (2014), to which jumps to asset returns and volatility are added.

The time dimension is discretised by replacing the partial derivative with respect to time with a backward Euler approximation for the first two time steps, and then the three level backward difference formula for the remainder of the time steps. The partial integro-differential equation is approximated using finite differences. All the derivatives with respect to volatility and interest rate are replaced with finite differences. Integral functions are approximated using Gaussian quadrature, namely, Gauss-Hermite quadrature and Gauss-Laguerre quadrature. The resulting equation is a second order ordinary differential equation, which must be solved at each time step, variance grid point, and interest-rate point.

Within each time step, the second order ordinary differential equation is solved using two-stage iterations. These iterations are done until the price converges to a desired level of accuracy, at which point computations proceed to the next time step. Hence, the MoL

approximation would be given by a boundary value problem, together with its boundary conditions. To solve this boundary value problem, it is first transformed into a system of two first-order equations. This system is then solved using the Riccati transformation, which consists of three steps, namely, the forward sweep, followed by the determination of the boundary values at the free boundary, and, finally, the reverse sweep of the appropriate equations. The resulting solution of the reverse sweep gives us the option delta, which is then used to obtain the option values.

2.3.1. Partial Derivatives Approximation. Let $V_m = m\Delta V$, $r_n = n\Delta r$ and $\tau_l = l\Delta\tau$ for $m = 0, 1, 2, \dots M$, and $n = 0, 1, 2, \dots N$ and where $\tau_L = T$. The call option price along the variance line V_m, the interest rate line r_n and the time line τ_l is given by:

$$C\left(\tau_l, S, V_m, r_n\right) = C^l_{m,n}\left(S\right).$$

The option delta at the grid point is given by:

$$V\left(\tau_l, S, V_m, r_n\right) = \frac{\partial C\left(\tau_l, S, V_m, r_n\right)}{\partial S} = V^l_{m,n}\left(S\right).$$

The partial derivative discretised with respect to time, $\frac{\partial C}{\partial \tau}$. For the first two time steps, the backward Euler approximation is used:

$$\frac{\partial C}{\partial \tau} = \frac{C^l_{m,n} - C^{l-1}_{m,n}}{\Delta\tau}. \tag{2.3.1}$$

For subsequent steps, a three-level backward difference formula is used:

$$\frac{\partial C}{\partial \tau} = \frac{3}{2}\frac{C^l_{m,n} - C^{l-1}_{m,n}}{\Delta\tau} + \frac{1}{2}\frac{C^{l-1}_{m,n} - C^{l-2}_{m,n}}{\Delta\tau}. \tag{2.3.2}$$

Using (2.3.1) and (2.3.2) together yields a stable numerical method for the solution of the PIDE (Meyer (2015)). The derivative terms are approximated with respect to V and r using finite differences.

$$\frac{\partial C}{\partial V} = \frac{C^l_{m+1,n} - C^l_{m-1,n}}{2\Delta V}, \quad \frac{\partial C}{\partial r} = \frac{C^l_{m,n+1} - C^l_{m,n-1}}{2\Delta r},$$

$$\frac{\partial^2 C}{\partial V^2} = \frac{C^l_{m+1,n} - 2C^l_{m,n} + C^l_{m-1,n}}{\left(\Delta V\right)^2}, \quad \frac{\partial^2 C}{\partial r^2} = \frac{C^l_{m,n+1} - 2C^l_{m,n} + C^l_{m,n-1}}{\left(\Delta r\right)^2},$$

$$\frac{\partial^2 C}{\partial S \partial V} = \frac{V^l_{m+1,n} - V^l_{m-1,n}}{2\Delta V}, \quad \frac{\partial^2 C}{\partial S \partial r} = \frac{V^l_{m,n+1} - V^l_{m,n-1}}{2\Delta r},$$

$$\frac{\partial^2 C}{\partial V \partial r} = \frac{C^l_{m+1,n+1} - C^l_{m+1,n-1} + C^l_{m-1,n+1} + C^l_{m-1,n-1}}{4\Delta V \Delta r}.$$

2.3.2. Integral Terms Approximation. Gaussian quadrature is used to approximate the integral terms. For an integral function

$$I = \int_a^b f(x)\, dx,$$

if $W(x)$ and an integer N are given, weights w_j and abscissas x_j can be found such that

$$\int_a^b W(x) f(x)\, dx \approx \sum_{j=0}^{N-1} w_j f(x_j)$$

is exact if $f(x)$ is a polynomial (William H. Press & Flannery (2002)).

The first integral term is

$$\int C(YS,\tau) - C(S,\tau) G^*(Y)\, dY = \int C(YS,\tau) G^*(Y)\, dY - \int C(S,\tau) G^*(Y)\, dY$$

$$= \int C(YS,\tau) G^*(Y)\, dY - C(S,\tau).$$

Following Merton (1976), Y is log-normally distributed and thus $G^*(Y)$ is given as

$$G^*(Y) = \frac{1}{Y\delta\sqrt{2\pi}} \exp\left\{ -\frac{\left[\ln Y - \left(\gamma - \frac{\delta^2}{2}\right)\right]^2}{2\delta^2} \right\}, \tag{2.3.3}$$

where γ is the mean and δ is the standard deviation. From equation (3.2.2), it follows that

$$k = \boldsymbol{E}^{\mathbb{Q}}(Y-1) = \boldsymbol{E}^{\mathbb{Q}}(Y) - \boldsymbol{E}^{\mathbb{Q}}(1) = \boldsymbol{E}^{\mathbb{Q}}(Y) - 1 = \exp\left(\left(\gamma - \frac{\delta^2}{2}\right) + \frac{1}{2}\delta^2\right) - 1 = \exp(\gamma) - 1.$$

The remaining integral is approximated using Gauss-Hermite quadrature where

$$W(x) = e^{-x^2} \quad -\infty < x < \infty.$$

Changing variables in this integral, let $X = \left[\ln Y - \left(\gamma - \frac{\delta^2}{2}\right)\right]$. It is transformed to

$$\int_{-\infty}^{\infty} C\left(YS, \tau\right) G^*\left(Y\right) dY = \frac{1}{\sqrt{\pi}} \int_{-\infty}^{\infty} e^{-X^2} C\left(\tau, S\exp\left(\left(\gamma - \frac{\delta^2}{2}\right) + \sqrt{2}\delta X\right), V, r\right) dX. \tag{2.3.4}$$

Using the Gauss-Hermite quadrature formula, equation (2.3.4) is discretised,

$$\frac{1}{\sqrt{\pi}} \int_{-\infty}^{\infty} e^{-X^2} C\left(\tau, S\exp\left(\left(\gamma - \frac{\delta^2}{2}\right) + \sqrt{2}\delta X\right), V, r\right) dX,$$

$$= \frac{1}{\sqrt{\pi}} \sum_{j=0}^{J} w_j C_{m,n}\left(S\exp\left(\left(\gamma - \frac{\delta^2}{2}\right) + \sqrt{2}\delta X_j\right)\right),$$

where w_j and X_j are the weights and the abscissas. To obtain the value of the option at the computed point, which might not necessarily lie on the grid, the cubic spline interpolation is used to interpolate between values which lie on the grid. Summing this product gives the value of the integral at the required point.

The second integral term is

$$\int \left(C\left(V + y, \tau\right) - C\left(V, \tau\right)\right) g^*\left(y\right) dy.$$

In their "Double Jump" illustrative model, Duffie et al. (2000) assumed that the volatility jump size is exponentially distributed. This ensures that the jumps are always positive. The same assumption of exponential distribution with parameter $\lambda > 0$ is made, regarding the size of the volatility jump. Thus,

$$y \sim \exp\left(\lambda\right),$$

where

$$g^*\left(y\right) = \lambda e^{-\lambda y}.$$

This integral term is approximated using the Gauss-Laguerre quadrature where

$$W\left(x\right) = x^{\alpha} e^{-x}, \quad 0 < x < \infty. \tag{2.3.5}$$

Changing variables in this integral, let

$$X = \lambda y \implies y = \frac{X}{\lambda} \implies dy = \frac{dX}{\lambda}.$$

Substituting back into the equation

$$\int_0^\infty \left(C\left(V+y,\tau\right) - C\left(V,\tau\right)\right) g^*\left(y\right) dy = \int_0^\infty C\left(V+y,\tau\right) g^*\left(y\right) dy - \int_0^\infty C\left(V,\tau\right) g^*\left(y\right) dy,$$

$$= \int_0^\infty C\left(V+\frac{X}{\lambda},\tau\right) \lambda e^{-X} \frac{dX}{\lambda} - C\left(V,\tau\right) = \int_0^\infty C\left(V+\frac{X}{\lambda},\tau\right) e^{-X} dX - C\left(V,\tau\right).$$

Using the Gauss-Laguerre quadrature formula

$$\int_0^\infty C\left(V+\frac{X}{\lambda},\tau\right) e^{-X} dX = \sum_{j=0}^{J} w_j C_{m,n}\left(V+\frac{X_j}{\lambda}\right),$$

where w_j and X_j are the weights and the abscissas. Similarly, as in the previous integral approximation, cubic spline interpolation is used to interpolate between values that lie on the grid to obtain option prices for an asset price, which does not lie on a grid point. Summing this product gives the value of the integral at the required point.

2.3.3. The Riccati Transformation. From equation (3.2.4), the PIDE becomes

$$\begin{aligned}
&\left(r-q-\lambda_1 k\right) S\frac{\partial C}{\partial S} + \left(\kappa\left(\theta - V\right) - \lambda_V V\right)\frac{\partial C}{\partial V} + \left(\left(a\left(b\left(\tau\right)-r\right)\right) - \lambda_r\right)\frac{\partial C}{\partial r} + VS^2\frac{1}{2}\frac{\partial^2 C}{\partial S^2} \\
&+ \sigma_V^2 V\frac{1}{2}\frac{\partial^2 C}{\partial V^2} + \sigma_r^2\frac{1}{2}\frac{\partial^2 C}{\partial r^2} + VS\sigma_V\rho_{12}\frac{\partial^2 C}{\partial S\partial V} + \sqrt{V}S\sigma_r\rho_{13}\frac{\partial^2 C}{\partial S\partial r} + \sigma_r\sigma_V\sqrt{V}\rho_{23}\frac{\partial^2 C}{\partial V\partial r} \\
&+ \lambda_1\int\left(C\left(YS,\tau\right) - C\left(S,\tau\right)\right) G^*\left(Y\right) dY + \lambda_2\int\left(C\left(V+y,\tau\right) - C\left(V,\tau\right)\right) g^*\left(y\right) dy - rC = \frac{\partial C}{\partial \tau}.
\end{aligned} \tag{2.3.6}$$

Substituting for the partial derivatives with respect to time, V and r, together with the mixed partial derivatives using the approximating equations above, an ODE is obtained. The option price For the first two time steps, this is given by:

$$
\begin{aligned}
&VS^2\frac{1}{2}\frac{d^2C^l_{m,n}}{dS^2}+\left(r-q-\lambda_1 k\right)S\frac{dC^l_{m,n}}{dS}-rC^l_{m,n}-\frac{C^l_{m,n}-C^{l-1}_{m,n}}{\Delta\tau}\\
&+\left(\kappa\left(\theta-V\right)-\lambda_V V\right)\frac{C^l_{m+1,n}-C^l_{m-1,n}}{2\Delta V}+a\left(b\left(\tau\right)-r\right)\frac{C^l_{m,n+1}-C^l_{m,n-1}}{2\Delta r}\\
&+\sigma_V^2 V\frac{1}{2}\frac{C^l_{m+1,n}-2C^l_{m,n}+C^l_{m-1,n}}{\left(\Delta V\right)^2}+\sigma_r^2\frac{1}{2}\frac{C^l_{m,n+1}-2C^l_{m,n}+C^l_{m,n-1}}{\left(\Delta r\right)^2}\\
&+VS\sigma_V\rho_{12}\frac{V^l_{m+1,n}-V^l_{m-1,n}}{2\Delta V}+\sqrt{V}S\sigma_r\rho_{13}\frac{V^l_{m,n+1}-V^l_{m,n-1}}{2\Delta r}\\
&+\sigma_r\sigma_V\sqrt{V}\rho_{23}\frac{C^l_{m+1,n+1}-C^l_{m+1,n-1}+C^l_{m-1,n+1}+C^l_{m-1,n-1}}{4\Delta V\Delta r}\\
&+\lambda_1\int\left(C\left(YS,\tau\right)-C\left(S,\tau\right)\right)G^*\left(Y\right)dY+\lambda_2\int\left(C\left(V+y,\tau\right)-C\left(V,\tau\right)\right)g^*\left(y\right)dy=0.
\end{aligned}
\tag{2.3.7}
$$

For subsequent time steps, this becomes:

$$
\begin{aligned}
&VS^2\frac{1}{2}\frac{d^2C^l_{m,n}}{dS^2}+\left(r-q-\lambda_1 k\right)S\frac{dC^l_{m,n}}{dS}-\frac{3}{2}\frac{C^l_{m,n}-C^{l-1}_{m,n}}{\Delta\tau}+\frac{1}{2}\frac{C^{l-1}_{m,n}-C^{l-2}_{m,n}}{\Delta\tau}-rC^l_{m,n}\\
&+\left(\kappa\left(\theta-V\right)-\lambda_V V\right)\frac{C^l_{m+1,n}-C^l_{m-1,n}}{2\Delta V}+a\left(b\left(\tau\right)-r\right)\frac{C^l_{m,n+1}-C^l_{m,n-1}}{2\Delta r}\\
&+\sigma_V^2 V\frac{1}{2}\frac{C^l_{m+1,n}-2C^l_{m,n}+C^l_{m-1,n}}{\left(\Delta V\right)^2}+\sigma_r^2\frac{1}{2}\frac{C^l_{m,n+1}-2C^l_{m,n}+C^l_{m,n-1}}{\left(\Delta r\right)^2}\\
&+VS\sigma_V\rho_{12}\frac{V^l_{m+1,n}-V^l_{m-1,n}}{2\Delta V}+\sqrt{V}S\sigma_r\rho_{13}\frac{V^l_{m,n+1}-V^l_{m,n-1}}{2\Delta r}\\
&+\sigma_r\sigma_V\sqrt{V}\rho_{23}\frac{C^l_{m+1,n+1}-C^l_{m+1,n-1}+C^l_{m-1,n+1}+C^l_{m-1,n-1}}{4\Delta V\Delta r}\\
&+\lambda_1\int\left(C\left(YS,\tau\right)-C\left(S,\tau\right)\right)G^*\left(Y\right)dY+\lambda_2\int\left(C\left(V+y,\tau\right)-C\left(V,\tau\right)\right)g^*\left(y\right)dy=0,
\end{aligned}
\tag{2.3.8}
$$

subject to the boundary conditions:

$$
C^l_{m,n}\left(0\right)=0,\ \ C^l_{m,n}\left(d^l_{m,n}\right)=d^l_{m,n}-K,\ \ \tfrac{dC^l_{m,n}}{dS}\left(d^l_{m,n}\right)=1.
$$

where the free boundary point, along the variance line V_m, the interest rate line r_n and the time line τ_l is given by:

$$
d\left(\tau_l,V_m,r_n\right)=d^l_{m,n}.
$$

For a put option, the boundary conditions are given as

$$P^l_{m,n}(0) = 0, \quad P^l_{m,n}\left(d^l_{m,n}\right) = K - d^l_{m,n}, \quad \frac{dP^l_{m,n}}{dS}\left(d^l_{m,n}\right) = -1.$$

The boundary conditions discussed in the previous section are imposed. The integrals are approximated using the Gaussian quadrature explained above. To solve equations (2.3.7) and (2.3.8), each equation is first transformed into two equations of first order.

$$\begin{aligned} \frac{dC^l_{m,n}}{dS} &= V^l_{m,n} \\ \frac{dV^l_{m,n}}{dS} &= A_{m,n}(S)\, C^l_{m,n} + B_{m,n}(S)\, V^l_{m,n} + P^l_{m,n}(S). \end{aligned} \tag{2.3.9}$$

This is done by grouping together all the $C^l_{m,n}$ terms, $V^l_{m,n}$ terms and the rest of the terms in $C^l_{m+1,n},\ C^l_{m-1,n}\ C^l_{m,n+1},\ C^l_{m,n-1}, V^l_{m+1,n},\ V^l_{m-1,n}\ V^l_{m,n+1},\ V^l_{m,n-1}$ and the integral terms make up the $P^l_{m,n}(S)$ term. This first order system of equations is then solved using a Riccati transformation,

$$C^l_{m,n}(S) = R_{m,n}(S)\, V^l_{m,n}(S) + W^l_{m,n}(S), \tag{2.3.10}$$

in which $R_{m,n}(S)$ and $W^l_{m,n}(S)$ are solutions of the initial value problems,

$$\frac{dR_{m,n}}{dS} = 1 - B_{m,n}(S)\, R_{m,n}(S) - A_{m,n}(S)\left(R_{m,n}(S)\right)^2, \quad R_{m,n}(0) = 0, \tag{2.3.11}$$

$$\frac{dW^l_{m,n}}{dS} = -A_{m,n}(S)\, R_{m,n}(S)\, W^l_{m,n} - R_{m,n}(S)\, P^l_{m,n}(S), \quad W^l_{m,n}(0) = 0. \tag{2.3.12}$$

The integration of equation (4.3.8) and equation (4.3.9) from 0 to S_{max} is called the forward sweep. In the case of a put option, the integration of (4.3.8) and equation (4.3.9) begins from S_{max} to 0. S_{max} is chosen large enough such that the free boundary point between 0 and S_{max} is obtained. Using each of the $R_{m,n}$ and the $W^l_{m,n}$ values obtained from the integration, the value of the free boundary $S^\bullet$ is between the two consecutive points, where the sign changes on computing values for the following equation:

$$S^\bullet - K - R_{m,n}(S^\bullet) - W^l_{m,n}(S^\bullet) = 0.$$

For a put option, this equation will be formulated as

$$K - S^{\bullet} - R_{m,n}\left(S^{\bullet}\right) - W^{l}_{m,n}\left(S^{\bullet}\right) = 0.$$

$d^{l}_{m,n}$ along the S-grid is defined as the free boundary at the grid point (V_m, r_n, τ_l). In obtaining this free boundary point and the values required for computing the option price at the free boundary, cubic spline interpolation is used as it is most likely that the free boundary point does not lie on the given grid points. The following equation is integrated for the option delta from $d^{l}_{m,n}$ to 0. This is known as the backward sweep. For a put option, the integration of this equation is from $d^{l}_{m,n}$ to S_{max}.

$$\frac{dV^{l}_{m,n}}{dS} = A_{m,n}\left(S\right)\left(R\left(S\right)V + W^{l}_{m,n}\left(S\right)\right) + B_{m,n}\left(S\right)V + P^{l}_{m,n}\left(S\right), \quad V^{l}_{m,n}\left(d^{l}_{m,n}\right) = 1. \tag{2.3.13}$$

At all stages of the calculation the boundary conditions discussed in the previous section are considered. Having obtained the values for $R_{m,n}$, $W^{l}_{m,n}$ and $V^{l}_{m,n}$, the option values from the Riccati transformation equation (4.3.7) are obtained.

Within each time step, each ordinary differential equation is solved using iterations. Chiarella et al. (2009) look at a similar problem, but with only one jump in the asset dynamics. They use a two stage iterative scheme. In the first stage, they treat the IDEs as ODEs by using $C^{l-1}_{m,n}$ as an initial approximation for $C^{l}_{m,n}$ in the integral term. The same procedure is followed, the only difference being that there are now two integrals and not one. However, it is the same set of option values that will be used in both integral terms. An initial guess is begun with. For each time period, in each iteration, equations for $m = 1, \ldots, M$ are solved, using the latest values available for $C^{l}_{m+1,n},\ C^{l}_{m-1,n}\ C^{l}_{m,n+1},\ C^{l}_{m,n-1}$ and $V^{l}_{m+1,n},\ V^{l}_{m-1,n}\ V^{l}_{m,n+1},\ V^{l}_{m,n-1}$, obtained by using the Riccati transformation. When the difference between the option values for the $(k-1)^{th}$ and the k^{th} iteration is less than 10^{-6}, the iterations are terminated.

In the second stage of iterations, the integral is updated with this new option value and the process is repeated until the price converges at this level, i.e. the difference between

the option value in the integral and new computed option value is less than 10^{-6}. The iterations are terminated and the computations are made at the next time step.

2.3.4. Complexity of computing using the MoL. One of the complexities in using the MoL is that not all parameter values chosen for the different models can lead to convergence. Hence for the purposes of analysis, we use parameter values that have been shown to converge from previous literature. The PIDE to be solved is given by:

$$\begin{aligned}&(r-q-\lambda_1 k)\,S\frac{\partial f}{\partial S}+\left(\kappa\left(\theta-V\right)-\lambda_V V\right)\frac{\partial f}{\partial V}+\left(\left(a\left(b\left(\tau\right)-r\right)\right)-\lambda_r\right)\frac{\partial f}{\partial r}+VS^2\frac{1}{2}\frac{\partial^2 f}{\partial S^2}\\&+\sigma_V^2 V\frac{1}{2}\frac{\partial^2 f}{\partial V^2}+\sigma_r^2\frac{1}{2}\frac{\partial^2 f}{\partial r^2}+VS\sigma_V\rho_{12}\frac{\partial^2 f}{\partial S\partial V}+\sqrt{V}S\sigma_r\rho_{13}\frac{\partial^2 f}{\partial S\partial r}+\sigma_r\sigma_V\sqrt{V}\rho_{23}\frac{\partial^2 f}{\partial V\partial r}\\&+\lambda_1\int\left(f\left(YS,\tau\right)-f\left(S,\tau\right)\right)G^*\left(Y\right)dY+\lambda_2\int\left(f\left(V+y,\tau\right)-f\left(V,\tau\right)\right)g^*\left(y\right)dy-rf=\frac{\partial f}{\partial\tau}.\end{aligned}\tag{2.3.14}$$

One of the difficulties arise when $rS\frac{\partial f}{\partial S}$ dominates the term $VS^2\frac{1}{2}\frac{\partial^2 f}{\partial S^2}$ as this results in a solution with oscillations that are not normal. This is solved by refining the mesh points used in this problem. In the computations, the term $VS^2\frac{1}{2}\frac{\partial^2 f}{\partial S^2}$ has been redefined as

$$\max\left(\epsilon, VS^2\frac{1}{2}\frac{\partial^2 f}{\partial S^2}\right),\qquad \epsilon<1$$

to avoid degeneracy at $S=0$. Another difficulty arises when the maximum value of the asset price is close to the strike value, as this can have a non-negligible impact on the option price. According to Meyer (2015), a maximum asset value that is at least three times the strike price is recommended. Lastly, with the inclusion of each jump, the rate at which the code runs is affected, resulting in more run time.

2.4. Numerical Results

In this section, a numerical study is conducted to assess the impact of jumps and the stochastic dynamics of interest rates and volatility on American option prices, and their free boundaries and Greeks. By using the model proposed in Section 3.2, the MoL is implemented to price an American call option with strike $K=100$ maturing in six months on an asset paying a dividend yield of 5%.

TABLE 2.4.1. Parameter values used to compute American call option prices. The Heston (1993) stochastic volatility model and a Hull-White stochastic interest rate model is used. Asset jumps are log-normally distributed, and volatility jumps are exponentially distributed.

Parameters	**Value**	**SV**	**Value**	**SI**	**Value**	**Jumps**	**Value**
T	0.5	θ	0.04	σ_r	0.1	λ_1	5
q	0.05	σ_V	0.4	a	0.3	λ_2	5
K	100	κ	2.0	λ_r	0.0	λ	200
		λ_V	0.0	ρ_{13}	0.5	γ	0.0
		ρ_{12}	-0.5	ρ_{23}	0.0	δ	0.1
				c_1	0.04		
				c_2	0.00		
				c_3	1.0		

To implement the MoL, S, V, r and τ are discretised, in line with the asset dynamics in equation (4.2.26). Along the S dimension, a non-uniform mesh is used to handle the lack of smoothness in this problem. There are 50 time steps (L) with the maturity time being $T = 0.5$. $S_{\min} = 0$ and $S_{\max} = 800$ with 50 grid points on $[0, 50]$, 50 grid points on $[50, 100]$, 200 grid points on $[100, 200]$ and 500 grid points on $[200, 800]$, thus totalling 800 grid points. There are 25 variance points with $V_{\min} = 0$ and $V_{\max} = 0.5$ or 50%, and 25 interest rates points with $r_{\min} = 0$ and $r_{\max} = 25\%$. By including jumps, assumptions that the asset price jumps follow a Poisson process and that the volatility jump size is exponentially distributed are made. To approximate the jump integrals, 50 abscissa points are used for the Hermite integration and 5 abscissa points for the Gauss-Laguerre integration. The α of equation (4.3.1) is assumed to be 0. The correlation between S and V, ρ_{12} = -0.5, and between V and r, ρ_{23}= 0.0. Fama (1981*b*), Li, Yang, Hsiao & Chang (2005), Giot (2005) and Fama (1981a) found a significant negative relationship between expected returns and volatility. Cheng, Nikitopoulos & Schlögl (2018) show empirically that, in their data (crude oil futures and USD Treasuries), the correlation between asset volatility and interest rates is almost zero. A similar assumption in this analysis is made. The correlation between S and r (ρ_{13}) can be positive/negative, and it is 0.5 for this analysis. Table 2.4.1 presents the parameter values used in the numerical study. Using these parameter values, option prices are computed using the MoL when there are both asset and volatility jumps. [5]

[5]The parameter values used have been taken from a paper by Chiarella et al. (2009) in which they price American call options with asset dynamics that have stochastic volatility and asset jumps.

TABLE 2.4.2. This table presents a comparison of put option prices for two different pricing methods at different interest rate and volatility levels when $S = 100$ using parameter values in Samimi et al. (2017). The American put option prices obtained using the MoL are stated in the 4^{th} column and Monte Carlo prices are in the 5^{th} and 6^{th} columns. LSM1 are prices obtained from Samimi et al. (2017), whilst LSM2 are the prices obtained using the python LSM algorithm by Hilpisch (2011), for 1 million paths and 100 time steps. The standard error given in the 7^{th} column is for the prices obtained using LSM2. The resulting upper and lower price bounds at 95% confidence interval for the LSM2 prices are given in the 8^{th} column and 9^{th} column.

T	**r**	**V**	**MoL**	**LSM1**	**LSM2**	**SE**	**LB**	**UB**
0.2	**0.04**	**0.09**	4.7061	4.689	4.7066	0.0037	4.6993	4.7139
0.2	**0.04**	**0.25**	7.9274	7.907	7.9193	0.0055	7.9085	7.9301
0.2	**0.09**	**0.09**	4.3516	4.337	4.3560	0.0038	4.3486	4.3634
0.2	**0.09**	**0.25**	7.5360	7.511	7.5344	0.0058	7.5230	7.5458
0.3	**0.04**	**0.09**	5.5270	5.490	5.5268	0.0043	5.5184	5.5352
0.3	**0.04**	**0.25**	9.2832	9.245	9.2769	0.0064	9.2644	9.2894

To test the correctness of the MoL implementation, American put prices computed by MoL are compared with prices obtained using the Monte Carlo technique commonly attributed to Longstaff & Schwartz (2001). Several papers provide prices for American put options using the Heston (1993) and Hull & White (1987) model, and which, in particular, use this similar method in their implementation. Some of these results are used for comparison purposes. Samimi et al. (2017) provides tables of values which will be used for comparison. In addition to this Python code by Hilpisch (2011)is run in order to obtain the option prices, including the standard errors. Table 2.4.2 presents the results for these two different pricing methods for put options.

As indicated in Table 2.4.2, the values for the American put option obtained using the MoL are within the Monte Carlo bounds at the 99% confidence interval. The run time for the MoL is more efficient especially when the computation of Greek letters is included, given that MoL computes that as part of the computations. Chiarella et al. (2009) have demonstrated the time efficiency of the MoL in comparison to component-wise splitting (CS) method and Crank-Nicholson with PSOR method, thus Monte Carlo is only used for comparison purposes.

A sensitivity analysis is conducted next to first examine the impact of stochastic volatility and stochastic interest rates on the shape of the free boundary surfaces in the presence of jumps. Thus, by using jump-diffusion models with jumps in both asset and volatility, an assessment on how the asset prices, stochastic volatility, and stochastic interest rates

affect the free boundaries is made. Since this model has non-constant values of volatility and interest rates, an investigation into the effects of changing maximum volatility and maximum interest rate used in the MoL algorithm for discretisation purposes is made, see equation (3.2.5).

2.4.1. Sensitivity analysis. The sensitivity of the free boundary is assessed in terms of asset prices, volatility levels, and interest rate levels. Figure 2.6.1 displays the impact of interest rates on the free boundary surfaces under two volatility scenarios; a low volatility at 4% and a high volatility environment at 30%. Figure 2.6.2 shows the impact of volatility on free boundary surfaces under two interest rates scenarios; a low interest rate at 4% and a high interest rate at 16%. Figure 2.6.3 summarises the impact of both volatility and interest rates on the free boundary of an American call option at its maturity date of six months.

As expected, the free boundary value for American call options holds a positive relation with both interest rates and volatility. As interest rates increase, early exercise for a call option is less likely (due to the consequent higher option prices)[6], which drives their free boundaries high. An increase in volatility is expected to increase the free boundary. An increase in volatility increases the time value of the option, thus as the option becomes more valuable, the free boundary value rises. These effects are more pronounced for longer maturity options and for relatively high levels of volatility and interest rates. For example, an American call option with maturity of 6 months, interest rate at 10% and a volatility of 24% implies a free boundary value of about 290, while for a volatility of 40%, the boundary value is around 307, see Figure 2.6.3. The shapes of the free boundary surfaces are similar to the ones produced by models without jumps, see Pantazopoulos, Zhang & Houstis (1996) who use front-tracking finite difference methods, Chiarella & Ziogas (2005) who use an iterative numerical integration scheme, Hirsa (2013) who uses the ADI method, and Kang & Meyer (2014) who also use the MoL for a model with stochastic volatility. The free boundary surfaces are smooth, an advantage of using the MoL. This is a feature that is not shared with other methods, for instance, the finite difference methods, which typically require a smoother (Ikonen & Toivanen (2009)) to be used.

[6]Early exercise for a call option occurs when asset value is above the free boundary. The free boundary of a call option increase as interests rates increase, since call options become "better" investments, providing substantially higher returns (compared to positions in the underlying asset), which increases their prices.

2.4.1.1. *Impact of volatility of volatility.* The volatility of financial products is likely to be stochastic. Heston (1993) found that volatility of volatility increases the kurtosis of spot returns. Using a stochastic volatility model, an investigation on the impact of volatility of volatility on the free boundary is made. Figure 2.6.6 displays the free boundaries for American call options in the presence of jumps in both asset and volatility dynamics for different volatility of volatility: 4%, 14%, and 40% when $r = 4\%$ and $V = 4\%$. An increase in the volatility of volatility tends to shift up the free boundary curve, an effect that is more pronounced further from expiry, see Figure 2.6.6. Thus, the volatility of volatility (or kurtosis of returns) has a positive effect on free boundary surfaces, making it less likely for the option to be exercised early.

2.4.1.2. *Impact of volatility of interest rate.* Next, an investigation on the effect of increasing the volatility of interest rate on the free boundary is made. Figure 2.6.7 displays the free boundaries for American call options in the presence of jumps in both the asset and volatility dynamics for different volatility of interest rates: 8%, 10%, and 12% when $r = 4\%$ and $V = 4\%$. As in the previous analysis, as the volatility of interest rates is increased, the free boundary values also increase, similarly making it less likely for the option holder to exercise the option early. Ho et al. (1984) illustrate that the value of an American option increases as the volatility of interest rates increase, a change that also depends on asset volatility. Further from expiry, the impact of the interest rate volatility is stronger than the impact of the volatility of volatility.

2.4.1.3. *Impact of r_{Max} and V_{Max}.* As part of the analysis, an investigation on how the choice of r_{Max} and V_{Max} used in the MoL impacts the free boundary values is made. Selection of this value will depend on several factors, including the prevailing market conditions, convergence of values depending on the pricing method being used, the purpose for which the pricing is being done, etc. For instance, a variance that is greater than 100% is a possibility in some markets, especially for small cap stocks or shares from troubled companies (www.macroption.com). Hirsa (2013) discussed the importance of V_{Max} on obtaining good estimates for approximate boundary conditions. Some markets experience negative interest rates; hence, this might also influence the selection of r_{Max} as it will not be as large as when markets experience positive interest rates.

Figure 2.6.8a plots the free boundary surfaces for three levels of r_{Max}; r_{Max} = 0.2, 0.25, and 0.3. In Figure 2.6.8a, as r_{Max} increases, there is a negligible increase in the value of the free boundaries for the same interest rate level. Thus, the selection of r_{Max} does not have a big impact on the resulting free boundary values. An investigation on how the choice of V_{Max} impacts free boundary values is performed. Figure 2.6.8b plots the free boundary surfaces for $V_{Max} = 0.5, 0.75, 1.0$.V_{Max} again has negligible impact on the free boundary values, see also Kang & Meyer (2014) for similar conclusions. Thus, the numerical application is robust with regards to the discretisation limits with inconsequential impact on free boundaries.

2.5. Impact of jumps

To assess the impact of jumps on American call prices, their free boundary surfaces and Greek values, three models are compared: Heston Hull White (HHW), the Heston Hull White with asset jumps (HHWJ) and the Heston Hull White with asset and volatility jumps (HHWJJ). To maintain consistent variance for the three models for comparison, some parameter values have been adjusted as explained next.

Using a spot variance of 4% (or standard deviation of 20%), for the HHWJJ model, the global variance for $\ln S$ is computed by finding the first and second moment of the characteristic function of the model with both jumps and the formula for finding variance being:

$$S^2 = E\left[X^2\right] - E\left[X\right]^2$$

The characteristic function for a 3-D model with no jumps is given by Grzelak et al. (2012), in which asset jump (Kangro et al. (2003)) and volatility jumps (Lutz (2010)) are included. The first and second moments are the first and second derivatives of this characteristic function. For this analysis, the correlation between S and r ρ_{12} is 0.0, the correlation between V and r ρ_{23} is 0.0, and the correlation between S and V ρ_{12} is ± 0.5. There is evidence that the sign of this correlation affects the free boundary differently, see Chiarella et al. (2009). Using these parameter values, the value of the global variance is 24.3% when $\rho_{12} = -0.5$ and 22.1% when $\rho_{12} = 0.5$. This global variance is used as the standard value for the remaining two models (HHWJ and HHW) in which some of the model parameters are changed such that the same global variance is obtained. The difference in

the formulation rises from the fact that, for the case with only asset jumps, λ_2 is 0, and when there are no jumps, both λ_1 and λ_2 are zero. In determining these parameter values, which match global variance, an assumption that the spot variance V is equal to the long run mean of V, which is given by θ_V is made, see Chiarella et al. (2009). The interest rate is then adjusted, rounding it off to the nearest percentage, so that, overall, the condition is met. In Table 2.5.1, the new parameters for each model are listed, which ensure that this global variance is the same across all models.

TABLE 2.5.1. Parameter values for the models with no jumps and asset jumps, which ensure that the global variance for these models is similar to that of the model with asset and volatility jumps when ρ_{12} is negative (-0.5) and positive (0.5). ρ_{13} and ρ_{23} is 0 in this analysis. $\theta_V = 0.04$, $V = 0.04$, $r = 0.04$ have been selected to be 0.04, 0.04 and 0.04 respectively when there are asset and volatility jumps, giving us a global variance (S^2) of 24.3% (negative correlation) and 22.1% (positive correlation). The rest of the parameters in Table 2.4.1 remain the same.

	$\rho_{12} = -0.5$		$\rho_{12} = 0.5$	
Model Parameter	**No Jumps**	**Asset Jumps**	**No Jumps**	**Asset Jump**
V	0.08	0.06	0.08	0.06
θ_V	0.08	0.06	0.08	0.06
r	0.04	0.02	0.05	0.03
λ_1	0.0	0.5	0.0	0.5
λ_2	0.0	0.0	0.0	0.0

2.5.1. Free boundary surfaces. The impact of asset and volatility jumps on the free boundary is assessed by considering the three models; namely, HHW, HHWJ and HHWJJ. Using the values in Table 2.4.1 and Table 2.5.1, the free boundary values for the three models are plotted, see Figure 2.6.4 for the negative asset volatility correlation case and Figure 2.6.5 for the positive asset volatility correlation case. The red line represents the free boundary curve for the HHWJJ model. The black line represents the free boundary curve for the HHWJ model, whilst the blue line is the free boundary curve for the HHW model. The free boundary values for the model with no jumps is lower than the free boundary values for the models with jumps towards the options expiration. However, as the time to maturity increases, the relation reverses and the free boundaries for the model with no jumps becomes higher than the free boundary for models with jumps. The inclusion of asset jumps and asset-volatility jumps (in comparison to the no jumps case) has a significant impact on free boundaries, especially away from expiry, as it lowers the free boundaries. Thus, in the presence of jumps, the investor is more likely to exercise the option early rather than closer to maturity. This is attributed to the fact that towards expiry,

asset and volatility jumps have a direct effect on the option value. When there is sufficient time left to maturity, jumps in asset prices can be balanced out by upcoming offsetting jumps or by long-term mean reverting diffusion.

Further from expiry, adding asset jumps to the HHW model leads to lowering the free boundary. Yet, when volatility jumps are further added to the asset jumps, the free boundary curve elevates, making it less likely for the option holder to exercise the option. Indeed, the HHWJJ model consistently shifts up the free boundary curve, and their difference widens as time-to-maturity increases. In financial terms, this implies that the impact of volatility jumps on the call options prices, when these are added to the asset jumps, is incremental. Note that the global variance between the different model specifications has been held constant. By holding the global variance constant, the variation is entirely allocated in the asset price dynamics in the models with asset jumps only, while the same variance is distributed in both the asset and volatility dynamics for models with asset and volatility jumps.

The behaviour of the models is similar for positive and negative correlation. The only difference is in the magnitude of the variation between the model with no jumps and the models with jumps, with positive correlation having greater impact on the free boundary surfaces. Similar results were obtained by Chiarella et al. (2009) when contrasting the stochastic volatility model and the stochastic volatility model with jumps for negative and positive correlation.[7] When the correlation is positive, there is a small window period near to expiry in which the model without jumps results in a lower free boundary than the model with asset-volatility jumps.

2.5.2. American option price. Next, an investigation on the impact of jumps on the American call option price is made, under the assumption of the same global variance across all the three models. Figure 2.6.9 shows the differences in the option prices between the three models. The parameter values similar as those used in Figure 2.6.4 have been used, where an assumption that the correlation between S and V is -0.5 is made. Negative (positive) differences in the graphs imply that the option price for that particular model

[7]Yet, these results depend on the quantitative relation between the interest rate and dividend yield in addition to the sign of the mean asset price jump size, see Chiarella & Ziogas (2009) and Chapter 3 of this thesis.

(asset jumps or asset-volatility jumps) is greater (lower) than the option price for the HHW model.

Figure 2.6.9 describes the behaviour of the options in terms of moneyness, as jumps are included in the model. When the call option is out-the-money (OTM) or at-the-money (ATM), the option prices for the models with asset jumps and asset volatility jumps are greater than the option price for the no jumps model. Furthermore, the American call price with asset jumps is consistently higher than the American call price with asset-volatility jumps. However, for in-the-money (ITM) call options this relationship reverses and call prices with asset-volatility jumps are worth more than the options with asset jumps. In addition, for ITM options, the prices for models with jumps are worth less than the prices from no jumps models. Like the findings in Section 2.5.1, when holding global variance constant, options prices are more sensitive to asset jumps compared to the impact of adding volatility jumps to asset jumps. This may be because, under constant global variance between models, the variation is distributed between asset and volatility (instead of asset dynamics only). There is also possible offsetting in the overall variation in the presence of both asset and volatility jumps. Chiarella et al. (2009) made similar observations when comparing stochastic volatility models with jumps and no jumps. Hence the inclusion of asset jumps and asset-volatility jumps in the model is important when pricing options, as it can lead to the over- or under-estimating of values.

Figure 2.6.10 depicts the impact of volatility of volatility on the American call option price by considering the price differences for the models with no jumps, asset jumps, and asset-volatility jumps for $\rho_{12} = -0.5$. As the volatility of volatility decreases from 0.4 to 0.1, the option prices for the models with jumps approach the option prices for the no-jumps model.

2.5.3. Greeks. Another advantage of using the MoL is the fact that Greeks (Delta and Gamma) are computed at the same time as the option values. This helps in terms of time efficiency, in contrast to other methods, which require a separate computation of Greeks. In Figure 2.6.11, a comparison of the American call option delta value differences is made for the different models as jumps are included in the model without jumps when $\rho_{12} = -0.5$. The black line represents the model with asset jumps only, and the red line represents the model with asset and volatility jumps. Negative (positive) differences in the

graphs imply that the delta for that model (asset jumps or asset and volatility jumps) is greater (lower) than the delta for the pure diffusion model. From Figure 2.6.11, including asset jumps increases the delta for OTM options and decreases the delta for ATM and ITM options. For a model with asset-volatility jumps, the delta slightly decreases, although it is still greater than the delta for the no jumps model. When the call option is ITM, the delta for the model with asset jumps is less than the delta for the no-jumps model. Hence, inclusion of asset jumps and inclusion of asset-volatility jumps has a significant impact on the delta of an option, although the impact is slightly less when volatility jumps are added.

2.6. Conclusion

In this chapter, the problem of pricing American call options under jump diffusion versions of the Heston (1993) stochastic volatility model with Hull & White (1987) stochastic interest rate is considered. Asset jumps follow a log-normal distribution and volatility jumps follow an exponential distribution. Using the MoL, free boundaries, option prices, and Greeks are obtained. The MoL has been shown to be accurate and efficient. The correctness of MoL implementation has been confirmed through comparison with the Monte Carlo simulation (for demonstration purposes). A sensitivity analysis is performed to gauge the impact of volatility and interest rate parameters on the free boundaries. A further assessment on the impact of jumps on the option prices, the free boundaries, and Greeks is made.

The key findings of the numerical investigations include: The inclusion of asset-volatility jumps has a significant impact on free boundaries, especially far from expiry. Far from expiry, adding asset jumps to the HHW model leads to lowering the free boundary. Yet, when volatility jumps are further added to the asset jumps, the free boundary curve elevates, thus making it less likely for the option to be exercised. The inclusion of an asset-volatility jumps model was found to consistently shift up the free boundary curve, and the difference widens as time-to-maturity increases. The impact of jumps on option prices depends on the moneyness of the option. Option prices for models with both asset and asset volatility jumps are greater than the option price for the no jumps model when the call option is OTM or ATM. The American call prices with asset jumps are consistently higher than the American call price with asset-volatility jumps, a relationship that reverses when call

options are ITM. Further, asset jumps increase the delta for OTM options and reduces the delta for ATM and ITM options. On including the volatility jump, the delta slightly decreases, although it is still greater than the delta for the no jumps model. Lastly, the volatility of volatility and volatility of interest rates have a positive effect on free boundary surfaces, whilst rMax and VMax do not have any significant impact on free boundaries.

Possible directions for further research can be models that allow for jumps in interest rate dynamics, given that interest rates may experience sudden fluctuations from time to time. In addition, extensions with more industry relevance can be considered, including applications to financial products such as pension schemes, which is the topic of Chapter 4.

Figures

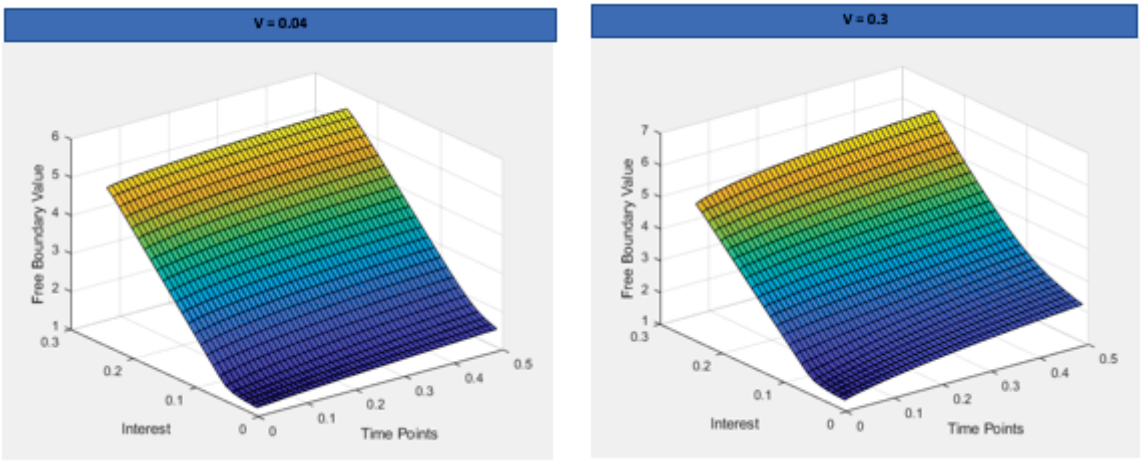

FIGURE 2.6.1. Free boundary surfaces for a six-month American call option obtained using the MoL for a range of interest rates. The left panel considers a low volatility of 4% and the centre panel a high volatility of 30%. The right panel plots the difference between these two sets of free boundary values. The parameter values used are given in Table 2.4.1.

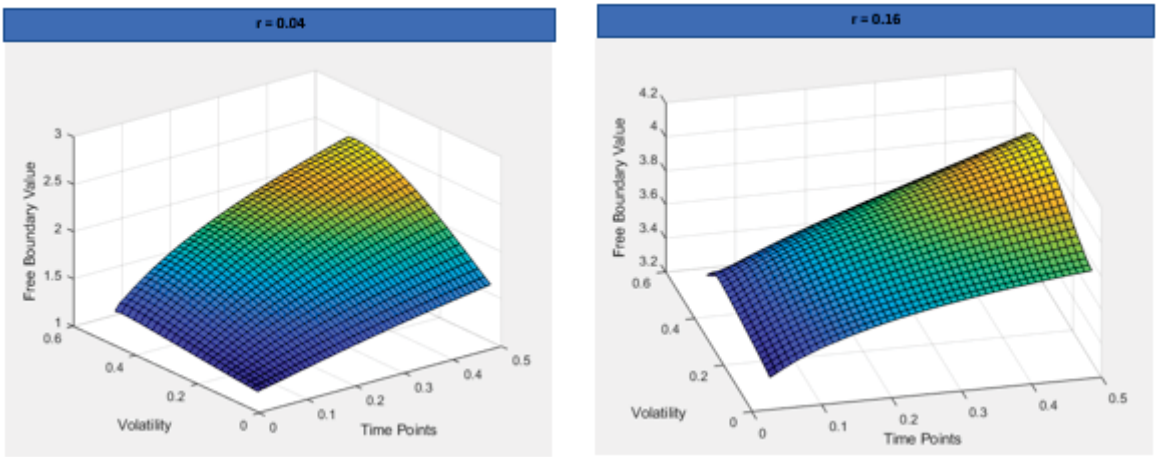

FIGURE 2.6.2. Free boundary surfaces for a six-month American call option obtained using the MoL for a range of volatilities. The left panel considers a low interest rate of 4% and the centre panel a high interest rate of 16%. The right panel plots the difference between these two sets of free boundary values. The parameter values used are given in Table 2.4.1.

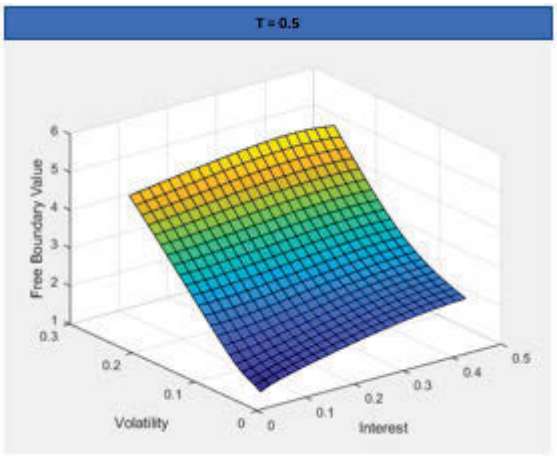

FIGURE 2.6.3. Free boundary surfaces for a six-month American call option for T = 0.5 as interest rates and volatility varies, obtained using the MoL. The parameter values used are given in Table 2.4.1.

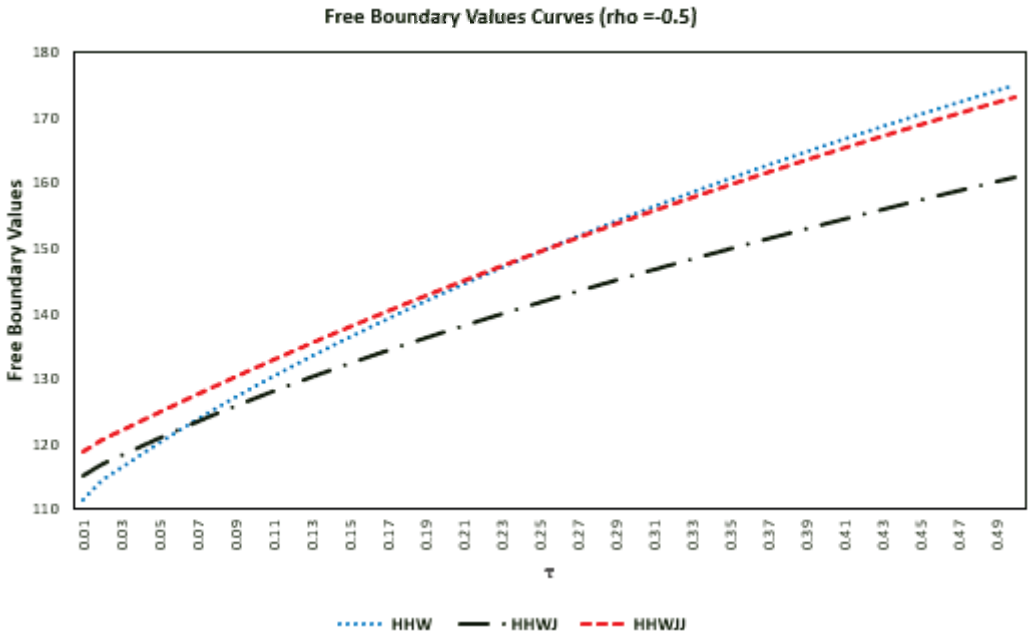

FIGURE 2.6.4. Free boundary surfaces for American call options when $\rho_{12} = -0.5$ under three model specifications: HHW, HHWJ and HHWJJ. The global variance for the three models is 24.3%. The parameter values which ensure the same global variance across all models are given in Table 2.5.1, whilst the rest of the parameter values are in Table 2.4.1.

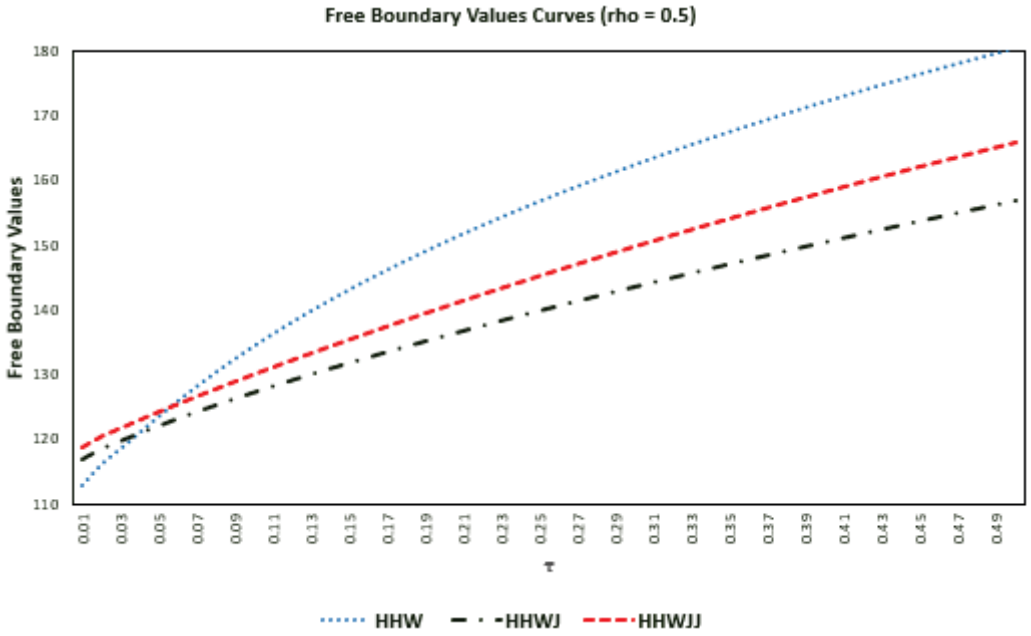

FIGURE 2.6.5. Free boundary surfaces for American call options when $\rho_{12} = 0.5$ under three model specifications: HHW, HHWJ and HHWJJ. The global variance for the three models is 22.25%. The parameter values, which ensure the same global variance across all models are given in Table 2.5.1, whilst the rest of the parameter values are in Table 2.4.1.

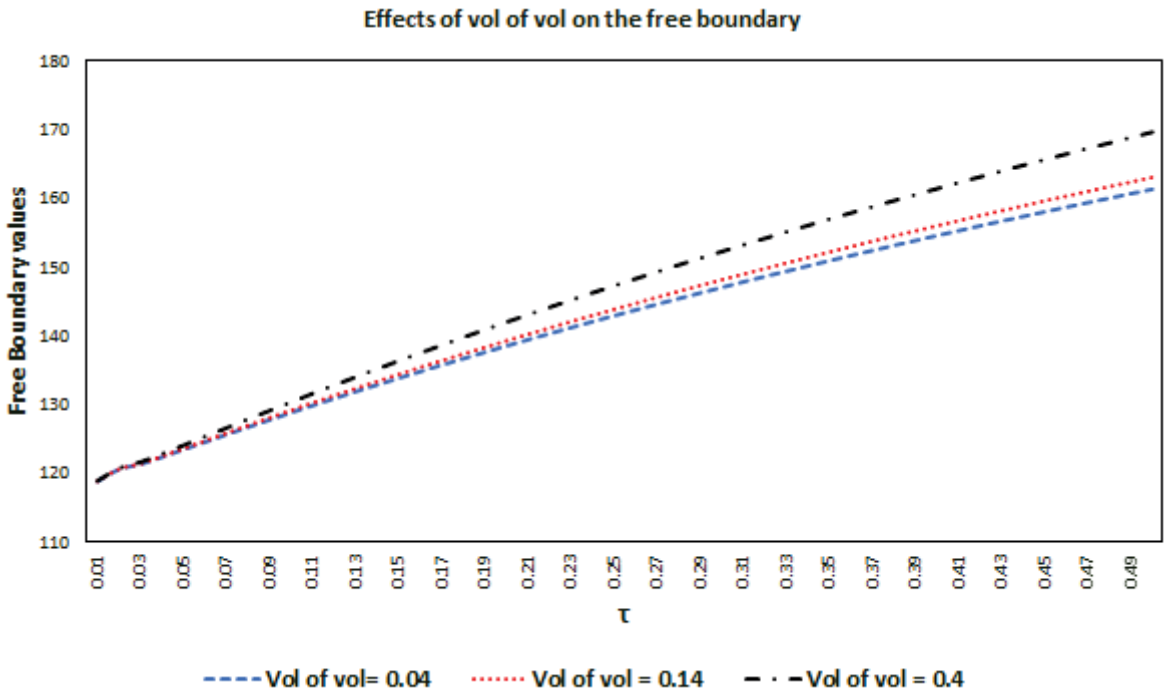

FIGURE 2.6.6. Free boundary surfaces of American call options for different levels of volatility of volatility in the presence of asset volatility jumps when $r = 0.04$ and $V = 0.04$. The parameter values are given in Table 2.4.1.

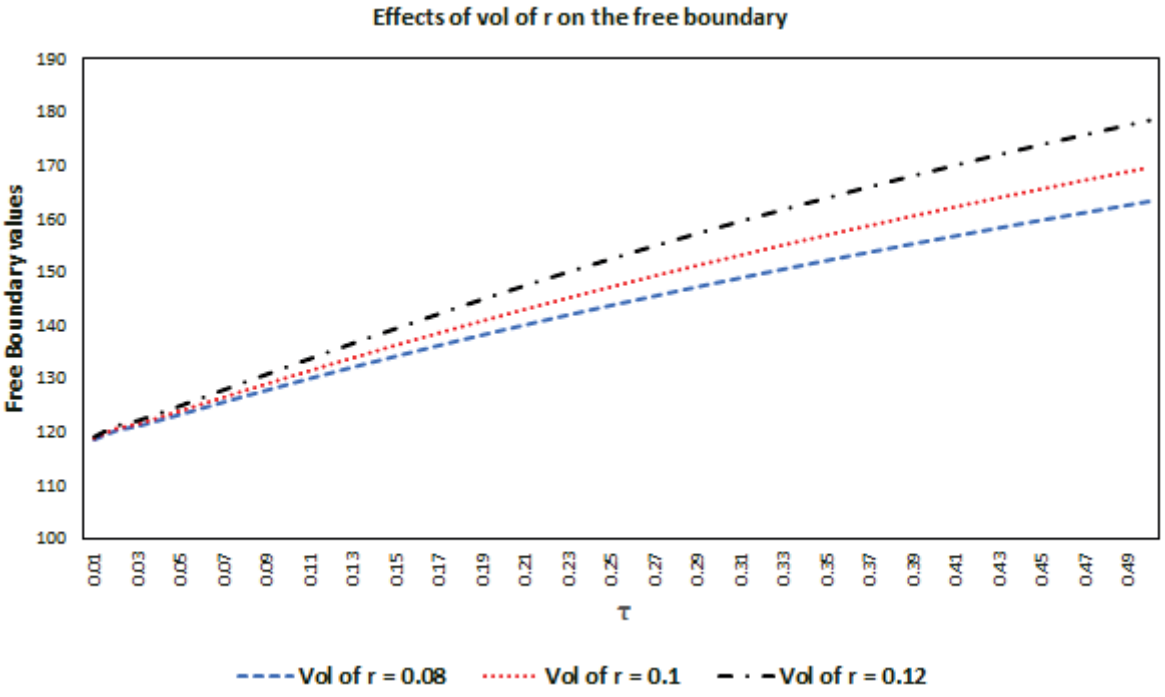

FIGURE 2.6.7. Free boundary surfaces of American call options for different levels of volatility of interest rates in the presence of asset volatility jumps when $r = 0.04$ and $V = 0.04$. The parameter values are given in Table 2.4.1.

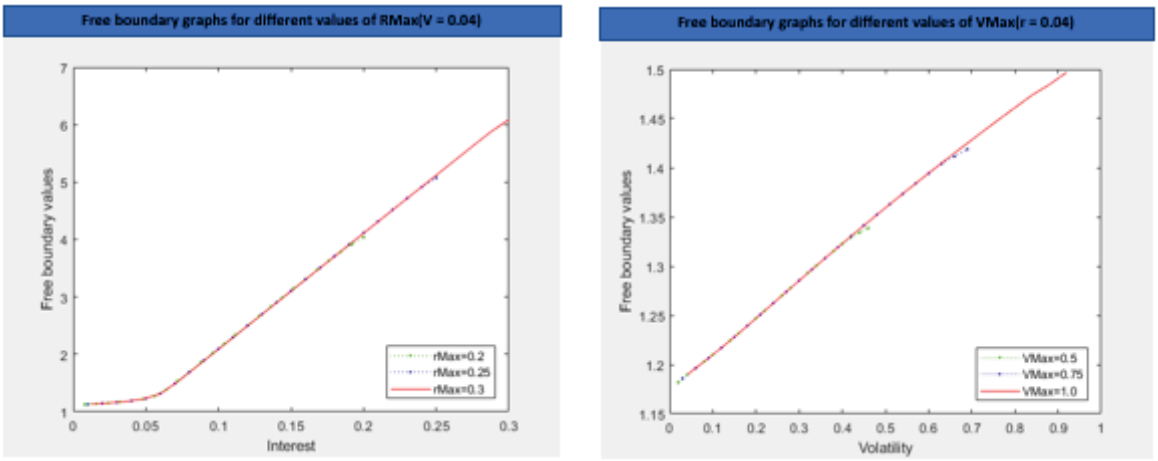

FIGURE 2.6.8. The impact of r_{Max} on the free boundary surfaces of an American call option in the presence of asset volatility jumps when $V = 0.04$ at maturity. The parameter values are given in Table 2.4.1.

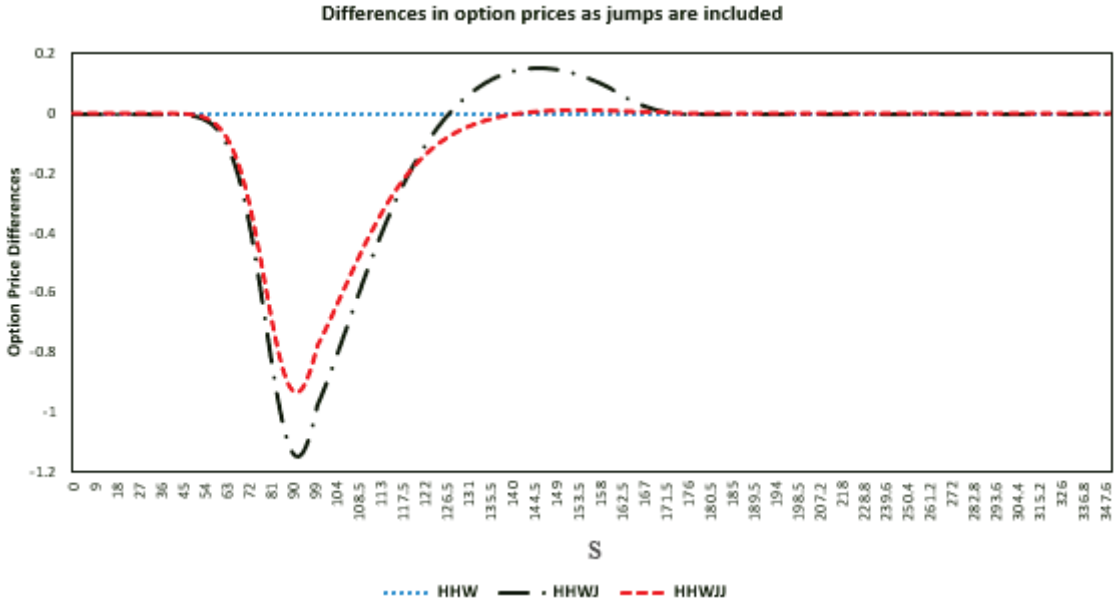

FIGURE 2.6.9. Comparison of American call option price differences for the HHW, HHWJ, and HHWJJ model (for $\rho_{12} = -0.5$). The global variance is 24.3%. The new parameter values, which ensure a similar global variance across all models, are given in Table 2.5.1, whilst the rest of the parameter values are in Table 2.4.1.

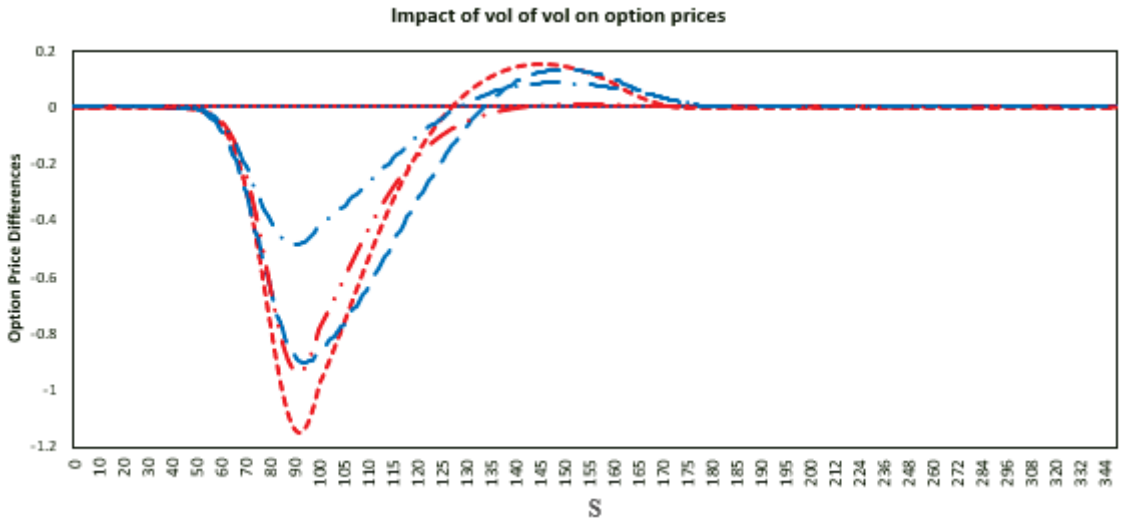

FIGURE 2.6.10. The impact of volatility of volatility on American call option price by considering the price differences for the HHW, HHWJ, and HHWJJ model (for $\rho_{12} = -0.5$). The global variance is 22.1%. The new parameter values, which ensure a similar global variance across all models are given in Table 2.5.1, whilst the rest of the parameter values are in Table 2.4.1.

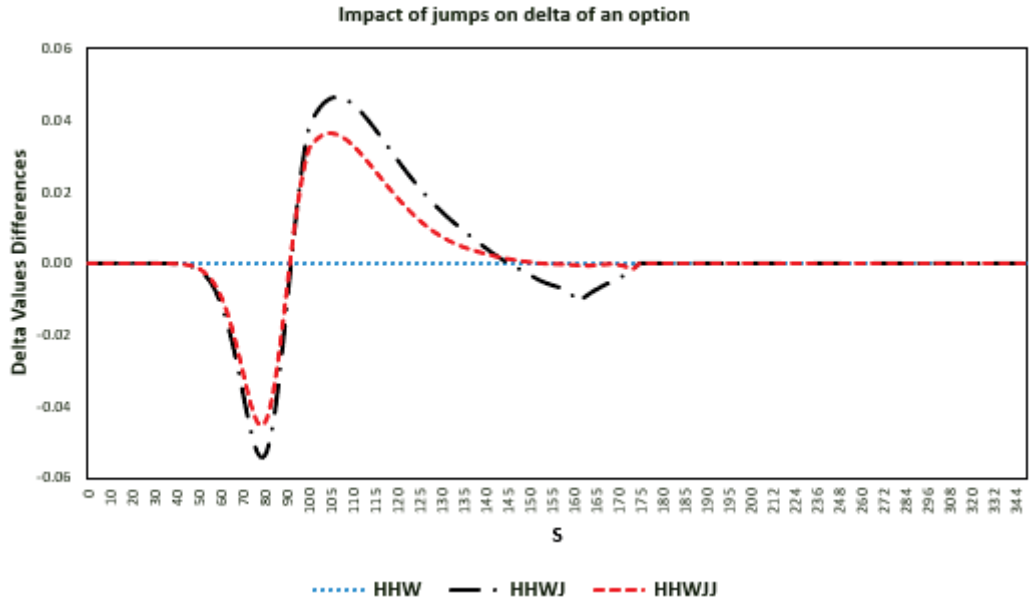

FIGURE 2.6.11. Comparison of American call option delta value differences for the HHW, HHWJ AND HHWJJ model (for $\rho_{12} = -0.5$). The global variance is 24.3%. The new parameter values, which ensure a similar global variance across all models are given in Table 2.5.1, whilst the rest of the parameter values are in Table 2.4.1.

Appendix 2.1 : Cholesky decomposition

Let the vector $(W_1, W_2, W_3)^T$ be a system of uncorrelated Wiener processes. The set of equations to be transformed are:

$$\begin{pmatrix} dZ_1 \\ dZ_2 \\ dZ_3 \end{pmatrix} = \begin{pmatrix} a_{11} & a_{12} & a_{13} \\ a_{21} & a_{22} & a_{23} \\ a_{31} & a_{32} & a_{33} \end{pmatrix} \begin{pmatrix} dW_1 \\ dW_2 \\ dW_3 \end{pmatrix}$$

where $(a_{ij})_{3\times 3}$ are chosen so as to preserve the correlation structure of the $Z_i(t)$ as given by the equations:

(1) $E(dZ_i) = 0$ for $i = 1, 2, 3$

(2) $E(dZ_i)^2 = dt$ for $i = 1, 2, 3$

(3) $E(dZ_1 dZ_2) = \rho_{12},\ E(dZ_1 dZ_3) = \rho_{13},\ E(dZ_2 dZ_3) = \rho_{23}$

From 1., since W_1, W_2, W_3 are Wiener processes, the condition:

$$E\left(dZ_i\right) = 0 \text{ for } i = 1, 2, 3$$

is satisfied for any choice of a_{ij}.

From 2., the condition $E\left(dZ_i\right)^2 = dt$ imposes three conditions:

$$\sum_{j=1}^{3} a_{ij}^2 = 1 \text{ for } i = 1, 2, 3$$

$$\begin{aligned} i = 1 &\longrightarrow a_{11}^2 + a_{12}^2 + a_{13}^2 = 1 \\ i = 2 &\longrightarrow a_{21}^2 + a_{22}^2 + a_{23}^2 = 1 \\ i = 3 &\longrightarrow a_{31}^2 + a_{32}^2 + a_{33}^2 = 1 \end{aligned} \tag{2.6.1}$$

From 3., the condition $E\left(dZ_1 dZ_2\right) = \rho_{12},\ E\left(dZ_1 dZ_3\right) = \rho_{13},\ E\left(dZ_2 dZ_3\right) = \rho_{23}$ imposes three conditions:

$$\sum_{k=1}^{3} a_{ik} a_{jk} = \rho_{ij} \text{ for } i = 1, 2, 3$$

$$\begin{aligned} i = 1 &\longrightarrow a_{11}a_{21} + a_{12}a_{22} + a_{13}a_{23} = \rho_{12} \\ i = 2 &\longrightarrow a_{11}a_{31} + a_{12}a_{32} + a_{13}a_{33} = \rho_{13} \\ i = 3 &\longrightarrow a_{21}a_{31} + a_{22}a_{32} + a_{23}a_{33} = \rho_{23} \end{aligned} \tag{2.6.2}$$

Since we have 6 conditions and 9 uknown coefficients, we let the remaining 3 conditions be equal to zero:

$$a_{12} = a_{13} = a_{23} = 0$$

The resulting system of equations is as follows:

$$
\begin{aligned}
a_{11}^2 &= 1 \\
a_{21} &= \rho_{12} \\
a_{22} &= \sqrt{1-\rho_{12}^2} \\
a_{12} &= 0 \\
a_{31} &= \rho_{13} \\
a_{32} &= \frac{\rho_{32}-\rho_{12}\rho_{13}}{\sqrt{1-\rho_{12}^2}} \\
a_{33} &= \left(\frac{1-\rho_{12}^2-\rho_{13}^2-\rho_{23}^2+2\rho_{12}\rho_{13}\rho_{23}}{1-\rho_{12}^2}\right)^{\frac{1}{2}}
\end{aligned}
\tag{2.6.3}
$$

If we substitute for a_{ij} in the matrix equation above, we have:

$$
\begin{pmatrix} dZ_1 \\ dZ_2 \\ dZ_3 \end{pmatrix} = \begin{pmatrix} 1 & 0 & 0 \\ \rho_{12} & (1-\rho_{12}^2)^{\frac{1}{2}} & 0 \\ \rho_{13} & \frac{\rho_{32}-\rho_{12}\rho_{13}}{\sqrt{1-\rho_{12}^2}} & \left(\frac{1-\rho_{12}^2-\rho_{13}^2-\rho_{23}^2+2\rho_{12}\rho_{13}\rho_{23}}{1-\rho_{12}^2}\right)^{\frac{1}{2}} \end{pmatrix} \begin{pmatrix} dW_1 \\ dW_2 \\ dW_3 \end{pmatrix}
$$

After the transformation we have the following set of equations:

$$
\begin{aligned}
dS &= (r-q-\lambda_1 k)\,Sdt + \sigma_{_L}\sqrt{V}SdW_1 + (Y-1)\,SdN_1 \\
dV &= \kappa(\theta-V)\,dt + \sigma_V\sqrt{V}\left(\rho_{12}dW_1 + \left(1-\rho_{12}^2\right)^{\frac{1}{2}}dW_2\right) + ydN_2 \\
dr &= a(b(t)-r)\,dt + \sigma_r\left(\rho_{13}dW_1 + \frac{\rho_{32}-\rho_{12}\rho_{13}}{\sqrt{1-\rho_{12}^2}}dW_2 + \left(\frac{1-\rho_{12}^2-\rho_{13}^2-\rho_{23}^2+2\rho_{12}\rho_{13}\rho_{23}}{1-\rho_{12}^2}\right)^{\frac{1}{2}}dW_3\right)
\end{aligned}
\tag{2.6.4}
$$

On expanding:

$$
\begin{aligned}
dS &= (r-q-\lambda_1 k)\,Sdt + \sigma_{_L}\sqrt{V}SdW_1 + (Y-1)\,SdN_1 \\
dV &= \kappa(\theta-V)\,dt + \sigma_V\sqrt{V}\rho_{12}dW_1 + \sigma_V\sqrt{V}\left(1-\rho_{12}^2\right)^{\frac{1}{2}}dW_2 + ydN_2 \\
dr &= a(b(t)-r)\,dt + \sigma_r\rho_{13}dW_1 + \sigma_r\frac{\rho_{32}-\rho_{12}\rho_{13}}{\sqrt{1-\rho_{12}^2}}dW_2 + \sigma_r\left(\frac{1-\rho_{12}^2-\rho_{13}^2-\rho_{23}^2+2\rho_{12}\rho_{13}\rho_{23}}{1-\rho_{12}^2}\right)^{\frac{1}{2}}dW_3
\end{aligned}
\tag{2.6.5}
$$

Appendix 2.2 : Code - Implementation of the MoL for the HHWJJ model

```
    MODULE modpar
       implicit none
       save

      integer :: n,n1,m,m1,nt,rN,r1
      Integer :: nn1,nn2,nn3,nn4,HM, alf, HM2
      Integer :: itime, itcoun

      Double precision,allocatable :: ry(:,:,:),w(:),un(:,:,:),&
uoo(:,:,:),uo(:,:,:),vn(:,:,:),option_price(:,:,:)
      Double precision,allocatable :: sny(:,:),time(:),sny2(:,:,:)
      Double precision,allocatable :: yy(:)
      Double precision,allocatable :: pd(:,:,:),aint1(:,:,:),aint2(:),&
aint3(:,:,:),aint3F(:,:,:)
      Double precision,allocatable :: ph(:)
      Double precision,allocatable :: ac(:,:,:),bc(:,:,:),cc(:,:,:),&
dc(:,:,:),f(:),g(:), g_gamma(:,:,:)
      Double precision,allocatable :: op(:), uui(:,:,:)
      Double precision :: t,dtau,rate,q,sigma,cap,thet,rho, &
sigmar,rhoSR,rhoVR,capr, cOne, cTwo, cThree, thetr
      Double precision :: om,dif,dif1,yf,zmax,dz,dz2,dr2
      Double precision :: alam,ak1,gam,del,aa,bb,sqpi,ufb,vfb, alamG, &
alamGExpo, aaG
      Double precision :: y0,y1,y2,y3,ymax,tol,tn
      Double precision :: pi,rMax,dr,rMin
    END MODULE

PROGRAM  JUMPSTOCHVOL
    USE modpar
```

```
    IMPLICIT NONE

      DOUBLE PRECISION, ALLOCATABLE :: Roots(:), Weights(:), &
RootsG(:), WeightsG(:)
      DOUBLE PRECISION :: start_time, end_time
      Double Precision, allocatable :: Spot_p(:), O_p(:,:)
      Double Precision, allocatable :: op_delta(:), op_gamma(:)
      Double precision :: dz_t
      Double Precision :: spot_t,strike_t,zmax_t
      Double precision :: dt,dif7
      double precision :: y,z,u,rate_disc
      double precision :: u0,v0,b_exp,find_b_start,told
      INTEGER :: icount,itcoun_i,case
      double precision ::coy,cony,beta,delta,eps
      double precision :: rin,dif_i,w1j,vin
      double precision :: stime, etime,spot,ex,p1,p2,strike
      Integer :: mj,j,i,k,l,kfb,iprice,rr
      CALL cpu_time(start_time)

      rate = 2.9999999E-02
      q = 6.0000001E-02
      cap = 1.5
      thet = 0.02
      sigma  =0.15
      rho = -0.5
      alam = 5.0000000
      gam = 0.0000000
      del = 0.1000000
      y0 = 0.00000500
      y1 = 0.500000
      y2 = 1.000000
      y3 = 2.000000
```

```
ymax = 8.00000
nn1 = 50
nn2 = 50
nn3  =200
nn4  =500
zmax  =1.5
m = 25
tol = 1.0000000E-06
tn = 0.5
nt = 50
HM = 50
alf = 0
alamG =5.0
HM2 = 5
alamGExpo = 250
rN  =25
rMax = 0.25
rMin = 0.0
sigmar = 0.10000000000
rhoSR = 0.5
rhoVR = 0.5
capr = 0.30000
cOne = 0.040
cTwo =0.0000
cThree = 1.0000
thetr = 0.04
strike = 1.0000

aa=del*del/2-gam
bb=sqrt(2.)*del
pi=acos(0.0D0)*2.0D0
sqpi=sqrt(pi)
```

```
      aaG = 1/alamGExpo

      n=nn1+nn2+nn3+nn4
      n1=n+1
      m1=m+1
      dz=zmax/m
      dz2=dz*dz
      r1=rN+1
      dr=(rMax-rMin)/rN
      dr2=dr*dr

      Allocate(ry(n1,m1,r1),w(n1),un(n1,m1,r1), &
uoo(n1,m1,r1),uo(n1,m1,r1), &
      vn(n1,m1,r1), option_price(n1,m1,r1))
      Allocate (sny(nt+1,m1),time(nt+1),sny2(nt+1,m1,r1))
      Allocate (yy(n1))
      Allocate (pd(n1,m1,r1),aint1(n1,m1,r1),aint2(n1), &
aint3(n1,m1,r1),aint3F(m1,n1,r1))
      Allocate (ph(n1))
      Allocate (ac(n1,m1,r1),bc(n1,m1,r1),cc(n1,m1,r1), &
dc(n1,m1,r1),f(n1),g(n1) )
      Allocate (op(n1), uui(n1,m1,r1),op_delta(n1),op_gamma(n1), &
g_gamma(n1,m1,r1))

      call grid()

      open (9, FILE='Jump_Stvol.dat', STATUS='unknown')

       write (9,*) 'The risk-free rate of interest r:', rate
       write (9,*) 'The rate of dividend yield q:', q
       write (9,*) 'The rate of mean reversion:', cap
       write (9,*) 'The long run mean of the volatility:', thet
```

```
      write (9,*) 'The instantaneous volatility of v:', sigma
      write (9,*) 'The correlation rho:', rho
      write (9,*) 'The lambda for the Hermite jump:', alam
      write (9,*) 'The gamma for the jumps:', gam
      write (9,*) 'The delta for the jumps:', del
      write (9,*) 'The splitting price for the spot:', &
y0, y1, y2, ymax
      write (9,*) 'The number of points between &
splitting price', nn1, nn2, nn3
      write (9,*) 'The maximal volatility:', zmax
      write (9,*) 'The number of volatilities:', m
      write (9,*) 'The tolerance:', tol
      write (9,*) 'The expire date:', tn
      write (9,*) 'The number of time steps:', nt
      write (9,*) 'The number of hermite &
polynomials:', HM
      write (9,*) 'The alpha of of Lagaurre polynomials:', alf
      write (9,*) 'The lambda for the Gauss-Laggaure jump:', alamG
      write (9,*) 'The lambda for the Gauss-Laggaure exponential &
distribution :', alamGExpo
      write (9,*) 'The number of interest rate points:', rN
      write (9,*) 'The maximum interest:', rMax
      write (9,*) 'The instantaneous volatility of r:', sigmar
      write (9,*) 'The correlation rhoSR:', rhoSR
      write (9,*) 'The correlation rhoVR:', rhoVR
      write (9,*) 'The rate of mean reversion for r:', capr
      write (9,*) 'Interest rate parameter c1:', cOne
      write (9,*) 'Interest rate parameter c2:', cTwo
      write (9,*) 'Interest rate parameter c3:', cThree

     open (10, FILE='plot_mol.dat', STATUS='unknown')
     open (11, FILE='mol_results.dat', STATUS='unknown')
```

```
    if(alam.ne.0.) then

    ALLOCATE (Roots(1:HM), Weights(1:HM))
    ALLOCATE (RootsG(1:HM2), WeightsG(1:HM2))

    do k = 1, HM
    Roots(k) = 0.0D0
    end do

    do k = 1, HM2
    RootsG(k) = 0.0D0
    end do

    call gauher(Roots,Weights,HM)
    call gaulag(RootsG,WeightsG,HM2,alf)

    do 10 k=1,n1
    aint2(k)=0.00D0
 10 continue

    do 11 l=1,HM
    Roots(l) = exp(bb*Roots(l) - aa)
 11 continue

do 1111 l=1,HM2
    RootsG(l) = RootsG(l)*aaG
 1111 continue
    end if

    do 15 rr=1,r1
    do 15 j=1,m1
```

```
      sny2(1,j,rr)=1
      do 15 k=1,n1
      y=yy(k)
      z=(j-1)*dz
      rate_disc=(rr-1)*dr
      un(k,j,rr)=u0(y,z)
      vn(k,j,rr)=v0(y,z)
      uo(k,j,rr)=un(k,j,rr)
15    continue

      b_exp = Find_b_start(rate_disc, q, alam, gam, del)
      write (10,1101) (0.0D0,(j-1)*dz, b_exp,j=2,m1)

      t=0
      itime=1
20    continue
      icount=0
      told=t
      dtau=(tn-t)/nt

      do 30 rr=2,r1
      do 30 j=2,m1
      do 30 k=1,n1
      y=yy(k)
      z=(j-1)*dz
      rate_disc = (rr-1)*dr
      u=un(k,j,rr)
      coy=cony(y,z,u)
      ac(k,j,rr)=0
      bc(k,j,rr)=1
      dc(k,j,rr)=-beta(y,z,u,rate_disc)/coy
      f(k)=0
```

```
   30 continue

   40 continue
      if(t.ge.tn-1.e-6) go to 1100
      itime=itime+1
      icount=icount+1
      t=told+icount*dtau

      if(itime.eq.2) then
      do 60 rr=2,r1
      do 60 j=2,m1
      do 50 k=1,n1
      y=yy(k)
      z=(j-1)*dz
      rate_disc=(rr-1)*dr
      u=un(k,j,rr)
      coy=cony(y,z,u)
      cc(k,j,rr)=(eps(y,z,u)/dtau-delta(y,z,u,rate_disc))/coy
      ry(1,j,rr)=0
      rin=ry(1,j,rr)
      call riccati(1,n1,rin,j,rr)
50 continue
60 continue
end if

if(itime.eq.4) then
      do 80 rr=2,r1
      do 80 j=2,m1
      do 70 k=1,n1
      y=yy(k)
      z=(j-1)*dz
      rate_disc=(rr-1)*dr
```

```
      u=un(k,j,rr)
      coy=cony(y,z,u)
      cc(k,j,rr)=(3*eps(y,z,u)/(2*dtau)-delta(y,z,u,rate_disc))/coy
      ry(1,j,rr)=0
      rin=ry(1,j,rr)
      call riccati(1,n1,rin,j,rr)
 70   continue
 80   continue
      end if

itcoun_i = 0
109   continue
      if(alam.ne.0) then
      call cpu_time(stime)
call hermite(Roots, Weights)
call GaussLaguerre(RootsG, WeightsG)

      itcoun_i = itcoun_i+1
      dif_i = 0.0d0
      uui = un
      end if

      itcoun=0
110   continue
      itcoun=itcoun+1
      dif=0

      do 378 j=1,m1
      do 378 k=1,n1
      un(k,j,1)=un(k,j,4)-3*(un(k,j,3)-un(k,j,2))
      vn(k,j,1)=vn(k,j,4)-3*(vn(k,j,3)-vn(k,j,2))
      sny2(itime,j,1)=sny2(itime,j,4)- &
```

```
3*(sny2(itime,j,3)-sny2(itime,j,2))
  378 continue

      do 380 rr=1,r1
      do 380 k=1,n1
      un(k,1,rr)=un(k,4,rr)-3*(un(k,3,rr)-un(k,2,rr))
      vn(k,1,rr)=vn(k,4,rr)-3*(vn(k,3,rr)-vn(k,2,rr))

      sny2(itime,1,rr)=sny2(itime,4,rr) &
-3*(sny2(itime,3,rr)-sny2(itime,2,rr))
  380 continue

do 700 rr=2,r1
do 700 j=2,m1
      w1j=0
      rin=ry(1,j,rr)
      call forward(rin,w1j,1,n1,j,rr)
      call freboun(1,n1,kfb,j,rr)
      vin=vn(kfb,j,rr)
      call backward(kfb,1,vin,j,rr)
      time(itime)=t
      sny2(itime,j,rr)=yf
  700 continue
      print *,'itime,itcoun,dif'
      print 709,itime,itcoun,dif
  709 format(2i10,f15.8)
   if(itcoun.gt.1000) then

      stop
      end if

      if(dif.ge.tol) go to 110
```

```
      if(alam.ne.0) then
      do 720 rr = 2, r1
      do 720 j = 2, m1
      do 720 k = 1, n1
      dif_i = max(dif_i,abs(uui(k,j,rr)-un(k,j,rr)))
  720 continue
      print *,'itime,itcoun_i,dif_i'
      print 722,itime,itcoun_i,dif_i
  722 format(2i10,f15.8)

  if(itcoun_i.gt.1000) then
      stop
      end if
      if(dif_i.ge.tol) go to 109
      itcoun_i = 0
      end if

      do 750 rr=1,r1
      do 750 j=1,m1
      do 750 k=1,n1
      uoo(k,j,rr)=uo(k,j,rr)
      uo(k,j,rr)=un(k,j,rr)

      if(yy(k).ge.sny2(itime,j,rr)) then
      uo(k,j,rr)=yy(k)-1
      vn(k,j,rr)=1
      end if
      if(j.eq.3) then
      WRITE (222222,*) itime, (rr-1)*dr, (j-1)*dz, &
yy(k), un(k,j,rr)*100, vn(k,j,rr)
      end if
  750 continue
```

```
    write (10,1101) (t,(j-1)*dz,sny2(itime,j,5),j=2,m1)
    write (19,1101) (t,(rr-1)*dr,sny2(itime,3,rr),rr=2,r1)
    write (20202020,1101) (((j-1)*dz,(rr-1)*dr, &
sny2(itime,j,rr),j=2,m1),rr=2,r1)
     go to 40

1100 continue
    write (10,1101) (t,(j-1)*dz,sny2(itime,j,17),j=2,m1)
    write (19,1101) (t,(rr-1)*dr,sny2(itime,15,rr),rr=2,r1)
    write (20202020,1101) (((j-1)*dz,(rr-1)*dr, &
sny2(itime,j,rr),j=2,m1),rr=2,r1)
1101 format(2f12.4,f15.6)

   call cpu_time(end_time)
     print *, 'Runtime: ', end_time - start_time
     write (9,*) 'Runtime', end_time - start_time

   do i=0,5
     spot=80.0d0+i*10.0d0
     ex=spot/100.0d0

     if(ex.lt.ymax) then
     do 1210 rr=1,r1
     do 1210 j=1,m1
     do 1200 k=1,n1
     if(ex.le.yy(k+1).and.ex.gt.yy(k)) then
     p1=(ex-yy(k))/(yy(k+1)-yy(k))
     p2=1-p1
     op(j)=(p1*un(k+1,j,rr)+p2*un(k,j,rr))*100.0d0
     op_delta(j)=(p1*vn(k+1,j,rr)+p2*vn(k,j,rr))
     op_gamma(j)=p1*(cc(k+1,j,rr)*un(k+1,j,rr) &
```

```
+(dc(k+1,j,rr)-ac(k+1,j,rr))*vn(k+1,j,rr) &
+g_gamma(k+1,j,rr))+ p2*(cc(k,j,rr)*un(k,j,rr) &
+(dc(k,j,rr)-ac(k,j,rr))*vn(k,j,rr)+g_gamma(k,j,rr))
      end if
 1200 continue
 1210 continue
      end if

write (9, *) spot, 0.04*m*dz, op(nint(0.04*m+1)), &
op_delta(nint(0.04*m+1)), op_gamma(nint(0.04*m+1))
 WRITE (11,*) 'spot=', spot
      do j=1,5
      WRITE (11,*) (j-1)*dz, (rr-1)*dr, op(j), &
op_delta(j), op_gamma(j)
      end do
    end do

do 12100 rr=1,r1
do 12100 j=1,m1
do 12100 k=1,n1
    y=yy(k)
    z=(j-1)*dz
    rate_disc=(rr-1)*dr
  option_price(k,j,rr)=(p1*un(k+1,j,rr)+p2*un(k,j,rr))*100.0d0
  WRITE (11111,*) itime, rate_disc, z, y, option_price(k,j,rr)
12100 continue
      END program

subroutine grid()
      use modpar
      IMPLICIT NONE
      DOUBLE PRECISION :: dy
```

```
      INTEGER :: i,k

      dy=(y1-y0)/nn1
      yy(1)=y0
      do 16 k=1,nn1
      yy(k+1)=yy(1)+k*dy
   16 continue
      dy=(y2-y1)/nn2
      do 17 i=1,nn2
      k=nn1+i
      yy(k+1)=yy(nn1+1)+i*dy
   17 continue
      dy=(y3-y2)/nn3
      do 18 i=1,nn3
      k=nn1+nn2+i
      yy(k+1)=yy(nn1+nn2+1)+i*dy
   18 continue
      dy=(ymax-y3)/nn4
      do 19 i=1,nn4
      k=nn1+nn2+nn3+i
      yy(k+1)=yy(nn1+nn2+nn3+1)+i*dy
   19 continue
      return
      end

double precision function u0(y,z)
      use modpar
      IMPLICIT NONE
      DOUBLE PRECISION :: y,z
      u0=max(0.0d0,y-1)
      return
      end
```

```
double precision function v0(y,z)
      use modpar
      IMPLICIT NONE
      double PRECISION :: y,z
      v0=0
      if(y.gt.1) v0=1
      return
      end

DOUBLE PRECISION FUNCTION Find_b_start(r, q, lambda, gamma, delta)
        IMPLICIT NONE
        DOUBLE PRECISION :: r, q, lambda, gamma, delta
        DOUBLE PRECISION :: TOL, x0, x1, fx0, fx0d, diff
        DOUBLE PRECISION :: du, dl, PI, temp
        DOUBLE PRECISION :: CND

        PI = 2.0D0*ACOS(0.0D0)
        TOL = 1.0D-15
        x0 = MAX(1.0D0, r/q)
        diff = 1.0D0
        DO WHILE (diff .GE. TOL)

              du = (-LOG(x0) - (gamma - 0.50D0*delta*delta))/delta
            dl = (-LOG(x0) - (gamma + 0.50D0*delta*delta))/delta
              fx0 = (r + lambda * CND(du))
              fx0 = fx0/(q + lambda*EXP(gamma)*CND(dl)) - x0

              fx0d = (q + lambda*EXP(gamma)*CND(dl))
              fx0d = fx0d*EXP(-0.50D0*du*du)
              temp = EXP(gamma)*EXP(-0.50D0*dl*dl)
              fx0d = fx0d - (r + lambda*CND(du))*temp
```

```
                fx0d = -fx0d * lambda / (SQRT(2.0D0*PI)*delta*x0)
                fx0d = fx0d / (q + lambda*EXP(gamma) &
*CND(dl))**2.0D0 -1.0D0

                x1 = x0 - fx0/fx0d
                diff = ABS(x1-x0)
                x0 = x1
        END DO
        Find_b_start = MAX(x0, 1.0D0)
      END

DOUBLE PRECISION FUNCTION CND( X )
IMPLICIT DOUBLE PRECISION( A - H , O - Z )
PARAMETER( MAXN = 10 )
DOUBLE PRECISION, DIMENSION( -MAXN : MAXN ) :: CN , EA

        CN( -10 ) = 0.7619853024160526D-23
        CN(  -9 ) = 0.1128588405953841D-18
        CN(  -8 ) = 0.6220960574271784D-15
        CN(  -7 ) = 0.1279812543885835D-11
        CN(  -6 ) = 0.9865876450376981D-9
        CN(  -5 ) = 0.2866515718791939D-6
        CN(  -4 ) = 0.3167124183311992D-4
        CN(  -3 ) = 0.1349898031630095D-2
        CN(  -2 ) = 0.2275013194817921D-1
        CN(  -1 ) = 0.1586552539314571D0
        CN(   0 ) = 0.5000000000000000D0
        CN(   1 ) = 0.8413447460685429D0
        CN(   2 ) = 0.9772498680518208D0
        CN(   3 ) = 0.9986501019683699D0
        CN(   4 ) = 0.9999683287581669D0
        CN(   5 ) = 0.9999997133484281D0
```

```
        CN(   6 ) = 0.9999999990134124D0
        CN(   7 ) = 0.9999999999987202D0
        CN(   8 ) = 0.9999999999999994D0
        CN(   9 ) = 0.1000000000000000D1
        CN(  10 ) = 0.1000000000000000D1

EA(  0 ) = 0.3989422804014327D0
EA(  1 ) = 0.2419707245191433D0
EA(  2 ) = 0.5399096651318805D-1
EA(  3 ) = 0.4431848411938007D-2
EA(  4 ) = 0.1338302257648854D-3
EA(  5 ) = 0.1486719514734298D-5
EA(  6 ) = 0.6075882849823285D-8
EA(  7 ) = 0.9134720408364593D-11
EA(  8 ) = 0.5052271083536892D-14
EA(  9 ) = 0.1027977357166891D-17
EA( 10 ) = 0.7694598626706419D-22

IF( X .LE. -10.0D0 ) THEN
    CND = 0.0D0
ELSEIF( X .GE. 10.0D0 ) THEN
    CND = 1.0D0
ELSE
    NA  = NINT( X )
    Z   = X - NA
    H0  = 1.0D0
    H1  =-NA
    F2  = 1.0D0
    SUM = 0.0D0
    DO  N = 1 , 20 , 1
        F2  = F2 * Z / N
        SUM = SUM + H0 * F2
```

```
          H2  =-NA * H1 - N * H0
          H0  = H1
          H1  = H2
           END DO
     CND = CN( NA ) + EA( ABS( NA ) ) * SUM
ENDIF
RETURN
      END

double precision function cony(y,z,u)
      use modpar
      IMPLICIT NONE
      DOUBLE PRECISION :: y,z,u,rate_disc
      cony=z*y*y/2
      cony=amax1(cony,1.e-5)
      return
      end

DOUBLE PRECISION function beta(y,z,u,rate_disc)
      use modpar
      IMPLICIT NONE
      DOUBLE PRECISION :: y,z,u,rate_disc
      beta=(rate_disc-q-alam*ak1)*y
      return
      end

DOUBLE PRECISION function eps(y,z,u)
      use modpar
      IMPLICIT NONE
      DOUBLE PRECISION :: y,z,u,rate_disc
      eps=1.0d0
      return
```

```
      end

double precision function delta(y,z,u,rate_disc)
use modpar
IMPLICIT NONE
DOUBLE PRECISION ::y,z,u,rate_disc,funcOne,funcTwo
funcOne = sigma*sigma*z/dz2
funcTwo = sigmar*sigmar/dr2
if(z.eq.zmax) then
    funcOne = 0.0
else if(rate_disc.eq.rMax) then
    funcTwo = 0.0
end if

delta=-rate_disc-funcOne-funcTwo
delta=delta-alam-alamG
return
end

subroutine riccati(kbeg,kend,rin,j,rr)
      use modpar
      IMPLICIT NONE

      Double precision :: c1,c2,c3,rin,dy
      Integer ::k1,k,inc,j,kbeg,kend,rr

      ry(kbeg,j,rr)=rin
      if(kbeg.lt.kend) then
      inc=-1
      else
      inc=1
      end if
```

```
      do 600 k=kbeg-inc,kend,-inc
      k1=k+inc
      dy=yy(k)-yy(k1)
      c1=cc(k,j,rr)
      c2=2/dy-ac(k,j,rr)+dc(k,j,rr)
      c3=(-ac(k1,j,rr)+dc(k1,j,rr)-2/dy)*ry(k1,j,rr) &
-bc(k,j,rr)-bc(k1,j,rr)+cc(k1,j,rr) &
*ry(k1,j,rr)*ry(k1,j,rr)
      ry(k,j,rr)=-2*c3/(c2+sqrt(c2*c2-4*c1*c3))
  600 continue
      return
      end

subroutine forward(rin,win,kin,kend,j,rr)
      use modpar
      IMPLICIT NONE

      double precision :: y,z,u,um,up,vm,vp,v, &
rate_disc,umr,upr,vmr,vpr,umru,umrd,upru,uprd
      integer :: k,j,jp1,kend,kin,rr,rrp1,jm1
      double precision :: rin,win,coy,cony,st,eps,currTime

      do 160 k=1,n1
      jp1=j+1
      rrp1 = rr+1
      if(j.eq.m1) jp1=m
      if(rr.eq.r1) rrp1 = rN
      y=yy(k)
      z=(j-1)*dz
      rate_disc=(rr-1)*dr
      u=un(k,j,rr)
      um=un(k,j-1,rr)
```

```
      umr=un(k,j,rr-1)
      umru=un(k,jp1,rr-1)
      umrd=un(k,j-1,rr-1)
      up=un(k,jp1,rr)
      upr=un(k,j,rrp1)
      upru=un(k,jp1,rrp1)
      uprd=un(k,j-1,rrp1)
      v=vn(k,j,rr)
      vm=vn(k,j-1,rr)
      vmr=vn(k,j,rr-1)
      vp=vn(k,jp1,rr)
      vpr=vn(k,j,rrp1)
      coy=cony(y,z,u)
      currTime = itime*dtau
      g(k)=st(y,z,um,u,up,vm,v,vp,j,k,rr,umr,upr, &
vmr,vpr,umru,umrd,upru,uprd,currTime,rate_disc)

      if(itime.le.3) then
      g(k)=g(k)-eps(y,z,u)*uo(k,j,rr)/dtau
      else
      g(k)=g(k)-eps(y,z,u)*(4*uo(k,j,rr) &
-uoo(k,j,rr))/(2*dtau)
      end if
      g(k)=g(k)/coy
      g_gamma(k,j,rr)=g(k)

  160 continue
      call fwswp(kin,kend,win,j,rr)
      return
      end

      double precision function st(y,z,um,u,up,vm, &
```

```
v,vp,j,k,rr,umr,upr,vmr,vpr,umru,umrd,upru, &
uprd,currTime,rate_disc)
      use modpar
      IMPLICIT NONE
      DOUBLE PRECISION :: y,z,um,u,up,vm,v,vp, &
rate_disc,umr,upr,vmr,vpr,umru,umrd,upru,uprd
      INTEGER :: j,k,rr
      DOUBLE PRECISION :: upwind,currTime

      if(itime.le.3) then
        umru = 0.0
        umrd = 0.0
        upru = 0.0
        uprd = 0.0
        vmr = 0.0
        vpr = 0.0
      end if


      upwind=um
      if(z.lt.thet) upwind=up
      st=-sigma*sigma*z/2*(um+up)/dz2-(cap*(thet-z)) &
/2.0*dz*(up-um)-sigma*rho*y*z*(vp-vm)/&
      (2*dz)-sigmar*sigmar/2*(umr+upr)/dr2&
      -sqrt(z)*y*sigmar*rhoSR*(vpr-vmr)/(2*dr) &
-sigma*sigmar*sqrt(z)*rhoVR*(upru-uprd-umru &
+umrd)/(4.0*dz*dr)&
      -capr*((cOne-cTwo*exp(-cThree*currTime)) &
-rate_disc)*(upr-umr)/(2*dr)

      if(z.eq.zmax) then
      st=-(cap*(thet-z))/dz*(u-um)&
```

```
       -sigmar*sigmar/2*(umr+upr)/dr2&
       -sqrt(z)*y*sigmar*rhoSR*(vpr-vmr)/(2*dr) &
       -capr*((cOne-cTwo*exp(-cThree*currTime)) &
-rate_disc)*(upr-umr)/(2*dr)

      else if(rate_disc.eq.rMin) then
        st=-sigma*sigma*z/2*(um+up)/dz2 &
-(cap*(thet-z))/dz*(up-um)&
       -sigma*rho*y*z*(vp-vm)/(2*dz)&
       -capr*((cOne-cTwo*exp(-cThree*currTime)) &
-rate_disc)*(upr-u)/(dr)

     else  if(rate_disc.eq.rMax) then
        st=-sigma*sigma*z/2*(um+up)/dz2 &
-(cap*(thet-z))/dz*(up-um) &
       -sigma*rho*y*z*(vp-vm)/(2*dz) &
       -capr*((cOne-cTwo*exp(-cThree*currTime)) &
-rate_disc)*(u-umr)/(dr)
       end if

     st = st-alam*(aint1(k,j,rr))-alamG*(aint3(k,j,rr))
       return
       end


 subroutine fwswp(kbeg,kend,win,j,rr)
       use modpar
       IMPLICIT NONE

       double precision :: c1, c2, c3,win,dy
       integer :: k1,k,kbeg,kend, inc,j,rr
       w(kbeg)=win
```

```
      if(kbeg.lt.kend)then
      inc=-1
      else
      inc=1
      end if
      do 600 k=kbeg-inc,kend,-inc
      k1=k+inc
      dy=yy(k)-yy(k1)
      c1=(1/dy+(ac(k1,j,rr)-cc(k1,j,rr)*ry(k1,j,rr))/2)
      c2=(1/dy-(ac(k,j,rr)-cc(k,j,rr)*ry(k,j,rr))/2)
      c3=(f(k)+f(k1)-(ry(k,j,rr)*g(k)+ry(k1,j,rr)*g(k1)))/2
      w(k)=(c1*w(k1)+c3)/c2
  600 continue
      return
      end


subroutine freboun(kbeg,kend,kfb,j,rr)
      use modpar
      IMPLICIT NONE

      integer :: kbeg,kend,j,kleft,kright,inc,k,kfb,ic,rr
      double precision :: r,phi,phii,pho,phoo,yn
      double precision:: y,c1,c2,c3,c4
      double precision :: fnf,fnp,p1,p2
      double precision :: ww2,rr2,aav2,bav2,cav2,dav2,fav2,gav2
      double precision :: dy

      if(kbeg.lt.kend) then
      inc=1
      else
      inc=-1
```

```
      end if
      kleft=min0(kbeg,kend)
      kright=max0(kbeg,kend)
      do 100 k=kleft,kright
      y=yy(k)

      ufb=max(0.0d0,y-1)
      vfb=1
      ph(k)=ufb-ry(k,j,rr)*vfb-w(k)

  100 continue
      kleft=kleft+2
      kright=kright-2
      do 150 k=kright,kleft,-1
      phii=ph(k+1)
      phi=ph(k)
      pho=ph(k-1)
      phoo=ph(k-2)
      if(phi*pho.le.0) go to 200
  150 continue
      print *,' no free boundary at t =',t
     print *, sny2(itime-1,j,rr), yy(1)
  160 continue
      stop
  200 continue
      r=yy(k)*pho/(pho-phi)-yy(k-1)*phi/(pho-phi)
      c1=phoo/((yy(k-2)-yy(k-1))*(yy(k-2) &
-yy(k))*(yy(k-2)-yy(k+1)))
      c2=pho/((yy(k-1)-yy(k-2))*(yy(k-1)-yy(k)) &
*(yy(k-1)-yy(k+1)))
      c3=phi/((yy(k)-yy(k-2))*(yy(k)-yy(k-1)) &
*(yy(k)-yy(k+1)))
```

```
      c4=phii/((yy(k+1)-yy(k-2))*(yy(k+1)-yy(k-1)) &
*(yy(k+1)-yy(k)))
      yf=r
      do 300 ic=1,10
      fnf=c1*(r-yy(k-1))*(r-yy(k))*(r-yy(k+1)) &
+c2*(r-yy(k-2))*(r-yy(k))*(r-yy(k+1)) &
      +c3*(r-yy(k-2))*(r-yy(k-1))*(r-yy(k+1)) &
+c4*(r-yy(k-2))*(r-yy(k-1))*(r-yy(k))

      fnp=c1*((r-yy(k))*(r-yy(k+1))+(r-yy(k-1)) &
*(r-yy(k+1))+(r-yy(k-1))*(r-yy(k)))  &
      +c2*((r-yy(k))*(r-yy(k+1))+(r-yy(k-2)) &
*(r-yy(k+1))+(r-yy(k-2))*(r-yy(k)))     &
      +c3*((r-yy(k-1))*(r-yy(k+1))+(r-yy(k-2)) &
*(r-yy(k+1))+(r-yy(k-2))*(r-yy(k-1))) &
      +c4*((r-yy(k-1))*(r-yy(k))+(r-yy(k-2)) &
*(r-yy(k))+(r-yy(k-2))*(r-yy(k-1)))

      yn=r-fnf/fnp
      if(abs(yn-r).lt.1.e-6) go to 400
      r=yn
  300 continue
      print *,' no newton convergence at t=  ',t
      print *,' linear interpolation is used'
      yn=yf
  400 continue
      yf=yn
      p1=(yy(k)-yf)/(yy(k)-yy(k-1))
      p2=1-p1
      if(inc.eq.1) then
      kfb=k-1
      else
```

```
      kfb=k
      end if

      ww2=p1*w(k-1)+p2*w(k)
      rr2=p1*ry(k-1,j,rr)+p2*ry(k,j,rr)
      aav2=p1*ac(k-1,j,rr)+p2*ac(k,j,rr)
      bav2=p1*bc(k-1,j,rr)+p2*bc(k,j,rr)
      cav2=p1*cc(k-1,j,rr)+p2*cc(k,j,rr)
      dav2=p1*dc(k-1,j,rr)+p2*dc(k,j,rr)
      fav2=p1*f(k-1)+p2*f(k)
      gav2=p1*g(k-1)+p2*g(k)
      ufb=max(0.0d0,yf-1)
      vfb=1
      dy=yy(kfb)-yf
      c1=2+dy*(dav2+cav2*rr2)
      c2=2+dy*(-dc(kfb,j,rr)-cc(kfb,j,rr)*ry(kfb,j,rr))
      c3=dy*(cc(kfb,j,rr)*w(kfb)+cav2*ww2+gav2+g(kfb))
      vn(kfb,j,rr)=(c1*vfb+c3)/c2
      return
      end

subroutine backward(kbeg,kend,vin,j,rr)
      use modpar
      IMPLICIT NONE
      double precision :: uu,vin
      integer :: j,kbeg,kend,inc,k,rr

      call bwswp(kbeg,kend,vin,j,rr)
      if(kbeg.lt.kend) then
      inc=1
      else
      inc=-1
```

```
      end if
      do 400 k=kbeg,kend,inc
      uu=ry(k,j,rr)*vn(k,j,rr)+w(k)
      dif=max(dif,abs(uu-un(k,j,rr)))
      un(k,j,rr)=uu
400   continue
      if(kbeg.lt.kend) then
      do 315 k=1,kbeg-1
      uu=ufb+vfb*(yy(k)-yf)
      dif=max(dif,abs(uu-un(k,j,rr)))
      un(k,j,rr)=uu
      vn(k,j,rr)=vfb
315   continue
      else
      do 320 k=kbeg+1,n1
      uu=ufb+vfb*(yy(k)-yf)
      dif=max(dif,abs(uu-un(k,j,rr)))
      un(k,j,rr)=uu
      vn(k,j,rr)=vfb
320   continue
      end if
      return
      end

      subroutine bwswp(kbeg,kend,vin,j,rr)
      use modpar
      IMPLICIT NONE
      Integer :: inc,kbeg,kend,j,k1,k,rr
      Double precision :: vin,dy,c1,c2,c3

      vn(kbeg,j,rr)=vin
      if(kbeg.lt.kend) then
```

```
      inc=-1
      else
      inc=1
      end if
      do 600 k=kbeg-inc,kend,-inc
      k1=k+inc
      dy=yy(k)-yy(k1)
      c1=2/dy+dc(k1,j,rr)+cc(k1,j,rr)*ry(k1,j,rr)
      c2=2/dy-dc(k,j,rr)-cc(k,j,rr)*ry(k,j,rr)
      c3=cc(k,j,rr)*w(k)+cc(k1,j,rr)*w(k1)+g(k1)+g(k)
      vn(k,j,rr)=(c1*vn(k1,j,rr)+c3)/c2
  600 continue
      return
      end

      subroutine hermite(Roots, Weights)
      use modpar
      IMPLICIT NONE
      INTEGER :: FoC,j,k,l,rr
      DOUBLE PRECISION :: Roots(1:HM), Weights(1:HM)
      DOUBLE PRECISION :: b_sp(0:n1), c_sp(0:n1), d_sp(0:n1-1)
      DOUBLE PRECISION :: alpha, beta
      DOUBLE PRECISION :: xy(1:n1), fxy(1:n1,1:m1,1:r1)
      DOUBLE PRECISION :: Spline_Int, uy, uxi

      FoC = 1
      alpha = 0.0D0
      beta = 1.0D0

      do rr=1,r1
      do j=1,m1
      do k=1,n1
```

```
      xy(k) = yy(k)
      fxy(k,j,rr) = un(k,j,rr)
      end do
      end do
      end do

      do 20 rr=1,r1
      do 20 j=1,m1
      CALL SmallSpline(xy, fxy(:,j,rr), b_sp, &
c_sp, d_sp, n1-1, FoC,alpha, beta)
      do 20 k=1,n1
      aint1(k,j,rr)=0.0D0
      do 10 l=1,HM
      uxi = xy(k)*Roots(l)
      uy = Spline_Int(uxi, n1-1, xy, fxy(:,j,rr), &
b_sp, c_sp, d_sp)
      aint1(k,j,rr)=aint1(k,j,rr)+Weights(l)*uy

   10 continue
   20 continue
      aint1 = aint1/sqrt(acos(0.0D0)*2.0D0)
      return
      end

      subroutine GaussLaguerre(RootsG, WeightsG)
      use modpar
      IMPLICIT NONE
      INTEGER :: FoC,j,k,l,rr
      DOUBLE PRECISION :: RootsG(1:HM2), WeightsG(1:HM2)
      DOUBLE PRECISION :: b_sp(0:n1), c_sp(0:n1), d_sp(0:n1-1)
      DOUBLE PRECISION :: alpha, beta
      DOUBLE PRECISION :: xy(1:n1), fxy(1:n1,1:m1,1:r1), &
```

```
xz(1:m1), fxySwap(1:m1,1:n1,1:r1)
      DOUBLE PRECISION :: Spline_Int, uy, uxi2,uxi3

      FoC = 1
      alpha = 0.0D0
      beta = 1.0D0

      do rr=1,r1
      do k=1,n1
      do j=1,m1
      xz(j) = (j-1)*dz
      fxySwap(j,k,rr) = un(k,j,rr)
      end do
      end do
      end do

       do 20 rr=1,r1
       do 20 k=1,n1

       CALL SmallSpline(xz, fxySwap(:,k,rr), b_sp, &
 c_sp, d_sp, m1-1, FoC,alpha, beta)
       do 20 j=1,m1

      aint3(k,j,rr)=0.0D0
      do 10 l=1,HM2
      uxi2 = xz(j)+RootsG(l)
      uy = Spline_Int(uxi2, m1-1, xz, fxySwap(:,k,rr), &
b_sp, c_sp, d_sp)

      if(j.eq.m1) then
        uxi3 = xz(j)
       uy = Spline_Int(uxi3, m1-1, xz, fxySwap(:,k,rr), &
```

```
b_sp, c_sp, d_sp)
      end if
      aint3(k,j,rr)=aint3(k,j,rr)+WeightsG(l)*uy
   10 continue
   20 continue
      return
      end

SUBROUTINE SmallSpline(x, f_x, b_spl, c_spl, d_spl, &
N, FoC, alpha, beta)
        IMPLICIT NONE
        INTEGER :: N, FoC, i
        DOUBLE PRECISION :: alpha, beta, Spline_Int
        DOUBLE PRECISION :: x(0:N), f_x(0:N)
        DOUBLE PRECISION :: b_spl(0:N), c_spl(0:N), &
d_spl(0:N-1)

        DO i = 0, N
                b_spl(i) = 0.0D0
                c_spl(i) = 0.0D0
        END DO

        DO i = 0, N-1
                d_spl(i) = 0.0D0
        END DO

        CALL CubicSpline(x, f_x, N, FoC, alpha, beta, &
b_spl,c_spl, d_spl)
      END SUBROUTINE

DOUBLE PRECISION FUNCTION Spline_Int(x_bar, N, x, a, &
b, c, d)
```

```
  IMPLICIT NONE
  INTEGER :: N
  INTEGER :: i, Lower, Upper, j
  DOUBLE PRECISION :: x_bar, x(0:N), a(0:N), b(0:N)
  DOUBLE PRECISION :: c(0:N), d(0:N-1)
  DOUBLE PRECISION :: Interp
  LOGICAL :: Exact

  i =  INT(N/2)
Upper = N
  Lower = 0
  Exact = .FALSE.

  IF ( x_bar .LE. x(N) .AND. x_bar .GE. x(0) ) THEN
          DO WHILE (Upper - Lower .NE. 1)
                  IF (x_bar < x(i)) THEN
                          Upper = i
                          i = INT(i/2)
          ELSEIF (x_bar > x(i)) THEN
                          Lower = i
                          i = INT((Upper + i)/2)
                  ELSE
                          Exact = .TRUE.
                          Upper = i
                          Lower = i-1
                  END IF
          END DO

          IF (Exact) THEN
           Lower = Upper
  END IF
```

```
                i = Lower
                Interp = a(i) + b(i)*(x_bar - x(i)) &
+c(i)*(x_bar - x(i))**2 + d(i)*(x_bar-x(i))**3

        ELSE

            Interp = MAX(x_bar - 1.0D0, 0.0D0)

        END IF

        Spline_Int = Interp
      END

      SUBROUTINE CubicSpline(x, a_spl, N, FoC, alpha, &
beta,b_spl, c_spl, d_spl)
IMPLICIT NONE
        INTEGER :: N, FoC
        INTEGER :: MSize, i
        DOUBLE PRECISION :: alpha, beta
        DOUBLE PRECISION :: x(0:N), a_spl(0:N)
        DOUBLE PRECISION :: b_spl(0:N), c_spl(0:N), d_spl(0:N-1)
        DOUBLE PRECISION, ALLOCATABLE :: Ad(:), Al(:), Au(:)
        DOUBLE PRECISION, ALLOCATABLE :: b(:), c(:), b_temp(:)

        ALLOCATE ( b(0:N) )
        IF (FoC == 0) THEN
                MSize = N-1
        ELSE
                MSize = N+1
        END IF
```

```
        ALLOCATE( Ad(1:MSize), Al(2:MSize), Au(1:MSize-1) )
        CALL BuildMatrix(N, FoC, alpha, beta, x, &
a_spl, b,MSize, Ad, Al, Au)
        ALLOCATE( c(1:MSize), b_temp(1:MSize) )

        IF (FoC == 0) THEN
                DO i = 1, MSize
                        b_temp(i) = b(i)
                END DO
        ELSE
                DO i = 0, N
                        b_temp(i+1) = b(i)
                END DO
        END IF

        CALL TriSolver(MSize, Ad, Al, Au, b_temp, c)
        DEALLOCATE (b, b_temp, Ad, Al, Au)

        IF (FoC == 1) THEN
                DO i = 1, MSize
                        c_spl(i-1) = c(i)
                END DO
        ELSE
                DO i = 1, MSize
                        c_spl(i) = c(i)
                END DO
        END IF
        DEALLOCATE (c)
        CALL FitSpline(N, FoC, alpha, beta, x, a_spl, &
c_spl, b_spl, d_spl)
      END SUBROUTINE
```

```
SUBROUTINE BuildMatrix(N, FoC, alpha, beta, x, a, b,MSize, Ad, Al, Au)

        IMPLICIT NONE
        INTEGER :: N, i, FoC, Start, Finish, MSize, j
        DOUBLE PRECISION :: x(0:N), a(0:N), b(0:N)
        DOUBLE PRECISION :: Ad(1:MSize), Al(2:MSize), Au(1:MSize-1)
        DOUBLE PRECISION, ALLOCATABLE :: Hd(:), h(:)
        DOUBLE PRECISION :: alpha, beta

        ALLOCATE ( h(0:N-1) )

DO i = 1, N
        h(i-1) = x(i) - x(i-1)
        END DO

        ALLOCATE ( Hd(1:N-1) )

        DO i = 1, N-1
                Hd(i) = 2.0D0 * ( h(i) + h(i-1) )
                 b(i) = 3.0D0 * ( ( (a(i+1) - a(i))/h(i) ) &
- ( (a(i) - a(i-1))/h(i-1) ) )
        END DO

        IF (FoC == 0) THEN
                Start = 2
                Finish = N-2
        ELSE
                Start = 1
         Finish = N-1

                b(0) = 3.0D0 * ( (a(1) - a(0))/h(0) - alpha )
                b(N) = 3.0D0 * ( beta- (a(N) - a(N-1))/h(N-1) )
```

```
        END IF

        IF (FoC == 0) THEN
                Ad(1) = Hd(1)
                Au(1) = h(1)
        ELSE
                Ad(1) = 2.0D0*h(0)
                Au(1) = h(0)
        END IF

        j = 2
        DO i = Start, Finish
                Al(j) = h(i-1)
                Ad(j) = Hd(i)
                Au(j) = h(i)
                j = j + 1
        END DO

        IF (FoC == 0) THEN
                Al(MSize) = h(N-2)
                Ad(Msize) = Hd(N-1)
        ELSE
                Al(MSize) = h(N-1)
                Ad(MSize) = 2.0D0*h(N-1)
        END IF
      END SUBROUTINE

SUBROUTINE TriSolver(N, Ad, Al, Au, b, x)

IMPLICIT NONE
        INTEGER :: N, i
        DOUBLE PRECISION :: Ad(1:N), Al(2:N), &
```

```
Au(1:N-1), b(1:N), x(1:N)
        DOUBLE PRECISION, ALLOCATABLE :: Ld(:), Uu(:)
        DOUBLE PRECISION, ALLOCATABLE :: y(:)

        ALLOCATE( Ld(1:N), Uu(1:N-1) )
        ALLOCATE( y(1:N) )

        Ld(1) = Ad(1)
        DO i = 2, N
                Uu(i-1) = Au(i-1) / Ld(i-1)
                Ld(i)   = Ad(i) - Al(i) * Uu(i-1)
        END DO

        y(1) = b(1) / Ld(1)
        DO i = 2, N
                y(i) = ( b(i) - Al(i) * y(i-1) ) / Ld(i)
        END DO

        x(N) = y(N)
        DO i = N-1, 1 ,-1
                x(i) = y(i) - Uu(i) * x(i+1)
        END DO
      END SUBROUTINE

SUBROUTINE FitSpline(N, FoC, alpha, beta, x, a, c, b, d)

        IMPLICIT NONE
        INTEGER :: N, i, FoC, Start
        DOUBLE PRECISION :: x(0:N), a(0:N), c(0:N), b(0:N), d(0:N-1)
        DOUBLE PRECISION :: alpha, beta
        DOUBLE PRECISION, ALLOCATABLE :: h(:)
```

```
        ALLOCATE ( h(0:N-1) )
        IF (FoC == 1) THEN
                b(0) = alpha
                b(N) = beta
        END IF

        DO i = 1, N
        h(i-1) = x(i) - x(i-1)
        END DO

        IF (FoC == 0) THEN
                c(0) = 0.0D0
                c(N) = 0
                Start = 0
        ELSE
                Start = 1
                d(0) = ( c(1) - c(0) )/( 3.0D0 * h(0) )
        END IF

        DO i = Start, N-1
                b(i) = ( a(i+1) - a(i) )/h(i) &
- h(i) * ( c(i+1) + 2.0D0*c(i) )/3.0D0
        d(i) = ( c(i+1) - c(i) )/( 3.0D0 * h(i) )
        END DO
      END SUBROUTINE

SUBROUTINE gauher(Roots,Weights,N)
IMPLICIT NONE
INTEGER :: N,MAXIT
DOUBLE PRECISION :: Roots(1:N), Weights(1:N)
DOUBLE PRECISION EPS,PIM4
PARAMETER (EPS=3.D-14,PIM4=.7511255444649425D0,MAXIT=10)
```

```
INTEGER i,its,j,m
DOUBLE PRECISION p1,p2,p3,pp,z,z1
m=(N+1)/2
do i=1,m
if(i.eq.1)then
z=sqrt(float(2*N+1))-1.85575*(2*N+1)**(-.16667)
else if(i.eq.2)then
z=z-1.14*N**.426/z
else if (i.eq.3)then
z=1.86*z-.86*Roots(1)
else if (i.eq.4)then
z=1.91*z-.91*Roots(2)
else
z=2.*z-Roots(i-2)
endif
do  its=1,MAXIT
p1=PIM4
p2=0.d0
do  j=1,N
p3=p2
p2=p1
p1=z*sqrt(2.d0/j)*p2-sqrt(dble(j-1)/dble(j))*p3
enddo
pp=sqrt(2.d0*N)*p2
z1=z
z=z1-p1/pp
if(abs(z-z1).le.EPS)goto 1
enddo
1 Roots(i)=z
Roots(N+1-i)=-z
Weights(i)=2.d0/(pp*pp)
Weights(N+1-i)=Weights(i)
```

```
enddo
return
END

SUBROUTINE gaulag(RootsG,WeightsG,N,alf)
IMPLICIT NONE
INTEGER :: N,MAXIT, alf
DOUBLE PRECISION ::  RootsG(1:N), WeightsG(1:N)
DOUBLE PRECISION EPS
PARAMETER (EPS=3.D-14,MAXIT=10)
INTEGER i,its,j
REAL ai,gammln
DOUBLE PRECISION p1,p2,p3,pp,z,z1

do i=1,N
if(i.eq.1)then
z=(1.+alf)*(3.+.92*alf)/(1.+2.4*N+1.8*alf)
else if(i.eq.2)then
z=z+(15.+6.25*alf)/(1.+.9*alf+2.5*N)
else
ai=i-2
z=z+((1.+2.55*ai)/(1.9*ai)+1.26*ai*alf/(1.+3.5*ai)) &
*(z-RootsG(i-2))/(1.+.3*alf)
endif
do its=1,MAXIT
p1=1.d0
p2=0.d0
do j=1,N
p3=p2
p2=p1
p1=((2*j-1+alf-z)*p2-(j-1+alf)*p3)/j
enddo
```

```
pp=(N*p1-(N+alf)*p2)/z
z1=z
z=z1-p1/pp
if(abs(z-z1).le.EPS)goto 1
enddo
pause 'too many iterations in gaulag'
1 RootsG(i)=z
WeightsG(i)=-exp(gammln(alf+N)-gammln((N)))/(pp*N*p2)
enddo
return
END

FUNCTION gammln(xx)
IMPLICIT NONE
REAL gammln
INTEGER j, xx
DOUBLE PRECISION :: ser,stp,tmp,x,y
DOUBLE PRECISION :: cof(1:6)
DATA cof/76.18009172947146d0,-86.50532032941677d0, &
24.01409824083091d0,1.231739572450155d0,0.1208650973866179d-2, &
-.5395239384953d-5/

stp = 2.5066282746310005d0
x=xx
y=x
tmp=x+5.5d0
tmp=(x+0.5d0)*log(tmp)-tmp
ser=1.000000000190015d0
do j=1,6
y=y+1.d0
ser=ser+cof(j)/y
enddo
```

```
gammln=tmp+log(stp*ser/x)
return
END
```

CHAPTER 3

The impact of jumps on American option pricing: The S&P 100 options case.

3.1. Introduction

Since Merton (1976) introduced jumps in the Black & Scholes (1973) model, there has been several studies about jumps and their suitability for the pricing of options; see Naik & Lee (1990) and Bates (1996) for earlier studies. The inclusion of jumps to the Black-Scholes model may explain shorter maturity smiles, which cannot be explained by stochastic volatility models (see Bakshi et al. (1997), Bates (2000) and Pan (2002)).[1] Eraker et al. (2003) demonstrated that including jumps in returns explains the large movements in the S&P 500 and Nasdaq option prices, whilst including volatility jumps allows it to rapidly increase, since jumps in returns are a rapidly moving, but persistent, factor that drives volatility. Broadie, Chernov & Johannes (2007) found strong evidence in support of the presence of jumps in volatility as they are essential in explaining the time series of returns, together with option prices. Bakshi & Cao (2003) also find that jumps in the asset returns are of a higher-order importance than jumps in volatility. A stochastic volatility model with jumps in returns improves the model more than a stochastic volatility model with jumps in volatility only. Yet, most of the above-mentioned research papers deal with European option pricing.

American option pricing has been also studied extensively with a variety of models including stochastic volatility models (Rambharat & Brockwell (2010) and Ruckdeschela, Sayera & Szimayerb (2011)), stochastic volatility and stochastic interest rate models, e.g. Kang & Meyer (2014) and Samimi et al. (2017)) and stochastic volatility models with asset jumps, e.g. Chiarella et al. (2009), Ballestra & Sgarra (2010), Salmi, Toivanen & Sydow (2013), and Cheang et al. (2013). According to Das & Sundaram (1999), stochastic

[1] Bakshi et al. (1997) observed that on including jumps in volatility, pricing errors no longer showed any clear systematic biases. Duffie et al. (2000) and Pan (2002) observe that jumps in volatility increase the Black-Scholes implied volatility for ITM options and they labelled this as the 'hook' or 'tipping at the end' effect.

volatility models can produce sufficiently realistic conditional nonnormalities, but only over longer periods of time resulting in rather flat implied volatility surfaces for short-dated options contracts. On the other hand, stochastic volatility models with asset jumps capture unconditional and conditional nonnormalities well, but they fail to explain the persistence of the conditional volatility of returns (Bates (2000)). The inclusion of jumps in volatility in addition to asset jumps[2] produces the empirically observed volatility that is persistent and "rapidly moving", see Eraker et al. (2003)). Thus, stochastic volatility and stochastic interest rate models with asset and volatility jumps are employed to study the impact of these jumps on American option prices and their early exercise boundaries.

The American option pricing problem typically relies on numerical solutions. The convectional numerical methods employed in the literature are Monte Carlo simulations including mesh and tree methods, e.g. Broadie & Glasserman (1996), Broadie & Glasserman (1997), Broadie & Glasserman (2004) and Tavakkoli & Thomas (2014), regression based methods, e.g. Carriere (1996), Longstaff & Schwartz (2001) and Samimi et al. (2017), finite difference methods, e.g. Meyer (1998), Zhao et al. (2007) and Ikonen & Toivanen (2009), and, finally, a combination of those (Tsitsiklis & Roy (1999), Fu et al. (2001), Lindset & Lund (2007), and Agarwal et al. (2016)). These time-recursive methods are liable to approximation errors and their efficiency relies on required computational times. Front-fixing methods use non-linear transformations to generate a fixed boundary and avoid the time-backward computation of the optimal boundary (Wu & Kwok (1997) and Nielsen & Tveito (2002)). Several works also propose analytical solutions of American option prices for basic models (Geske & Johnson (1984), Barone-Adesi & Whaley (1987), Hansen & Jorgensen (2000) and Zhu (2005)). This chapter contributes to this literature by employing the MoL to price American options under stochastic volatility and stochastic interest-rate models with jumps in assets and volatility.

This chapter deals with the pricing of American call index options by using the Heston (1993) stochastic volatility model and the Hull & White (1987) short rate model in the presence of asset (index) and volatility jumps. As demonstrated in Chapter 2, the inclusion of stochastic interest rates is an important addition to the modelling framework since the free boundaries of American option prices are sensitive to interest rates dynamics, see also

[2]Eraker et al. (2003) support the notion that jumps in volatility should always complement asset jumps in a model as both jumps are important in explaining market behaviour over periods of financial turmoil.

Chiarella et al. (2009). Hull & White (1987) allow for negative interest rates with positive probability, which reflects occasional market conditions.[3] American options are priced by using the MoL. The application of this method to option pricing was first developed by Meyer (1998) in the case of a one-dimensional option pricing model. Subsequently, several extensions have been proposed in the literature including jump-diffusion models, e.g. Meyer (1998) and Chiarella et al. (2009).

By using this computational method, alternative models are directly calibrated to market prices for American options, which enables an analysis of the impact of modelling jumps on option prices and their exercise boundary, while holding the observed market prices fixed for options. The stochastic interest rate model is calibrated to OIS data while the jump-diffusion stochastic volatility options pricing model is calibrated to S&P 100 American options prices. To gauge the effect of the asset and volatility jumps to American options prices, their boundaries and their deltas, three models are considered for the calibration; the Heston-Hull-White (HHW), the Heston-Hull-White with asset jumps (HHWJ), and the Heston-Hull-White with asset and volatility jumps (HHWJJ). By using both global and local optimisation,[4] these models are calibrated to four distinct dates characterised by different volatility levels and interest rates levels.

Findings reveal that consistently with the literature, models with asset jumps improve the overall pricing performance compared to the corresponding diffusion models independent of moneyness and market conditions, while the addition of volatility jumps tend to further improve pricing performance. The impact of jumps on free boundaries is more pronounced during high volatility regimes. Inclusion of asset jumps tend to increase the free boundary, while the addition of volatility jumps marginally drops the free boundary. Chiarella & Ziogas (2009) and Chiarella et al. (2009) found that when the asset jumps are lognormal, their inclusion in the model significantly postpones early exercise, especially when the time-to-maturity is short and the mean asset jump size is negative. They also showed that even small probabilities of jumps can significantly alter the optimal exercise decision in comparison to the early exercise decision based on the Black-Scholes model. As shown

[3]Bakshi et al. (1997), Kim (2002) and Cheng et al. (2018) have shown that stochastic interest rates matter for longer maturity options. Even though this chapter studies pricing of short-dated options, stochastic interest rates affect the free boundary of American options.

[4]The global optimisation was conducted by the Controlled Random Search (CRS) algorithm (Price (1978), Price (1983) and Kaelo & Ali (2006)) and the local optimisation by Constrained Optimisation by Linear Approximations (COBYLA) algorithm (Powell (1994) and Powell (1998)).

in Chapter 2, the inclusion of jumps impacts differently on free boundaries as it lowers (lifts) the free boundaries for options away from (near) expiry. Including further volatility jumps in the asset jumps model results in an increasing free boundary value, and the option holder is less likely to exercise the option.

The results in these studies were obtained under the typical assumption (in this literature) that the overall variance within the models should remain the same - this means that the models (with and without jumps) were compared only on an approximately like-to-like basis. The current study is the first study in which models are compared by fitting to the same market prices of American options. As a result, a more accurate like-to-like comparison is achieved to analyse properly the impact of introducing jumps into a model when the prices of a given set of calibrated instruments with American exercise features are held fixed, allowing us to identify more accurately the effects on the early exercise boundary.

This chapter is structured as follows. Section 3.2 discusses the numerical evaluation of American options with jump-diffusion stochastic volatility and stochastic interest rate models. Section 3.3 describes the data and the methodology in a calibration application to S&P 100 American options. The results of the study that assesses the impact of jumps in the American option pricing problem are presented in Section 3.4. Section 3.5 concludes.

3.2. American Option Pricing Model

American call index options are priced with the Heston (1993) stochastic volatility model and the Hull & White (1987) short rate model in the presence of asset (index) and volatility jumps. Subject to an appropriate filtered probability space, and under the risk-neutral measure $\mathbb{Q}$, the following system of stochastic differential equations is considered:

$$\begin{aligned} dS &= (r - q - \lambda_1 k)\, S dt + \sqrt{V} S dZ_1 + (Y - 1)\, S dN_1, \\ dV &= \kappa\,(\theta - V)\, dt + \sigma_V \sqrt{V} dZ_2 + y dN_2, \\ dr &= a\,(b\,(t) - r)\, dt + \sigma_r dZ_3, \end{aligned} \tag{3.2.1}$$

where, S is the index price process, V is the stochastic variance process, and r is the instantaneous interest rate process. In relation to the index price process S, q is the

continuously compounded dividend yield, λ_1 is the asset jump frequency and

$$k = E^{\mathbb{Q}}(Y-1) = \int_0^{\infty} (Y-1)\, G(Y)\, dY, \tag{3.2.2}$$

where $G(Y)$ is the probability distribution of Y under the risk-neutral measure $\mathbb{Q}$. In line with Merton (1976), Y is log-normally distributed with mean γ and standard deviation δ. Z_1 is the Wiener process driving the index price, $Y-1$ is the random variable percentage change in the index price on the occurrence of a jump, and dN_1 is a Poisson increment for the asset dynamics given by

$$dN_1 = \begin{cases} 1, & \text{with probability} \quad \lambda_1 dt, \\ 0, & \text{with probability} \quad 1-\lambda_1 dt, \end{cases} \tag{3.2.3}$$

in relation to the variance process V, κ is the rate of mean reversion, θ is the long run mean, σ_V is the instantaneous volatility, Z_2 is the Wiener process driving the stochastic volatility process, and dN_2 is defined similarly as equation (3.2.3), with the jump intensity being λ_2. y is the absolute jump size of the volatility process and is exponentially distributed (Duffie et al. (2000)) with mean λ where $\lambda > 0$. The components of the interest rate process r are the rate of mean reversion a, the instantaneous volatility σ_r, the standard Wiener process Z_3, the long run mean $b(t) = c_1 - c_2 e^{-c_3 t}$ where c_1, c_2 and c_3 are positive constants with $c_1 > c_2$. The Wiener processes have a correlation structure given as

$$E^{\mathbb{Q}}(dZ_1 dZ_2) = \rho_{12} dt, E^{\mathbb{Q}}(dZ_1 dZ_3) = \rho_{13} dt, E^{\mathbb{Q}}(dZ_2 dZ_3) = \rho_{23} dt,$$

Let $\tau = T - t$ be the time to maturity. The associated partial-integro differential equation (PIDE) is discussed in detail in Chapter 2, Section 2.2 using the Martingale approach and is given by

$$\begin{aligned} &(r - q - \lambda_1 k) S \frac{\partial C}{\partial S} + (\kappa(\theta - V) - \lambda_V V) \frac{\partial C}{\partial V} + ((a(b(\tau) - r)) - \lambda_r r) \frac{\partial C}{\partial r} + \sigma_V^2 V \frac{1}{2} \frac{\partial^2 C}{\partial V^2} \\ &+ VS^2 \frac{1}{2} \frac{\partial^2 C}{\partial S^2} + \sigma_r^2 \frac{1}{2} \frac{\partial^2 C}{\partial r^2} + VS\sigma_V \rho_{12} \frac{\partial^2 C}{\partial S \partial V} + \sqrt{V} S \sigma_r \rho_{13} \frac{\partial^2 C}{\partial S \partial r} + \sigma_r \sigma_V \sqrt{V} \rho_{23} \frac{\partial^2 C}{\partial V \partial r} \\ &+ \lambda_1 \int (C(YS, \tau) - C(S, \tau)) G(Y)\, dY + \lambda_2 \int (C(V + y, \tau) - C(V, \tau)) g(y)\, dy - rC = \frac{\partial C}{\partial \tau}, \end{aligned} \tag{3.2.4}$$

in the region

$$0 \le \tau \le T, \quad 0 < S \le d(\tau, V, r), \quad 0 < V < \infty, \quad -\infty < r < \infty,$$

where $d(\tau, V, r)$ is the early exercise boundary. The computational domain is

$$0 \leq \tau \leq T, \;\; S_{\min} < S \leq S_{\max}, \;\; V_{\min} < V < V_{\max}, \;\; r_{\min} < r < r_{\max}. \tag{3.2.5}$$

Boundary conditions imposed on this PIDE include the initial condition (payoff function)

$$\lim_{\tau \to 0} C(\tau, S, V, r) = C(0, S, V, r) = \max(S - K, 0),$$

the value matching condition

$$C(\tau, d(\tau, V, r), V, r) = d(\tau, V, r) - K$$

at the free boundary point and the smooth pasting conditions

$$\lim_{S \to d(\tau,V,r)} \frac{\partial C}{\partial S} = 1, \quad \lim_{S \to d(\tau,V,r)} \frac{\partial C}{\partial V} = 0, \quad \lim_{S \to d(\tau,V,r)} \frac{\partial C}{\partial r} = 0 \tag{3.2.6}$$

at the free boundary. Further to this, boundary conditions are imposed on the points S_{min}, S_{max}, V_{min}, V_{max}, r_{min} and r_{max} (Kang & Meyer (2014), Meyer (2015)). At $S = S_{max}$, the value of the call option is

$$C(\tau, S_{max}, V, r) = S_{max} - K,$$

and at $S_{\min}$ the value of the call option is

$$C(\tau, 0, V, r) = 0.$$

At the point $V = V_{\min}$, the PIDE becomes

$$\begin{aligned} &\sigma_r^2 \frac{1}{2} \frac{\partial^2 C}{\partial r^2} + (r - q - \lambda_1 k) S \frac{\partial C}{\partial S} + \kappa\theta \frac{\partial C}{\partial V} + ((a(b(\tau) - r)) - \lambda_r r) \frac{\partial C}{\partial r} - rC \\ &+ \lambda_1 \int (C(YS, \tau) - C(S, \tau)) G(Y) \, dY + \lambda_2 \int (C(y, \tau) - C(0, \tau)) g(y) \, dy = \frac{\partial C}{\partial \tau}, \end{aligned} \tag{3.2.7}$$

and at $r_{\min}$ the PIDE reduces to

$$\begin{aligned} &(r - q - \lambda_1 k) S \frac{\partial C}{\partial S} + (\kappa(\theta - V) - \lambda_V V) \frac{\partial C}{\partial V} + a(b(\tau)) \frac{\partial C}{\partial r} \\ &+ VS^2 \frac{1}{2} \frac{\partial^2 C}{\partial S^2} + VS\sigma_V \rho_{12} \frac{\partial^2 C}{\partial S \partial V} + \sigma_V^2 V \frac{1}{2} \frac{\partial^2 C}{\partial V^2} \\ &+ \lambda_1 \int (C(YS, \tau) - C(S, \tau)) G(Y) \, dY + \lambda_2 \int (C(V + y, \tau) - C(V, \tau)) g(y) \, dy = \frac{\partial C}{\partial \tau}. \end{aligned} \tag{3.2.8}$$

At the boundary points $V_{\min}$ and $r_{\min}$, a quadratic extrapolation is used to obtain the option price by using option values on the first three points along the V- and the r-direction respectively. These were computed by solving the PIDE using a Riccati transformation. The general formula used for quadratic extrapolation is:

$$f(0) = 3f(\Delta x) - 3f(2\Delta x) + f(3\Delta x).$$

At $V = V_{max}$ the PIDE is:

$$\begin{aligned}
&(r - q - \lambda_1 k) S\frac{\partial C}{\partial S} + (\kappa(\theta - V_{max}) - \lambda_V V_{max})\frac{\partial C}{\partial V} + ((a(b(\tau) - r)) - \lambda_r r)\frac{\partial C}{\partial r} \\
&+ V_{max}S^2\frac{1}{2}\frac{\partial^2 C}{\partial S^2} + \sigma_r^2\frac{1}{2}\frac{\partial^2 C}{\partial r^2} + \sqrt{V_{max}}S\sigma_r\rho_{13}\frac{\partial^2 C}{\partial S\partial r} - rC \qquad (3.2.9)\\
&+ \lambda_1\int (C(YS,\tau) - C(S,\tau))\, G(Y)\, dY + \lambda_2\int (C(V_{max} + y,\tau) - C(V_{max},\tau))\, g(y)\, dy = \frac{\partial C}{\partial \tau}.
\end{aligned}$$

At $r = r_{max}$ the PIDE is given as:

$$\begin{aligned}
&(r_{max} - q - \lambda_1 k) S\frac{\partial C}{\partial S} + (\kappa(\theta - V) - \lambda_V V)\frac{\partial C}{\partial V} + ((a(b(\tau) - r_{max})) - \lambda_r r_{max})\frac{\partial C}{\partial r} \\
&+ VS^2\frac{1}{2}\frac{\partial^2 C}{\partial S^2} + \sigma_V^2 V\frac{1}{2}\frac{\partial^2 C}{\partial V^2} + VS\sigma_V\rho_{12}\frac{\partial^2 C}{\partial S\partial V} - r_{max}C \qquad (3.2.10)\\
&+ \lambda_1\int (C(YS,\tau) - C(S,\tau))\, G(Y)\, dY + \lambda_2\int (C(V + y,\tau) - C(V,\tau))\, g(y)\, dy = \frac{\partial C}{\partial \tau},
\end{aligned}$$

and for $V = V_{max}$ and $r = r_{max}$ the PIDE is

$$\begin{aligned}
&(r_{max} - q - \lambda_1 k) S\frac{\partial C}{\partial S} + (\kappa(\theta - V_{max}) - \lambda_V V_{max})\frac{\partial C}{\partial V} + ((a(b(\tau) - r_{max})) - \lambda_r r_{max})\frac{\partial C}{\partial r} - r_{max}C \qquad (3.2.11)\\
&+ \lambda_1\int (C(YS,\tau) - C(S,\tau))\, G(Y)\, dY + \lambda_2\int (C(V + y,\tau) - C(V,\tau))\, g(y)\, dy = \frac{\partial C}{\partial \tau}.
\end{aligned}$$

The index call option price is computed using the MoL by using these boundary conditions and the PIDE at the non-boundary points. For a detailed description of this numerical method, see Chapter 2, Section 2.3.

3.3. Calibration

To assess the impact of jumps on American option prices and their boundaries, a calibration to market data is performed using the stochastic volatility-stochastic interest rate American option pricing models with asset and volatility jumps, see equation (3.2.1). Three models are considered: the Heston-Hull-White (HHW) model, the HHW model with asset jumps

(HHWJ), and the HHW model with asset and volatility jumps (HHWJJ). These models are calibrated to the data of four distinct dates and the significance of the jumps is evaluated accordingly. The data used, and the calibration methodology, are discussed next.

3.3.1. Data. For this study, OIS rates and American S&P 100 index options traded on the Chicago Board of Options Exchange (CBOE) are used. The OIS data was collected from Bloomberg and the S&P 100 index options data was obtained from Wharton School at the University of Pennsylvania through Wharton Research Data Services (WRDS) database.[5]

The OIS rates are being used as a proxy for the risk-free rate. Before the Global Financial Crisis (GFC), LIBOR rates were used mostly for this purpose. There have been discussions about the appropriate risk-free proxy to use, especially when assets do not have any collateral. Hull & White (2013) concluded that OIS rates should be used when both collateralised and non-collateralised assets are being valued. The last panel of Figure 3.5.1 shows the OIS rates from 2006 to 2017 for four tenors: three months, six months, nine months and one year, which are of interest in this chapter since options with short maturities are being considered. OIS rates decreased during the GFC, while they remained very close to zero post-GFC. Since 2015, OIS rates have started to increase.

The first panel of Figure 3.5.1 displays the S&P 100 index over the last ten years. The S&P 100 index has been steadily increasing, with large price fluctuations being experienced in times of market distress. For example, during the GFC, it decreased to a low of 325 index points, and steadily increased to 1,162 in December 2017. The second panel of Figure 3.5.1 displays VXO, the volatility index based on the S&P 100 index. It fluctuates mostly between 10% and 30%, with occasional higher spikes like the one during the GFC, which reached a level of almost 90%.

[5]The S&P 100 is a subset of S&P 500, constituting 100 major US companies, which form around 63% of the total market value of the S&P 500. The S&P 100 index was first traded in the CBOE on the 15th of June 1983, being used to measure the performance of large cap companies in the US. Before long, large volumes of OEX index options were being traded at the CBOE, i.e. in December 1984, the average daily volume of these options was 296,230 contracts which was greater than the average daily volume of the 231,917 contracts for all equity options (Sheikh (1991)). Since then, more than a billion S&P 100 option contracts have been traded, making it one of the most commonly used tools in portfolio management. S&P 100 index call/put options are both European and American, in contrast to S&P 500 index options, which are only European. At inception, only the OEX American style options were being used. In 1993, VXO, a volatility index based on the S&P 100 index, was introduced by CBOE. The OEX European style options were introduced in July 2001, to cater for all type of investors, since some investors prefer certainty associated with the European style feature (http://www.cboe.com).

For this calibration, four dates are selected, each one representing different market conditions in terms of volatility and the level of interest rates. These dates are: 10th October 2008, 10th August 2011, 20th June 2014 and 18th May 2017. The first two dates are characterised by high volatility, however in 2008 interest rates were relatively high between $2\% - 4\%$, while in 2011 interest rates were around 0%. On 10 October 2008, one of the highest volatilities was recorded, with VXO reaching 89% as a result of the GFC. During the Eurozone debt crisis, VXO reached 46.6% on 10th August 2011, marking another high volatility regime for VXO. On 10th June 2014 and 18th May 2017, the market experienced low volatilities with VXO at 9.81% and 13.52% respectively. Indeed, in June 2014, one of the lowest volatilities over the past 10 years was observed. Further, in June 2014, interest rates were extremely low, while in May 2017, interest rates had risen. These dates are marked in the middle panel of Figure 3.5.1.

TABLE 3.3.1. Bid/Ask OIS rates and corresponding discount factors on four dates: the 10th October 2008, 10th August 2011, 10th June 2014, and 18th May 2017.

	10/08/08		**10/08/11**		**10/06/14**		**18/05/17**	
T	**Bid**	**Ask**	**Bid**	**Ask**	**Bid**	**Ask**	**Bid**	**Ask**
0.25	1.149	1.170	0.07	0.09	0.091	0.1063	1.0104	1.0172
0.5	1.135	1.159	0.075	0.083	0.103	0.109	1.0591	1.0636
0.75	1.193	1.213	0.074	0.081	0.114	0.12	1.0986	1.0986
1	1.316	1.335	0.0725	0.0825	0.139	0.144	1.1295	1.1295
2	1.929	1.931	0.113	0.1175	0.42	0.425	1.2386	1.2480
3	2.577	2.577	0.251	0.301	0.823	0.863	1.3520	1.3620
4	2.973	2.990	0.563	0.592	1.22	1.27	1.4210	1.4710
5	3.266	3.266	0.914	0.954	1.552	1.602	1.5200	1.5300
6	–	–	–	–	1.843	1.853	1.5810	1.6310
7	–	–	–	–	2.046	2.096	1.6430	1.6930
8	–	–	–	–	2.239	2.249	1.7010	1.7510
9	–	–	–	–	2.384	2.394	1.7560	1.8060
10	3.850	3.887	2.145	2.185	2.490	2.540	1.8380	1.8380
	Discount	**Rates**	**Discount**	**Rates**	**Discount**	**Rates**	**Discount**	**Rates**
0.25	0.99714	0.99708	0.99983	0.99978	0.99977	0.99973	0.99748	0.99746
0.5	0.99436	0.99424	0.99963	0.99959	0.99949	0.99946	0.99473	0.99471
0.75	0.99113	0.99098	0.99945	0.99939	0.99915	0.99910	0.99183	0.99183
1	0.98697	0.98678	0.99928	0.99918	0.99861	0.99856	0.98880	0.98881
2	0.96240	0.96236	0.99774	0.99765	0.99164	0.99154	0.97567	0.97549
3	0.92590	0.92590	0.99250	0.99101	0.97559	0.97441	0.96045	0.96017
4	0.88811	0.88750	0.97766	0.97653	0.95220	0.95028	0.94501	0.94311
5	0.84935	0.84937	0.95501	0.95309	0.92483	0.92251	0.92709	0.92665
6	–	–	–	–	0.89426	0.89380	0.90978	0.90701
7	–	–	–	–	0.86492	0.86181	0.89159	0.88844
8	–	–	–	–	0.83352	0.83299	0.87291	0.86939
9	–	–	–	–	0.80358	0.80300	0.85381	0.84994
10	0.57997	0.57661	0.73378	0.72955	0.77553	0.77139	0.83620	0.83199

TABLE 3.3.2. Dividend yields, VOX price and index level of four days: the 10th October 2008, 10th August 2011, 10th June 2014, and 18th May 2017.

	10/10/2008	**10/08/2011**	**10/06/2014**	**18/05/2017**
Dividend yield	2.71%	2.12%	1.94%	1.81%
VOX Price	89.74%	41.47%	9.81%	13.52%
S&P 100 Index Level	427.45	506.61	864.67	1044.44

Table 3.3.1 displays the OIS data and corresponding discount factors for these four days. Credit Support Annex (CSA) agreements under the International Swaps and Derivatives Association Master Agreement require that collateral calls be made daily to mitigate risks associated with respective transactions. An overnight rate (OIS) is used in computing discount factors for these transactions, and this is known as OIS discounting. An OIS rate is used as a proxy for risk-free interest rates in the discounting equation. The OIS discount equation under the risk neutral measure $\mathbb{Q}$, when borrowing from t to T is given in equation (3.3.1) below:

$$DF_{OIS} = E_t^{\mathbb{Q}}\left[e^{-\int_t^T r_c(s)ds}\right] \tag{3.3.1}$$

where r_c is the continuously compounded interbank overnight rate. The OIS discount factor curve is obtained by bootstrapping using the OIS curve. This is discussed in detail by Alfeus, Grasselli & Schlögl (2017). The discount factors obtained are used to calibrate the parameters of the Hull-White interest rate model, whose bond pricing formula is given in equation (3.3.3).

The S&P 100 index option prices are given as the highest closing bid across all exchanges and the lowest closing ask across all exchanges. To filter this data, quotes have been removed based on the following criteria: (i) bid/ask price quotes that are small in value, i.e. less than 0.1 to avoid microstructure biases (Abudy & Izhakian (2013)); (ii) bid/ask prices with call option values, such that $C < \max(S-K, 0)$ to avoid arbitrage opportunities ; (iii) bid/ask price quotes whose moneyness $K/S - 1 > 0.5$ (Kokholm & Stisen (2015)). Based on the index level on each of these days, the moneyness intervals are selected. Thus, on 10th October 2008, the models are calibrated to deep ITM $(320-360)$, ITM $(380-400)$, ATM $(420-440)$, OTM $(460-560)$ and deep OTM $(580-740)$ S&P 100 index American call options. There are 22 quoted prices of American call options on 10 October 2008 with

an expiration of 0.4438 years. By filtering out bid price quotes that are equal to zero, 17 bid/ask price quotes are used for the calibration. On 10th August 2011, the models are calibrated to deep ITM $(300-380)$, ITM $(400-480)$, ATM $(500-520)$, OTM $(540-580)$ and deep OTM $(600-700)$ S&P 100 index American call options. There are 21 quoted prices of American call options on 10 August 2011 with an expiration of 0.3534 years. After filtering out bid/ask quotes that are less than 0.01, 17 bid/ask price quotes are left. On 10th June 2014, the models are calibrated to deep ITM $(360-680)$, ITM $(700-850)$, ATM $(860-880)$ and OTM $(900-920)$ S&P 100 index American call options. There are 30 quoted prices of American call options on this date with an expiration of 0.4438 years and after filtering out[6], 25 bid/ask price quotes for the calibration are left. Finally, on 18th May 2017, the models are calibrated to four subsets: deep ITM $(300-740)$, ITM $(760-980)$, ATM $(1000-1060)$ and OTM $(1080-1260)$ S&P 100 index American call options. There are 49 quoted prices of American call options on this date with an expiration of 0.578 years, which after filtering leaves us with 29 bid-ask quotes for the calibration. In addition to the S&P 100 index options data, information on the S&P 100 index dividend yield, the VOX index price, and the S&P 100 index price data is obtained from the same database for all four dates, and the data is given in Table 3.3.2.

For ease of calibration, calibration for each day is performed in two steps using these two sets of data. Firstly, calibration to the US OIS rates data is performed and then to the S&P 100 American call options data.

3.3.2. Calibration Methodology. By considering three American option pricing models, namely HHW, HHWJ, and HHWJJ, the aim is to obtain optimum parameter values such that the model prices are between the bid/ask prices for each of these days. First, calibration of Hull & White (1987) interest rate model parameters to the US OIS rates data is done. Using these parameter values, a calibration of the remaining model parameters to S&P 100 index options data is performed. Lastly, a comparison of model prices obtained using these new parameters to market data is carried out, to assess the impact of jumps on the pricing performance of these models.

[6]Bid price quotes that are equal to zero, and bid/ask price quotes whose money-ness $K/S-1>0.5$ are filtered out (Kokholm & Stisen (2015)).

3.3.2.1. *Calibration to OIS data.* To calibrate the Hull & White (1987) interest rate model to US OIS rates, the objective function

$$\min_{x} \left\{ \left| g\left(x\right) - market_{bid} \right| + \left| g\left(x\right) - market_{ask} \right|, \right\} \tag{3.3.2}$$

where $market_{bid}$ is the market bid price, $market_{ask}$ is the market ask price for US OIS interest rates and $g\left(x\right)$ is the model price is considered. This model price is the price of a zero-coupon bond, which is given by Kang & Ziveyi (2018)

$$\begin{aligned} g_{model}\left(t,T\right) &= \widehat{H}\left(t,T\right) e^{-\beta(t,T)r(t)}, \\ \widehat{H}\left(t,T\right) &= H\left(t,T\right) \exp\left(-a \int_{t}^{T} b\left(u\right) \beta\left(u,T\right) du \right), \\ H\left(t,T\right) &= \exp\left(-\frac{\sigma_r^2}{2a^2} \left(\beta\left(t,T\right) - \left(T-t\right) \right) - \frac{\sigma_r^2}{4a} \beta\left(t,T\right)^2 \right), \\ \beta\left(t,T\right) &= \frac{1 - e^{-a(T-\tau)}}{a}. \end{aligned} \tag{3.3.3}$$

All the input parameters have been defined in Section 3.2. This non-linear objective function is used to obtain the Hull & White (1987) interest rate model parameters using both local and global optimisation algorithms, which will be discussed in Section 3.3.3.1.

3.3.2.2. *Calibration to S&P 100 index options data.* The interest rate parameter values obtained from the first calibration are used as inputs to calibrate the Heston (1993) model with jumps in both asset and volatility dynamics to S&P 100 index options data. The non-linear objective function used to obtain the parameter values for the three models is:

$$\min_{x} \left\{ \sum^{N} \left(\left(\frac{\max\left(market_{bid} - \left(f\left(x\right) \right), 0.0 \right)}{market_{bid}} \right) + \left(\frac{\max\left(\left(f\left(x\right) - market_{ask} \right), 0.0 \right)}{market_{ask}} \right) \right)^2 \right\}, \tag{3.3.4}$$

where $market_{bid}$ is the market bid price, $market_{ask}$ is the market ask price for S&P 100 index options, $f\left(x\right)$ is the model price obtained using the MoL (see Chapter 2), and N is the total number of options being used in the calibration.[7]

[7]For the application of the MoL, S, V, r and τ are discretised. For example, on the 18th of May 2017, in the S direction, a non-uniform mesh is used in which $S_{\min} = 0$ and $S_{\max} = 4000$ with 300 grid points on $[100, 920]$, 205 grid points on $[920, 1120]$, 210 grid points on $[1120, 3000]$ and 100 grid points on $[3000, 4000]$, thus in total, there are 815 grid points. In the r direction, there are 10 grid points in which $r_{\min} = 0$ and $r_{\max} = 2\%$. There are 10 grid points in the V direction with $V_{\min} = 0$ and $V_{\max} = 0.16$. Discretisations on other dates have been amended accordingly, depending on the interest rates and the volatilities on the day, together with the asset prices.

3.3.3. Optimization. For this non-linear calibration, both global and local optimisers are used.[8]

3.3.3.1. *Global Optimisation - Controlled Random Search (CRS) with local mutation.* A global optimisation algorithm that is available in the open-source library NLopt for non-linear optimisation, namely, the Controlled Random Search (CRS) with local mutation, named $NLOPT\_GN\_CRS2\_LM$ is used firstly. The NLopt library contains local and global algorithms, and for local algorithms, both derivative-free and gradient-based methods have been provided. The Controlled Random Search (CRS) with a local mutation algorithm was originally discussed by Price (1978) and Price (1983), and most recently by Kaelo & Ali (2006). It is a type of search method that starts with a random number of points, which are evolved heuristically, like the Nelder-Mead algorithm (NLOPT Documentation). Initially, a set S is filled with N points. The current worst point is replaced with a trial point if it is better than the worst point. This process is repeated until a certain specified condition is met. This algorithm type also requires a specification of boundary constraints.

3.3.3.2. *Local Optimisation - Constrained Optimisation BY Linear Approximations (COBYLA).* Having obtained the parameter values using the global optimiser, the values are refined to improve accuracy. As a starting point, the global optimum values obtained in the Controlled Random Search (CRS) with local mutation optimisation are used. The Constrained Optimisation BY Linear Approximations (COBYLA) algorithm, found in the open-source library NLopt, is used for this purpose. It is a derivative free algorithm, which was derived from an implementation discussed in the paper by Powell (1994), and is suitable for use when it is not possible to obtain first derivatives. It supports both linear and nonlinear constraints.[9]

3.3.4. Model Comparison. To compare the performance of the models, in terms of the contribution of asset and volatility jumps in improving pricing performance, three measures are employed: the Average Relative Pricing Error (ARPE) and the Average Relative Bid-Ask Error (ARBAE) (Kokholm & Stisen (2015)). $E_{Objective}$ is the error

[8]Codes on Intel Fortran for both the Intel optimiser and the NLOPT optimization algorithms are run on a PC with Intel CORE i7, 2.70GHz processer, 8.00G of RAM on a Windows 10 64-bit operating system.

[9]Originally local optimisation involving trust region methods was used. As the fit to the data was not good, both the global and local optimisers discussed above were employed. For comparison purposes, a summary of the results with the trust region methods is given in the Appendix 3.1

obtained after minimising the objective function (Alfeus et al. (2017)). The benchmark is the quoted S&P 100 call option values and an analysis into which of the three models reports a lesser pricing error when calibrated to quoted market prices is performed. The ARBAE is used to measure the average error of model prices which fall outside of the bid-ask spread (Kokholm & Stisen (2015)). A model with a smaller value of ARPE/ARBAE indicates a better fit to the market data. These performance measures are defined below as follows:

$$ARPE = \frac{1}{N}\sum_{i=1}^{N}\frac{\left|market_i^{Mid} - market_i^{Model}\right|}{market_i^{Mid}},$$

$$ARBAE = \frac{1}{N}\sum_{i=1}^{N}\frac{\max\left\{\left(market_i^{Model} - market_i^{Ask}\right)^+, \left(market_i^{Bid} - market_i^{Model}\right)^+\right\}}{market_i^{Mid}},$$

$$E_{Objective} = \sum^{N}\left(\left(\frac{\max\left(market_i^{bid} - \left(f\left(x\right)\right), 0.0\right)}{market_i^{bid}}\right) + \left(\frac{\max\left(\left(f\left(x\right) - market_i^{ask}\right), 0.0\right)}{market_i^{ask}}\right)\right)^2 \tag{3.3.5}$$

where $market_i^{Bid}$ is the i^{th} market bid price, $market_i^{Ask}$ is the i^{th} market ask price, $market_i^{Mid}$ is the i^{th} market mid-price and $market_i^{Model}$ is the i^{th} model price for S&P 100 index options. N is the total number of quotes.

3.4. Numerical Results

This section discusses the results of the calibration application. The calibrated parameters are first presented and analysed, after which an assessment on the importance of jumps when fitting to market data is performed. Then the impact of jumps on the free boundaries and the option's Delta is assessed.

3.4.1. Calibrated parameters. The stochastic volatility - stochastic interest rate American option pricing models (with asset and volatility jumps) are calibrated to four dates: 10th October 2008, 10th August 2011, 10th June 2014, and 18th May 2017.

3.4.1.1. *Calibration to OIS rates.* In the first stage of this calibration, a calibration of the Hull & White (1987) interest rate model to OIS rates is done. Parameter values for σ_r and a are obtained from Cheng et al. (2018) as the associated period partly overlaps with the selected dates for this study. r_o is the observed OIS rate for the corresponding date. To avoid different tenors being outside the bid/ask values, a value for $b(t)$ in each tenor is obtained, such that the model discount factor is between the bid/ask discount factors. Table 3.4.1 presents the calibrated parameter values of the stochastic interest rate model on the four selected dates. Figure 3.5.3 plots the errors between the bid/ask OIS discount factors and the model discount factors using the parameter values of Table 3.4.1. These graphs show that the OIS discount factors are within the bid/ask values, which is indicative of parameter values that reflect market data.

TABLE 3.4.1. Parameter values obtained from calibrating the Hull & White (1987) interest rate model to OIS data. $b(u)$ has been defined separately in each tenor, such that the resulting discount factors are within the bid/ask values. Trust Region Methods and CRS with local mutation algorithms have been used for optimisation.

Parameters	10/10/2008	10/08/2011	10/06/2014	18/05/2017
σ_r	0.0058	0.0058	0.0058	0.0058
a	0.0492	0.0492	0.0492	0.0492
r_0	0.0115	0.00079	0.0011	0.0106
$b(u)$				
$[0 \leq u \leq 0.25]$	0.00828	0.00087	0.00037	0.00745
$[0.25 < u \leq 0.5]$	0.02652	0.00260	0.00356	0.02547
$[0.5 < u \leq 0.75]$	0.04703	0.00484	0.00712	0.04405
$[0.75 < u \leq 1]$	0.10099	0.00735	0.01392	0.07990
$[1 < u \leq 2]$	0.05563	0.00523	0.01651	0.03496
$[2 < u \leq 3]$	0.14939	0.02355	0.06197	0.07015
$[3 < u \leq 4]$	0.24010	0.07394	0.13032	0.10702
$[4 < u \leq 5]$	0.33214	0.15356	0.20626	0.14717
$[5 < u \leq 6]$	-	-	0.28480	0.19331
$[6 < u \leq 7]$	-	-	0.36341	0.23248
$[7 < u \leq 8]$	-	-	0.42979	0.27726
$[8 < u \leq 9]$	-	-	0.50079	0.32346
$[9 < u \leq 10]$	0.39996	0.24518	0.57359	0.34610

3.4.1.2. *Calibration to S&P 100 American call options.* In the second stage of this calibration, a calibration to American option prices is performed to three American option pricing models, namely, HHW, HHWJ and HHWJJ. Table 3.4.2 displays the calibrated parameter values of these models in the four selected dates.

During the GFC, the S&P 100 index experienced a decline in a regime of extremely high volatility. At the same time, interest rates had started to drop, and they were around 2% at the time. Accordingly, on 10th October 2008, the parameter values reveal high volatility levels and high volatility of the volatility (with the long run mean of the variance at 6.51%, the volatility of volatility at 81.66% and the level of the variance at 42% for the HHWJJ model). The second highest volatilities occurred on 10th August 2011, with the lowest volatility estimates took place on 10th June 2014. These volatility calibrated values are consistent with the market observed conditions on these days as displayed in Figure 3.5.1.

In the absence of jumps, the volatility estimates are typically higher, with the inclusion of jumps lowering the values of these estimates. As jumps are added into the models, the variation is distributed between the diffusion component and the jump components of the variance, causing the estimates of the long run mean of variance, the volatility of volatility and the level of variance to decrease. This is also found in previous literature including Eraker (2004), Bates (1996), Bakshi et al. (1997), Chiarella et al. (2009), and in Chapter 2.

Empirical evidence of a strong negative correlation in the index returns and volatility is found. Depending on the model specifications, this correlation ranges between -0.9 and -0.6 in all the dates, see Table 3.4.2. The models with jumps exhibit lower correlations in magnitude which are typically more representative parameter values. This well documented negative relation between equity returns and volatility (known also as asymmetric volatility) has been credited to the leverage effect and the volatility feedback effect, and, more recently, to behavioural effects.[10] An empirical study by Giot (2005), where S&P 100 and NASDAQ 100 are considered, reveals a negative relationship between the returns of the stock index and the corresponding volatility index. Further, negative correlation between the S&P 100 index and the interest rates is found, which is supported by Fama (1981*b*) and Fama (1981*a*). Several papers focus on different economic environments, which enable stocks and interest rates to move together or in different directions, i.e. Stivers & Sun (2002)

[10]According to the leverage effect (Black (1976)), negative equity return shocks increase firms leverage and consequently volatility. The volatility feedback effect introduced by Campbell & Hentschel (1992) suggests that any change (and in particular increase) in volatility causes a reduction in stock returns. In line with behavioural effects, representativeness, affect and extrapolation bias make positions with high returns and low risk preferred due to a good investment representation (Hibbert, Daigler & Dupoyet (2008)). Farid AitSahlia & Guha (2010) show accordingly that the equity markets react more to negative news than otherwise.

found that shares and bonds tend to move together when stock market uncertainty is low, and they have a very low/negative correlation when uncertainty is high.

TABLE 3.4.2. **Parameters Estimates** Parameter estimates obtained from calibrating the HHW, HHWJ, and HHWJJ models to S&P 100 American call option prices on 10th October 2008, 10th August 2011, 10th June 2014, and 18th May 2017. Both the Constrained Optimisation BY Linear Approximations (COBYLA) algorithm and the Controlled Random Search (CRS) with local mutation algorithm have been used for optimisation. Parameter values from the calibration of the Hull & White (1987) stochastic interest rate model to OIS data are used as inputs to obtain the remaining of the model parameters.

	κ	θ	σ_V	ρ_{12}	ρ_{13}	λ_1	δ	γ	λ_2	λ	V_0
10/10/2008											
HHW	2.2369	0.0798	0.9613	-0.891	-0.33	-	-	-	-	-	0.52
HHWJ	2.1111	0.0718	0.8506	-0.762	-0.31	0.1196	0.8071	-1.5169	-	-	0.42
HHWJJ	2.0811	0.0651	0.8166	-0.757	-0.20	0.1013	0.8071	-1.5169	3.33	238	0.42
10/08/2011											
HHW	12.992	0.0386	1.3355	-0.78	-0.31	-	-	-	-	-	0.41
HHWJ	12.988	0.0356	1.3254	-0.74	-0.25	0.0532	0.4510	-1.0852	-	-	0.39
HHWJJ	12.957	0.0201	1.2947	-0.73	-0.25	0.0512	0.4510	-1.0106	2.95	320	0.39
10/06/2014											
HHW	0.6569	0.014	0.2873	-0.78	-0.10	-	-	-	-	-	0.134
HHWJ	0.6271	0.0107	0.2573	-0.68	-0.33	0.0223	4.9646	-1.3266	-	-	0.105
HHWJJ	0.5771	0.0097	0.2512	-0.66	-0.20	0.0217	4.0647	-2.9562	2.92	299	0.098
18/05/2017											
HHW	0.9795	0.0199	0.82094	-0.78	-0.35	-	-	-	-	-	0.1765
HHWJ	0.9714	0.0198	0.62100	-0.61	-0.35	0.01881	5.7841	-1.0019	-	-	0.1286
HHWJJ	0.9639	0.0168	0.61935	-0.60	-0.30	0.01818	4.8946	-2.7962	2.96	299	0.1257

Finally, the asset jump intensities tend to depend on the level of volatility experienced on the day, i.e. when the volatility was at the highest on 10th October 2008, the highest asset jump intensity of 0.1013 was observed, while on the 10th of June 2014, the date with the lowest volatility, the asset jump intensity was very low, with an estimate of 0.0217 for a HHWJJ model. During the Eurozone debt crisis and on 10th of August 2011, the asset and volatility jump intensities were lower compared to the 10th of October 2008; the expected volatility jump size was 1/238 = 0.0042 in 2008 and 1/320 = 0.031 in 2011.

Overall, the calibrated parameter values capture effectively the changing market conditions on these four selected dates in terms of the level of volatility, correlations, and jump specifications.

3.4.2. Pricing performance. Table 3.4.3 compares the pricing performance of the three models over the four dates by considering three measures; the ARPE, ARBAE and $E_{Objective}$ function. All three measures demonstrate an overall good fit of the models to the market data, where the dates in 2011, 2014 and 2017 displaying very small errors, while in the most volatile date in 2008 higher (yet acceptable) errors are reported. Typically, models fit better to ITM options with some deterioration when considering the fit to ATM and OTM options. The results suggest that when the volatility is high, the model with asset and volatility jumps is closer to the mid-price for deep ITM and deep OTM options in comparison to the model with asset jumps only and asset and the model with no jumps. When the volatility is low, it is observed that the model with asset and volatility jumps is closer to the mid-price when options are deep ITM, ATM, and OTM.

To gauge the performance of the calibrated models to reflect market data, the model prices are compared to quoted bid/ask prices. Figure 3.5.4, Figure 3.5.5, Figure 3.5.6 and Figure 3.5.7 depict the differences between the model index prices and the quoted bid/ask prices over different moneyness intervals on the four selected dates, respectively. Three main observations are made. First, for all four dates, the model with no jumps exhibits the least performance with an improvement in the fit when asset jumps and volatility jumps are included in the model. Second, with regards to moneyness, typically, OTM, ATM, and ITM options fit well within the bounds. Deep ITM options are mostly within the bid-ask range with the occasional exemption on 18th May 2017, which is slightly below the bid price, although the difference is very small. Thirdly, the model with assets and volatility jumps consistently provides a significant improvement (over the other two models) in fitting within the boundaries, especially over the volatile dates in 2008 and 2011.

3.4.3. The impact of jumps on the free boundaries. Figure 3.5.8, Figure 3.5.9, Figure 3.5.10 and Figure 3.5.11 depict the impact of the jumps on the free boundaries (over different moneyness intervals) on the four selected dates respectively. Each date has a fixed asset price, and a range of strikes used for calibration. For each strike, the option prices together with the free boundaries and Greeks have been computed for a different combination of S, V and r. Certain strikes for the analysis have been selected depending on whether the strike price is less than/greater than/equal to the fixed asset price for the day

and have defined this in terms of moneyness ($S > K$ being in-the-money, $S < K$ being out-of-money and $S = K$ being at-the-money).

The models with asset jumps and volatility jumps bring an increase in the level of the free boundaries compared to the models with no jumps. However, when volatility jumps are added to asset jumps, the level of free boundaries is marginally reduced. This holds consistently at all levels of the options moneyness and for all market environments (for all the four selected days). However, the magnitude of these changes varies over the four dates. On 10th of October 2008 (see Figure 3.5.8), the free boundary for near to maturity contracts almost doubles compared to a moderate 20% increase in 2011, 15% in 2014 and 50% in 2017 as shown in Figure 3.5.9 - Figure 3.5.11, respectively. The magnitude of these changes tend to be analogous to the volatility levels on the selected days. However, the higher interest rates in 2017 may have played a role in augmenting the impact of the jumps in the free boundary, even though the volatility on 18th May 2017 was relatively low.

To analyse the impact of jumps on early exercise boundaries, the general approach adopted in most literature is to fix the variance in all the nested models, to ensure consistent variance over the corresponding time period (Chiarella & Ziogas (2009), Chiarella et al. (2009)), which is also the approach used in Chapter 2 of the thesis. However, in this chapter, the calibration determines the parameter values, including variance, the models are fitted to the same American option prices, yet similar results are obtained. Chiarella & Ziogas (2009) show the impact of jumps on free boundary changes, depending on the options expiration and market conditions. When the risk-free rate is lower than the dividend yield and the mean asset jump size of the lognormal jumps is positive then near (far from) expiry, the free boundaries for the HHW model is lower (higher) than the free boundaries for the HHWJ and the HHWJJ models. However, when the mean asset jump size is negative then the free boundaries for the HHW model is always lower than the free boundaries for the jump-diffusion HHW models. Table 3.4.2 provides evidence of negative mean asset jumps size while Table 3.3.1 and Table 3.3.2 reveals that risk-free rate was lower to the dividend yield (on the four dates). Accordingly, the early exercise boundary of the models with jumps are always found to be above the boundary of the HHW model, implying that

holders of American call options tend to delay early exercise in order to eliminate the impact of downward jumps.

TABLE 3.4.3. **Pricing Performance** The table reports the pricing performance of the three models HHW, HHWJ, and HHWJJ depending on the level of moneyness by using Average Relative Pricing Error (ARPE), Average Relative Bid-Ask Error (ARBAE), and $E_{Objective}$ error. The benchmark is the bid/ask prices of the S&P 100 index options data.

	10 October 2008				10 August 2011			
Model	Moneyness (S/K)	ARPE	ARBAE	$E_{Objective}$	Moneyness (S/K)	ARPE	ARBAE	$E_{Objective}$
HHW	**Deep-OTM**	40.26%	0.00%	0.00%	**Deep-OTM**	2.70%	0.00%	0.00%
HHWJ	$(S/K < 0.75)$	14.81%	0.00%	0.00%	$(S/K < 0.85)$	5.67%	0.00%	0.00%
HHWJJ		11.49%	0.00%	0.00%		0.70%	0.00%	0.00%
HHW	**OTM**	6.62%	0.00%	0.00%	**OTM**	2.11%	0.00%	0.00%
HHWJ	$(0.75 < S/K < 0.95)$	8.45%	0.00%	0.00%	$(0.85 < S/K < 0.95)$	0.68%	0.00%	0.00%
HHWJJ		7.58%	0.00%	0.00%		2.49%	0.00%	0.00%
HHW	**ATM**	4.92%	0.00%	0.00%	**ATM**	1.32%	0.00%	0.00%
HHWJ	$(0.95 < S/K < 1.05)$	2.41%	0.00%	0.00%	$(0.95 < S/K < 1.05)$	1.19%	0.00%	0.00%
HHWJJ		0.58%	0.00%	0.00%		1.38%	0.00%	0.00%
HHW	**ITM**	2.51%	0.00%	0.00%	**ITM**	0.29%	0.00%	0.00%
HHWJ	$(1.05 < S/K < 1.15)$	2.22%	0.00%	0.00%	$(1.05 < S/K < 1.3)$	0.44%	0.00%	0.00%
HHWJJ		0.50%	0.00%	0.00%		0.26%	0.00%	0.00%
HHW	**Deep-ITM**	0.46%	0.00%	0.00%	**Deep-ITM**	0.43%	0.00%	0.00%
HHWJ	$(S/K > 1.15)$	1.53%	0.00%	0.00%	$(S/K > 1.3)$	0.19%	0.00%	0.00%
HHWJJ		0.21%	0.00%	0.00%		0.28%	0.00%	0.00%
HHW	**Overall**	12.76%	0.00%	0.00%	**Overall**	0.88%	0.00%	0.00%
HHWJ		7.28%	0.00%	0.00%		0.82%	0.00%	0.00%
HHWJJ		5.54%	0.00%	0.00%		0.74%	0.00%	0.00%
	10 June 2014				18 May 2017			
Model	Moneyness (S/K)	ARPE	ARBAE	$E_{Objective}$	Moneyness (S/K)	ARPE	ARBAE	$E_{Objective}$
HHW	**OTM**	2.85%	0.00%	0.00%	**OTM**	5.47%	0.00%	0.00%
HHWJ	$(S/K < 0.97)$	3.30%	0.00%	0.00%	$(S/K < 0.98)$	4.39%	0.00%	0.00%
HHWJJ		1.94%	0.00%	0.00%		1.48%	0.00%	0.00%
HHW	**ATM**	1.92%	0.00%	0.00%	**ATM**	2.52%	0.00%	0.00%
HHWJ	$(0.97¡S/K < 1.01)$	1.69%	0.00%	0.00%	$(0.97 < S/K < 1.01)$	2.04%	0.00%	0.00%
HHWJJ		0.15%	0.00%	0.00%		0.79%	0.00%	0.00%
HHW	**ITM**	0.48%	0.00%	0.00%	**ITM**	0.32%	0.00%	0.00%
HHWJ	$(1.01 < S/K < 1.40)$	0.48%	0.00%	0.00%	$(1.05 < S/K < 1.40)$	0.56%	0.00%	0.00%
HHWJJ		0.58%	0.00%	0.00%		0.78%	0.00%	0.00%
HHW	**Deep-ITM**	0.06%	0.00%	0.00%	**Deep-ITM**	0.39%	0.0805%	0.08%
HHWJ	$(S/K > 1.40)$	0.06%	0.00%	0.00%	$(S/K > 1.40)$	0.22%	0.0123%	0.01%
HHWJJ		0.06%	0.00%	0.00%		0.23%	0.0161%	0.02%
HHW	**Overall**	0.54%	0.00%	0.00%	**Overall**	0.94%	0.029%	0.93%
HHWJ		0.54%	0.00%	0.00%		0.84%	0.006%	0.18%
HHWJJ		0.42%	0.00%	0.00%		0.59%	0.007%	0.22%

3.4.4. Greeks. The MoL conveniently allows the obtaining of Greeks at the same computational level as the option price. Hence, an investigation into the impact of jumps on the options delta is performed. Figure 3.5.12, Figure 3.5.13, Figure 3.5.14 and Figure 3.5.15 show the differences in the values of delta between the diffusion models and the corresponding jump-diffusion models on 10th October 2008, 10th August 2011, 10th June 2014, and 18th May 2017, respectively. Regarding these figures, the red dotted line represents the differences in delta between the diffusion model with stochastic volatility and stochastic interest rate and the corresponding model with asset and volatility jumps. The

black dotted line represents the differences in delta between the same diffusion model and the corresponding model with asset jumps only. Negative (positive) differences indicated by the graphs mean that model delta (asset jumps or asset and volatility jumps) is greater (lower) than the delta in the case of a pure diffusion model.

Figures 3.5.12–3.5.15 show that the inclusion of jumps impacts on the option delta with the most impact being on OTM and ATM options. The impact of jumps on the delta for deep-ITM and deep-OTM options is marginal. Further, including asset jumps typically increases the delta for OTM options and reduces the delta for ATM and ITM options. The delta decreases slightly for the case of a model with asset-volatility jumps. For ITM call option, the delta for the asset jumps model is lower than the delta for the model without jumps. Thus, including asset jumps and volatility jumps impacts significantly the option delta, although the impact is slightly less with the addition of volatility jumps. Hence, the inclusion of jumps impacts the free boundary differently, and tends to depend on the volatility level.

3.5. Conclusion

This chapter evaluates the significance of asset and volatility jumps in pricing American index call options. The study examines the ability of jump-diffusion models to improve option pricing performance and analyses the impact of jumps in the free boundary and delta of the options. To this end, the Heston-Hull-White model with asset and volatility jumps is solved numerically by using the MoL and is then calibrated to OIS data and S&P 100 index call options data.

Models with asset jumps consistently improve the overall pricing performance compared to the corresponding diffusion models, with further improvement occurring when the volatility jumps are added. The addition of the asset jumps provides a consistent improvement independent of moneyness and market conditions, while the addition of volatility jumps tend to improve the pricing performance further. In accordance with previous literature, empirical evidence of the importance of jumps in improving the ability of models to better price short-dated American options is provided, especially when markets experience financial stress.

The impact of jumps on the free boundaries is significant and more pronounced during volatile market conditions. Inclusion of asset jumps tend to increase the free boundary, while the addition of volatility jumps marginally drops the free boundary with more noticeable effects on near maturity options. An analysis of the impact of jumps on options delta shows that, asset jumps typically increase the delta for OTM options with asset jumps, and reduce the delta for ATM and ITM options, while volatility jumps marginally reduce the delta.

As expected, models with more parameters tend to fit better market data compared to simpler nested models and a back testing exercise will provide a more solid assessment on pricing performance. However, the objective of this study is to compare nested models when fitted to the same market prices (e.g. American options). Calibrating different models to the same traded option prices should remove any model risk (at least for those instruments to which the model is calibrated). We find substantial differences that imply that model risk still remains in optimal exercise strategies

These results highlight the significance of including asset and volatility jumps in American options pricing and hedging applications, which are of critical importance to hedge funds and financial investors. American option holders become more skeptical with their exercise decision with increasing volatility and market conditions liable to jumps.

In this calibration a smaller subset of data with specific maturity is considered. As an extension to this chapter, calibration to a larger data set, i.e. consisting of all maturities for the day can be considered to observe if the impact of jumps on the free boundary remains similar.

Figures

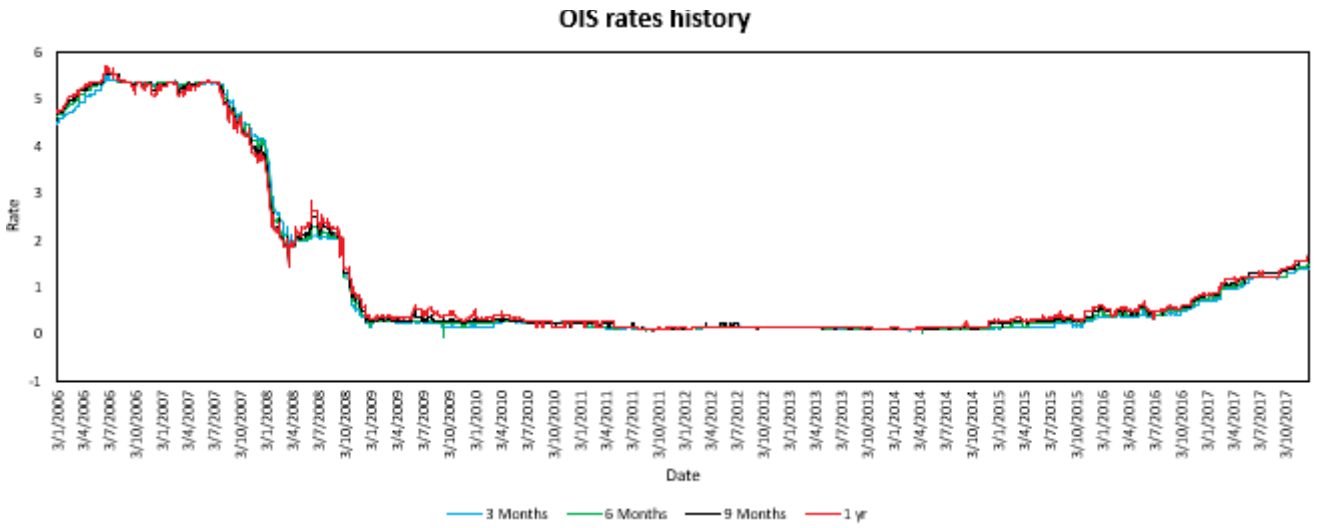

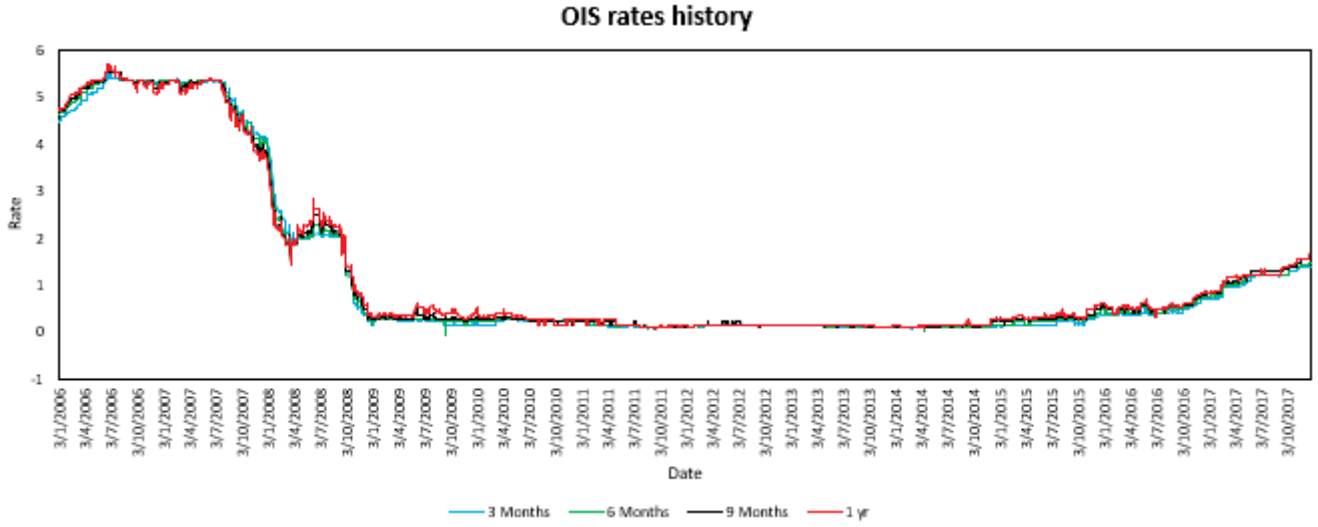

FIGURE 3.5.1. Historical prices of the S&P 100 Index (OEX), the S&P 100 Volatility Index (VXO) and the OIS rates from January 2006 to December 2017. The red vertical lines on the second graph indicate the dates at which the empirical analysis is based. (Source - WRDS (OEX data), CBOE (VXO data) and Bloomberg (OIS Data))

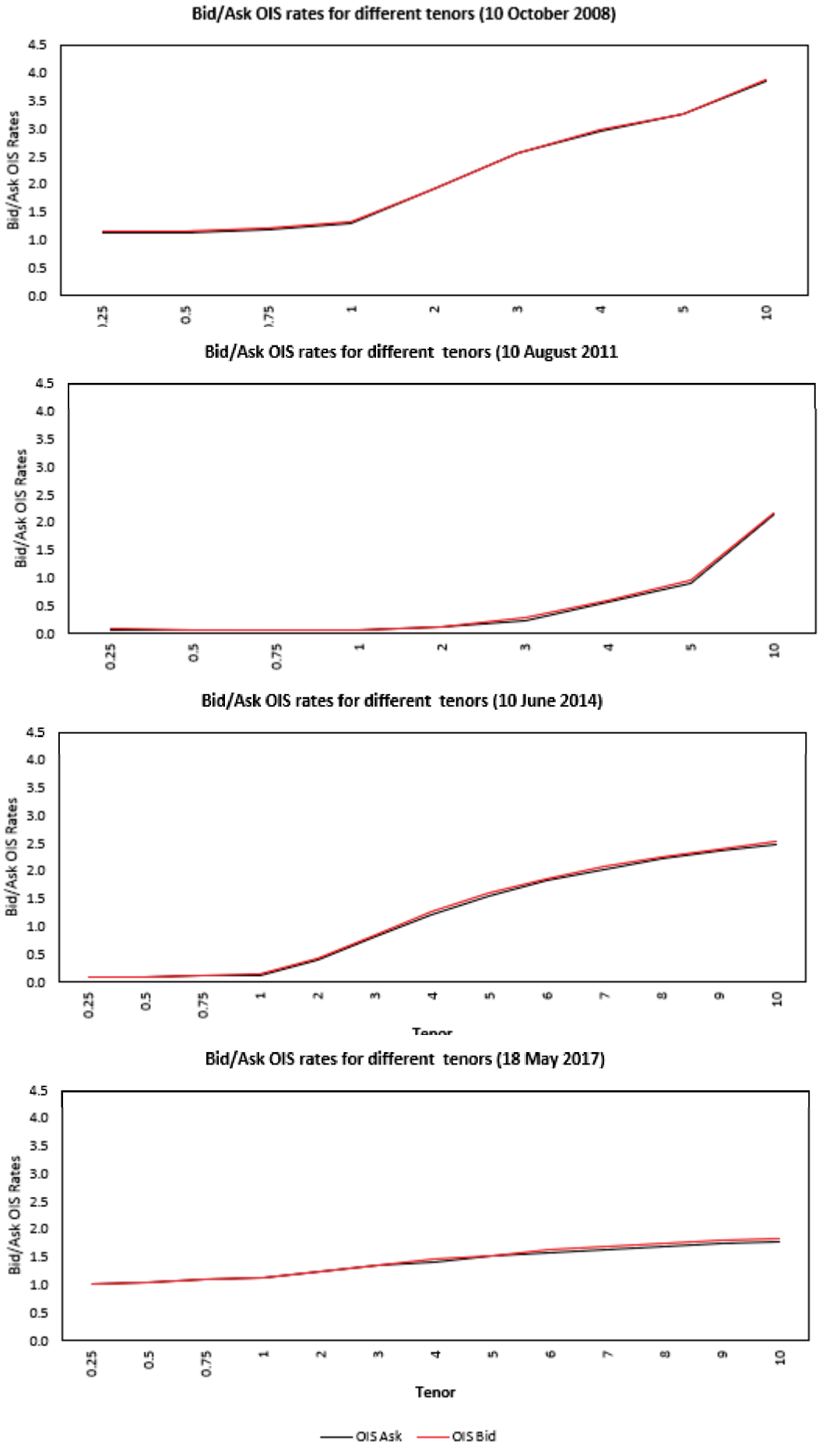

FIGURE 3.5.2. The bid/ask prices for the OIS rates on 10th October 2008, 10th August 2011, 10th June 2014, and 18th May 2017 collected from Bloomberg. These will be used to calibrate the Hull-White interest rate model.

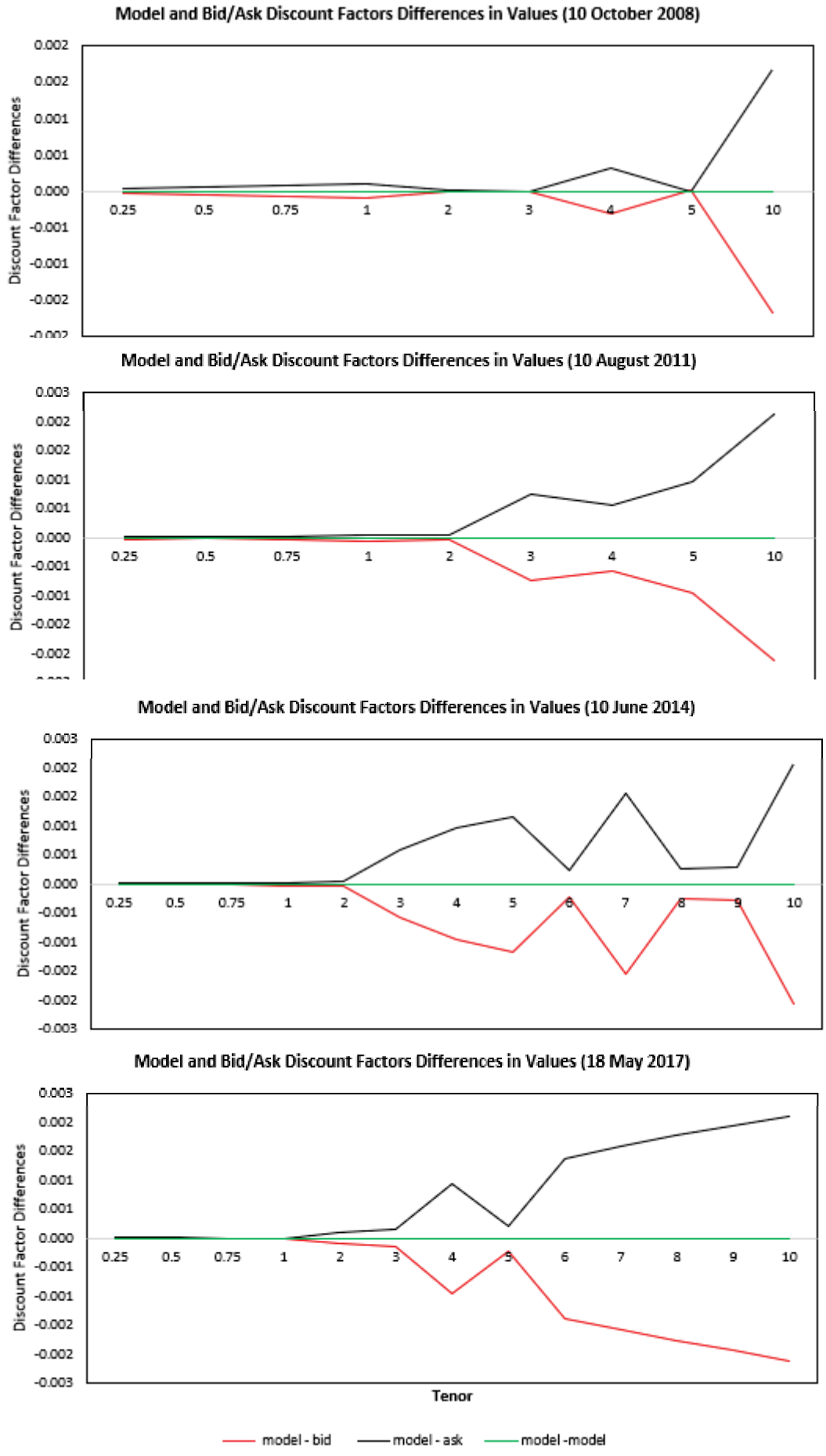

FIGURE 3.5.3. Discount factor differences between the model and the bid/ask prices on computing OIS discount factors using the parameter values from the calibration on the listed dates. Optimisation was done using Trust Region Methods and Controlled Random Search optimisation. The parameter values used are given in Table 3.4.1.

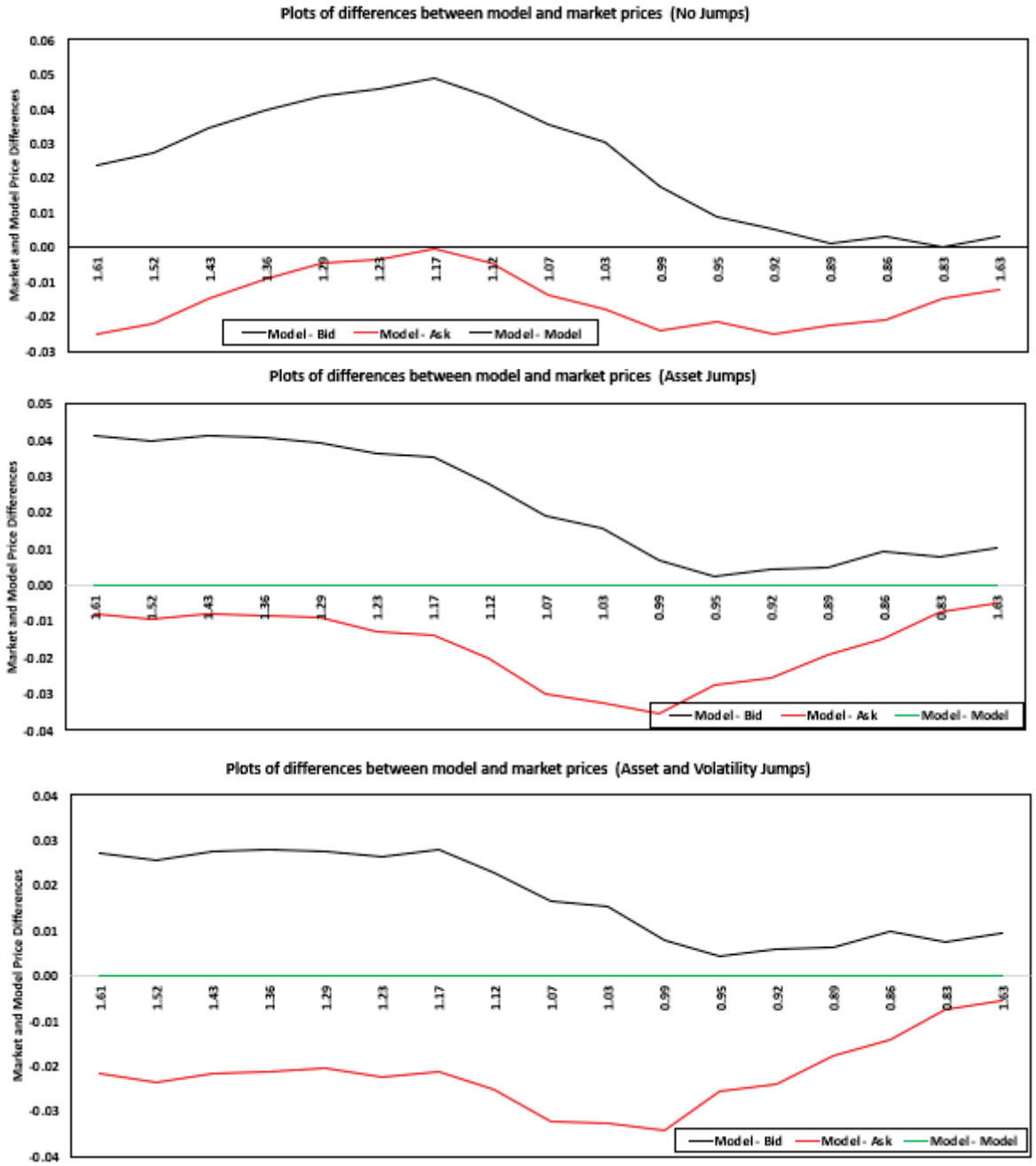

FIGURE 3.5.4. Option price differences between the model and the bid/ask prices on 10th October 2008, regarding computing the American call option prices, using the resulting parameter values from the calibration. Optimisation has been done using Trust Region Methods. The parameter values used are given in Table 3.4.1 and Table 3.4.2.

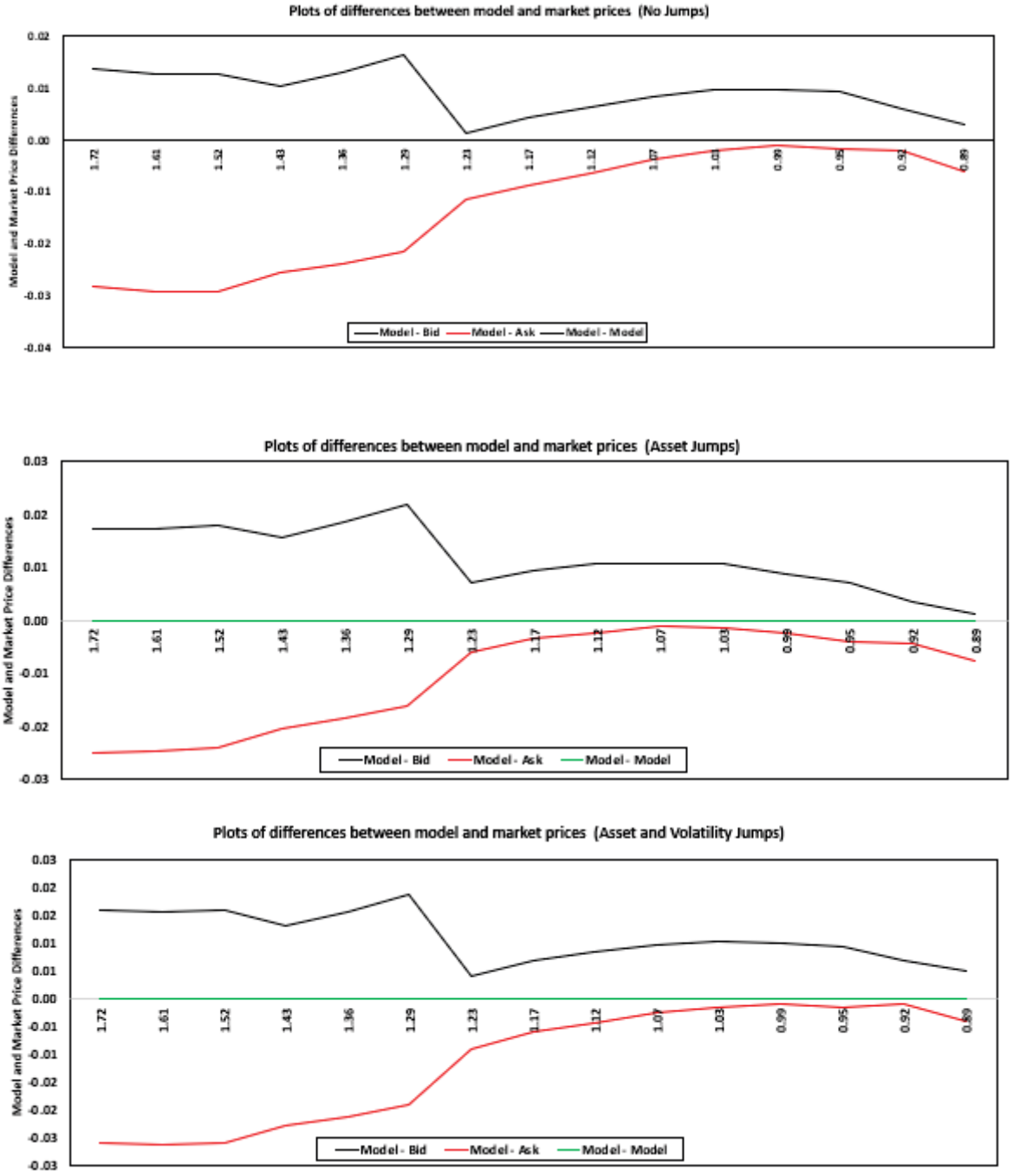

FIGURE 3.5.5. Option price differences between model and the bid/ask prices on the 10th of August 2011, on computing the American call option prices using the resulting parameter values from the calibration. These parameter values are given in Table 3.4.1 and Table 3.4.2.

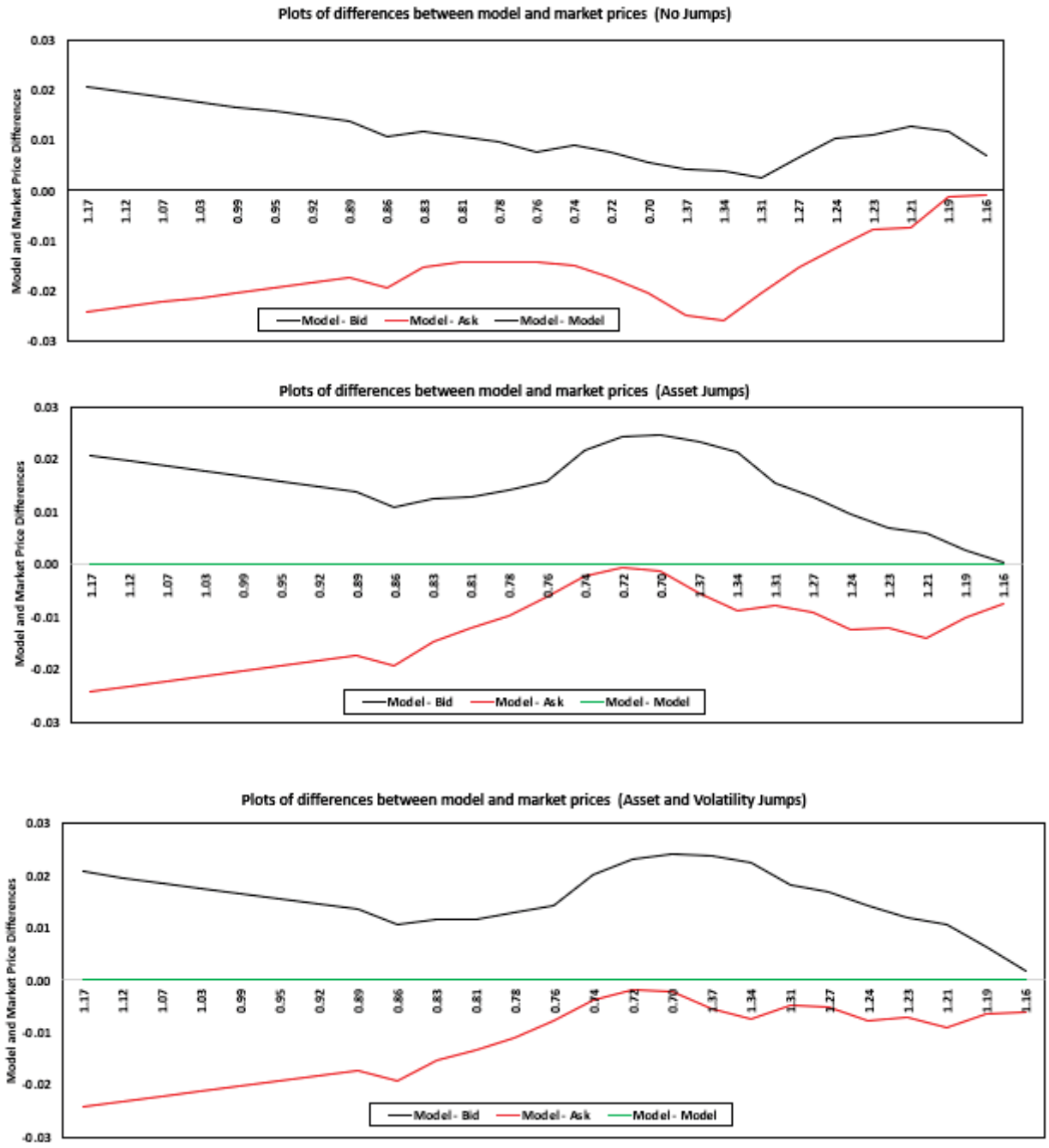

FIGURE 3.5.6. Option price differences between the model and the bid/ask prices on 10th June 2014 on computing the American call option prices, using the resulting parameter values from the calibration. These parameter values are given in Table 3.4.1 and Table 3.4.2.

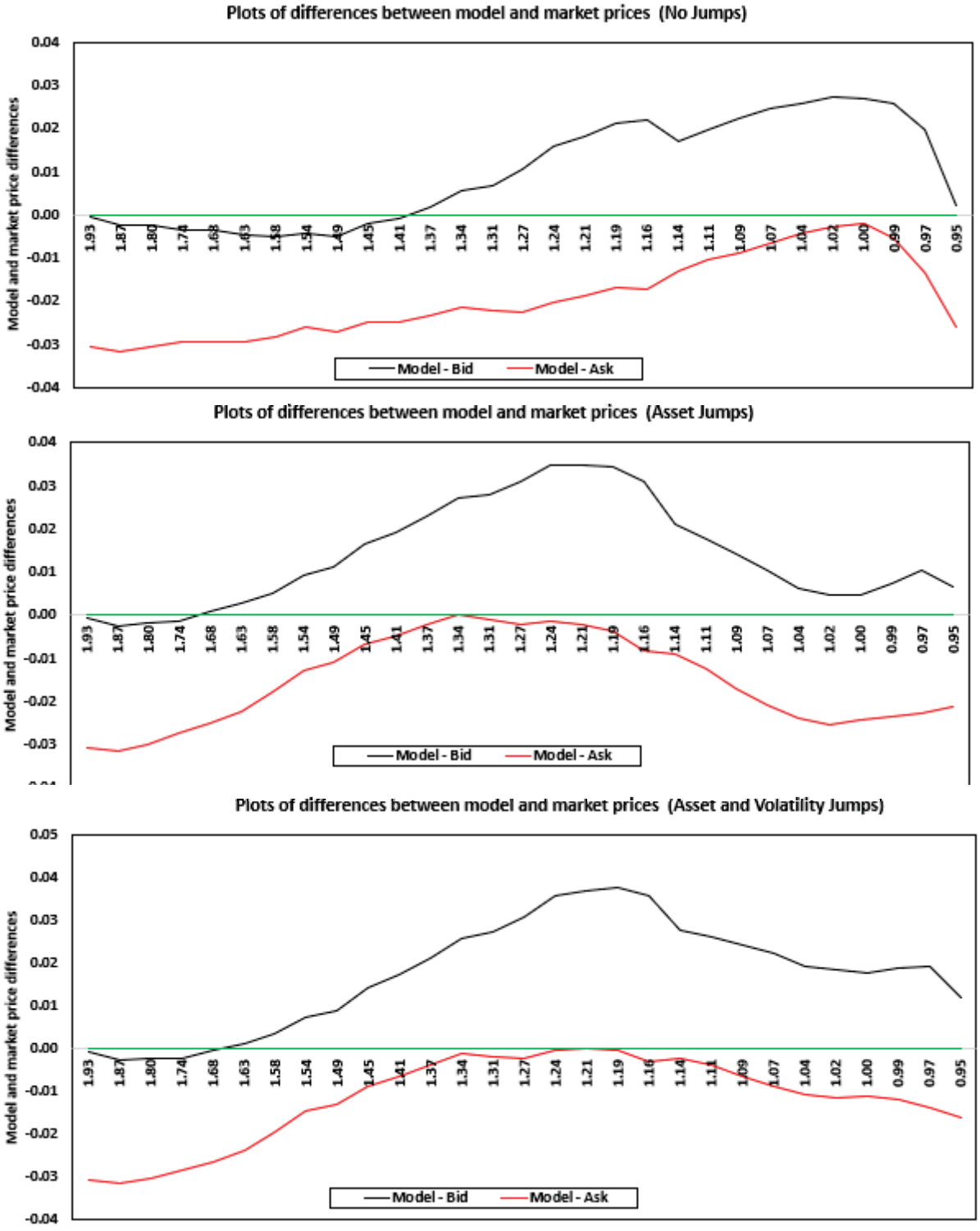

FIGURE 3.5.7. Option price differences between the model and the bid/ask prices on 18th May 2017, on computing American call option prices using the resulting parameter values from the calibration. These parameter values are given in Table 3.4.1 and Table 3.4.2.

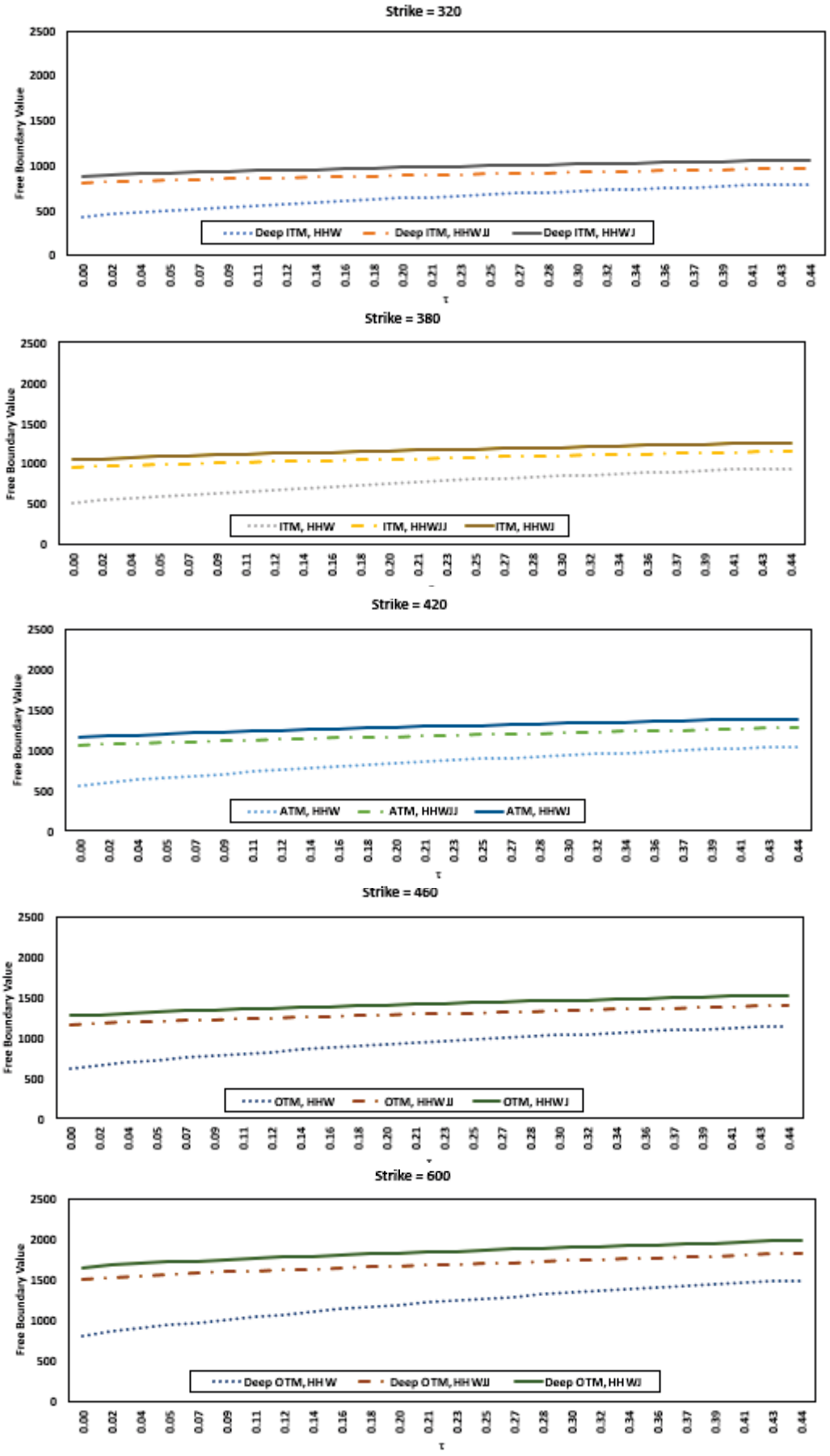

FIGURE 3.5.8. Free boundary surfaces for the $S\&P$ 100 index American call option on 10th October 2008 with an expiry of 0.44-years, obtained using the resulting parameter values from the calibration of HHW, HHWJ, and HHWJJ models. From the top, the graph represent deep ITM, ITM, ATM, OTM, and deep OTM-free boundaries respectively. Parameter values are given in Table 3.4.1 and Table 3.4.2.

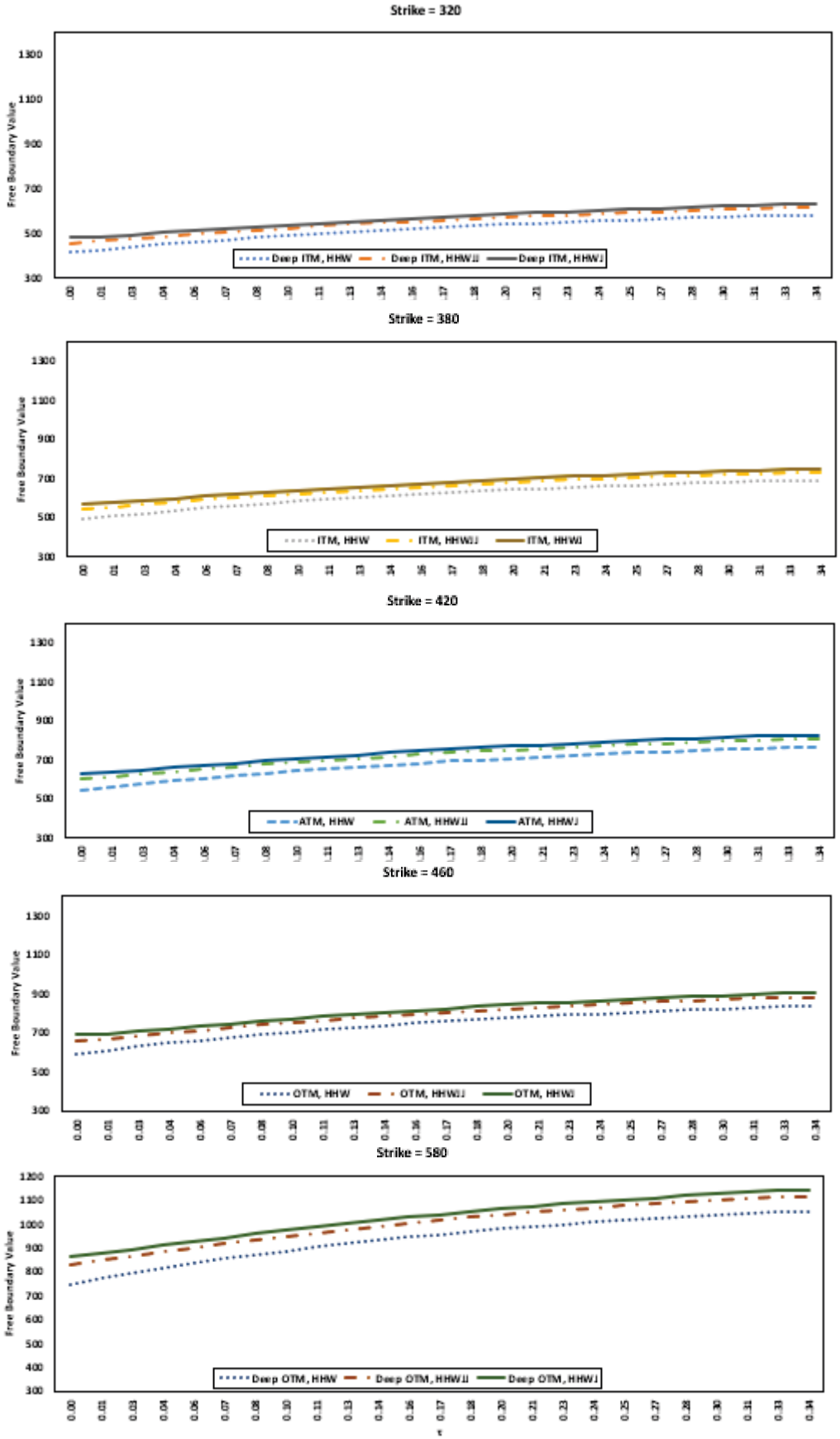

FIGURE 3.5.9. Free boundary surfaces for the *S&P* 100 index American call option on 10th August 2011, with an expiry of 0.35-years, obtained using the resulting parameter values from the calibration of HHW, HHWJ, and HHWJJ models. From the top, the graph represent deep ITM, ITM, ATM, OTM,and deep OTM-free boundaries respectively. Parameter values are given in Table 3.4.1 and Table 3.4.2.

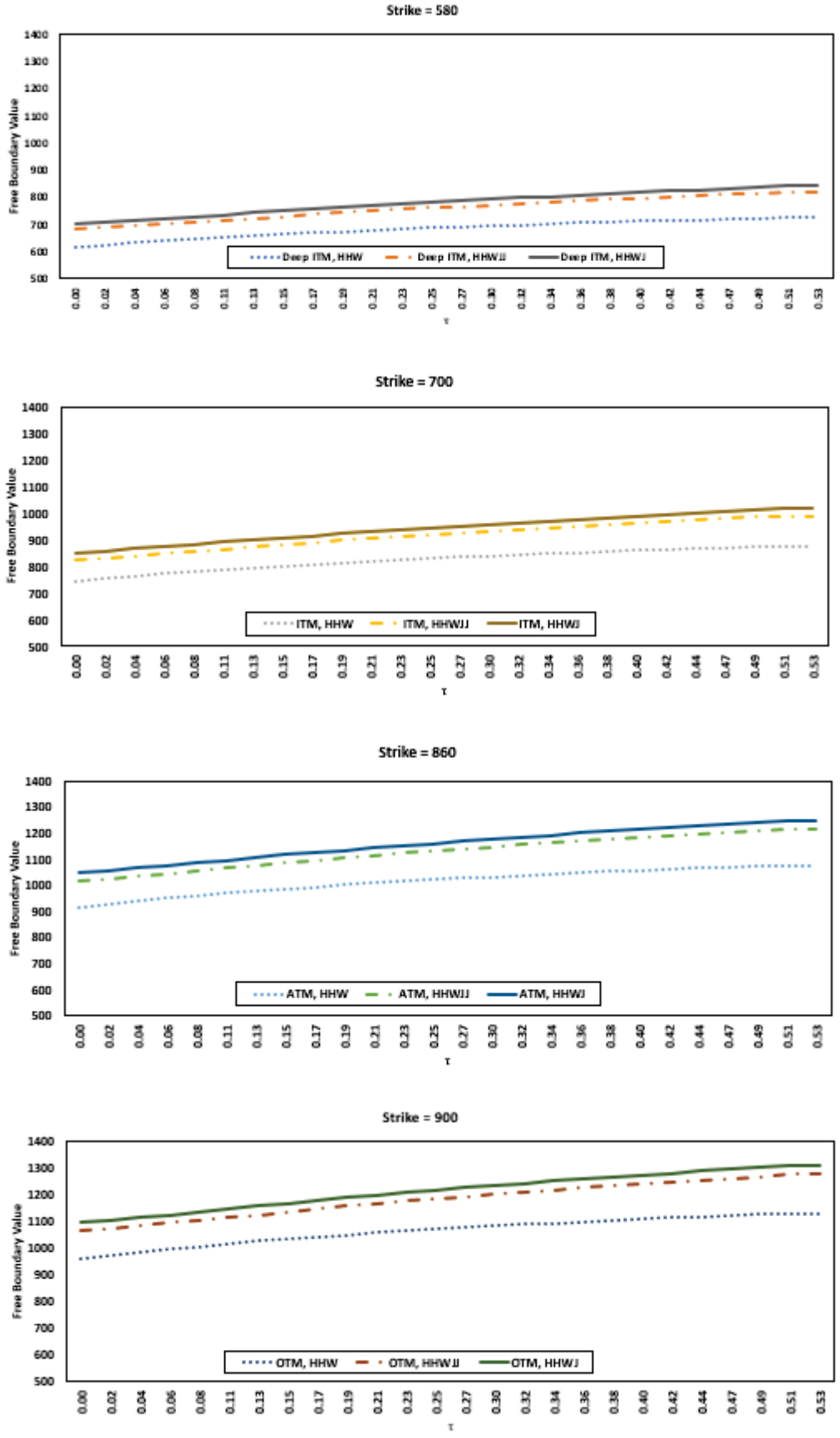

FIGURE 3.5.10. Free boundary surfaces for the $S\&P$ 100 index American call option on 10th June 2014 with an expiry of 0.53-years, obtained using the resulting parameter values from the calibration of HHW, HHWJ, and HHWJJ models. From the top, the graph represents deep ITM, ITM, ATM, and OTM-free boundaries respectively. Parameter values are given in Table 3.4.1 and Table 3.4.2.

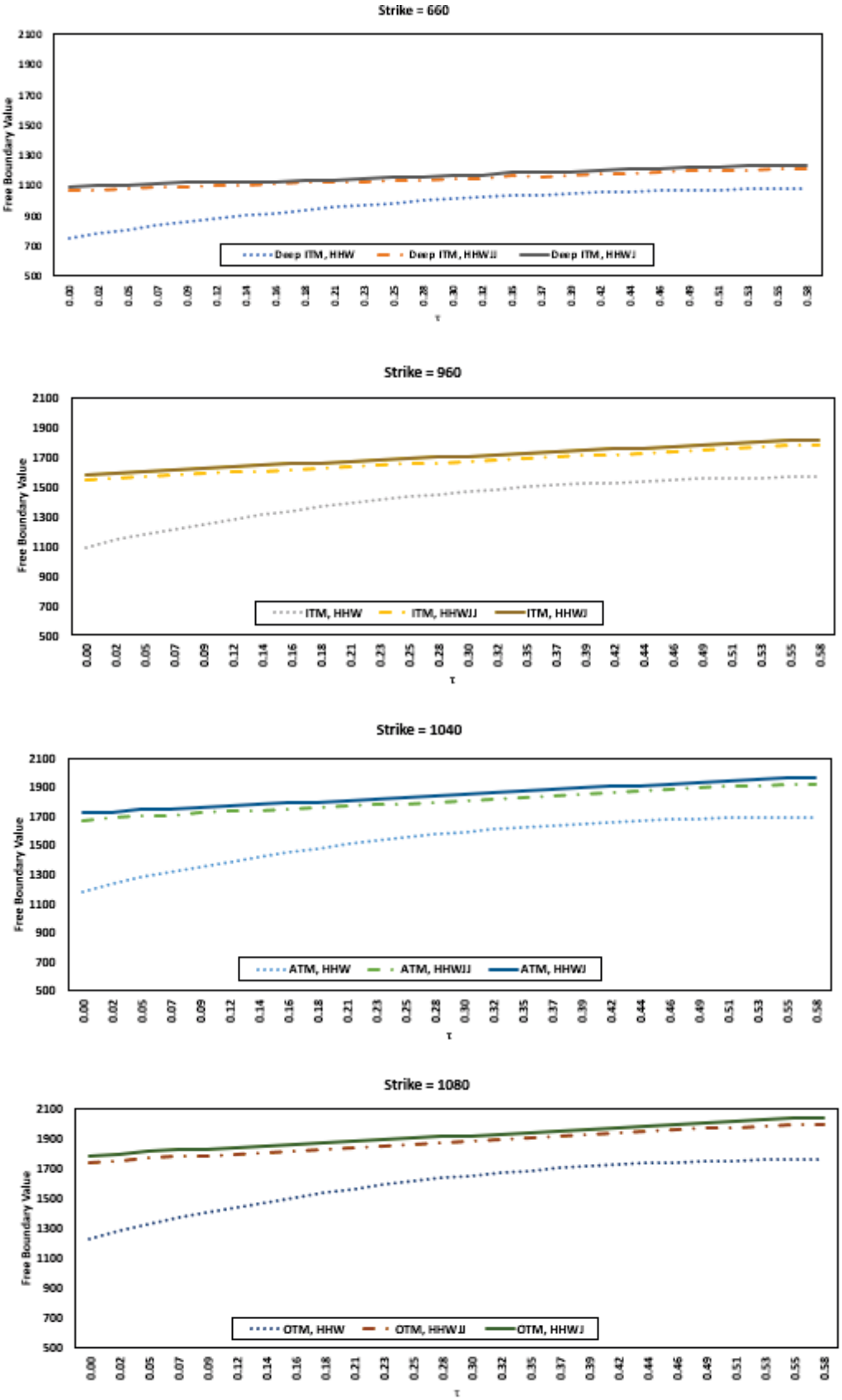

FIGURE 3.5.11. Free boundary surfaces for the $S\&P$ 100 index American call option on 18th May 2017 with an expiry of 0.58-years, obtained using the resulting parameter values from the calibration of HHW, HHWJ, and HHWJJ models. From the top, the graph represents deep ITM, ITM, ATM, and OTM-free boundaries respectively. Parameter values are given in Table 3.4.1 and Table 3.4.2.

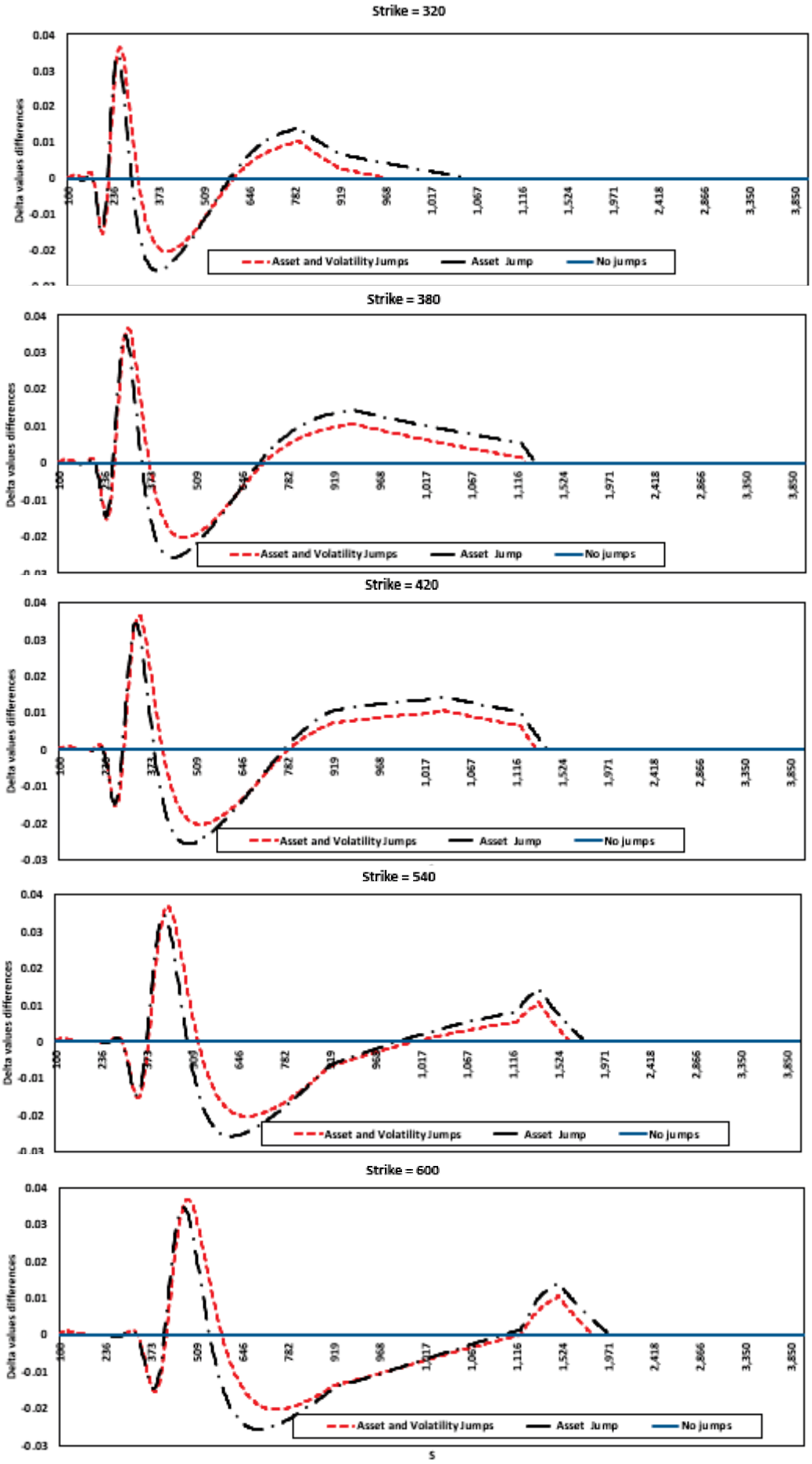

FIGURE 3.5.12. The impact of jumps on the option delta values for the $S\&P$ index American call option on 10th October 2008, obtained using the parameter values in Table 3.4.1 and Table 3.4.2. The red dotted line represents the difference in delta values for the model with no jumps and the model with both asset and volatility jumps, whilst the black dotted line represents the difference in delta values for the model with no jumps and the model with asset jumps only.

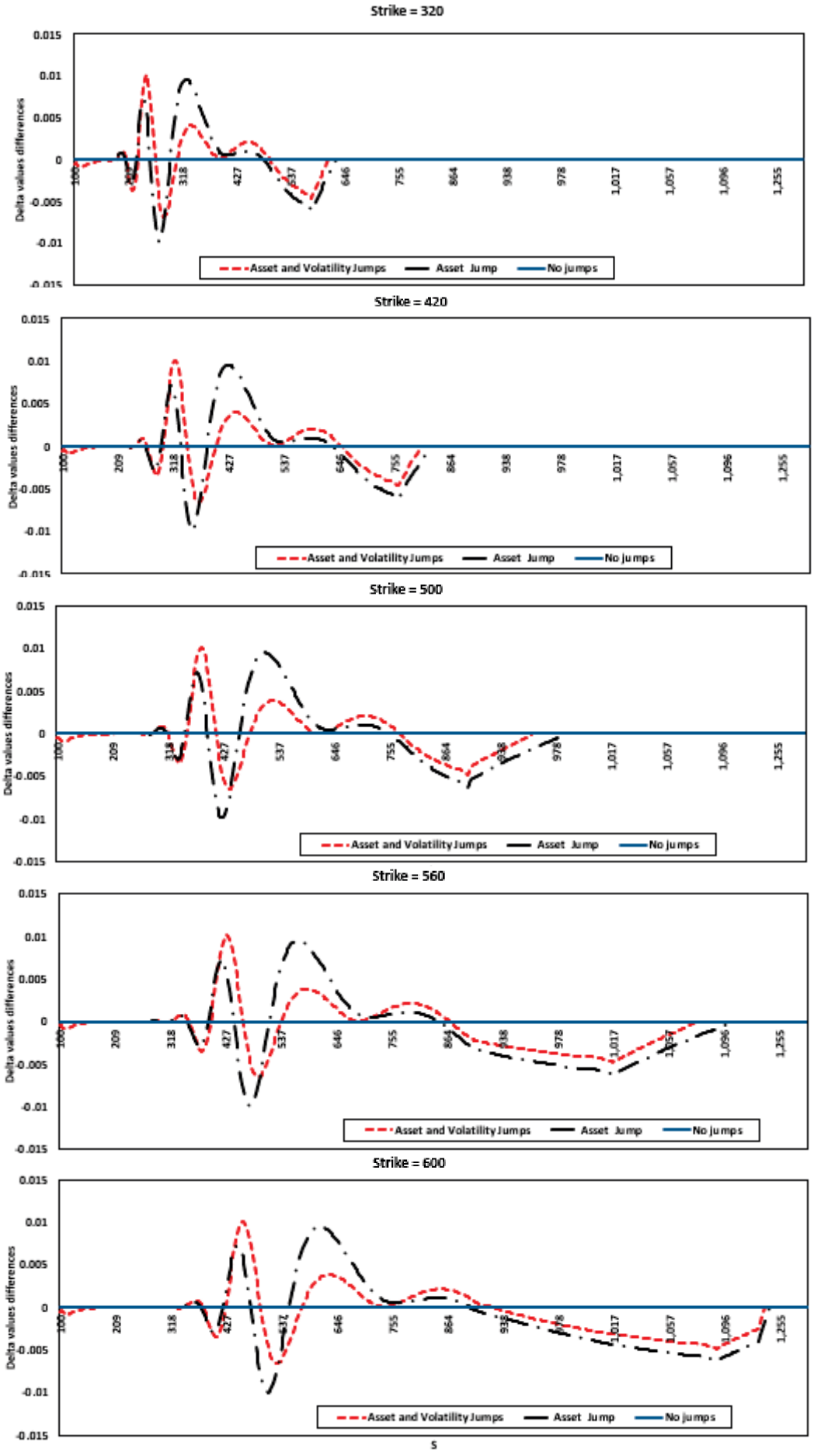

FIGURE 3.5.13. The impact of jumps on the option delta values for the $S\&P$ index American call option on 10th August 2011, obtained using the parameter values in Table 3.4.1 and Table 3.4.2. The red dotted line represents the difference in delta values for the model with no jumps and the model with both asset and volatility jumps, whilst the black dotted line represents the difference in delta values for the model with no jumps and the model with asset jumps only.

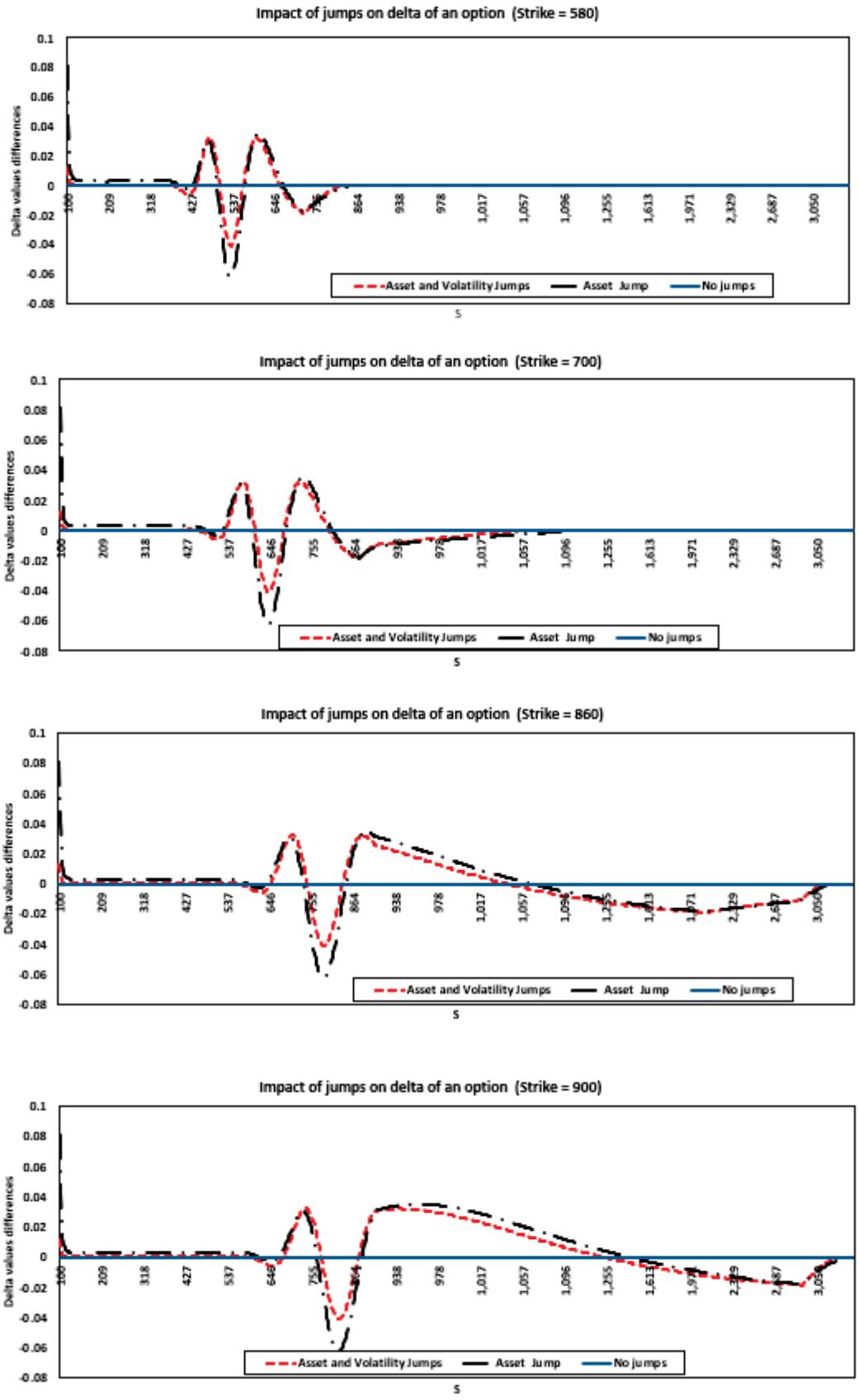

FIGURE 3.5.14. The impact of jumps on the option delta values for the $S\&P$ index American call option on 10th June 2014, obtained using the parameter values in Table 3.4.1 and Table 3.4.2. The red dotted line represents the difference in delta values for the model with no jumps and the model with both asset and volatility jumps, whilst the black dotted line represents the difference in delta values for the model with no jumps and the model with asset jumps only.

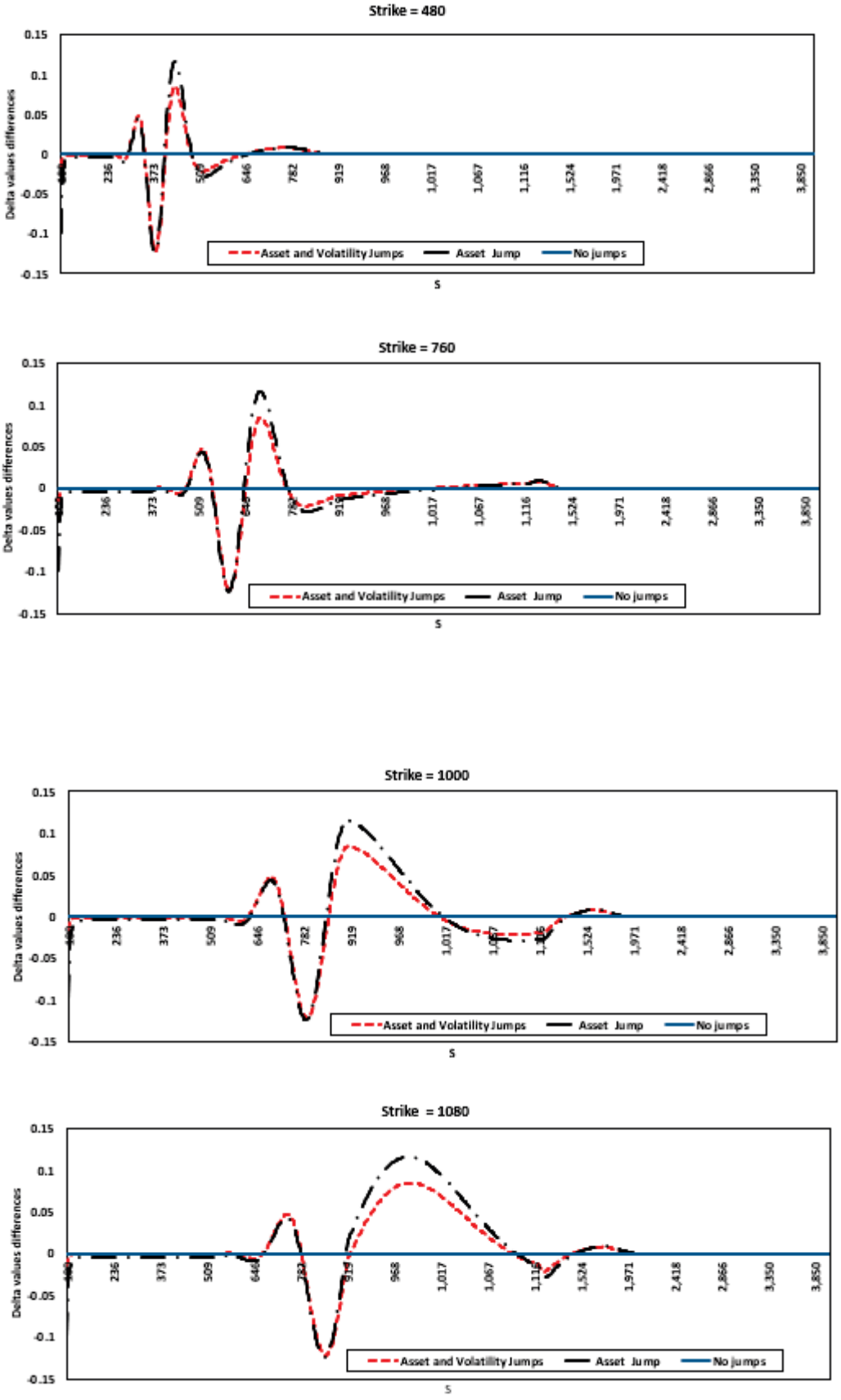

FIGURE 3.5.15. The impact of jumps on the option delta values for the $S\&P$ index American call option on 18 May 2017, obtained using the parameter values in Table 3.4.1 and Table 3.4.2. The red dotted line represents the difference in delta values for the model with no jumps and the model with both asset and volatility jumps, whilst the black dotted line represents the difference in delta values for the model with no jumps and the model with asset jumps only.

Appendix 3.1 : Local Optimisation - Trust Region Methods

A local optimiser is first used, namely, the Trust Region Method algorithm. The trust region method is one of the ways of solving non-linear optimisation problems that were used in this chapter. The objective function is approximated within a certain region in each iteration. In this chapter, an optimiser for the Non-linear Least Square Problem with Linear (Boundary) Constraints in the FORTRAN language is used, and is available in the Intel Math Kernel Library (Intel MKL). The methodology has been described in detail by Conn, Gould & Toint (2000). An Intel compiler on an Intel microprocessor is used for this optimisation.

In Table 3.5.1 parameter values that were obtained from this calibration for the different models are shown. To assess the effectiveness of the parameters obtained from the calibration using Trust Region Method algorithm, a comparison of the model prices obtained to bid/ask prices is made. A plot of the errors obtained between the bid/ask S&P 100 American option prices and the model prices using these parameter values, is given in Figure 3.5.16. Out-of-money options are not fitted well by all models, whilst most at-the-money options and in-the-money options fit well with the models. Deep in-the-money options are slightly below the market bid prices. By observing the graphs, it is seen that as jumps are included, the model fit improves.

TABLE 3.5.1. Parameter values obtained from calibrating the Heston-Hull-White model with asset and volatility jumps to S&P 100 American call option prices on 18th May 2017. Trust Region methods have been used for optimization. Parameter values from the calibration of the Hull & White (1987) stochastic interest rate model to OIS data are used as inputs to obtain the rest of the model parameters. HHW is the stochastic volatility and stochastic interest rate model, HHWJ is the stochastic volatility and stochastic interest rate model with asset jumps, and HHWJJ is the stochastic volatility and stochastic interest rate model with asset and volatility jumps.

Parameter	κ	θ	σ_V	ρ_{SV}	ρ_{Sr}	λ_1	δ	γ	λ_2	λ
HHW	0.890	0.578	0.801	-0.400	-0.195	-	-	-	-	-
HHWJ	0.875	0.542	0.751	-0.414	-0.276	0.005	-2.317	0.026	-	-
HHWJJ	0.905	0.538	0.689	-0.504	-0.300	0.0046	2.9890	-3.085	0.0045	1.698

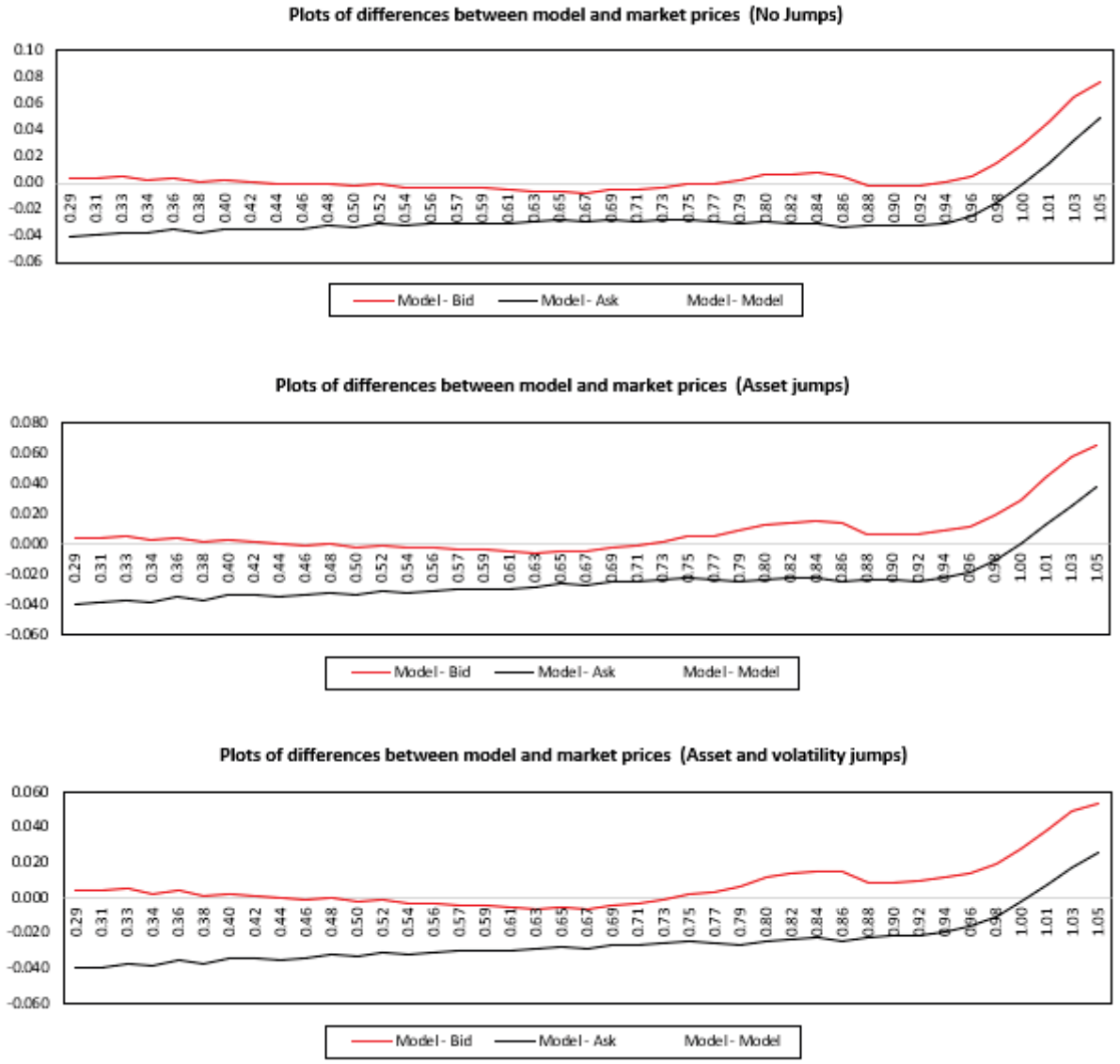

FIGURE 3.5.16. Option price differences between the model and the bid/ask prices on 18th May 2017, on computing the American call option prices, using the resulting parameters values from the calibration. Optimisation has been done using Trust Region Methods. The parameter values used are given in Table 3.4.1 and Table 3.4.2.

CHAPTER 4

Evaluation of Equity Linked Pension Schemes With Guarantees.

4.1. Introduction

Following the Global Financial Crisis, which led to substantial losses in pension schemes, the protection of such pension schemes has gained considerable attention. Empirical evidence suggests that it was only in the 1990s that pension schemes were realising high returns and surpluses and that the recent unfavourable conditions were a result of, among other things, low interest rates, underfunded pensions, and stock market corrections (Stewart (2007)). This culminated in the need for alternative investments that would help protect pension benefits, as this represented a substantial risk for managing financial institutions. As indicated by Bernard, MacKay & Muehlbeyerb (2014), one of the risks arises because selling such contracts can be expensive and financial institutions can only recover costs during the first year of receiving premiums from the investor. These alternative investments can take different forms. One of the ways that this can be achieved is by introducing a return guarantee of a pension plan (Nielsen et al. (2011)). This is a type of insurance in which premiums are paid to finance this return guarantee. Typically, the investor would pay frequent premiums and for each premium, a proportion would be used for investment purposes and the remainder to finance the guarantee. A guarantee on a defined contribution pension scheme is like a guarantee on the minimum maturity cash value of equity-linked life insurance policies (Pennacchi (1999)). Equity-linked policies are attractive because they give investors the exposure to financial indices, which can lead to improving investment performance (Bacinello, Biffis & Millossovich (2009)).

Pricing of equity-linked insurance contracts is closely related to option pricing. Brennan & Schwartz (1976) assumes the equilibrium pricing of equity-linked life insurance policies with an asset value guarantee and computes the value of the call option numerically. Boyle & Schwartz (1977)'s provide a theoretical basis by studying equity-linked contracts used in pricing death benefit guarantees and maturity benefit guarantees. They consider these contracts as options that can be exercised at maturity, during which the investor is entitled

to the maximum of the value of unit amounts and the specified guarantee. Nielsen & Sandmann (1995), Bacinello & Persson (2002) and Bacinello & Ortu (1994) use models with stochastic interest rate dynamics. Melnikov & Romanyuk (2008) uses the method of efficient hedging to price and hedge equity-linked life insurance contracts optimally with payoffs that depend on the performance of several risky assets.

As these financial products have evolved, some features such as early policy surrender have been included. From an insurer's perspective, one of the reasons for allowing early policy surrender is to ensure that investors view these policies as liquid investments, which is likely to boost sales (Bacinello et al. (2009)). Early policy surrenders are not always welcome because they result in the depletion of assets under management. Bernard & Lemieux (2008) classifies the reasons for surrender into two categories: exogenous (personal reasons) and endogenous (economic conditions). When the interest rates are high and the investment performance is low, investors are likely to surrender their policies to invest in better performing financial products (endogenous condition). The risk faced by the insurer as a result of endogenous surrender is difficult to estimate since using historical data might lead to pricing errors. Option pricing theory is used as an alternative method to pricing this risk, by looking at the option to surrender as an American option (Bernard & Lemieux (2008)). If early exercise is optimally done (endogenous surrender), it results in profitability to the investor. One of the assumptions made by Bernard et al. (2014) is that the investor is completely rational and will surrender the policy only if is optimal to do so. Bernard et al. (2014) further mention that even if this occurs later, surrendering a policy is very expensive. Hence, all this needs to be considered when the contract is being priced and an analysis of all the risks involved with optimal surrender should be taken into account so that the risks can be minimised. Kling, Ruez & Rub (2014) investigate the effects of the behaviours of policy holders in the pricing of variable annuities and one of the types of behaviours they consider is policy surrender, which occurs due to the 'moneyness' of the guarantee. This presents a significant risk to the financial institution.

Early withdrawal of the whole pension amount is allowed in some countries, e.g. UK and USA, with the only disadvantage being that a portion or all the withdrawn pension money could be taxed at a higher rate. Adding a penalty in the form of high tax discourages people from withdrawing from their funds early. In some countries, such as Australia,

the government allows one to only withdraw a portion of the pension fund under special circumstances. A lot of insurers impose a high penalty in the case of early surrender. Regulators also protect investors if insurers deal unfairly with the investors in cases of early surrender.

There has been literature that discusses the inclusion of this early exercise feature. Bernard & Lemieux (2008) considered equity life insurance contracts with the possibility of early surrender, using the least-squares Monte Carlo approach. Bacinello et al. (2009) discuss a pricing algorithm for life insurance contracts, which embed American options using a similar approach. Bacinello (2005) discussed the modelling of surrender conditions in equity-linked life insurance in the American style framework. Grosena & Jorgensen (2000) looks at the impact of interest rate guarantees, surrender options, and bonus policies in the pricing of American options.

Different approaches have been used in literature to price these contract types. Nielsen & Sandmann (1995) apply Monte Carlo simulations with a variance reduction technique to price an equity- linked life insurance contract under the stochastic interest rate process. Gaillardetz & Lin (2006) value equity linked insurance and annuity products using binomial models. Fusai, Marena & Roncoroni (2008) compute an analytical expression, which allows them to obtain a closed form formula for Asian-style options using a two-step procedure, which is very fast and effective. Xu, Wang & Chen (2010) by following the work by Milevsky & Salisbury (2006) and Dai, Kwok & Zongi (2008), use a stochastic control approach to price guaranteed equity-linked insurance. Nielsen et al. (2011) focus on a European Asian option and consider the upper and lower bounds. Anzilli (2012) uses a possibilistic approach to evaluate equity-linked life insurance products under uncertainty of randomness and fuzziness. Li & Szimayer (2014) formulate the valuation problem using a PDE approach and solve it using finite difference methods for a unit-linked life insurance contract.

This chapter provides pricing solutions to the American Asian option to include the possibility of withdrawal from the fund at any time, prior to the maturity of the contract. The effects of two different types of return guarantees on equity-linked pension schemes are analysed, namely, the investment guarantee and the contribution guarantee (Nielsen et al. (2011)). The asset dynamics are stochastic, with deterministic volatility and Hull

& White (1987) stochastic interest rates. Since these are long-dated options contracts, stochastic interest rates are important.[1] The relationship between the return guarantee and the proportion of the investor's finance contribution is analysed. The impact of the parameter values on the optimal surrender region is also investigated. This type of numerical analysis will help in decision making meant to minimise the risks associated guarantees offered by financial institutions and can be used as a tool for contract design. Although the optimal surrender strategy as treated in this thesis does not consider the possibility that a policy holder might choose not to surrender the policy optimally in this sense due to other (unmodelled) circumstances, for pricing and risk management purposes the policy issuer should take the worst case perspective. This is to ensure that the insurer manages their risk conservatively, i.e., any departure from the optimal surrender strategy by the policy holder will simply result in a windfall gain for the insurer. To value these contracts, an American Asian option is priced using the MoL, see Chapter 2.

The remainder of the chapter is structured as follows. In Section 4.2, the valuation model used to price the American Asian option is discussed. Given this valuation model, the associated partial differential equation (PDE) using the Feynman-Kac theorem, is obtained. Section 4.3 describes the valuation method, which is the MoL. The results are discussed in Section 4.4, together with a sensitivity analysis. Section 4.5 concludes.

4.2. Model Description

This section describes the evaluation method of equity-linked pension schemes, which is represented as an American Asian option pricing problem. Using the Feynman-Kac theorem, the associated PDE, which is used to compute the optimal surrender region, is obtained.

Nielsen & Sandmann (1995) define an equity-linked contract as being an agreement between a buyer and a seller, in which the buyer pays a predetermined premium to the seller at frequent intervals until the expiry of the contract or until the death of the buyer, and after which the seller pays the buyer of the contract according to the stipulations in the initial agreement. This benefit is the maximum of two specified amounts: the first one being a fixed guaranteed amount of which the value depends on the amount of premiums

[1] Bacinello & Ortu (1994) made a similar observation on the importance of the behaviour of the term structure of interest rates.

that are being paid over the life of the contract. The second is the total value of the portfolio, which is random in nature and for which the value depends on the premium amount being paid, the previous values of the share price, and the current value of the stock. Hence the value of this benefit depends on the stock's performance.

Under the risk-neutral measure $\mathbb{Q}$, the dynamics of the share price are log normally distributed and they follow a stochastic process with a deterministic volatility and stochastic interest rate. These dynamics are expressed as:

$$dS(t) = S(t) r(t) dt + \sigma_s(t) S(t) dW_\beta(t), \tag{4.2.1}$$

where $S(t)$ is the stock price, $r(t)$ is the continuously compounded short rate of interest, $\sigma_s(t)$ is the deterministic volatility and $W_\beta(t)$ is a standard Wiener process.

Market prices become insensitive to volatility assumptions for long term contracts (Boyle & Hardy (2003), Nielsen et al. (2011)), thus deterministic volatility specifications are considered for long term contracts.

Since the interest rate risk affects the terms at which contracts sell in a market that is free of arbitrage, it becomes important to consider the behaviour of the term structure of interest rates (Bacinello & Ortu (1994)). The dynamics of stochastic short rate of interest $r(t)$ are of the Hull & White (1987) type [2]:

$$dr(t) = a(b(t) - r(t)) dt + \sigma_r dW_r(t), \tag{4.2.2}$$

where a is the rate of mean reversion, $b(t)$ is the long run mean of r and is computed as (Haentjens & Hout (2012))

$$b(t) = c_1 - c_2 \exp(-c_3 t),$$

σ_r is the instantaneous variance of $r(t)$. W_β and W_r are correlated Wiener processes. Under the risk-neutral measure $\mathbb{Q}$ the assumed correlation structure is

$$\boldsymbol{E}^{\mathbb{Q}}(dW_\beta dW_r) = \rho_{\beta r} dt.$$

[2]The Hull & White (1987) type model has been chosen because it allows for negative interest rates with positive probability. In the current market environment, negative interest rates are a possibility (Euro Libor, JPY Libor).

For modelling convenience, the correlated Wiener processes are transformed into independent Wiener processes using Cholesky decomposition. Thus,

$$\begin{pmatrix} dW_\beta \\ dW_r \end{pmatrix} = \begin{pmatrix} 1 & 0 \\ \rho_{12} & (1-\rho_{12}^2)^{\frac{1}{2}} \end{pmatrix} \begin{pmatrix} dZ_\beta \\ dZ_r \end{pmatrix},$$

where dZ_β and dZ_r are independent Wiener processes. Hence, the risk-neutral dynamics of the share price are given by (see equation (4.2.1) and equation (4.2.2))

$$\begin{aligned} dS(t) &= S(t)\, r(t)\, dt + \sigma_s S(t)\, dZ_\beta(t), \\ dr(t) &= a(b(t) - r(t))\, dt + \rho_{12}\sigma_r dZ_\beta + \left(1-\rho_{12}^2\right)^{\frac{1}{2}} \sigma_r dZ_r(t). \end{aligned} \tag{4.2.3}$$

In line with Nielsen et al. (2011) an investor who purchases an equity-linked pension scheme by making constant and equal periodical contributions $K(t_i)$ at each time t_i, whilst this investor is alive, until surrendering the contract on or before maturity is considered. Contribution dates are denoted as $t_0,\ t_1,\ t_2, \ldots,\ t_{N-1}$ where t_N is the maximum maturity. Let $t_n \in t_N$ be the date at which the contract is terminated. A portion of this contribution is used to buy shares of a risky fund, which make up his investment portfolio at the same frequency as the contributions being made. The benefit that the investor obtains when surrendering the policy before, or at, expiration largely depends on the market value of this investment portfolio for which the value would have accumulated over time with the addition of shares at each frequency. The choice of selection of these shares depends on the level of risk that the investor is willing to take. Since the market value of these shares is random, so is the value of this portfolio. The associated risks can be mitigated by purchasing an investment guarantee, which is financed using the remainder of the contribution portion. Although there are many types of risk that could be factored into the model, interest rate risk will only be considered and the performance of the stock market. At this stage, mortality risk and transaction costs are not included in the modelling framework. One of the reasons for contract termination could be due to the death of the policy holder, thus factoring in mortality is important. This has been left for future research.

Let $k(t_i)$ be the portion of the contribution, which is used to purchase the shares (using the investment amount) at each time point t_i for which the price is denoted as $S(t_i)$. Further,

$\alpha \in [0,1]$ defines the fraction of the contribution premium used for investment. $k(t_i)$ is

$$k(t_i) = \alpha K(t_i),$$

where $K(t_i)$ has been defined above as a constant periodical contribution. Since the portfolio is made up of these shares, its value is not certain and is dependent on the amount invested at each period (see Kurz (1996)), the share price at the previous periodic dates $t_i < t$ and the share price at time t and is given by

$$P(t,k) = \sum_{i=0}^{\min\{n^*(t),N-1\}} k(t_i) \frac{S(t)}{S(t_i)}, \tag{4.2.4}$$

where $n^*(t) = \max\{j \in \aleph_0 | t_j < t\}$. One will also note that $\frac{k(t_i)}{S(t_i)}$ is the number of shares that can be bought with each investment amount at each time point. If these are summed up and multiplied by the share price at time t, the total value of the portfolio is obtained at that time. In terms of $K(t_i)$, the value of this investment at time t is given by

$$P(t,\alpha K) = \alpha \sum_{i=0}^{\min\{n^*(t),N-1\}} K(t_i) \frac{S(t)}{S(t_i)}. \tag{4.2.5}$$

To define this portfolio value in the continuous sense, the summation is expressed as the equivalent integrals representation:

$$P(t,k) = P(t,\alpha K) = \alpha \sum_{i=0}^{\min\{n^*(t),N-1\}} \frac{K(t_i)}{\Delta t_i} \frac{S(t)}{S(t_i)} \Delta t_i. \tag{4.2.6}$$

Hence for a continuous stream of fund inflows,

$$\bar{K}(t_i) = K(t_i)/\Delta t_i$$

and

$$\bar{k}(t_i) = k(t_i)/\Delta t_i,$$

where

$$\Delta t_i = \frac{t}{n}.$$

From the definition of a definite integral

$$\int_a^b f(x)\,dx = \lim_{n\to\infty} \sum_{k-1}^{n} f(x_k)\,\Delta x. \tag{4.2.7}$$

Using this definition, the value of the investment portfolio is expressed in the continuous sense. Under the assumption of no transaction costs, perfect competitiveness and no arbitrage, this value is given as:

$$P\left(t,\alpha\bar{K}\right)=\lim_{n\to\infty}\alpha\sum_{i=0}^{\min\{n^{*}(t),N-1\}}\bar{K}\left(t_{i}\right)\frac{S\left(t\right)}{S\left(t_{i}\right)}\Delta t_{i}=\alpha S\left(t\right)\int_{0}^{t}\frac{\bar{K}\left(u\right)}{S\left(u\right)}du. \tag{4.2.8}$$

By taking differentials of this expression:

$$\begin{aligned}dP\left(t,\bar{k}\right)&=\alpha dS\left(t\right)\int_{0}^{t}\frac{\bar{K}\left(u\right)}{S\left(u\right)}du+\alpha S\left(t\right)\frac{\bar{K}\left(t\right)}{S\left(t\right)}dt\\&=\alpha dS\left(t\right)\int_{0}^{t}\frac{\bar{K}\left(u\right)}{S\left(u\right)}du+\alpha\bar{K}\left(t\right)dt.\end{aligned}$$

But since

$$\int_{0}^{t}\frac{\bar{K}\left(u\right)}{S\left(u\right)}du=\frac{P\left(t,\alpha\bar{K}\right)}{\alpha S\left(t\right)},$$

we get

$$\begin{aligned}dP\left(t,\bar{k}\right)&=\alpha dS\left(t\right)\left[\frac{P\left(t,\alpha\bar{K}\right)}{\alpha S\left(t\right)}\right]+\alpha\bar{K}\left(t\right)dt\\&=P\left(t,\alpha\bar{K}\right)\frac{dS\left(t\right)}{S\left(t\right)}+\alpha\bar{K}\left(t\right)dt\\&=P\left(t,\alpha\bar{K}\right)\left[r\left(t\right)dt+\sigma_{s}\left(t\right)dZ_{B}\left(t\right)\right]+\alpha\bar{K}\left(t\right)dt\\&=\left[r\left(t\right)P\left(t,\alpha\bar{K}\right)+\alpha\bar{K}\left(t\right)\right]dt+\sigma_{s}P(\left(t,\alpha\bar{K}\right)dZ_{B}\left(t\right).\end{aligned}$$

Since

$$P\left(t,\alpha\bar{K}\right)=\alpha P\left(t,\bar{K}\right),$$

then,

$$dP\left(t,\bar{k}\right)=\alpha\left[r\left(t\right)P\left(t,\bar{K}\right)+\bar{K}\left(t\right)\right]dt+\alpha\sigma_{s}P\left(t,\bar{K}\right)dZ_{B}\left(t\right).$$

Thus the risk-neutral dynamics of the portfolio value are determined by

$$\begin{aligned}dP\left(t,\bar{k}\right)&=\alpha\left[r\left(t\right)P\left(t,\bar{K}\right)+\bar{K}\left(t\right)\right]dt+\alpha\sigma_{s}P\left(t,\bar{K}\right)dZ_{\beta}\left(t\right),\\dS\left(t\right)&=S\left(t\right)r\left(t\right)dt+\sigma_{s}S\left(t\right)dZ_{\beta}\left(t\right),\\dr\left(t\right)&=a\left(b\left(t\right)-r\left(t\right)\right)dt+\rho_{12}\sigma_{r}dZ_{\beta}+\left(1-\rho_{12}^{2}\right)^{\frac{1}{2}}\sigma_{r}dZ_{r}\left(t\right).\end{aligned} \tag{4.2.9}$$

Guarantees on different investments can be defined in terms of a specific payoff or a return on the invested amount. In this chapter, the guarantee is defined in terms of the latter. Let g be the guaranteed rate of return on this investment. The total value of these n payment

streams, where $n \in N$ can be computed at this guaranteed rate. $A(t_n, g)$ is defined as the compounded total contribution amount at maturity, inclusive of the guaranteed return earned during the period. Mathematically, this is expressed as

$$A(t_n, g) = \sum_{i=0}^{n-1} K(t_i) \exp[g(t_n - t_i)]. \tag{4.2.10}$$

The payoffs at maturity for the different investment schemes are expressed in terms of this guaranteed return, see Nielsen et al. (2011).

Investment guarantee scheme (IG Scheme)

The guarantee is defined in terms of the investment amount which is given by $\alpha A(t_n, g)$. It is the maximum of the guaranteed amount and the invested amount, namely,

$$G_{IG}(t_n, \alpha, g) = \max[\alpha P(t_n, K), \alpha A(t_n, g)]. \tag{4.2.11}$$

It allows one to have exposure to the investment market, at the same time protecting them against losing the invested premiums. These do not include the cost of purchasing the guarantee. From an investor's perspective, this payoff can be expressed as a sum of this guaranteed amount and a call option:

$$G = \alpha A(T, g) + \alpha \max\{P(T, K) - A(T, g), 0\} \text{ (IG-Scheme)}. \tag{4.2.12}$$

If $\alpha = 1$ all the proceeds of the investments are given to the investor and there would be nothing left to finance this guarantee. Hence in this case, the investment fraction is always assumed to be less than 1.

Contribution guarantee scheme (CG Scheme)

The guarantee is defined again in terms of the contribution amount, which is given by $\alpha A(t_n, g)$ and is the maximum of the guaranteed amount and the total contributed amount,

$$G_{CG}(t_n, \alpha, g) = \max[\alpha P(t_n, K), A(t_n, g)]. \tag{4.2.13}$$

This type of payoff allows one to have exposure to the investment market, at the same time protecting them against losing the contributed premiums, which include the cost of purchasing the guarantee. From an investor's perspective, this payoff is also expressed as a

sum of this guaranteed amount and a call option,

$$G = A(T, g) + \max\{\alpha P(T, K) - A(T, g), 0\} \text{ (CG-Scheme)}. \tag{4.2.14}$$

These two payoffs mentioned so far are similar when $\alpha = 1$. However, note that $\alpha < 1$. One of the goals of this chapter is to obtain the relationship between the investment fraction α and the guaranteed return. To establish this relationship, the following definition which extends the no-arbitrage pricing principle for contingent claims for instances where there are periodic payments is used.

DEFINITION 4.2.1. Let $K(t_0), \ldots K(t_{n-1})$ be a sequence of constant periodical contributions, $D(t_0, t_i)$ the discounting factor at t_0 and maturity t_i and $Z(t_n)$ be random payoff at time t_n. $Z(t_n)$ is called admissible if the following relationship is satisfied:

$$C_{initial} = \sum_{i=0}^{n-1} K(t_i) D(t_0, t_i), \tag{4.2.15}$$

where $C_{initial}$ is option value at the initial time.

From equation (4.2.11), it is noted that if $\alpha = 0$, the payoff of the IG scheme becomes zero. Following equation (4.2.13) and equation (4.2.14), if $\alpha = 0$ for the CG scheme, the payoffs equate to $A(t_n, g)$ which is a contract on a set of fixed payments, which are being compounded at a rate of g.

All the payoffs depend on $A(t_n, g)$. (Nielsen et al. (2011)) shows that this function converges to zero if the guaranteed rate of return approaches $-\infty$. Since a negative guaranteed return implies a cost to the investor, there is no guarantee on this investment, and, hence, no hedging costs. In the light of this, the two payoffs defined above are considered as pure investments.

4.2.1. Partial Differential Equation using the Feynman-Kac theorem. The infinitesimal generator $\boldsymbol{K}$ for the system of equations (4.2.9) is given as:

$$\begin{aligned}\boldsymbol{K} = \rho_{sr}\frac{\partial^2}{\partial S \partial r}\sigma_s\sigma_r S + \frac{1}{2}\frac{\partial^2}{\partial^2 S}S^2\sigma_s^2 + \frac{1}{2}\frac{\partial^2}{\partial^2 r}\sigma_r^2 + rS\frac{\partial}{\partial S} + a(b(t) - r(t))\frac{\partial}{\partial r} \\ +\alpha(rP + K)\frac{\partial}{\partial P} + \frac{1}{2}P^2\sigma_S^2\alpha^2\frac{\partial^2}{\partial P^2} + \rho_{Pr}\alpha\frac{\partial^2}{\partial P \partial r}\sigma_s\sigma_r P + PS\alpha\sigma_s^2\rho_{PS}\frac{\partial^2}{\partial S \partial P}.\end{aligned} \tag{4.2.16}$$

Let f, a function of t, P, S, r be the price of an Asian option given by $f(t, P, S, r)$. Under the risk neutral measure, it would be a martingale if:

$$f(t, P, S, r) = \boldsymbol{E}_t^{\mathbb{Q}} \left[e^{-\int_t^T r(s)ds} f(T, P, S, r) \right].$$

Applying the Feynman-Kac formula, $f(t, P, S, r)$ satisfies the partial differential equation:

$$\frac{\partial f}{\partial t} + \mathbf{K} f - rf = 0,$$

subject to the initial condition

$$\lim_{t \to T} f(t, P, S, r) = f(T, P, S, r).$$

Using the infinitesimal generator in 4.2.16, the PDE that needs to be solved to obtain $f(t, P, S, r)$ is given as:

$$\begin{aligned} &\frac{\partial f}{\partial t} + \rho_{sr} \frac{\partial^2 f}{\partial S \partial r} \sigma_s \sigma_r S + \frac{1}{2} \frac{\partial^2 f}{\partial^2 S} S^2 \sigma_s^2 + \frac{1}{2} \frac{\partial^2 f}{\partial^2 r} \sigma_r^2 + rS \frac{\partial f}{\partial S} \\ &+ a(b(t) - r(t)) \frac{\partial f}{\partial r} + \alpha (rP + K) \frac{\partial f}{\partial P} + \alpha^2 \frac{1}{2} P^2 \sigma_S^2 \frac{\partial^2 f}{\partial P^2 f} \\ &+ \alpha \rho_{Pr} \frac{\partial^2 f}{\partial P \partial r} \sigma_s \sigma_r P + \alpha P S \sigma_s^2 \rho_{PS} \frac{\partial^2 f}{\partial S \partial P} - rf = 0. \end{aligned} \tag{4.2.17}$$

4.2.2. The partial differential equation for a call option and the boundary conditions. Let $C(t, P, S, r)$ be the call option price. Using similar arguments as in Chapter 2, Section 2.2 for option pricing using the Martingale approach, the corresponding PDE is given as

$$\begin{aligned} &\frac{\partial C}{\partial t} + \rho_{sr} \frac{\partial^2 C}{\partial S \partial r} \sigma_s \sigma_r S + \frac{1}{2} \frac{\partial^2 C}{\partial S^2} S^2 \sigma_s^2 + \frac{1}{2} \frac{\partial^2 C}{\partial r^2} \sigma_r^2 + rS \frac{\partial C}{\partial S} \\ &+ a(b(t) - r(t)) \frac{\partial C}{\partial r} + \alpha (rP + K) \frac{\partial C}{\partial P} + \frac{1}{2} \alpha^2 P^2 \sigma_S^2 \frac{\partial^2 C}{\partial P^2} \\ &+ \alpha \rho_{Pr} \frac{\partial^2 C}{\partial P \partial r} \sigma_s \sigma_r P + \alpha P S \sigma_s^2 \rho_{PS} \frac{\partial^2 C}{\partial S \partial P} - rC = 0, \end{aligned} \tag{4.2.18}$$

in the domain:

$$D^* = \{(t, P, S, r) \,|t > 0, P \geq 0, S \geq 0, -\infty \leq r \leq \infty)\}, \tag{4.2.19}$$

The value of the portfolio at the free boundary is denoted by $d(t, P, S, r)$ and for the IG scheme it will be determined as the maximum of the investment amount and the guaranteed value in a case in which the investor decides to terminate the policy early for some reason. For the CG scheme, it will be determined as the maximum of total contributions and the

guaranteed amount. The present value of the remainder of the contributions is added to all these payoffs because they will be invested in a bank account. Let t_{n^*} be the time point at which early termination occurs. For the IG Scheme, the PDE is solved, subject to the conditions:

$$C_{IG}\left(T,P,S,r\right)=\max\left\{\alpha P\left(T,K\right),\alpha A\left(T,g\right)\right\}, \tag{4.2.20}$$

$$\begin{aligned}&C_{IG}\left(t_{n^*},d\left(t_{n^*},P,S,r\right),S,r\right)\\&=\max\left\{\alpha d\left(t_{n^*},P,S,r\right),\alpha\sum_{i=0}^{n^*}K\left(t_i\right)\exp\left[g\left(t_{n^*}-t_i\right)\right]\right\}\\&+\sum_{i=n^*+1}^{n-1}K\left(t_i\right)Z\left(t_i,t_n\right),\end{aligned} \tag{4.2.21}$$

$$C_{IG}\left(t,0,S,r\right)=Z\left(t,T\right)\alpha A\left(t,g\right). \tag{4.2.22}$$

For the CG scheme, the PDE is solved subject to the conditions

$$C_{CG}\left(T,P,S,r\right)=\max\left\{\alpha P\left(T,K\right),A\left(T,g\right)\right\}, \tag{4.2.23}$$

$$\begin{aligned}&C_{CG}\left(t_{n^*},d\left(t_{n^*},P,S,r\right),S,r\right)\\&=\max\left\{\alpha d\left(t_{n^*},P,S,r\right),\sum_{i=0}^{n^*}K\left(t_i\right)\exp\left[g\left(t_{n^*}-t_i\right)\right]\right\}\\&+\sum_{i=n^*+1}^{n-1}K\left(t_i\right)Z\left(t_i,t_n\right),\end{aligned} \tag{4.2.24}$$

$$C_{CG}\left(t,0,S,r\right)=Z\left(t,T\right)A\left(t,g\right), \tag{4.2.25}$$

where $Z\left(t,T\right)$ is the price of a zero-coupon bond defined as (Kang & Ziveyi (2018))

$$\begin{aligned}Z\left(t,T\right)&=\widehat{H}\left(t,T\right)e^{-\beta(t,T)r(t)},\\\widehat{H}\left(t,T\right)&=H\left(t,T\right)\exp\left(-a\int_t^T b\left(u\right)\beta\left(u,T\right)du\right),\\H\left(t,T\right)&=\exp\left(-\frac{\sigma_r^2}{2a^2}\left(\beta\left(t,T\right)-\left(T-t\right)\right)-\frac{\sigma_r^2}{4a}\beta\left(t,T\right)^2\right),\\\beta\left(t,T\right)&=\frac{1-e^{-a(T-\tau)}}{a}.\end{aligned} \tag{4.2.26}$$

Equations (4.2.20) and (4.2.23) represent the payoffs of the two guarantees at maturity. These payoffs can be further expressed in terms of call options as below:

$$C_{IG}\left(T,P,S,r\right)=\alpha A\left(T,g\right)+\alpha\max\left\{P\left(T,K\right)-A\left(T,g\right),0\right\}\ \text{(IG-Scheme)}\,, \tag{4.2.27}$$

$$C_{CG}\left(T,P,S,r\right)=A\left(T,g\right)+\max\left\{\alpha P\left(T,K\right)-A\left(T,g\right),0\right\}\ \text{(CG-Scheme)}\,. \tag{4.2.28}$$

Equations (4.2.21) and (4.2.24) are value matching conditions required to eliminate arbitrage. If the investor chooses to terminate early, the value of the free boundary would be the sum of the maximum of the value of portfolio and the guaranteed value at the point of termination of the contract and the present value of all contributions not made due to early termination. If the guaranteed amount is the total accumulated contribution amount at maturity, the investor can exercise early, only if the current value of the portfolio is greater than the guaranteed value at maturity. Kang & Ziveyi (2018) makes similar assumptions in their model, which evaluates variable annuity contracts with guaranteed minimum maturity benefits. In this case, the value-matching condition at the free boundary will be represented as:

$$\begin{aligned}C_{IG}\left(t_{n^*},d\left(t_{n^*},S,r\right),S,r\right)&=\alpha A\left(t_{n^*},g\right)+\alpha\left(d\left(t_{n^*},S,r\right)-A\left(t_{n^*},g\right)\right)\\&=\alpha d\left(t_{n^*},S,r\right),\end{aligned} \tag{4.2.29}$$

$$\begin{aligned}C_{CG}\left(t_{n^*},d\left(t_{n^*},S,r\right),S,r\right)&=A\left(t_{n^*},g\right)+\left(\alpha d\left(t_{n^*},S,r\right)-A\left(t_{n^*},g\right)\right)\\&=\alpha d\left(t_{n^*},S,r\right).\end{aligned} \tag{4.2.30}$$

If the value of the portfolio diminishes, the investor will receive the present value of the guarantee, as equations (4.2.22) and (4.2.25) illustrate. The smooth pasting condition requires us to obtain the following limits at the free boundary:

$$\lim_{P\to d(t,S,r)}\frac{\partial C}{\partial P},\qquad\lim_{P\to d(t,S,r)}\frac{\partial C}{\partial S},\qquad\lim_{P\to d(t,S,r)}\frac{\partial C}{\partial r}.$$

The following boundary conditions are imposed at the points $P_{\min}$, $S_{\min}$, $S_{\max}$, $r_{\min}$ and $r_{\max}$. The boundary conditions at $P=P_{\min}$, $S=S_{\min}$ and $r=r_{\min}$ can be obtained by using the algebraic sign of the Fichera function for the PDE (Kang & Meyer (2014) and

Meyer (2015)). At the point $S = S_{\min}$, the PDE is given as

$$\frac{\partial C}{\partial t} + rS\frac{\partial C}{\partial S} + a\left(b\left(t\right) - r\left(t\right)\right)\frac{\partial C}{\partial r} + \alpha\left(rP + K\right)\frac{\partial C}{\partial P} + \frac{1}{2}\frac{\partial^2 C}{\partial r^2}\sigma_r^2 - rC = 0, \tag{4.2.31}$$

and at $r = r_{\min}$ the PDE is given as

$$\begin{aligned}\frac{\partial C}{\partial t} + \frac{1}{2}\frac{\partial^2 C}{\partial S^2}S^2\sigma_s^2 + rS\frac{\partial C}{\partial S} + a\left(b\left(t\right)\right)\frac{\partial C}{\partial r} \\ +\alpha\left(rP + K\right)\frac{\partial C}{\partial P} + \alpha^2\frac{1}{2}P^2\sigma_S^2\frac{\partial^2 C}{\partial P^2} + \alpha PS\sigma_s^2\rho_{PS}\frac{\partial^2 C}{\partial S\partial P} = 0.\end{aligned} \tag{4.2.32}$$

At $S = S_{max}$ the PDE is given as:

$$\begin{aligned}\frac{\partial C}{\partial t} + \frac{1}{2}\frac{\partial^2 C}{\partial r^2}\sigma_r^2 + rS_{\max}\frac{\partial C}{\partial S} + a\left(b\left(t\right) - r\left(t\right)\right)\frac{\partial C}{\partial r} \\ +\alpha\left(rP + K\right)\frac{\partial C}{\partial P} + \alpha^2\frac{1}{2}P^2\sigma_S^2\frac{\partial^2 C}{\partial P^2} + \alpha\rho_{Pr}\frac{\partial^2 C}{\partial P\partial r}\sigma_s\sigma_r P - rC = 0.\end{aligned} \tag{4.2.33}$$

At $r = r_{max}$ the PDE is given as:

$$\begin{aligned}\frac{\partial C}{\partial t} + \frac{1}{2}\frac{\partial^2 C}{\partial S^2}S^2\sigma_s^2 + rS\frac{\partial C}{\partial S} + a\left(b\left(t\right) - r_{\max}\left(t\right)\right)\frac{\partial C}{\partial r} \\ +\alpha\left(r_{\max}P + K\right)\frac{\partial C}{\partial P} + \alpha^2\frac{1}{2}P^2\sigma_S^2\frac{\partial^2 C}{\partial P^2} + \alpha PS\sigma_s^2\rho_{PS}\frac{\partial^2 C}{\partial S\partial P} - r_{\max}C = 0,\end{aligned} \tag{4.2.34}$$

and for $S = S_{max}$ and $r = r_{max}$ the PDE is

$$\frac{\partial C}{\partial t} + rS\frac{\partial C}{\partial S} + a\left(b\left(t\right) - r\left(t\right)\right)\frac{\partial C}{\partial r} + \alpha\left(rP + K\right)\frac{\partial C}{\partial P} - rC = 0. \tag{4.2.35}$$

At the boundary points $S = S_{\min}$ and $r = r_{\min}$, a similar procedure to the one described in Section 2.2 is performed to obtain the option values and the quadratic extrapolation formula given by

$$f\left(0\right) = 3f\left(\Delta x\right) - 3f\left(2\Delta x\right) + f\left(3\Delta x\right)$$

is used to obtain the price of the call option. In the section that follows, the method used to solve this problem is discussed.

4.3. Methodology

To solve the partial differential equation of the price dynamics, the MOL is used, see Chapter 2, Section 2.3 for details. Time is discretised in a similar manner as discussed in the referred section. The derivatives with respect to asset price and interest rates are

discretised using finite difference schemes. The equation obtained after discretisation is a second-order ordinary differential equation, which is solved at each time step, asset price grid point, and interest rate point. The form of this equation is similar to that obtained in Section 2.3, without integral equations.

4.3.1. A Mathematical Description. Let $S_m = m\Delta S$, $r_n = n\Delta r$ and $\tau_l = l\Delta\tau$ for $m = 0, 1, 2, \ldots M$, and $n = 0, 1, 2, \ldots N$ and where $\tau = T - t$ and $\tau_L = T$. The call option price along the asset price line S_m, the interest rate line r_n and the time line τ_l is given by:

$$C\left(\tau_l, P, S_m, r_n\right) = C^l_{m,n}\left(P\right).$$

The option delta at the grid point is given by:

$$V\left(\tau_l, P, S_m, r_n\right) = \frac{\partial C\left(\tau_l, P, S_m, r_n\right)}{\partial P} = V^l_{m,n}\left(P\right).$$

The partial derivative is discretised with respect to time, $\frac{\partial C}{\partial \tau}$. A backward Euler approximation is used for the first two time steps:

$$\frac{\partial C}{\partial \tau} = \frac{C^l_{m,n} - C^{l-1}_{m,n}}{\Delta\tau}. \tag{4.3.1}$$

For the subsequent remaining time steps, a three level backward difference formula is applied:

$$\frac{\partial C}{\partial \tau} = \frac{3}{2}\frac{C^l_{m,n} - C^{l-1}_{m,n}}{\Delta\tau} + \frac{1}{2}\frac{C^{l-1}_{m,n} - C^{l-2}_{m,n}}{\Delta\tau}. \tag{4.3.2}$$

By using equation (4.3.1) and equation (4.3.2) together ensures that a stable numerical method for the solution of this PDE is obtained (Meyer (2015)). Derivative terms are approximated with respect to S and r using finite differences:

$$\frac{\partial C}{\partial S} = \frac{C^l_{m+1,n} - C^l_{m-1,n}}{2\Delta S}, \quad \frac{\partial C}{\partial r} = \frac{C^l_{m,n+1} - C^l_{m,n-1}}{2\Delta r},$$

$$\frac{\partial^2 C}{\partial S^2} = \frac{C^l_{m+1,n} - 2C^l_{m,n} + C^l_{m-1,n}}{\left(\Delta S\right)^2}, \quad \frac{\partial^2 C}{\partial r^2} = \frac{C^l_{m,n+1} - 2C^l_{m,n} + C^l_{m,n-1}}{\left(\Delta r\right)^2},$$

$$\frac{\partial^2 C}{\partial P \partial S} = \frac{V^l_{m+1,n} - V^l_{m-1,n}}{2\Delta S}, \quad \frac{\partial^2 C}{\partial P \partial r} = \frac{V^l_{m,n+1} - V^l_{m,n-1}}{2\Delta r},$$

$$\frac{\partial^2 C}{\partial S \partial r} = \frac{C^l_{m+1,n+1} - C^l_{m+1,n-1} + C^l_{m-1,n+1} + C^l_{m-1,n-1}}{4\Delta S \Delta r}.$$

From equation (4.2.18), the PDE is given as

$$\rho_{sr}\frac{\partial^2 C}{\partial S\partial r}\sigma_s\sigma_r S+\frac{1}{2}\frac{\partial^2 C}{\partial S^2}S^2\sigma_s^2+\frac{1}{2}\frac{\partial^2 C}{\partial r^2}\sigma_r^2+rS\frac{\partial C}{\partial S}+a\left(b\left(t\right)-r\left(t\right)\right)\frac{\partial C}{\partial r}$$
$$+\alpha\left(rP+K\right)\frac{\partial C}{\partial P}+\alpha^2\frac{1}{2}P^2\sigma_S^2\frac{\partial^2 C}{\partial P^2}+\alpha\rho_{Pr}\frac{\partial^2 C}{\partial P\partial r}\sigma_s\sigma_r P+\alpha PS\sigma_s^2\rho_{PS}\frac{\partial^2 C}{\partial S\partial P}-rC=\frac{\partial C}{\partial \tau}. \tag{4.3.3}$$

Substituting the partial derivatives and the mixed partial derivatives with respect to time, S and r by using the approximating equations discussed, an ODE is obtained. For the first two time steps, it is given by:

$$\begin{aligned}
&\rho_{sr}\frac{C^l_{m+1,n+1}-C^l_{m+1,n-1}+C^l_{m-1,n+1}+C^l_{m-1,n-1}}{4\Delta S\Delta r}\sigma_s\sigma_r S\\
&\frac{1}{2}\frac{C^l_{m+1,n}-2C^l_{m,n}+C^l_{m-1,n}}{\left(\Delta S\right)^2}S^2\sigma_s^2+\frac{1}{2}\frac{C^l_{m,n+1}-2C^l_{m,n}+C^l_{m,n-1}}{\left(\Delta r\right)^2}\sigma_r^2\\
&+rS\frac{C^l_{m+1,n}-C^l_{m-1,n}}{2\Delta S}+a\left(b\left(t\right)-r\left(t\right)\right)\frac{C^l_{m,n+1}-C^l_{m,n-1}}{2\Delta r}\\
&+PS\alpha\sigma_s^2\rho_{PS}\frac{V^l_{m+1,n}-V^l_{m-1,n}}{2\Delta S}+\alpha\rho_{Pr}\frac{V^l_{m,n+1}-V^l_{m,n-1}}{2\Delta r}\sigma_s\sigma_r P\\
&-rC+\alpha\left(rP+K\right)\frac{\partial C}{\partial P}+\frac{1}{2}\alpha^2P^2\sigma_S^2\frac{\partial^2 C}{\partial P^2}-\frac{C^l_{m,n}-C^{l-1}_{m,n}}{\Delta\tau}=0.
\end{aligned} \tag{4.3.4}$$

For subsequent time steps, this is given by:

$$\begin{aligned}
&\rho_{sr}\frac{C^l_{m+1,n+1}-C^l_{m+1,n-1}+C^l_{m-1,n+1}+C^l_{m-1,n-1}}{4\Delta S\Delta r}\sigma_s\sigma_r S\\
&+\frac{1}{2}\frac{C^l_{m+1,n}-2C^l_{m,n}+C^l_{m-1,n}}{\left(\Delta S\right)^2}S^2\sigma_s^2+\frac{1}{2}\frac{C^l_{m,n+1}-2C^l_{m,n}+C^l_{m,n-1}}{\left(\Delta r\right)^2}\sigma_r^2\\
&+rS\frac{C^l_{m+1,n}-C^l_{m-1,n}}{2\Delta S}+a\left(b\left(t\right)-r\left(t\right)\right)\frac{C^l_{m,n+1}-C^l_{m,n-1}}{2\Delta r}\\
&+\alpha PS\sigma_s^2\rho_{PS}\frac{V^l_{m+1,n}-V^l_{m-1,n}}{2\Delta S}+\alpha\rho_{Pr}\frac{V^l_{m,n+1}-V^l_{m,n-1}}{2\Delta r}\sigma_s\sigma_r P\\
&-rC+\alpha\left(rP+K\right)\frac{\partial C}{\partial P}+\frac{1}{2}\alpha^2P^2\sigma_S^2\frac{\partial^2 C}{\partial P^2}-\frac{C^l_{m,n}-C^{l-1}_{m,n}}{\Delta\tau}=0.
\end{aligned} \tag{4.3.5}$$

The boundary conditions discussed in the previous section are also applied here. To solve equations (4.3.4) and (4.3.5), each equation is transformed into two equations of the first

order:

$$\begin{aligned}\frac{dC^l_{m,n}}{dS} &= V^l_{m,n},\\ \frac{dV^l_{m,n}}{dS} &= \mathbf{A}_{m,n}(P)\,C^l_{m,n} + \mathbf{B}_{m,n}(P)\,V^l_{m,n} + \mathbf{P}^l_{m,n}(P).\end{aligned} \tag{4.3.6}$$

A Riccati transformation is used to solve this system of first order equations and is given by:

$$C^l_{m,n}(P) = R_{m,n}(P)\,V^l_{m,n}(P) + W^l_{m,n}(P), \tag{4.3.7}$$

where $R_{m,n}(P)$ and $W^l_{m,n}(P)$ are solutions of the initial value problems,

$$\frac{dR_{m,n}}{dP} = 1 - \mathbf{B}_{m,n}(P)\,R_{m,n}(P) - \mathbf{A}_{m,n}(P)\,(R_{m,n}(P))^2, \quad R_{m,n}(0) = 0, \tag{4.3.8}$$

$$\begin{aligned}\frac{dW^l_{m,n}}{dP} &= -\mathbf{A}_{m,n}(P)\,R_{m,n}(P)\,W^l_{m,n} - R_{m,n}(P)\,\mathbf{P}^l_{m,n}(P),\\ W^l_{m,n}(0) &= \alpha A(\tau_l, g)\,Z(\tau_l, T) \quad (IG - Scheme),\\ W^l_{m,n}(0) &= A(\tau_l, g)\,Z(\tau_l, T) \quad (CG - Scheme),\end{aligned} \tag{4.3.9}$$

where $Z(\tau_l, T)$ is a zero-coupon bond.

The integration of equation (4.3.8) and equation (4.3.9) from 0 to P_{max} is called the forward sweep. The free boundary value $P^\bullet$ is computed using $R_{m,n}$ and the $W^l_{m,n}$ obtained from integration, and is between two consecutive points at which there is a sign change on computing values for the following equations:

$$\begin{aligned}&(\alpha A(\tau, g) + \alpha(d(\tau, S, r) - A(\tau, g))) - \alpha R_{m,n}(P^\bullet) - W^l_{m,n}(P^\bullet) = 0 \text{ (IG-Scheme)},\\ &(A(\tau, g) + (\alpha d(\tau, S, r) - A(\tau, g))) - \alpha R_{m,n}(P^\bullet) - W^l_{m,n}(P^\bullet) = 0 \text{ (CG-Scheme)}.\end{aligned} \tag{4.3.10}$$

$d^l_{m,n}$ is defined as the grid point at which there is this free boundary and is obtained using cubic spline interpolation.

An integration from $d^l_{m,n}$ to 0 for the option delta is performed. This is known as the backward sweep.

$$\frac{dV^l_{m,n}}{dP} = \mathbf{A}_{m,n}(P)\left(R(P)\,V + W^l_{m,n}(P)\right) + \mathbf{B}_{m,n}(P)\,V + \mathbf{P}^l_{m,n}(P), \quad V^l_{m,n}\left(d^l_{m,n}\right) = \alpha. \tag{4.3.11}$$

At all stages of the calculation the boundary conditions are considered. Having the values for $R_{m,n}$, $W^l_{m,n}$ and $V^l_{m,n}$ the option values from the Riccati transformation equation (4.3.7) are obtained. Iterations are used to solve ordinary differential equation in each time step.

When the difference between the option values is less than 10^{-5} for the $k^{th}-1$ and the k^{th} iteration, the iteration is stopped, and the procedure goes to the next step.

4.4. Numerical Results

A variety of numerical investigations are conducted to examine the impact of model parameters, such as the investment fraction, the interest rate and its volatility, to the early exercise boundary for the two types of pension schemes under consideration.

A 15-year contract with a periodic premium payment of 1 every two months is studied, implying 90 (15×6 payments per year) time points. To compute these American Asian call option prices using the MOL, the discretisation of the portfolio value, the asset price process, the interest rate process, and the time points are specified. r lies within the range $0 \leq r \leq 0.1$ with 10 grid points and similarly S lies within $0 \leq S \leq 0.1$ with 10 grid points. The grid for the portfolio values is not uniform, with P ranging between 0 and 10. In the interval $0 \leq P \leq 0.5$ there are 100 grid points. In the next interval $0.5 \leq P \leq 1.0$ there are 500 grid points and for the interval $1.0 \leq P \leq 2.0$ there are 1000 grid points. Lastly, in the interval $2 \leq P \leq 10$ there are 800 grid points. A finer grid for the interval $0.5 \leq P \leq 1.0$ has been chosen because there is a lack of smoothness of the solution around the points at which the strike price lies, and this interval is the range within which all the different strike prices lie (Meyer (2015)). Table 4.4.1 displays the parameter values used in the numerical investigations.

TABLE 4.4.1. Parameter values used to price American Asian options.

Parameter	σ_s	σ_r	a	c_1	c_2	c_3	ρ
Value	0.25	0.01	0.5	0.04	0.00	1	0.5

First, the relationship between the level of guaranteed investment return and the investment fraction to finance the guarantee is analysed. Second, a sensitivity analysis is conducted to gauge the impact of the interest rate and its volatility, of the portfolio volatility, and finally the correlation between the portfolio and the interest rate on the free boundary. Two sets of results denoted by Guarantee-Before-Maturity and Guarantee-At-Maturity will be shown. Guarantee-Before-Maturity are the results based on the equations (4.2.21) and (4.2.24). If the investor chooses to terminate early, these equations represent the value of the free

boundary being the sum of the maximum of the portfolio's value and the guaranteed value at the point of the termination of the contract and the present value of all contributions not made due to early termination. The guaranteed amount depends on the number of premiums paid until the point of termination. The other set of results will be denoted by Guarantee-At-Maturity and are based on equations (4.2.29) and (4.2.30). In this case, the guaranteed amount is the total accumulated contribution amount at maturity, and the investor can exercise early only if the current value of the portfolio is greater than the guaranteed value at maturity.

4.4.1. Relationship between the investment fraction α and the guaranteed return g. The purpose of this exercise is for a fixed level of guaranteed rate of return g, to find the value of α, such that the present value of the total contributions is equal to the value of the option, by solving a fixed-point problem. The total sum of the contributions is determined by Definition 1. The results of this analysis are presented in Table 4.4.2 for the Guarantee-At-Maturity case and Table 4.4.3 for the Guarantee-Before-Maturity case respectively, and for both the IG and CG schemes with the interest rate levels being $1\%,\ 4\%$ and 7%. The relationship between the investment fraction and the guaranteed return is depicted in Figure 4.5.1 for both schemes and at all interest rate levels, α is a decreasing function of the guaranteed return. However, α increases as the interest rate increases as shown by Table 4.4.2 and Table 4.4.3. This would be expected because option prices decrease as interest rates increase. Since the payment contribution amount remains constant, and part of it is used to purchase the options, the remainder is used for investment purposes. As the option prices decrease with increasing interest rates, the fraction of the amount to be invested gets larger.

Table 4.4.2 and Table 4.4.3 reveal that the differences between subsequent α values are greater for the CG Scheme compared to the IG scheme. As a result, the α values for the CG scheme approach zero much quicker than the IG scheme, as the guaranteed rate is increased. Note that the values start increasing once the guaranteed rate becomes greater than the interest rate. The results of this investigation show that for the Guarantee-At-Maturity case, the shape of the graph for the IG scheme is numerically close to linear, whilst for the CG scheme it is slightly concave down, see the top panel of Figure 4.5.1. Similar results were obtained by Nielsen et al. (2011). For the results based on the Guarantee-Before-Maturity

case, the shape of the graph for the IG scheme is also numerically close to linear, whilst for the CG scheme it is slightly concave up, see the bottom panel of Figure 4.5.1. The values of α obtained for the Guarantee-At-Maturity case have been observed to be higher than for the Guarantee-Before-Maturity case. This can be explained by the nature of the payoffs at the free boundaries as given by (4.2.21) and (4.2.24) for the Guarantee-Before-Maturity and (4.2.29) and (4.2.30) for the Guarantee-At-Maturity. A higher value at the free boundary results in a less investment fraction, since the premium amount is always constant. The α values for the Guarantee-At-Maturity case were observed to be higher than the α values for the Guarantee-Before-Maturity case and this can be explained by the nature of their payoff at the free boundaries.

TABLE 4.4.2. Guarantee-At-Maturity. Table displays the guaranteed return as a fraction of the investment fraction value α, for the IG and the CG schemes and for $r = 1\%$, $r = 4\%$ and $r = 7\%$. This pension scheme matures in 15 years and the investor pays constant premiums every two months.

	$r = 1\%$		$r = 4\%$		$r = 7\%$	
Guaranteed Return	α_{IG}	α_{CG}	α_{IG}	α_{CG}	α_{IG}	α_{CG}
7.5%					36.38%	
7.0%					37.72%	
6.5%					39.17%	6.61%
6.0%					40.64%	10.07%
5.5%					42.16%	13.06%
5.0%					43.80%	15.91%
4.5%			37.14%		45.38%	18.61%
4.0%			38.48%		46.97%	21.27%
3.5%			39.87%	6.38%	48.57%	23.97%
3.0%			41.30%	9.81%	50.18%	26.73%
2.5%			42.77%	12.72%	51.41%	29.48%
2.0%			44.26%	15.43%	52.65%	32.30%
1.5%	37.94%		45.58%	17.99%	53.89%	35.12%
1.0%	39.24%		46.76%	20.58%	55.13%	38.12%
0.5%	40.57%	6.17%	47.93%	23.15%	56.36%	41.08%
0.0%	41.92%	9.44%	49.01%	25.72%	57.60%	43.51%
-0.5%	43.07%	12.27%	50.08%	28.29%	58.84%	45.95%
-1.0%	44.22%	14.53%	51.15%	30.87%	60.07%	48.38%

An analysis of the payoffs of these schemes also helps in understanding these results. The payoffs are composed of two parts: the first being the guaranteed amount that is defined by equation (4.2.10) and the second being the expected payoff of a put option at maturity of

TABLE 4.4.3. Guarantee-Before-Maturity. The table displays the guaranteed return as a function of the investment fraction value α, for the IG and the CG schemes and for $r = 1\%$, $r = 4\%$ and $r = 7\%$. This pension scheme matures in 15 years and the investor pays constant premiums every two months.

	$r = 1\%$		$r = 4\%$		$r = 7\%$	
Guaranteed Return	α_{IG}	α_{CG}	α_{IG}	α_{CG}	α_{IG}	α_{CG}
7.5%					35.39%	
7.0%					36.79%	
6.5%					38.41%	9.03%
6.0%					39.84%	8.37%
5.5%					41.55%	9.25%
5.0%					43.36%	11.73%
4.5%			36.17%		45.05%	14.04%
4.0%			37.69%		46.64%	17.17%
3.5%			38.95%	5.43%	48.17%	20.18%
3.0%			40.72%	5.84%	49.64%	23.79%
2.5%			42.32%	7.10%	51.01%	27.17%
2.0%			43.96%	10.84%	52.32%	30.40%
1.5%	37.19%		45.03%	12.86%	53.54%	33.39%
1.0%	38.52%		46.09%	17.25%	54.73%	36.56%
0.5%	39.85%	3.82%	47.16%	18.29%	55.85%	39.57%
0.0%	41.24%	3.77%	48.23%	22.89%	56.91%	42.41%
-0.5%	42.73%	6.79%	49.29%	25.34%	57.94%	45.16%
-1.0%	44.22%	9.81%	50.36%	27.42%	58.79%	47.42%

the option, see equation (4.2.12) and (4.2.14). The guaranteed amount of the IG-Scheme, namely

$$G_{IG} = \alpha A\left(T, g\right),$$

is always less than the guaranteed amount of the CG-Scheme,

$$G_{CG} = A\left(T, g\right),$$

since α is always less than 1. Figure 4.5.3 compares directly the guaranteed benefit at maturity as a function of the guaranteed rate for the two schemes, namely, IG and CG, and demonstrates that CG scheme always provides higher guaranteed benefit compared to the IG scheme. Thus the IG scheme is more risky than the CG scheme since its guaranteed amount is less. Since each contribution amount is the same for each scheme and the guaranteed amount for the IG scheme is less, its investment amount will be more. In turn, the expected payoff for the IG-Scheme will be higher than that of the CG-scheme. These

results are in line with Nielsen et al. (2011) who specify that the relationship between the different investment fractions among the schemes is such that

$$\alpha_{IG} \geq \alpha_{CG}.$$

Since an American Asian option that can be exercised at, or prior to, maturity is being priced, the guaranteed benefit is illustrated as a function of time at the termination of the contract. Figure 4.5.3 shows a linear relationship between the guaranteed benefit and termination of the contract, with the guaranteed benefits from CG being considerably higher than the benefits for the IG scheme.

Comparing these results with the European style options case studied in Nielsen et al. (2011), it is evident that, for American options, the investment fraction is lower than in European options. This is expected, since American options are priced higher than European options and for a constant contribution, a lesser amount of the premium would be left for investment purposes. Looking at both schemes, the difference between subsequent values of the investment fraction as the guaranteed return increases is greater for the CG scheme, compared to the IG scheme. The results of the investigation show that the shape of the graph for the CG scheme is slightly concave for both the Guarantee-Before-Maturity and Guarantee-At-Maturity case, whilst for the IG scheme it is numerically close to linear, see also Nielsen et al. (2011) for similar results.

4.4.1.1. *Impact of speed of mean reversion of interest rates on the investment fraction.* The impact of the speed of mean reversion of interest rates (a) on the investment fraction (given the assumption of stochastic interest rates in the model) is also investigated. Table 4.4.4 reports the investment fraction values $a = 0.05$, $a = 0.125$ and $a = 0.2$ when the guaranteed return is 2% and the interest rate is 4%. In general, the speed of mean reversion

TABLE 4.4.4. Impact of the speed of mean reversion of interest rates on the investment fraction values for both the IG scheme and the CG scheme.

	$a = 0.05$	$a = 0.125$	$a = 0.2$
IG Scheme	46.38%	45.98%	45.82%
CG Scheme	17.44%	17.24%	17.19%

of interest rates has a small impact on the investment fraction, as an increase in a tends to

marginally reduce the investment fraction. The values for the investment fraction are very close to the ones obtained in the Table 4.4.2.

For the rest of the analysis, ATM options will be used, with $r = 0.04$. As S varies the option prices remain the same, hence an arbitrary value of S has been chosen. The guaranteed return is 2%. For convergence purposes of the MoL, the analysis will be done for $a = 0.05$. Using these parameter values, the results for the sensitivity analysis are discussed below.

4.4.2. Impact of interest rates on the free boundary. For American options, the early exercise premium depends on the term structure of interest rates. Hence interest rates are assumed to be stochastic. Figure 4.5.4 and Figure 4.5.5 plot the free boundary surface as a function of time to maturity and interest rates for the two cases, Guarantee-Before-Maturity and Guarantee-At-Maturity cases and for the IG and the CG scheme respectively. For all the schemes, the free boundary surface decreases in value as the risk-free rate increases. The high free boundary values for low interest rates can be explained by the fact that when interest rates are low, the investor would opt to exercise this option than when interest rates are high, hence the high value of the option. Kang & Ziveyi (2018) deduced that when interest rates are high, it would be optimal to surrender at lower fund values than when the interest rates are low.

The top panels of Figure 4.5.4 and Figure 4.5.5 show that the free boundary values increase as a function of time to maturity for the Guarantee-At-Maturity case. For call options, the longer the time to maturity, the higher the probability that the option will be in the money as a result of different events that are likely to occur in the long run. Hence, the price becomes higher as the time to maturity increases. Several papers report similar results, i.e. van Haastrecht, Plat & Pelsser (2010), Kang & Ziveyi (2018) and van Haastrecht, Lord, Pelsser & Schrager (2009). The panels at the bottom of Figure 4.5.4 and Figure 4.5.5 show decreasing free boundaries as the time to maturity increases for the Guarantee-Before-Maturity case. This can be explained by the fact that the option holder's decision to exercise is dependent on the value of the portfolio at that specific time, which is a decreasing function of time to maturity. This is different from the Guarantee-At-Maturity case discussed above, in which the investor's decision to exercise depends on the constant value of the portfolio at maturity time.

4.4.2.1. *Impact of the interest rate volatility on the free boundary.* Interest rate volatility determines the riskiness of interest rates and impacts the return of the portfolio. This is one of the most significant risks faced by pension fund managers. The longer the time to maturity, the greater the riskiness of interest rates because of the greater uncertainty regarding the level of interest rates. Since it is a part of market risk that cannot be diversified away, a proper analysis of the investor's behaviour will ensure correct decision making by fund managers, and, subsequently, accurate pricing (Shehu (2011)). The effect of interest rate volatility on the free boundary is investigated, with the proposed model specification of equation (4.2.2).

Figure 4.5.7 displays the optimal surrender curve for a range of interest rate volatilities. Accordingly, as the interest rate volatility increases, the optimal surrender curve is shifted up. This is expected, since call options are worth more if the volatility of interest rates goes up. This also implies that the investment fraction decreases as this parameter value is increased. Looking at the Guarantee-At-Maturity case, for a shorter time to maturity, the impact of changing interest volatility is negligible (ranging from $2\% - 3\%$ for the CG Scheme and $3\% - 6\%$ for the IG scheme), whilst for a longer time to maturity, the impact of interest rate volatility on the free boundary is relatively significant, as indicated by the plots (maximimum being 13% for the CG scheme and 17% for the IG Scheme). In the Guarantee-Before-Maturity case, the impact of interest rate volatility is greater for a shorter time to maturity for the IG scheme, and for the CG scheme the impact of interest rates looks similar across all maturities. Bacinello & Persson (2002) consider the pricing of equity-linked life insurance with stochastic interest rates and they found a positive relation between the premiums and volatility (when the volatility parameter is positive).

4.4.3. Impact of portfolio volatility on the free boundary. A sensitivity analysis is carried out to assess the impact of the portfolio volatility on the free boundary values. Asset volatility substantially impacts the value of options, thus increasing volatility presents a significant risk to pension schemes.

Under the assumption of deterministic volatility, the effect of portfolio volatility on the free boundary is investigated for $\sigma_S = 0.17,\ 0.20$ and 0.25. From Figure 4.5.8, it can be observed that generally, an increase in volatility also increases the free boundary value for both schemes and for both the Guarantee-Before-Maturity and Guarantee-At-Maturity

cases. This implies that if volatility is high, for the same asset price, interest rate, and time the investor will surrender the policy when the value of the fund is higher in comparison to when the volatility is low. Bernard et al. (2014) and Kang & Ziveyi (2018) concluded that guaranteed maturity minimum benefits are more valuable when the volatility is high. Bacinello & Persson (2002) did a similar analysis and found that increasing volatility of the asset price has an impact of increasing the premiums. For the Guarantee-Before-Maturity case it is observed that as time to maturity increases, the impact of volatility becomes more pronounced.

4.4.4. Impact of the correlation on the free boundary. The portfolio under consideration consists of shares. It is important to analyse the correlation between the portfolio and interest rates because shares are sensitive to the likelihood of interest rate movements. Also, since the present value of a pension increases as interest rates decrease, interest rates that are too low can lead to the insolvency of a fund. This analysis considers a positive correlation between the portfolio and interest rates, as empirical studies suggest. The empirical study by van Haastrecht et al. (2010) investigated the nature of the correlation between the long term interest rates and S&P 500 for US and EuroStoxx50 for EU. A significant positive relation was obtained. Figure 4.5.6 presents the results of the impact of this correlation on the free boundary when $\rho = 0.3,\ 0.5$ and 0.7. A positive relation between the correlation and the free boundary is evident. Ho et al. (1984) also found higher correlations to have a positive impact on option prices, especially when the interest rates are high.

In general, the correlation between the asset dynamics/portfolio value and the interest rate process have been found to impact the free boundary values differently, depending on the sign of the chosen correlation value as some of the studies have indicated, i.e. Kizaki & Muroi (2016). Boyle & Hardy (2003) found that as the correlation parameter increases, the option price also increases. Moreover, they found that when ρ is 0, the option price is double the case when ρ is -1, and one half of the case when ρ is 1.

4.5. Conclusion

In this chapter, the valuation of an American Asian option is considered, as applied to two types of equity-linked pension schemes with guarantee, namely, the investment

guarantee (IG) and the contribution guarantee (CG) scheme. This pricing occurs under the assumption of deterministic volatility and stochastic interest rates of the Hull & White (1987) type and the option is numerically evaluated using the MoL. Further, the relationship between the guaranteed return and the investment fraction of the different types of schemes is examined and the optimal surrender regions from the investor's perspective are also obtained using call options, which are used to compute call option prices. In the analysis, two sets of results are obtained, which differ in the way the guarantee has been defined. In the first set of results, denoted by Guarantee-Before-Maturity, the guarantee depends on the number of premiums made up to the point of termination and the investor will exercise only if the value of the portfolio is greater than this guaranteed amount. In the second set of results, denoted by Guarantee-At-Maturity, the guaranteed amount is the total accumulated contribution amount at maturity, and the investor can only exercise the option if the portfolio value is greater than this guaranteed amount.

In general, the investment fraction required to finance the guarantee is a decreasing function of the guaranteed return. For the CG scheme, this relation concaves down in the Guarantee-At-Maturity case and slightly concaves up in the Guarantee-Before-Maturity case. However, in our investigations of the IG scheme, this relationship is always numerically close to linear. Furthermore, the guarantee benefits for the CG scheme is considerably higher (especially as the maturity increases) than the guarantee benefits for the IG scheme, implying that the CG scheme is significantly less risky than the IG scheme. In relation to the interest rates, α is an increasing function of the interest rates because option prices decrease as interest rates increase. Since the premium is a constant amount, higher option prices result in a lower investment amount α. The difference between subsequent α values as the guaranteed amount increases was found to be greater for the CG scheme than for the IG scheme, resulting in the α values for the CG scheme approaching zero values much quicker than the IG scheme.

On investigating the impact of interest rates on free boundary values, the results for both schemes indicate that the free boundary is a decreasing function of interest rates. Accordingly, when interest rates are low, the investor would opt to exercise this option than when interest rates are high, hence the high value of the option. The speed of mean reversion has a small impact on the free boundary values. Further analysis indicates that

interest rate volatility, portfolio volatility, and correlation have a positive impact on the free boundary. The upward shift on the free boundary as interest rate volatility increases is expected, since call options are worth more if the volatility of interest rates goes up. However, the extent of this upward shift differs depending on the time to maturity for both schemes. The increasing free boundary, which results from increasing portfolio volatility implies that when volatility is high, for the same asset price, interest rate, and time the investor will surrender the policy when the value of the fund is higher compared to when volatility is low. The impact of the correlation between asset and interest rate dynamics impacts the free boundary depending on the sign of the correlation. A positive correlation has a positive impact on the free boundary, making it less likely for the option to be surrendered early.

By analysing this investor behaviour, the information can be used in decision making to minimise the risk faced by a financial institution as a result of early surrender of the policy by the investor. Mortality is one of the features that can be added in the proposed model and it can be considered for future research.

Figures

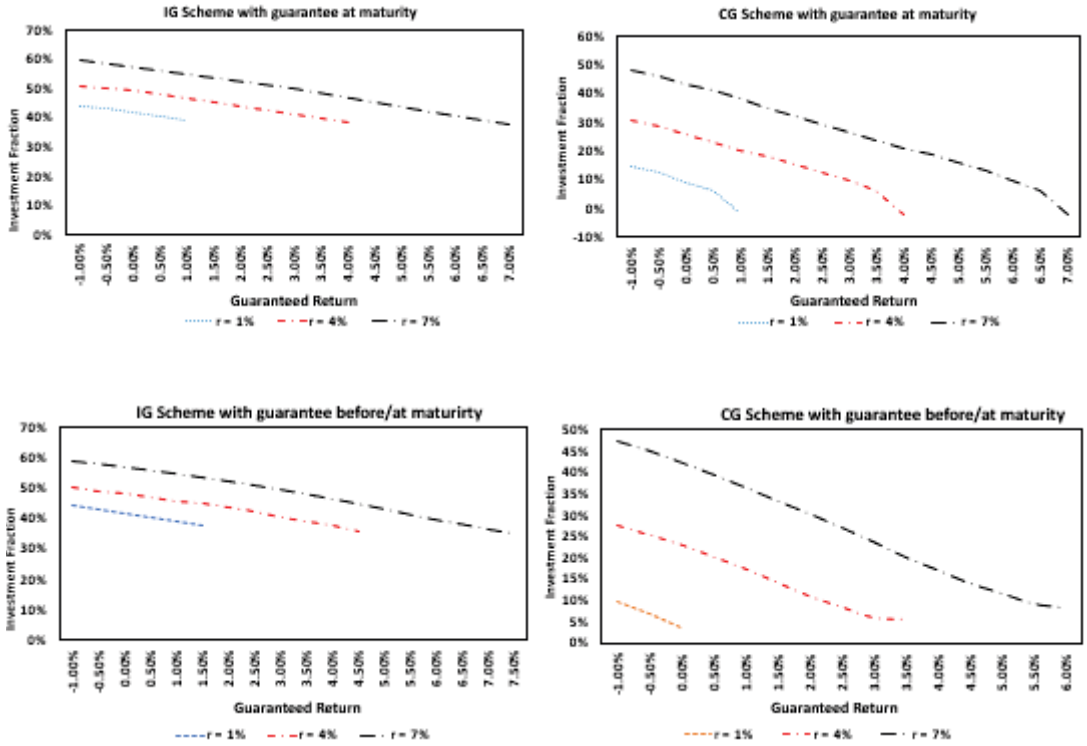

FIGURE 4.5.1. The graphs show the investment fraction α as a function of the guaranteed return for $r = 1\%$, $r = 4\%$ and $r = 7\%$. This pension scheme matures in 15 years and the investor pays constant premiums every two months. The top two panels depicts the investment fraction plots for the IG scheme and CG scheme for the Guarantee-At-Maturity case respectively whilst the bottom two panels are for the Guarantee-Before-Maturity case.

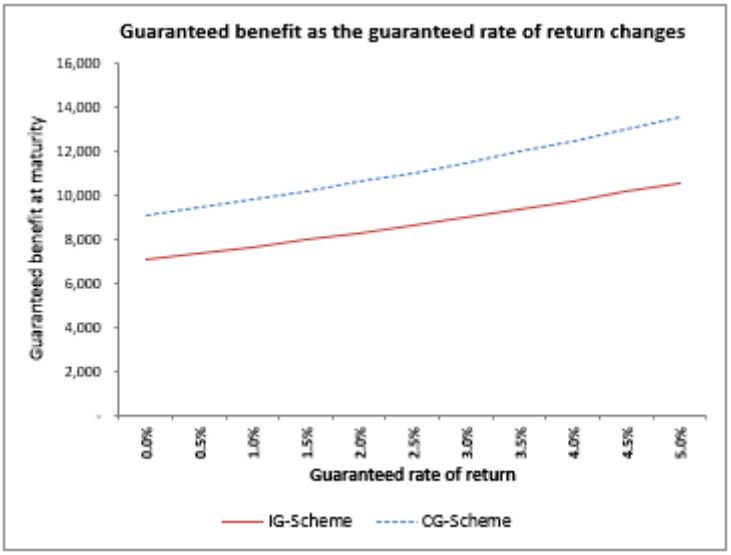

FIGURE 4.5.2. Guaranteed benefit at maturity as a function of the guaranteed rate of return for the IG-Scheme and the CG-Scheme. This pension scheme matures in 15 years and the investor pays constant premiums every two months.

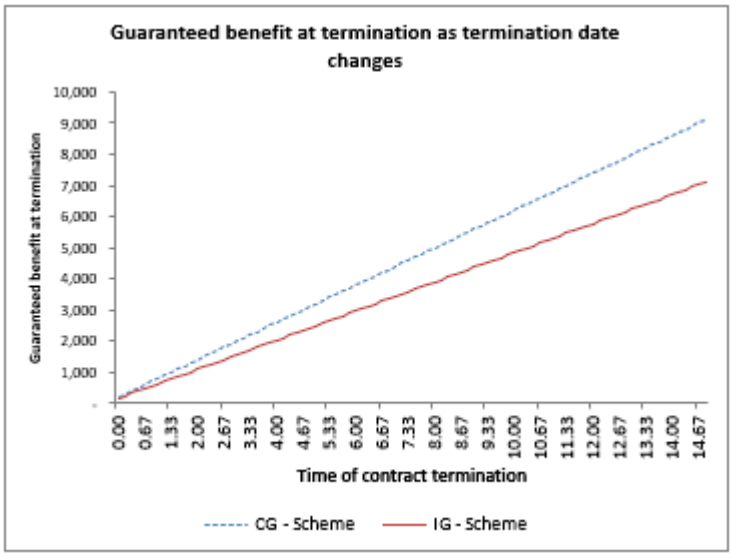

FIGURE 4.5.3. Guaranteed benefit at termination as a function of termination date for the IG-Scheme and the CG-Scheme. This pension scheme matures in 15 years and the investor pays constant premiums every two months.

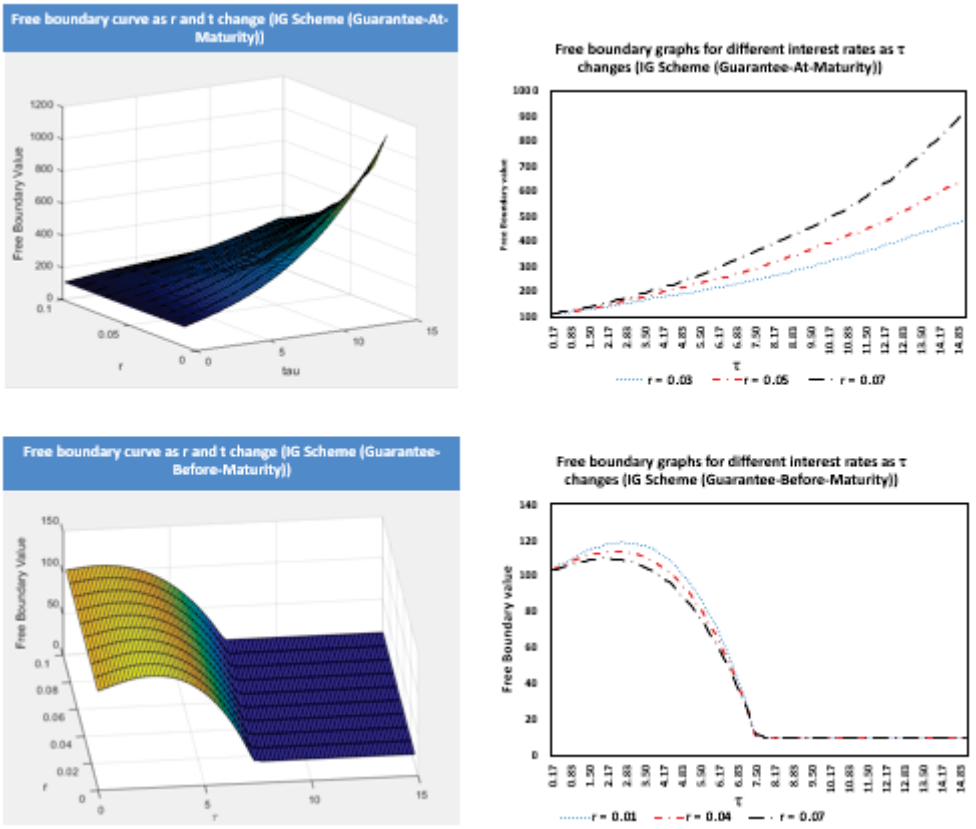

FIGURE 4.5.4. Free boundary curves for an American Asian option as a function of time to maturity and interest rate (left hand side). This pension scheme matures in 15 years and the investor pays constant premiums every two months. The graphs to the right show some cross-sectional values of the curve on the left hand side at different levels of interest rates. The top panels depicts the free boundary for the IG scheme for the Guarantee-At-Maturity case and the bottom panels for the Guarantee-Before-Maturity case. Parameter values are given in Table 4.4.1.

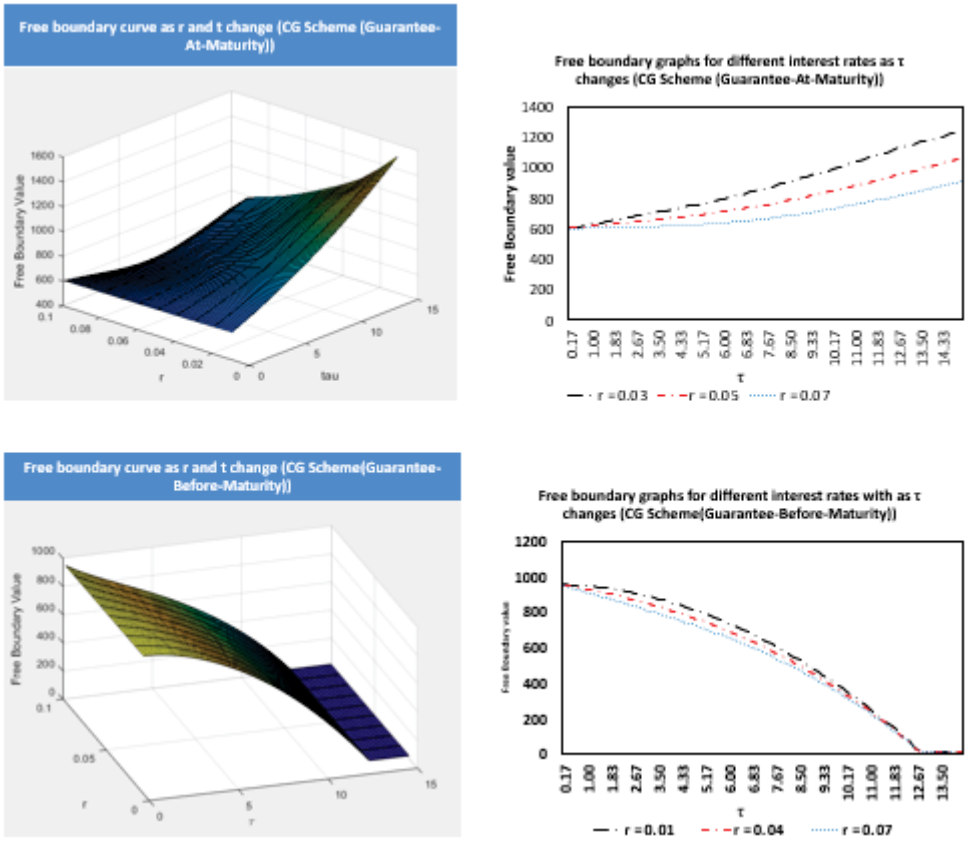

FIGURE 4.5.5. Free boundary curves for an American Asian option as a function of time to maturity and interest rate (left hand side). This pension scheme matures in 15 years and the investor pays constant premiums every two months. The graphs to the right show some cross-sectional values of the curve on the left hand side at different levels of interest rates. The top panels depicts the free boundary for the CG scheme for the Guarantee-At-Maturity case and the bottom panels for the Guarantee-Before-Maturity case. Parameter values are given in Table 4.4.1.

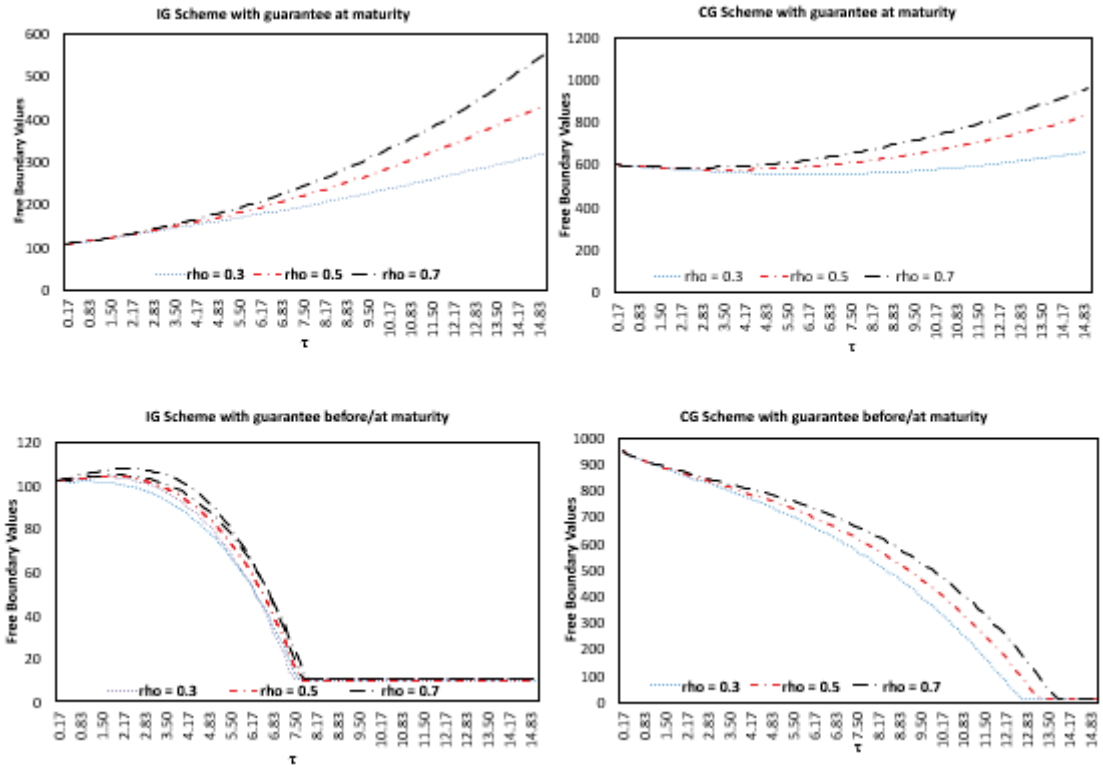

FIGURE 4.5.6. Free boundary curves for an American Asian option at different correlation values ($\rho = 0.16$, $\rho = 0.18$ and $\rho = 0.20$). This pension scheme matures in 15 years and the investor pays constant premiums every two months. The first two panels depicts the investment fraction plots for the IG scheme and CG scheme for the Guarantee-At-Maturity case, whilst the bottom two panels are for the Guarantee-Before-Maturity case. Parameter values are given in Table 4.4.1.

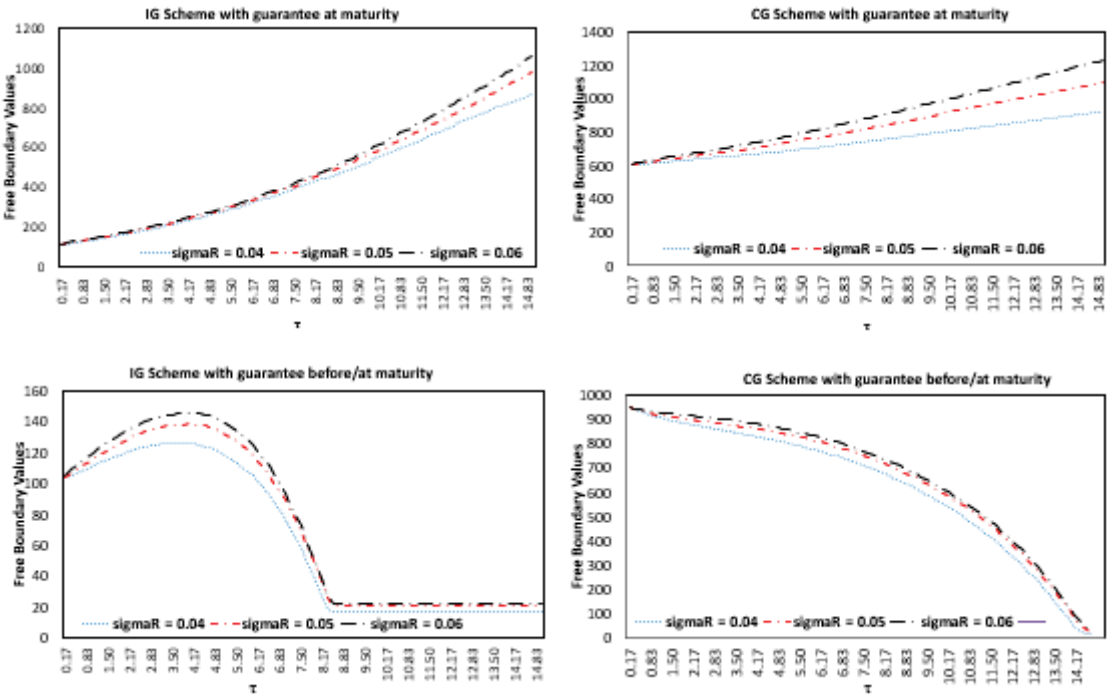

FIGURE 4.5.7. Free boundary curves for an American Asian option at different levels of interest rate volatility ($\sigma_r = 4\%$, $\sigma_r = 5\%$ and $\sigma_r = 6\%$). This pension scheme matures in 15 years and the investor pays constant premiums every two months. The first two panels depicts the investment fraction plots for the IG scheme and CG scheme for the Guarantee-At-Maturity case, whilst the bottom two panels are for the Guarantee-Before-Maturity case. Parameter values are given in Table 4.4.1.

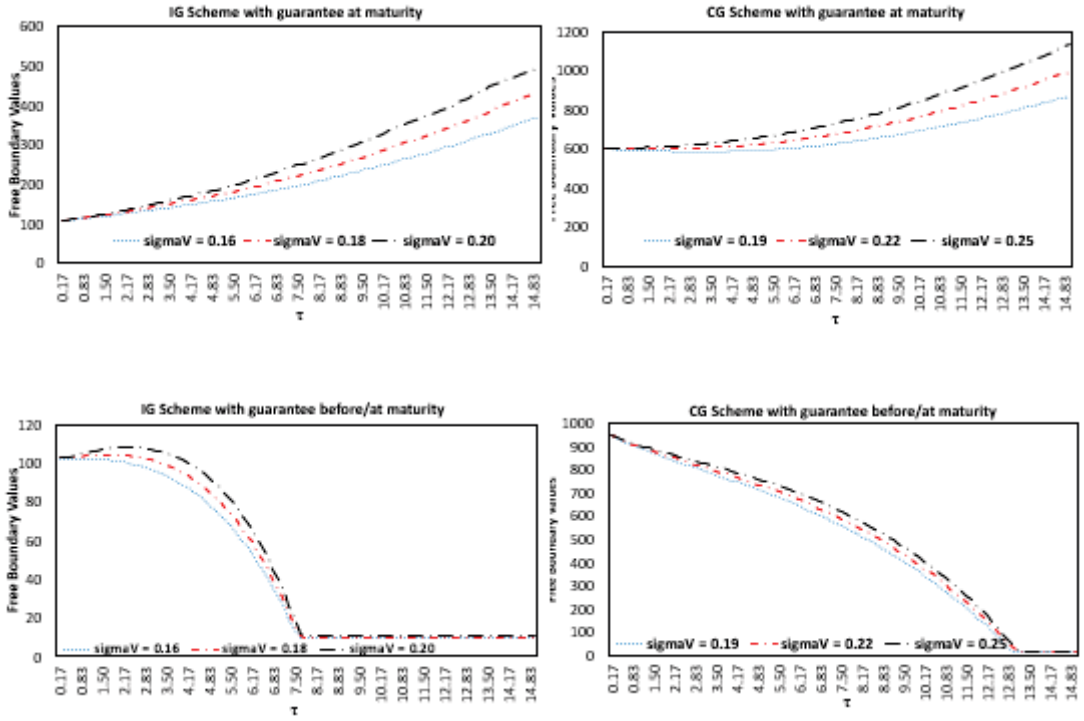

FIGURE 4.5.8. Free boundary curves for an American Asian option at different levels of volatility (SigmaV = 0.16, SigmaV = 0.18 and SigmaV = 0.20). This pension scheme matures in 15 years and the investor pays constant premiums every two months. The first two panels depicts the investment fraction plots for the IG scheme and CG scheme for the Guarantee-Before-Maturity case, whilst the bottom two panels are for the Guarantee-At-Maturity case.Parameter values are given in Table 4.4.1.

CHAPTER 5

Conclusion

Since the introduction of the Black & Scholes (1973) and Merton (1973) options pricing model, extensive literature has been dedicated on studying the pricing of options with the early exercise feature. The American option pricing problem rises from the fact that, in general, closed form solutions are not feasible. Thus, option pricing solutions rely on using efficient approximations or numerical schemes.

Classical modelling approaches have been employed for pricing American options, including stochastic volatility models, jump-diffusion models, and stochastic interest rates. Stochastic volatility models produce more realistic volatility smiles compared to the Black-Scholes-Merton model. The inclusion of asset jumps in option pricing models tends to improve stochastic volatility models, which are not capable of fully explaining the smile dynamics observed in the markets, in particular, short maturity smiles. Thus, they improve the pricing and hedging of short maturity options. Asset jumps can explain the negative skewness and kurtosis that are often observed in option prices. However, models with jumps in assets only are mis-specified. Eraker et al. (2003) report that although jumps in returns can generate large movements observed in financial markets, the impact only lasts for a short time and does not have an effect on future asset dynamics. They propose that adding volatility jumps to the asset jumps will provide '*a rapidly moving but persistent factor that drives the conditional volatility of returns*'. In the light of these findings, this thesis deals with the pricing of American options by using stochastic volatility option pricing models with asset and volatility jumps. As the free boundaries depend on the term structure of interest rates, stochastic interest rates have been considered. In the absence of closed form solutions, the option prices are evaluated by using the MoL. This numerical algorithm provides a satisfactory balance between pricing accuracy and computational effort, as free boundaries and Greeks can be obtained at the same computational level as the option prices. The thesis firstly conducts a numerical study to assess the impact of

jumps and stochastic interest rates on American options and their boundaries. A calibration application to S&P 100 American option prices follows in the next chapter.

Finally, an application of the MoL in valuing an American Asian option applied to two types of equity linked pension schemes with guarantees, namely, the investment guarantee and the contribution guarantee scheme is considered. Since these are long-term products, a deterministic volatility model without jumps is used to obtain the investment fraction that is required to achieve the required level of rate of return. Extending the Nielsen et al. (2011) pricing framework to American options allows the policy holder to surrender their policy any time before maturity if desired.

5.1. Pricing American Options with Jumps in Asset and Volatility

The second chapter considers the problem of pricing American call options for an asset for which dynamics follow the Heston (1993) stochastic volatility model with jumps in both the asset and volatility dynamics. The model also assumes Hull & White (1987) stochastic interest rates. Jumps in asset dynamics follow a log-normal distribution whilst jumps in volatility follow an exponential distribution. The MoL is used to numerically price the options and compute free boundaries. A comparison of the results obtained using the MoL with Monte Carlo simulation results confirms the correctness of this implementation. A sensitivity analysis is performed to assess the impact of volatility and interest rate parameters on the free boundaries and to investigate the impact of jumps on option prices, free boundaries, and the Greeks.

The results of the numerical investigations indicate that the inclusion of asset and volatility jumps has a significant impact on free boundaries, with more impact being observed with the increase in time to maturity. Adding asset jumps to the HHW model leads to lowering the free boundary when the option is far from expiry. When volatility jumps are further added to the model with asset jumps, the free boundary curve elevates. This results in the option being less likely to be exercised by the investor. The moneyness of the option also influences the impact of jumps on the option prices as option prices for models with both asset and volatility jumps are more than the prices for the model with no jumps for call options that are OTM or ATM.

The American call option prices for the model with asset jumps are higher than the American call prices for the model with asset-volatility jumps. This relationship reverses when the call options are ITM. Further, asset jumps increases the delta for OTM options and reduce the delta for ATM and ITM options. Including the volatility jump decreases the delta slightly, although this delta is still greater than that of the model with no jumps. Last, the volatility of volatility and volatility of interest rates have a positive impact on the free boundary surfaces. Further research could focus on option pricing models which allow for jumps in interest rate dynamics, and this extension can be handled using the MoL. More extensions that are relevant to industry can also be explored, e.g. studying applications to popular American style financial products, such as pension schemes, which is the topic of Chapter 4.

In the third chapter, the significance of asset and volatility jumps in pricing S&P American index call options is analysed. The study examines the ability of Heston-Hull-White models with asset and volatility jumps to improve options pricing performance and analyse the impact of jumps in the free boundary and delta of the options. To this end, the HHW model with asset and volatility jumps is solved numerically using the MoL and then is calibrated to OIS data and S&P 100 index call options data.

Models with asset jumps consistently improve the overall pricing performance compared to the corresponding diffusion models, with further improvement occurring when the volatility jumps are added. The addition of the asset jumps provides a consistent improvement that is independent of moneyness and market conditions, while the addition of volatility jumps tends to further improve pricing performance. In accordance with previous literature, empirical evidence is provided on the importance of jumps in improving the ability of models to better price short-dated American options, especially when markets experience financial stress.

The impact of jumps on free boundaries is significant and more pronounced during volatile market conditions. The inclusion of asset jumps tends to increase the free boundary, while the addition of volatility jumps marginally drops the free boundary with more noticeable effects on near maturity options. An analysis of the impact of jumps on options delta shows that asset jumps typically increase the delta for OTM options, increase with asset

jumps, and decrease the delta for ATM and ITM options while volatility jumps marginally decrease the delta.

These results highlight the significance of including asset and volatility jumps in American options pricing and hedging applications, which are of critical importance to hedge funds and financial investors. American option holders become more sceptical with their exercise decisions with increasing volatility and market conditions, liable to jumps.

In this calibration a small subset of data with a specific maturity is considered. A worthwhile extension could be a more rigorous calibration application to investigate the impact of jumps on the term structure of the volatility smile and the free boundaries for longer maturity options.

5.2. Evaluation of Equity-Linked Pension Schemes With Guarantees.

In the fourth chapter, the valuation of an American-Asian option is considered and applied to two types of equity-linked pension schemes with a guarantee, namely, the investment guarantee and the contribution guarantee scheme. This pricing occurs under the assumption of deterministic volatility and stochastic interest rates of the Hull-White type, as these are long-dated contracts.

Using the MoL, the relationship between the guaranteed return and the investment fraction of the different types of schemes is established. The optimal surrender regions from the investor's perspective, using call options, used to compute the call option prices have also been obtained. By considering this investor behaviour, as depicted by the graphs, the information can be used in decision making to minimise the risk faced by a financial institution as a result of early surrender of the policy by the investor. One of the features considered in the Nielsen et al. (2011) work was the mortality distribution, which can also be included in the model proposed in Chapter 4. This has been left for future research.

The results of the investigations undertaken in this thesis are indicative of the significance that asset jumps and volatility jumps play in the pricing of American options and on their free boundaries. As the impact of jumps and interest rate dynamics on American option prices and early exercise boundaries is significant, the revealed relationships can provide useful and helpful insights for market participants, such as hedge funds and financial investors in pricing and hedging applications.

Bibliography

Abudy, M. & Izhakian, Y. (2013), 'Pricing stock options with stochastic interest rate', *International Journal of Portfolio Analysis and Management* **1**(3), 2048–2361.

Adolfsson, T., Chiarella, C., Zioga, A. & Ziveyi, J. (2013), Representation and numerical approximation of American option prices under Heston stochastic volatility dynamics. Quantitative Finance Research Centre, Working paper 327, UTS.

Agarwal, A., Junega, S. & Sircar, R. (2016), 'American options under stochastic volatility: Control variates, maturity randomisation and multiscale asymptotics', *Quantitative Finance* **16**(1), 17–30.

AitSahlia, F. & Lai, T. L. (1999), 'A consistent stochastic model of the term structure of interest rates for multiple tenors', *Journal of Finance* **1**, 69–78.

Alfeus, M., Grasselli, M. & Schlögl, E. (2017), 'A consistent stochastic model of the term structure of interest rates for multiple tenors', *QFRC* (384), 1–33.

Amin, K. I. & Bodurtha, J. N. (1995), 'Discrete-time valuation of American options with stochastic interest rates', *The Society for Financial Studies* **8**(1), 193 – 234.

Amin, K. I. & Jarrow, R. A. (1992), 'Pricing options on risky assets in a stochastic interest rate economy', *Mathematical Finance* **2**(4), 217 – 237.

Anzilli, L. (2012), 'A possibilistic approach to evaluating equity-linked life insurance policies', *Advances in Computational Intelligence. IPMU 2012. Communications in Computer and Information Science* **300**.

Bacinello, A. & Ortu, F. (1994), 'Single and periodic premiums for guaranteed equity linked life insurance under interest-rate risk: the 'Lognormal + Vasicek' case', *Peccati, L., Viren, M. (Eds.), Financial Modelling. Physica-Verlag* p. 155.

Bacinello, A. & Persson, S. (2002), 'Design and pricing of equity-linked life insurance under stochastic interest rates', *The Journal of Risk Finance* **Vol. 3, Iss. 2**, 6–21.

Bacinello, A. R. (2005), 'Endogenous model of surrender conditions in equity-linked life insurance.', *Insurance: Mathematics and Economics* **37**(2), 270–296.

Bacinello, A. R., Biffis, E. & Millossovich, P. (2009), 'Pricing life insurance contracts with early exercise features', *Journal of Computational and Applied Mathematics* **233**, 27–35.

Bakshi, G. & Cao, C. (2003), 'Risk-neutral kurtosis, jumps, and option pricing: Evidence from 100 most actively traded firms on the CBOE', *Working paper, Smith School of Business, University of Maryland* pp. 1–48.

Bakshi, G., Cao, C. & Chen, Z. (1997), 'Empirical performance of alternative option pricing models', *Journal of Finance* **52**(5), 2003 – 2049.

Ballestra, L. V. & Sgarra, C. (2010), 'The evaluation of American options in a stochastic volatility model with jumps: An efficient finite element approach', *Computers and Mathematics with Applications* **60**(6), 1571–1590.

Barone-Adesi, G. & Whaley, R. E. (1987), 'Efficient analytic approximation of American option values', *The Journal of Finance* (2), 301–320.

Bates, D. S. (1996), 'Jumps and stochastic volatility: Exchange rate processes implicit in Deutsche Mark options', *The Review of Financial Studies* **9**(1), 69–107.

Bates, D. S. (2000), 'Post-'87 crash fears in the S&P 500 futures option market', *Journal of Econometrics* **94**, 181–238.

Beliaeva, N. A. & Nawalkha, S. K. (2010), 'A simple approach to pricing American options under the Heston stochastic volatility model', *The Journal of Derivatives* pp. 25–43.

Bensoussan, A. (1984), 'On the theory of option pricing.', *Acta Appl. Math.* **2**, 139–158.

Bernard, C. & Lemieux, C. (2008), 'Fast simulation of equity-linked life insurance contracts with a surrender option', *Proceedings of the 2008 Winter Simulation Conference* pp. 444–452.

Bernard, C., MacKay, A. & Muehlbeyerb, M. (2014), 'Optimal surrender policy for variable annuity guarantees', *Insurance: Mathematics and Economics* **55**, 116–128.

Black, F. (1975), 'Fact and fantasy in the use of options', *Financial Analysts Journal* **31**(4), 36–41+61–72.

Black, F. (1976), 'The dividend puzzle', *The Journal of Portfolio Management* **2**(2), 5–8.

Black, F. & Scholes, M. (1973), 'The pricing of options and corporate liabilities', *Journal of Political Economy* **81**, 637 – 659.

Boyarchenko, S. & Levendorski, S. (2007), 'American options in Levy models with stochastic interest rate of CIR - type', *Available at http://ssrn.com/abstract=1032716 or http://dx.doi.org/10.2139/ssrn.1032716* pp. 1–37.

Boyle, P. (1977), 'Options: A Monte Carlo approach,', *Journal of Financial Economics* **4**, 323–338.

Boyle, P. (1988), 'A lattice framework for option pricing with two state variables', *Journal of Financial and Quantitative Analysis* **23**(1), 1–12.

Boyle, P. & Hardy, M. (2003), 'Guaranteed annuity options', *Astin Bulletin* **Vol.33, No 2**, 125–152.

Boyle, P. P. & Schwartz, E. S. (1977), 'Equilibrium prices of guarantees under equity-linked contracts', *The Journal of Risk and Insurance* **44**, 639–660.

Brennan, M. J. & Schwartz, E. S. (1976), 'The pricing of equity-linked life insurance policies with an asset value guarantee', *Journal of Financial Economics* **3**, 195–213.

Brennan, M. J. & Schwartz, E. S. (1977), 'The valuation of American put options', *The Journal of Finance* **32**(2), 449–462.

Broadie, M., Chernov, M. & Johannes, M. (2007), 'Model specification and risk premia: Evidence from futures options', *The Journal of Finance* (3), 1453–1490.

Broadie, M. & Detemple, J. (1996), 'American option valuation: New bounds, approximations, and a comparison of existing methods', *The Review of Financial Studies* **9**(4), 1211–1250.

Broadie, M. & Glasserman, P. (1996), 'Estimating security price derivatives using simulation', *Management Science* **42**(2), 269–285.

Broadie, M. & Glasserman, P. (1997), 'Pricing American-style securities using simulation', *Journal of Economic Dynamics and Control* **21**, 1323–1352.

Broadie, M. & Glasserman, P. (2004), 'A stochastic mesh method for pricing high-dimensional American options', *Journal of Computational Finance* **7**, 35–72.

Campbell, J. Y. & Hentschel, L. (1992), 'No news is good news: An asymmetric model of changing volatility in stock returns.', *Journal of Financial Economics* **31**(3), 281–318.

Carr, P., Jarrow, R. & Myneni, R. (1996), 'Valuation of the early-exercise price for options using simulations and nonparametric regression', *Mathematical Finance* **2**(2), 87–106.

Carriere, J. F. (1996), 'Valuation of the early-exercise price for options using simulations and nonparametric regression', *Insurance: Mathematics and Economics* **19**, 19–30.

Cheang, G. H. L., Chiarella, C. & Ziogas, A. (2013), 'The representation of American options prices under stochastic volatility and jump-diffusion dynamics', *Quantitative Finance* **13**(2), 241–253.

Cheng, B., Nikitopoulos, C. S. & Schlögl, E. (2018), 'Pricing of long-dated commodity derivatives: Do stochastic interest rates matter?', *Journal of Banking and Finance* **95**, 148–166.

Chiarella, C. & Kang, B. (2011), 'The evaluation of American compound option prices under stochastic volatility and stochastic interest rates', *Journal of Computational Finance* **17**(1), 71–92.

Chiarella, C., Kang, B., Meyer, G. H. & Ziogas, A. (2009), 'The evaluation of American option prices under stochastic volatility and jump diffusion dynamics using the Method of Lines', *International Journal of Theoretical and Applied Finance* **12**(3), 393–425.

Chiarella, C., Nikitopoulos, C. S., Schlögl, E. & Yang, H. (2016), Pricing American options under regime switching using Method of Lines. Quantitative Finance Research Centre, Working paper 368, UTS.

Chiarella, C. & Ziogas, A. (2005), 'Pricing American options under stochastic volatility'.

Chiarella, C. & Ziogas, A. (2009), 'American call options under jump-diffusion processes: A Fourier transform approach', *Applied Mathematical Finance* **16**(1), 3779.

Chiarella, C. & Ziveyi, J. (2011), Two stochastic volatility processes - American option pricing. Quantitative Finance Research Centre, Working paper 292, UTS.

Chung, S.-L. (1999), 'American option valuation under stochastic interest rates', *Review of Derivatives Research* **3**, 283–307.

Clarke, N. & Parrott, K. (1999), 'Multigrid for American option pricing with stochastic volatility', *Applied Mathematical Finance* **6**(3), 177–195.

Conn, A. R., Gould, N. I. M. & Toint, P. L. (2000), 'Trust region methods', *SIAM* **1**, 1–959.

Cox, J. C., Ross, S. A. & Rubinstein, M. (1979), 'Option pricing: A simplified approach', *Journal of Financial Economics* **7**, 229–263.

Cox, J., Ingersoll, J. & Ross, S. (1985), 'A theory of the term structure of interest rates', *Econometrica* **53**, 385407.

Dai, M., Kwok, Y. & Zongi, J. (2008), 'Guaranteed minimum withdrawal benefit in variable annuities', *Mathematical Finance* **vol. 18**(4), 595–611.

Das, S. & Sundaram, R. K. (1999), 'Of smiles and smirks: A term structure perspective', *Journal of Financial and Quantitative Analysis* **34**(2), 211–239.

Detemple, J. & Tian, W. (2002), 'The valuation of American options for a class of diffusion processes', *Management Science* **48**(7), 917–937.

Doffou, A. & Hilliard, J. E. (2001), 'Pricing currency options under stochastic interest rates and jump-diffusion processes', *The Journal of Financial Research* (4), 565–585.

Duffie, D., Pan, J. & Singleton, K. (2000), 'Transform analysis and asset pricing for affine jump-diffusion', *Econometrica* **68**(6), 1343–1376.

Durhama, G. & Park, Y. (2013), 'Beyond stochastic volatility and jumps in returns and volatility', *Journal of Business and Economic Statistics* **31**(1), 107–121.

Eraker, B. (2004), 'Do stock prices and volatility jump? Reconciling evidence from spot and option prices', *The Journal Of Finance* (3), 1367–1403.

Eraker, B., Johannes, M. & Polson, N. (2003), 'The impact of jumps in volatility and returns', *The Journal of Finance* (3), 1269–1300.

Fama, E. F. (1981*a*), 'Stock returns, expected returns, and real activity', *The Journal of Finance* **45**(4), 1089–1108.

Fama, E. F. (1981*b*), 'Stock returns, real activity, inflation, and money', *The American Economic Review* **71**(4), 545–565.

Farid AitSahlia, M. G. & Guha, S. (2010), 'American option pricing under stochastic volatility: an empirical evaluation', *Comput Manag Sci* **7**, 189206.

Feller, W. (1951), 'Two singular diffusion problems', *Annals of Mathematics* **54**(1), 173–182.

Fu, M. C., Laprise, S. B., Madan, D. B., Su, Y. & Wu, R. (2001), 'Pricing American options: A comparison of monte carlo simulation approaches', *Journal of Computational Finance* **4**(3), 39–88.

Fusai, G., Marena, M. & Roncoroni, A. (2008), 'Analytical pricing of discretely monitored asian style options: Theory and application to commodity markets', *The Journal Of Banking and Finance* **32**, 2033–2045.

Gaillardetz, P. & Lin, X. S. (2006), 'Valuation of equity-linked insurance and annuity products with binomial models', *North American Actuarial Journal* **10:4**, 117–144.

Geske, R. (1981), 'Comments on Whaley's note', *Journal of Financial Economics* **9**(2), 213 –215.

Geske, R. & Johnson, H. (1984), 'The American put option valued analytically', *Journal of Finance* **39**(5), 1511–1524.

Giot, P. (2005), 'Relationships between implied volatility indices and stock index returns', *The Journal of Portfolio Management* **31**(3), 92–100.

Grosena, A. & Jorgensen, P. L. (2000), 'Fair valuation of life insurance liabilities: The impact of interest rate guarantees, surrender options, and bonus policies', *Insurance: Mathematics and Economics* **26**, 3757.

Grzelak, L. A., Oosterlee, C. W. & Weeren, S. V. (2012), 'Extension of stochastic volatility equity models with the HullWhite interest rate process', *Quantitative Finance* **12**(1), 89–105.

Guo, S., Grzelak, L. A. & Oosterlee, C. W. (2013), 'Analysis of an affine version of the Heston-Hull-White option pricing partial differential equation', *Applied Numerical Mathematics* **72**, 143–159.

Haentjens, T. & Hout, K. J. (2012), 'ADI finite difference schemes for the Heston-Hull-White PDE', *The Journal of Computational Finance* **16**, 83–110.

Haentjens, T. & Hout, K. J. (2015), 'ADI schemes for pricing American options under the Heston model', *Applied Mathematical Finance* **22**(3), 207–237.

Hansen, A. T. & Jorgensen, P. L. (2000), 'Analytical valuation of American-style Asian options', *Management Science* **46**(8), 1116–1136.

Hanson, F. & Westman, J. (2002), 'Stochastic analysis of jump-diffusions for financial log-return processes', *Springer-Verlag, New York* **280**, 169–184.

Hanson, F., Westman, J. & Zhu, Z. (2004), 'Multinomial maximum likelihood estimation of market parameters for stock jump-diffusion models', *Contemporary Mathematics* **351**, 155–169.

Haowen, F. (2012), 'European option pricing formula under stochastic interest rates', *Progress in Applied Mathematics* **4**(1), 14–21.

Harrison, J. & Pliska, S. R. (1981), 'Martingales and stochastic integrals in the theory of continuous trading', *Stochastic Processes and their Applications* **11**(3), 215–260.

Heston, S. (1993), 'A closed-form solution for options with stochastic volatility with applications to bond and currency options', *Review of Financial Studies* **6**(2), 327–343.

Hibbert, A. M., Daigler, R. T. & Dupoyet, B. (2008), 'A behavioral explanation for the negative asymmetric return-volatility relation.', *Journal of Banking and Finance* **32**(10), 2254–2266.

Hilpisch, Y. (2011), 'Fast Monte Carlo valuation of American options under stochastic volatility and interest rates.', *www.archive.euroscipy.org* pp. 1–21.

Hirsa, A. (2013), 'Computational methods in finance', *Chapman and Hall CRC Financial Maths Series* .

Ho, T. S., Stapleton, R. C. & Subrahmanyam, M. G. (1984), 'The valuation of American options with stochastic interest rates: A generalization of the Geske - Johnson technique', *The Journal of Finance* **52**(2), 827 –840.

Hua, J., Shancun, L. & Dianyu, S. (2012), 'Pricing options in a mixed fractional double exponential jump-diffusion model with stochastic volatility and interest rates', *Proceeding of 2012 International Conference on Information Management, Innovation Management and Industrial Engineering* **3**, 1–4.

Hull, J. & White, A. (1987), 'The pricing of options on assets with stochastic volatilities', *The Journal of Finance* **42**(2), 281–300.

Hull, J. & White, A. (1990), 'Pricing interest-rate-derivative securities', *Review of Financial Studies* **3**, 573592.

Hull, J. & White, A. (2013), 'Libor vs. OIS: The derivatives discounting dilemma', *Journal of Investment Management* **11**(3), 14–27.

Ikonen, S. & Toivanen, J. (2009), 'Operator splitting methods for pricing American options under stochastic volatility', *Numer. Math.* **113**, 299324.

Itkin, A. (2016), 'Lsv models with stochastic interest rates and correlated jumps', *International Journal of Computer Mathematics* **94**(7), 1291–1317.

Jaillet, P., L. & D. Lapeyre, B. (1990), 'Variational inequalities and the pricing of American options', *B. Acta Appl Math* **21**(3), 263–289.

Jeanblanc, M., Klöppel, S. & Miyahara, Y. (2007), 'Minimal f^Q-martingale measures for exponential levy processes', *Ann. Appl. Probab* **17**, 16151638.

Johnson, H. E. (1983), 'An analytic approximation for the American put price', *The Journal of Financial and Quantitative Analysis* **18**(1), 141–148.

Kaelo, P. & Ali, M. M. (2006), 'Some variants of the controlled random search algorithm for global optimization', *Journal of optimization theory and applications* **130**(2), 253 –264.

Kang, B. & Meyer, G. H. (2014), 'Pricing an American call under stochastic volatility and interest rates', *Nonlinear Economic Dynamics and Financial Modelling - Essays in Honour of Carl Chiarella* pp. 291–314.

Kang, B. & Ziveyi, J. (2018), 'Optimal surrender of guaranteed minimum maturity benefits under stochastic volatility and interest rates', *Insurance: Mathematics and Economics* **79**, 4356.

Kangro, R., Parna, K. & Sepp, A. (2003), 'Pricing European - style options under jump diffusion processes with stochastic volatility: Applications of Fourier transform', *Acta et Commentationes Universitatis Tartuensis de Mathematica* **8**, 123–133.

Karatzas, I. (1988), 'On the pricing of American options.', *Appl. Math. Optim.* **17**, 37–60.

Kaushik I. Amin, V. K. N. (1993), 'Option valuation with systematic stochastic volatility', *The Journal of Finance* **48**(3), 881–910.

Kim, I. J. (1990), 'The analytic valuation of American options', *Review of Financial Studies* **3**, 547–572.

Kim, Y.-J. (2002), 'Option pricing under stochastic interest rates: An empirical investigation', *Asia-Pacific Financial Markets* **9**(1), 23 –44.

Kim, Y. & Kunitomo, N. (1999), 'Pricing options under stochastic interest rates: A new approach', *Asia-Pacific Financial Markets* **6**, 49–70.

Kizaki, K. & Muroi, Y. (2016), 'Pricing of guaranteed annuity options in a stochastic volatility and interest rate environment.', *Asia-Pacific Journal of Risk and Insurance* **10**(2), 133–153.

Kling, A., Ruez, F. & Rub, J. (2014), 'The impact of policyholder behavior on pricing, hedging, and hedge efficiency of withdrawal benefit guarantees in variable annuities', *European Actuarial Journal* **Volume 4, Issue2**, 281314.

Kokholm, T. & Stisen, M. (2015), 'Joint pricing of VIX and SPX options with stochastic volatility and jump models', *The Journal of Risk Finance* **16**(1), 27–48.

Kou, S. (2002), 'A jump diffusion model for option pricing', *Management Science* **48**(8), 1086–1101.

Kurz, A. (1996), 'Pricing of equity-linked life insurance policies with an asset value guarantee and periodic premiums.', *Albrecht, P. (Ed.). Aktuarielle Anstze fr Finanz-Risiken AFIR 1996, Band II, 14851496. Verlag Versicherungswirtschaft, Karlsruhe.* p. 14851496.

Lamberton, D. & Mikou, M. (2008), 'The critical price for the American put in an exponential levy model', *Finance Stoch* **12**, 561–581.

Lamoureux, C. G. & Lastrapes, W. D. (1993), 'Forecasting stock-return variance: Toward an understanding of stochastic implied volatilities', *The Review of Financial Studies* **6**(2), 293–326.

Lauko, M. & Sevcovic, D. (2010), 'Comparison of numerical and analytical approximations of the early exercise boundary of the american put option', *arXiv.org* pp. 1–22.

Li, J. & Szimayer, A. (2014), 'The effect of policyholders rationality on unitlinked life insurance contracts with surrender guarantees', *Quantitative Finance* **14:2**, 327–342.

Li, Q., Yang, J., Hsiao, C. & Chang, Y. (2005), 'The relationship between stock returns, and volatility in international stock markets', *Journal of Banking and Finance* **12**, 650–665.

Lindset, S. & Lund, A.-C. (2007), 'A Monte Carlo approach for the American put under stochastic interest rates', *Journal of Economic Dynamics and Control* **31**, 10811105.

Longstaff, F. & Schwartz, E. (2001), 'Valuing American options by simulation: A simple least-squares approach', *The Review of Financial Studies* **14**(1), 113–147.

Lutz, B. (2010), 'Pricing of derivatives on mean-reverting assets', *Lecture Notes in Economics and Mathematical Systems* **630**, 1–137.

MacMillan, L. W. (1986), 'Analytic approximation for the American put option', *Advances in Futures and Options Research* **1**, 119–139.

Makate, N. & Sattayantham, P. (2011), 'Stochastic volatility jump-diffusion model for option pricing', *Journal of Mathematical Finance* **1**, 90–97.

Margrabe, W. (1978), 'The value of an option to exchange one asset for another', *The Journal of Finance* **33**(1), 177 –186.

McKean, H. P. J. (1965), 'Appendix: A free boundary problem for the heat equation arising from a problem of mathematical economics.', *Ind. Management* **6**, 32–39.

Medvedev, A. & Scaillet, O. (2010), 'Pricing American options under stochastic volatility and stochastic interest rates', *Journal of Financial Economics* **98**, 145–159.

Melnikov, A. & Romanyuk, Y. (2008), 'Efficient hedging and pricing of equity-linked life insurance contracts on several risky assets', *International Journal of Theoretical and Applied Finance* **11**(3), 295–323.

Merton, R. C. (1973), 'Theory of rational option pricing', *The Bell Journal of Economics and Management Science* **4**(1), 141–183.

Merton, R. C. (1976), 'Option pricing when underlying stock returns are discontinous', *Journal of Financial Economics* **3**, 125–144.

Meyer, G. H. (1998), 'The numerical valuation of options with underlying jumps', *Acta Mathematica Universitatis Comenianae* **67**(1), 69–82.

Meyer, G. H. (2015), 'The time-discrete Method of Lines for options and bonds: A PDE approach', *World Scientific* .

Meyer, G. H. & van der Hoek, J. (1997), 'The evaluation of American options with the Method of Lines', *Advances in Futures and Options Research* **9**, 265–285.

Milevsky, M. & Salisbury, T. (2006), 'Financial valuation of guaranteed minimum withdrawal benefits', *Insurance: Mathematics and Economics* **38**(1), 2138.

Minqiang, L. (2010), 'Analytical approximations for the critical stock prices of american options: a performance comparison', *Review of Derivatives Research* **13**, 7599.

Myneni, R. (1992), 'The pricing of the American option', *The Annals of Applied Probability* **2**(1), 123.

Naik, V. & Lee, M. (1990), 'General equilibrium pricing of options on the market portfolio with discontinuous returns', *Review of Financial Studies* **3**, 493521.

Nielsen, B. F.and Skavhaug, O. & Tveito, A. (2002), 'Penalty and front-fixing methods for the numerical solution of American option problems', *Journal of Computational Finance* **5**, 6997.

Nielsen, J. A. & Sandmann, K. (1995), 'Equity-linked life insurance: A model with stochastic interest rates', *Insurance: Mathematics and Economics* **16**, 225–253.

Nielsen, J. A., Sandmann, K. & Schlögl, E. (2011), 'Equity-linked pension schemes with guarantees', *Insurance: Mathematics and Economics* **49**, 547564.

Pan, J. (2002), 'The jump risk premia implicit in options: Evidence from an integrated time-series study', *Journal of Financial Economics* **63**, 3–50.

Pantazopoulos, K. N., Zhang, S. & Houstis, E. N. (1996), 'Front tracking finite difference methods for the American option valuation problem', *Department of Computer Science Technical Reports* **1288**, 1–15.

Pennacchi, G. G. (1999), 'The value of guarantees on pension fund returns', *The Journal of Risk and Insurance* **66**(2), 219–237.

Pinkham, S. & Sattayatham, P. (2011), 'European option pricing for a stochastic volatility Levy model with stochastic interest rates', *Journal of Mathematical Finance* **1**, 98–108.

Powell, M. J. D. (1994), 'A direct search optimization method that models the objective and constraint functions by linear interpolation.', *Advances in Optimization and Numerical Analysis* pp. 51–67.

Powell, M. J. D. (1998), 'Direct search algorithms for optimization calculations.', *Acta Numerica* **7**, 287–336.

Price, W. L. (1978), 'A controlled random search procedure for global optimization.', *Towards Global Optimization 2* pp. 71–84.

Price, W. L. (1983), 'Global optimization by controlled random search', *Journal of optimization theory and applications* **40**(3), 333–348.

Rabinovitch, R. (1989), 'Pricing stock and bond options when the default-free rate is stochastic', *The Journal of Financial and Quantitative Analysis* **24**(4), 447–457.

Rambharat, B. R. & Brockwell, A. E. (2010), 'Sequential Monte Carlo pricing of American-style options under stochastic volatility models', *The Annals of Applied Statistics* **4**(1), 222265.

Ribeiro, A. & Poulsen, R. (2013), 'Approximation behoves calibration', *Quantitative Finance Letters* **1**(1), 36–40.

Rindell, K. (1995), 'Pricing of index options when interest rates are stochastic: An empirical test', *Journal of Banking & Finance* **19**, 785–802.

Roll, R. (1977), 'An analytic valuation formula for unprotected American call options on stocks with known dividends', *Journal of Financial Economics* **5**(2), 251 –258.

Rubinstein, L. I. (1971), 'The Stefan problem', *American Mathematical Society, Providence* .

Ruckdeschela, P., Sayera, T. & Szimayerb, A. (2011), 'Pricing American options in the Heston model: a close look on incorporating correlation', *Berichte des Fraunhofer ITWM* (204), 1–41.

Salmi, S., Toivanen, J. & Sydow, L. (2013), 'Iterative methods for pricing American options under the bates model', *Procedia Computer Science* **18**, 1136–1144.

Salmi, S., Toivanen, J. & Sydow, L. (2014), 'An imex-scheme for pricing options under stochastic volatility models with jumps', *SIAM Journal on Scientific Computing* **36**(5), B817–B834.

Samimi, O., Mardani, Z. & Sharafpour, S. (2017), 'LSM algorithm for pricing American option under Heston-Hull-White's stochastic volatility model', *Comput Econ* **50**, 173–187.

Schobel, R. & Zhu, J. (1999), 'Stochastic volatility with an Ornstein - Uhlenbeck process: An extension', *European finance review* **3**(1), 23–46.

Scott, L. O. (1997), 'Pricing stock options in a jump-diffusion model with stochastic volatility and interest rates: Applications of Fourier inversion methods', *Mathematical Finance* **7**(4), 413–424.

Selby, M. & Hodges, S. (1987), 'On the evaluation of compound options', *Management Science* **33**(3), 347–355.

Shehu, A. A. (2011), 'A study on financial risk analysis in pension funds investment: An implication of exchange rate exposure', *Proceedings of the 8th International Conference on Innovation and Management* .

Sheikh, A. M. (1991), 'Transaction data tests of S&P 100 call option pricing', *The Journal of Financial and Quantitative Analysis* **26**(4), 459–475.

Stein, E. M. & Stein, J. C. (1991), 'Stock price distributions with stochastic volatility: An analytic approach', *The Review of Financial Studies* **4**(4), 727–752.

Stewart, F. (2007), 'Benefit security pension fund guarantee schemes', *OECD Working Papers on Insurance and Private Pensions* **No. 5**.

Stivers, C. & Sun, L. (2002), 'Stock market uncertainty and the relation between stock and bond returns', *Federal Reserve Bank of Atlanta* **2002**(3), 1–38.

Sullivan, M. A. (2000), 'Valuing American put options using Gaussian Quadrature', *The Review of Financial Studies* **13**(1), 75–94.

Tavakkoli, A. & Thomas, D. B. (2014), 'Low-latency option pricing using systolic binomial trees', *Proc. Int. Conf. Field-Program. Technol. (FPT)* p. 4451.

Tsitsiklis, J. N. & Roy, B. V. (1999), 'Optimal stopping of Markov processes: Hilbert space theory, approximation algorithms, and an application to pricing high-dimensional financial derivatives', *IEEE Transactions of automatic control* **44**(10), 1840–1851.

van Haastrecht, A., Lord, R., Pelsser, A. & Schrager, D. (2009), 'Pricing long-dated insurance contracts with stochastic interest rates and stochastic volatility', *Insurance: Mathematics and Economics* **45**, 436–448.

van Haastrecht, A., Plat, R. & Pelsser, A. (2010), 'Valuation of guaranteed annuity options using a stochastic volatility model for equity prices.', *Insurance: Mathematics and Economics* **47**, 266–277.

Van Moerbeke, P. L. (1976), 'On optimal stopping and free boundary problems', *Arch. Rational Mech. Anal.* **60**, 101–148.

Whaley, R. (1981), 'On the valuation of American call options on stocks with known dividends', *Journal of Financial Economics* **9**(2), 207 –211.

Whaley, R. (1986), 'On valuing American futures options', *Financial Analysts Journal* **42**(3), 207 –211.

William H. Press, Saul A. Teukolsky, W. T. V. & Flannery, B. P. (2002), 'Numerical recipes in c++: The art of scientific computing', *Cambridge University Press* .

Wu, L. X. & Kwok, Y. K. (1997), 'A front-fixing finite difference method for the valuation of American options', *Journal of Financial Engineering* **6**, 8397.

Xu, Z., Wang, Q. & Chen, H. (2010), 'A stochastic control model for pricing the guaranteed equity-linked insurance', *2010 International Conference on Management and Service Science* pp. 1–3.

Zhang, S. & Wang, L. (2013), 'A fast numerical approach to option pricing with stochastic interest rate, stochastic volatility and double jumps', *Commun Nonlinear Sci Numer Simulat* **18**, 1832–1839.

Zhao, J., Davison, M. & Corless, R. M. (2007), 'Compact finite difference method for American option pricing', *Journal of Computational and Applied Mathematics* **206**, 306321.

Zhu, S.-P. (2005), 'An exact and explicit solution for the valuation of American put options', *Quantitative Finance* **6**(3), 229242.